The nature of the base polymer and the properties of N.B.R. gum vulcanizates

Kiroski, Dusko

Award date:
1995

Awarding institution:
University of Bath

THE NATURE OF THE BASE POLYMER AND THE PROPERTIES OF N.B.R. GUM VULCANIZATES

submitted by Duško Kiroski
for the degree of PhD
of the University of Bath
1995

COPYRIGHT

ProQuest LLC
789 East Eisenhower Parkway
P.O. Box 1346
Ann Arbor, MI 48106-1346

ACKNOWLEDGEMENTS

I would like to take this opportunity to thank the Defence Research Agency for making possible this study by financially supporting the project and Mr. M. R. Bowditch and Dr. J. Lane for overlooking the work. Gratitude is extended to the N.B.R. manufacturers for donating free rubber samples. Most experimental work was carried out at the laboratories of the School of Materials Science, University of Bath and the Centre for Polymer Studies, Trowbridge Technical College, and I would like to thank both institutions and technical staff thereof for their support.

I acknowledge Dr. R. Ewan of the University of the West of England, Bristol, for his operation of the X.P.S., Dr. D. Apperley of the University of Durham for ^{13}C N.M.R. spectroscopy and Dr. K. Timmins of D.R.A. Farnborough for mass analysis of antioxidants. Further gratitude is extended to the following organisations: R.A.P.R.A. for G.P.C. analysis and Butterworth laboratories for elemental analysis.

I would also like to express sincere appreciation to the following people for their assistance in this project: Mr. M. G. Phillips of the University of Bath for his ideas and discussion following the first year of the project and to Mr. J. Hickman and Mr. A. L. Gregory of the Centre for Polymer Studies for sharing their considerable experience in polymer testing.

I reserve my greatest gratitude to Dr. D. E. Packham for his continuous encouragement, suggestions and discussion.

DEDICATION

This work is dedicated to those few who simply through example motivate and inspire in others, by their thoughtfulness, consideration and dedication. The following have given immeasurably: Mr. J. Hickman, Dr. M. Lotfipour, Dr. L. A. Reeves and Dr. D. E. Packham.

ABSTRACT

In order to assess the effect of differences in base polymer on cure, mechanical and ageing properties, five commercial N.B.R. polymers of c. 28 weight % combined ACN content and Mooney viscosity, (ML 1+4 at 100°C) c. 45 Mooney units were compounded with two sulphur based gumstock formulations and studied. The two formulations differed in diphenyl amine antioxidant addition.

Polymers were found to contain differences in structural parameters such as, molecular weight, molecular weight distribution, gel content, ACN distribution and elemental residue composition associated with coagulant, emulsifier, transfer agent and stabiliser residues. Molecular weight was found to influence polymer viscosity at low shear rates and vulcanizate network density. Coagulant residues, such as calcium chloride were observed to act as antioxidants through hydroperoxide stabilisation. Carboxylic acid emulsifier residues were found to be effective plasticisers and reduced viscosity, particularly at high shear rates. A high width of glass transition was associated with a high concentration of carboxylic acid residue. Unsaturated oleic acid residues reduce network density by preferential reaction with crosslinking agent. Sulphate emulsifier residues were demonstrated to interact with and deactivate diphenyl amine. Elemental sulphur residues cause an increase in network density.

In measurement of network density involving swelling it was found that uncombined polymer is extracted, therefore the volume element which is lost during swelling of networks should be included in network density determination. Measurement of weight loss enables calculation of chemical network density from molecular weight distribution curves. Vulcanization of N.B.R. is accelerated by diphenyl amine addition and the proportion of mono-sulphide crosslinks is increased due to catalysis of sulphide decomposition and interchange.

Oxidation of N.B.R., measured by rate of property change and hydroperoxide formation is strongly influenced by base polymer. Differences in stability between polymers without compounded-in antioxidant are caused by differences in antioxidant residues. Addition of diphenyl amine antioxidant improves oxidative stability at extended ageing times. The mechanism of oxidation at 100°C is simultaneous crosslink scission and crosslink formation with the latter process being dominant. Crosslink scission occurs mostly through cleavage of mono-sulphide crosslinks. Crosslink formation is directly between carbon atoms. Diphenyl amine catalyses desulphurisation and decomposition of poly-sulphide and di-sulphide crosslinks, and there is initially more rapid tensile property change during ageing in its presence.

The Choice

The intellect of a man is forced to choose
Perfection of the life, or of the work,
And if it take the second must refuse
A heavenly mansion raging in the dark
When all that story's finished, what's the news?
In luck or out the toil has left its mark:
That old perplexity an empty purse,
or the day's vanity, the night's remorse.

W. B. Yates.

CONTENTS

CHAPTER I

1.0. INTRODUCTION

1.1. INTRODUCTION TO N.B.R.

Acrylonitrile butadiene rubber, designated N.B.R., BS 3502, part 2, (1991), is commonly referred to as nitrile rubber. According to Franta (1989) the word 'rubber' was originally used by Priestly in 1770, to describe the dry latex of the Hevea Braziliensis tree, following his observation that this material was capable of erasing pencil marks. The name rubber was applied, thereafter to other natural and man made materials with a similar structure and elastic properties to natural rubber. Nitrile is the general name given to all polymers containing the nitrile, (cyanide) group.

In common with other rubbers N.B.R. is a material composed of linear, flexible polymer chains, termed macromolecules which are made up of covalently bonded repeat units, termed monomers. In N.B.R. the repeat units are butadiene and acrylonitrile, (ACN). Co-polymerisation of N.B.R. is in emulsion of ACN and butadiene by a free radical initiated chain addition reaction process.

N.B.R. can be used in the latex form or may be further processed to give solid rubber. Solid rubber is usually compounded with reinforcing fillers, plasticisers, vulcanizing agents, antioxidants and other additives, and processed to the required shape. The shaped form is converted into a mechanically strong and elastic product by loosely crosslinking polymer chains, usually by elemental sulphur, in a process termed vulcanization. The number of ingredients in a commercial mix formulation is often in excess of a dozen and final vulcanizate properties are strongly dependent on mix composition.

In comparison with other commercial rubber materials N.B.R. products are characterised by a relatively high resistance to swelling in petrol, oils and greases together with very good heat resistance, moderate tear strength, moderate tensile strength, moderate thermo-oxidative resistance, low gas permeability, poor ozone resistance and poor electrical insulation (Brydson, 1988). These properties are however greatly affected by combined ACN content.

N.B.R. is manufactured by over 30 companies world wide. The major producers are Bayer, Enichem, Goodrich, Goodyear, Nippon Zeon and Polysar (now part of Bayer). Total world consumption has remained rather static throughout the 1980's at 200 000 tpa. This figure represents approximately 2.4 % of total rubber consumption.

Solid N.B.R. grades differ mainly in combined ACN content and molecular weight (Mooney viscosity). The overwhelming majority of solid N.B.R. grades contain combined ACN content in the range of 18-53 weight % and Mooney viscosity in the region of 20-140 Mooney units. Polymers with combined ACN content in the region of 27-36 weight % are considered standard grades while grades outside this range are considered somewhat specialised. Latex grades, pre-crosslinked grades, grades containing network bound antioxidant, plasticised grades, powdered grades and carbon black containing grades are marketed so that the number of available grades is in excess of 500. Chemically modified grades such as carboxylated N.B.R., epoxy modified N.B.R., hydrogenated N.B.R., N.B.R./P.V.C. blends, co-polymers containing isoprene and alternating co-polymers have been introduced more recently.

Apart from combined ACN content and Mooney viscosity manufacturers also supply other information such as, polymerisation conditions, the nature of added stabilisers, (either staining or non-staining), volatile content and ash content. A range of compound properties, (not part of the specification), such as tensile strength, elongation at break, stress at 300 % elongation, hardness, resilience and swelling behaviour may also be provided by polymer manufacturers.

The large number of available commercial N.B.R. grades is reflected in the diversity of applications. Low ACN content N.B.R. is used for products requiring only limited non-polar oil resistance, good flexibility and low compression set, such as seals, hydraulic hose and injection moulded goods. High combined ACN content N.B.R. is used for products requiring excellent resistance to non-polar oils such as high temperature seals, diaphrams, seal packing and conveyer belt covers.

1.1.1. HISTORICAL BACKGROUND

The beginning of synthetic rubber development goes back to the middle of the nineteenth century when attempts to determine the chemical structure of natural rubber, by Faraday and later by Williams and also Bouchardt resulted in the discovery of isoprene (Franta, 1989). Isoprene was synthesized into polyisoprene rubber at the end of the nineteenth century by Kondakov and also by Tilden. Polymerisation of isoprene was followed by the polymerisation of dimethyl butadiene in 1909 and polybutadiene soon afterwards. Work at I.G. Farbenindustrie of Germany into the development of synthetic rubber based on butadiene monomer, in the 1920's, lead to the polymerisation of several butadiene based co-polymers, including N.B.R. (in

1930), in emulsion through the use of sodium initiator (Bertram, 1981). The discovery of N.B.R. is credited to Helmut Kleiner, an employee of I.G. Farbenindustrie.

Early investigations into the properties of nitrile rubber (known as BUNA N), had shown the material to have better abrasion resistance in addition to higher tensile strength than styrene butadiene rubber. In 1932 Stocklin in an internal report had shown that nitrile rubber vulcanizates with 25 weight% combined ACN content had superior oil swell resistance to natural rubber and other synthetic rubbers available at that time. It was this high oil resistance which provided the incentive for the development of N.B.R.

The construction of the first N.B.R. production plant for the manufacture of BUNA N was approved during a meeting by I.G. Farbenindustrie executives on October 11, 1934. Although this plant was a commercial failure, a full scale commercial plant was constructed in Schkopau, at the urging of the German government and full scale production at this site begun in 1937.

In the same year several tonnes of BUNA N were exported to the U.S. using the trade name Perbunan under a technology transfer agreement entered into by I.G. Farbenindustrie A.G. and the Standard Oil Company of New Jersey. Commercial production was commenced in the U.S. by the Standard Oil Company shortly after the advent of World War II. Goodyear Rubber Company and Sarnia of Canada started commercial production soon afterwards. After World War II commercial N.B.R. production was started in England, Italy, France, Japan and the 'former U.S.S.R.'.

1.2. INTRODUCTION TO THE PROJECT

It was already pointed out that N.B.R. is manufactured by over 30 companies world wide. Many of these manufacturers produce N.B.R. grades of identical specification. This is particularly true for standard grades of combined ACN content in the region of 27-36 weight % and Mooney viscosity in the region of 50 Mooney units. Such equivalent specification grades often contain differences in molecular structure and elemental composition which are not shown by the specification. Such subtle variation in raw polymer structure and elemental composition often manifests itself during compound processing and during product service.

Lotfipour, Reeves, Kiroski and Packham (1994) have shown significant

differences in mould fouling and mould release properties of identical specification polymers obtained from different manufacturers. Musci (1995) has shown a reduction in mould fouling of equivalent grade N.B.R. polymers through more stringent washing of product during final stages of manufacture. Differences in adhesion between metal and rubber when using equivalent specification grades of N.B.R. from different manufacturers have been reported by Lotfipour *et al.* (1994), Reeves and Packham (1992) and Lotfipour, Packham and Turner (1991). Reeves and Packham (1992) reported differences in apparent viscosity of two ostensibly equivalent N.B.R. grades, supplied by different manufacturers. Bond (1994) reported that in a lip type rotary seal moulding the level of rejects can increase from 0% to 7% when changing grades with equivalent combined ACN and Mooney viscosity, which were polymerised under different conditions. Recently Musci (1995) described improvements in low temperature flexibility, cure rate and oil swell resistance of identical specification grades through more stringent control of the polymerisation process. The observation that vulcanization behaviour is affected by polymerisation conditions would imply that network density and network structure are also affected.

Batch to batch variation in properties within a polymer grade has also been observed (Lotfipour, 1990). These findings illustrate that commercial method of specification of N.B.R. is insufficiently extensive to fully characterise the product.

In N.B.R. there is generally a lack of fundamental understanding of the relationship between changes in polymer structure and polymerisation residue composition and polymer and vulcanizate properties. Variation in polymer structure is introduced by variation of polymerisation conditions and process control. Differences in residue composition may be caused by variation in monomer feed purity, and variation of other components of the polymerisation process. Variation in trace residue concentration may also be caused by differences in the washing process of coagulated polymer.

It is largely recognised that many differences in properties of identical specification polymers may be associated with differences in polymerisation conditions. This is undoubtedly so because polymerisation is a complex heterogeneous process and there is therefore much scope for variation in polymer structure and polymerisation residue composition. Previous studies have reported that commercial N.B.R. contains significant concentrations of polymerisation residues (Musci, 1995; Lotfipour *et al.*, 1994; Reeves and Packham, 1992; Lotfipour *et al.*,

1991). Polymerisation residues, such as coagulant and emulsifier residues are found to differ between equivalent specification grades of N.B.R. which are polymerised by different manufacturers. It is recognised that emulsifier residue is particularly problematic because its presence adversely affects swelling resistance of N.B.R. vulcanizates (Musci, 1995).

Variability in N.B.R. properties implies a need for study of the influence of polymer structure and polymerisation residues on the properties of N.B.R. vulcanizates. This study addresses this need and reports on the relation between polymer structure and properties. The influence of polymerisation residues on vulcanizate network structure and vulcanizate properties is also reported.

A major area of interest is the study of the effect of polymer structure and polymerisation residue composition on oxidative stability of N.B.R. vulcanizates. Study of N.B.R. oxidation is important because N.B.R. products often require long term hot air resistance at temperatures in excess of 120°C, particularly for under the bonnet automobile applications.

Ageing is a complex process involving a variety of chemical reactions leading to main chain scission, crosslinking, main chain modification, crosslink scission and crosslink modification. In N.B.R., ageing causes an increase in hardness and loss of elasticity. A product compounded for optimum thermo-oxidative resistance has a useful service life in the region of 1 year at 90°C, 40 days at 120°C and only 3 days at 150°C (Brydson, 1988). Structural changes brought about by ageing and their effect on material properties makes this topic particularly suited to study by the interdisciplinary nature of materials science.

Past and present research into improving the inadequate thermo-oxidative stability of N.B.R. without changing the base polymer has been based largely on variation of compounding system (Kotani and Teramoto, 1980). Such studies have achieved significant improvement in thermo-oxidative stability through optimization of compound formulation. These improvements in thermo-oxidative stability have mainly been empirical and basic research into the mechanism of N.B.R. oxidation has received relatively little attention. The effect of polymer structure and polymerisation residue composition on N.B.R. oxidation has not been studied.

This study reports on the oxidation of sulphur cured N.B.R. vulcanizates using base polymer as a variable and keeping compound formulation constant. The role of trace impurities such as polymerisation residues in the ageing process of N.B.R. is of

particular interest because it is well known that trace impurities can have pro-oxidative and anti-oxidative effects (Lee, Stacy and Engel, 1966a; 1966b). Such impurities are present in commercial N.B.R. polymers as polymerisation contaminants.

At the outset of this study it was decided to work with five commercial N.B.R. polymers, of combined ACN content c. 28 % and Mooney viscosity (ML 1+4) at 100°C of c. 45 ± 5 Mooney units. This commercial specification was of interest to the sponsor. Commercial polymer grades were obtained from different N.B.R. manufacturers. The gumstock sulphur based compound formulations are based on an earlier project, of interest to the sponsor (Sims, 1988).

1.3. INTRODUCTION TO THE THESIS

This very broad introduction to the project is intended to present to the reader the rationale of this work.

The study reports on the nature of the base polymer and the properties of N.B.R. gum vulcanizates. A study into this area is of interest because available N.B.R. polymers often exhibit differences in structure and elemental residue composition whose effect on properties is poorly understood.

After describing the scope of the project in the present chapter, the relevant background literature is surveyed in chapter two. This review starts with a discussion of the commercial manufacture of N.B.R. and its vulcanization. The residues present come from these stages, and most of the molecular differences between polymers and variation in network structure originate here. This chapter also introduces and reviews the lesser known experimental techniques which have been used in polymer and network characterisation. Chapter two continues with a review of N.B.R. oxidation and illustrates effects of network structure and trace impurities on the process.

Experimental work begins with detailed elemental and structural characterisation of the five base polymers used in this study (chapters three and four). Results on polymer characterisation together with their discussion, presented in chapter four are intended to form the foundation around which the remainder of the project is built and later results are referenced to.

Characterisation of the base polymers is followed by study of vulcanization

behaviour and characterisation of network structure of vulcanizates. Differences in network structure caused by change in base polymer and compound formulation help to explain differences in static and dynamic tensile properties, reported at the end of this chapter.

In this study, structure-property relationships have been treated as topics of interest in their own right and also as a foundation for understanding the influence of base polymer on crosslink density.

Oxidation of N.B.R. is treated in chapters five and six. The room devoted to the study of oxidation reflects the importance of this subject and the complexity of the oxidation process in these systems.

Differences in oxidative stability between polymers and compounds may be caused by antioxidative and pro-oxidative effects of polymerisation residues, compounded-in antioxidants and differences in network structure.

The study of oxidation starts with an illustration of the effect of base polymer and compound formulation on static and dynamic tensile property change during oxidative ageing at 100°C. This is followed by study of the temperature-time dependence of ageing, measured through tensile property change. The influence of ageing on tensile properties is rationalised by determination of aged network density and structure. Network oxidation is studied further by ageing extracted networks and networks of uniform crosslink structures.

At the end of this chapter the effect of specific coagulants and emulsifier residues on ageing behaviour is studied by measuring ageing behaviour of compounds with such residues compounded-in.

Chapters four and six on results and discussion are followed by a chapter of more general discussion, (chapter seven). This brings together the points raised in previous discussions.

Conclusions on the nature of the base polymer, network structure, tensile properties and the thermo-oxidative stability of N.B.R. gum vulcanizates are drawn together and outlined in chapter eight. This is followed by suggestions for further work, (chapter nine).

CHAPTER II

2.1. PREPARATION OF N.B.R.

2.1.1. PREPARATION OF MONOMERS

2.1.1.1. Preparation of Acrylonitrile (ACN)

Commercially ACN is produced almost exclusively by the ammoxidation of propylene process, developed in the early 1960's (Wells, 1991).

$$CH_2=CHCH_3 + NH_3 + {}^3/_2O_2 \longrightarrow CH_2=CHCN + 3H_2O \qquad \text{I.}$$

A typical analysis of ACN monomer which is prepared by the Standard Company of Ohio, (SOHIO) process shows the presence of metal catalyst residues at < 0.5 parts per million, (ppm), hydrogen cyanide < 5 ppm and acetonitrile < 500 ppm (Hoffman, 1968).

ACN (2-propenenitrile) is a strongly polar monomer due to the presence of the electronegative nitrogen atom, the dipole moment being induced by the electronegativity of nitrogen and its uncombined lone pair electrons. At room temperature ACN is a colourless liquid, boiling point 77.3°C (Barlow, 1988).

2.1.1.2. Preparation of Butadiene

The overwhelming majority of butadiene is obtained from the C_4 fraction which is derived from steam cracking naphtha and gas oil (Wells, 1991). Naphtha contains 4.3 % butanes and butenes and 4.6 % butadiene. Gas oil contains 4.9-6.2 % butanes and butenes and 4.5-5.3 % butadiene.

Butadiene is obtained directly by extracting the C_4 stream from cracking naphtha, gas oil, butanes and propanes with n-methylpyrolidine or dimethylformamide. Butadiene is also obtained from dehydrogenation of butanes and butenes in the presence of metal oxide-chromium oxide catalyst mixtures at temperatures in the region of 600°C.

Separation of butadiene from other fractions is achieved by extraction with cuprous salts. Technical grades are of 99.6 % purity. Butadiene is often stabilised with p-tertiary-butyl pyrocatechol or 2,6-di-tertiary-butyl-p-cresol.

Butadiene, (1,3-butadiene) is a stable non polar hydrocarbon molecule, (boiling point -4.4°C), (Barlow, 1988).

2.1.2. EMULSION POLYMERISATION

Commercially the co-polymerisation of ACN and butadiene, to form N.B.R. is carried out in emulsion (Poehlein, 1986). Emulsion polymerisation is a heterogeneous reaction process in which the monomer is solubilised and dispersed in a continuous water phase by the use of emulsifier. Emulsifiers are molecules consisting of a polar hydrophilic part and a hydrophobic hydrocarbon part, which is an alkyl/aryl moiety. Orientation of emulsifiers at surfaces and interfaces of solutions results in lowering of surface tension, such that above a critical micelle concentration (C.M.C.) of emulsifier addition, micelles are formed and water insoluble materials are encapsulated within.

The micelles which form, become electrically charged and are stabilised by counterions of opposite charge in the solution (electrical double layer). Added monomer forms emulsified monomer droplets in the continuous water phase and also diffuses into micelles where polymerisation takes place. Some monomer may also dissolve in the water phase. This is observed to be the case with ACN monomer which is reported to have a solubility in water of 8.5 weight % at 50°C (Eliseeva, Ivanchev, Kuchanov and Lebedev, 1981). Radicals which are formed by the decomposition of initiators in the continuous phase react with monomer molecules to initiate polymerisation. Polymerisation is terminated by the addition of transfer agents and short stop.

The product of emulsion polymerisation, termed latex is a colloidal suspension of liquid polymer. In stable emulsions coalescence of individual latex particles is prevented by electrostatic repulsion. The addition of electrolytes above a critical concentration to emulsions leads to a rapid destruction in the particle surface charge potential of micelles. In the absence of electrostatic repulsion attractive forces between polymer particles become dominant and coagulation occurs.

2.1.2.1. Emulsion Polymerisation Components

Details of current commercial polymerisation recipes are not published and relevant literature on the subject, is invariably based on early polymerisation recipes which may no longer be in commercial use (Barlow, 1988; Hoffman, 1968). There is however much indirect information on current commercial emulsion polymerisation systems in studies reporting on the nature of polymerisation residues of commercial N.B.R (Reeves, Kiroski and Packham, 1995; Lotfipour *et al.*, 1994; Reeves and Packham, 1992; Lotfipour *et al.*, 1991).

In a detailed outline of N.B.R. polymerisation, Hoffman (1968) states that in a typical polymerisation recipe the water content may be 200 weight parts (parts per hundred parts of monomer feed). His remarks pointing out the need to use water of high purity, de-ionised and oxygen free, remain valid in present day polymerisation recipes. The pH of the system is controlled by addition of low levels of buffer such as sodium pyrophosphate (Eliseeva *et al.*, 1981). Control of pH is necessary because at strongly alkaline conditions ACN has been observed to hydrolise to amide (Frenkel, Duchacek and Maksutov, 1992).

Emulsifier addition may be in the region of 3-6 weight parts (Horvath, Purdon and Meyer, 1974). Study of emulsifier residues in commercial N.B.R. grades shows that emulsifiers are anionic surfactants, such as sodium salts of alkyl sulphate and sulphonate compounds. Sulphate/sulphonate compounds appear to be used often in combination with carboxylic acids. The length of the alkyl group is usually in the range C_{10}-C_{18} to balance conflicting demands for high reactivity and high solubility (Bhattacharjee, Bhowmick and Avasthi, 1993).

Company literature suggests that the overwhelming majority of N.B.R. grades are manufactured by the 'cold process' where polymerisation is primarily initiated with the use of water soluble free radical generating initiators. Initiators include potassium and ammonium salts of persulphuric acids, organic peroxides, hydroperoxides, peracids and perborates (Bhattacharjee *et al.*, 1993; Zachoval and Brajko, 1989). Reducing agents are based on iron sulphates and sodium sulphates. Systems comprising hydrogen peroxide (20 %) at 0.35 weight parts in combination with iron sulphate heptahydrate 0.02 weight parts and potassium persulphate 0.4 weight parts in combination with iron sulphate heptahydrate at 0.0005 weight parts are two published examples (Hoffman, 1968).

With the use of Redox systems emulsion polymerisation of N.B.R. is usually carried out at temperatures in the region of 5°C. The activation energy of Redox catalyst systems are quoted to be in the range of 50-65 $kJ.mole^{-1}$.

Molecular weight control, characterised by Mooney viscosity is achieved through incremental addition of modifiers which are almost exclusively alkyl mercaptan compounds (addition may be in the region of 0.2-0.75 weight parts) (Horvath *et al.*, 1974). Primary, secondary and tertiary mercaptans containing 8-16 methylene groups are used, often in combination. Accurate control of modifier addition is particularly important since a change in concentration from 0.4 to 0.6 weight parts is reported to cause a decrease in Mooney viscosity of 80 Mooney units (Zachoval and Brajko, 1989). Chemicals such as di-isopropyl xanthogen disulphide are used to retard the polymerisation initiation of ACN in low ACN content polymers (Hoffman, 1968).

Polymerisation is terminated by the addition of water soluble reducing agents, such as sodium hydrogen sulphite, sodium dithionite, hydroxylamine, hydrazine and its salts or sodium dimethyldithiocarbamate (Bhattacharjee *et al.*, 1993).

Non-staining stabilisers described by Hoffamn (1984) are usually bis-p-cresol, alkylated phenols and bis-phenols. These are added at concentrations in the region of 1-1.5 weight parts at the end of the polymerisation process, to protect polymer during coagulation, washing, drying and storage.

Coagulation in commercial N.B.R. is made with an aqueous solution of an inorganic salt such as aluminium sulphate, sodium chloride, calcium chloride or magnesium chloride as described by Hoffman (1968). This early publication by Hoffman has been shown to be relevant to current commercial N.B.R. polymers (Reeves *et al.*, 1995; Lotfipour *et al.*, 1994; Reeves and Packham, 1992; Lotfipour *et al.*, 1991).

2.1.2.2. Polymerisation Apparatus

N.B.R. is manufactured by a batch process and a continuous process, the choice of process being influenced by the level of production (Poehlein, 1986).

The batch process is carried out in individual, stainless steel, chrome-nickel or glass lined reactors.

In the commercially more important continuous process, polymerisation is carried in polymerisation lines which consist of a train of continuous stirred tank reactors (C.S.T.R's) connected in series. The average number of reactors is usually 10-15. Polymerisation components are fed into the first tank, by means of measuring pumps. Variations on the process use multiple point feed injection, different size reactors and a different number of reactors. The polymerisation charge is transferred to subsequent reactors along the polymerisation line and removed from the last C.S.T.R. as a partly converted latex stream. Temperature control is achieved through heat exchange between the polymerisation charge and cooled reactor walls and baffles. Polymerisation reactors also have mechanical stirrers to provide mixing and increased cooling efficiency.

2.1.2.3. Polymerisation Process Control

In the first step of the polymerisation process a fraction of the water of the polymerisation feed is introduced directly into the polymerisation reactor (Hoffman, 1968). The remainder of the water is used to dissolve other components of the recipe. A solution of premixed emulsifier is then fed into the reactor. Remaining emulsifier is added at a gradual rate to avoid problems with variations in latex viscosity.

The initiator is dissolved in water and introduced into the charge in the absence of co-agent. Addition of initiator is followed by the introduction of monomers and modifier. Polymerisation starts with the addition of initiator co-agent.

After monomer introduction the reaction vessel is closed and pressurised to increase the polymerisation rate. Air is removed and replaced by evaporated butadiene. A gradual drop in pressure caused by butadiene monomer depletion is used to measure the progress of polymerisation.

Modifier is pre-dissolved in butadiene and added gradually to obtain a uniform molecular weight distribution.

Polymerisation is terminated between 70 % and 80 % conversion by the addition of short stop. With an increase in conversion there is increased tendency for polymer chains to branch and crosslink. The termination step is carried out in a separate vessel. At the end of the polymerisation process stabilisers are added to the emulsion. Free monomer is recovered from the emulsion by 2-column steam distillation. The control of ACN, which is highly toxic is particularly stringent. For food contact

applications free ACN content needs to be less than 1 ppm (parts per million) (Musci, 1995).

N.B.R. latex is precipitated in separate vessel by addition of a concentrated electrolyte solution. Fatty acid soaps are converted to free fatty acids by treating with dilute acid solution. The rubber crumbs are washed with an weakly alkaline water solution after coagulation to extract water soluble polymerisation residues.

The washed polymer crumb is hot air dried in rotary or belt dryers at temperatures up to approximately 70°C. At these temperatures the porous surface of the product is maintained and the interior is also dried. Alternatively the rubber is dried in screw conveyer dryers. After drying the polymer crumb is compacted into bales and wrapped.

2.1.2.4. Summary on Polymerisation Residues

Detailed study of the elemental composition of commercial N.B.R. polymers has shown that polymers contain residues of the polymerisation process (Reeves and Packham, 1992). A typical polymer contains emulsifier residues at a few weight percent. These may be sulphate/sulphonate emulsifiers and carboxylic acids. Coagulant residues, such as magnesium chloride, calcium chloride and sodium chloride are present at a total concentration of less than 1 weight %. Mercaptan residues and initiator residues are combined with the polymer and their residual concentration is therefore negligible. Total antioxidant concentration will depend upon its addition level and may typically be in the region of 1 weight %.

2.1.3. N.B.R. STRUCTURE

2.1.3.1. Polymer Microstructure

N.B.R. is an unsaturated essentially linear random co-polymer of ACN and butadiene. Long chain branching and crosslinking may be introduced during latter stages of polymerisation but the concentration of such structural features is usually negligible (Brydson, 1988).

The microstructure of polymer chains varies due to the ability of butadiene monomer to add onto the growing chain in several ways. 1,4-addition gives rise to cis-

1,4-butadiene and trans-1,4-butadiene structures. 1,2- or 3,4-additions give rise to a vinyl, butadiene structure. These microstructures are illustrated in reaction scheme II. Some branching and crosslinking may be caused through polymerisation of vinyl-1,2-units. Willoughby (1989) showed that the butadiene fraction in N.B.R. containing 28 weight % combined ACN content is made up of 89.6 mole % 1,4-butadiene and 10.4 mole % 1,2-butadiene. The cis:trans ratio is in the region of 12:78 mole %, respectively. The results of Willoughby (1989) have been confirmed in other publications (Hertz, Bussem and Ray, 1994; Zachoval and Brajko, 1989; Brydson, 1988).

The low microstructural regularity of N.B.R. ensures that the polymer is amorphous and does not crystallise on stretching.

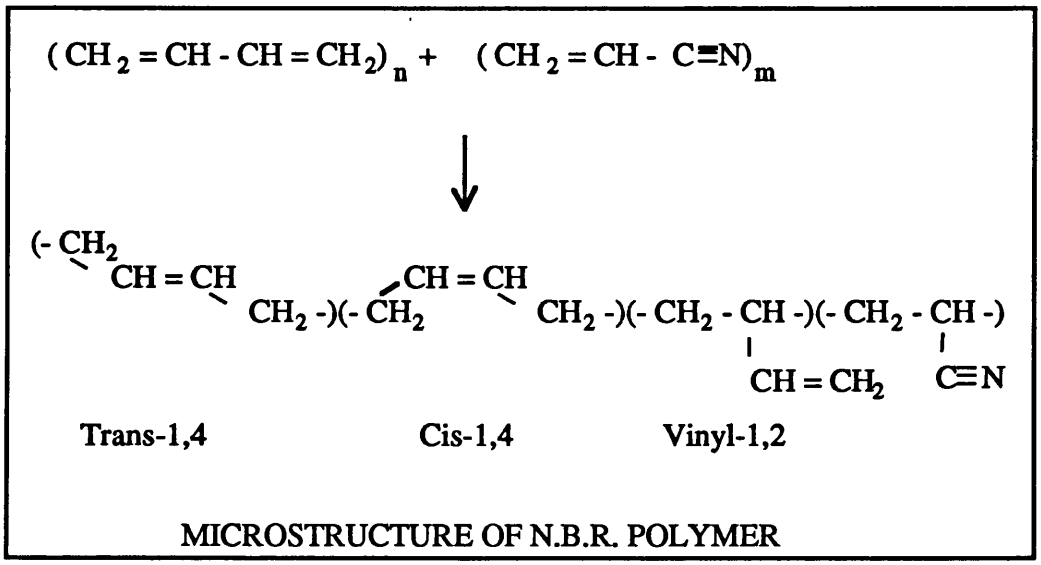

MICROSTRUCTURE OF N.B.R. POLYMER

II.

The molecular weight of polymer is strongly dependent on the degree of conversion. At high conversions there is an increase in molecular weight and molecular weight distribution due to branching and crosslinking.

Commercial polymers (such as Krynac 803, Mooney viscosity 47 Mooney units) have chains with molecular weight in the region of 30 000-300 000 $g.mole^{-1}$, with average molecular weight being in the region of 200 000 $g.mole^{-1}$ (Zachaval and Brajko, 1989). The molecular weight of butadiene and ACN are 54 and 53 $g.mole^{-1}$ respectively, hence the average degree of polymerisation is in the region of 5 500. Different polymer grades of Mooney viscosity in this region may have different

molecular weight since Mooney viscosity is also affected by the extent of branching and molecular weight distribution .

2.1.3.2. Monomer Sequence Distribution

As explained by Musci (1995) obtaining a uniform composition ACN rubber requires careful control of feed composition due to the large difference in reactivity ratios between ACN and butadiene. The reactivity ratios of ACN and butadiene at 5°C are stated to be r_A, (reaction rate of ACN with ACN relative to reaction rate with butadiene) 0.02 and r_B (reaction rate of butadiene with butadiene relative to reaction rate with ACN) 0.28, respectively (Hoffman, 1968).

At 5°C, the azeotropic feed composition at which both monomers polymerise at an equal rate is 36 % A.C.N. and 64 % butadiene. Away from the azeotropic ratio, there is compositional drift. With higher ACN content N.B.R., butadiene polymerises initially at a faster rate whereas with lower ACN content N.B.R., ACN polymerises initially at a faster rate.

In commercial N.B.R. co-polymerisation compositional drift is reduced by using a multi-increment (semi-continuous) polymerisation process where polymerisation is initiated with 10-20 % of total charge of the monomer which polymerises at a faster rate. The remaining monomer is added in increments at predetermined polymerisation intervals, or continuously at a rate which is lower than the overall rate of polymerisation.

There appears to be no published data on the extent of compositional drift in commercial N.B.R.. This may be because of the difficulty of measuring compositional drift. Publications on monomer sequence distribution in commercial N.B.R. grades with combined ACN content ranging from 27-50 weight %, such as that by Willoughby (1989) using the technique of high resolution ^{13}C nuclear magnetic spectroscopy (^{13}C N.M.R.) suggets high degree of alternation between ACN. and butadiene. However the high alternation suggested by the results of Willoughby may be misleading because the technique did not allow for estimation of the length of ACN and butadiene blocks, beyond tri-additions.

Willoughby (1989) found that in a typical commercial N.B.R with 28 weight % combined ACN, all ACN units are alternating but 60 mole % of butadiene is present in butadiene blocks containing more than 2-3 butadiene units. With an increase in

combined ACN content the level of alternation increases. The level of alternation increases to 70 mole % in an N.B.R. grade containing 50 weight % combined ACN content. The remainder monomer is enchained in ACN di-addition and butadiene di-addition.

2.1.3.3. Structure-Property Relationship

Properties of N.B.R. polymer are strongly influenced by the concentration of combined ACN content and also by polymer structure such as molecular weight and gel content (Chang, 1981). Properties are therefore extremely sensitive to variation in polymerisation conditions.

The density of N.B.R. is reported to be 1010 kg/m^3, 1050 kg/m^3 and 1070 kg/m^3 for grades containing 18 weight %, 28 weight % and 38 weight %, combined ACN content, respectively (Yehia and Stoll, 1982).

The Hilderbrand solubility parameter δ, (square root of cohesive energy density) of N.B.R. increases from 8.8 to 10.5 $(cal/cm^3)^{0.5}$ as combined ACN content increases from 20 to 45 weight % (Hoffman, 1984). The swelling parameter of a 28 weight % combined ACN content grade is 9.5 $(cal/cm^3)^{0.5}$.

N.B.R. vulcanizates swell readily in polar solvent such as aromatic hydrocarbons and ketones (Starmer, 1993a; 1993b; 1993c). With slightly polar solvents such as ethyl acetate a Gaussian distribution function describes the dependence of volume swell on combined ACN content. It is further reported that swelling is inversely related to molecular weight and gel content (Bhattarcharjee *et al.*, 1993; Chang, 1981).

The glass transition temperature and brittleness temperature of N.B.R. vulcanizates is strongly dependent on combined ACN content (Stolfuss and Warrach, 1991; Hoffman, 1984; Chang, 1981). With combined ACN content increasing from 28 to 39 weight % glass transition temperature increases from -28 to -8°C and brittleness point increases from -40 to -24°C. The glass transition temperature of N.B.R. with combined ACN content of 28 weight % is in the region of -28°C. Glass transition temperature and the width of transition is also affected by heterogeneity in polymer composition. It is reported that polymers of high heterogeneity have poor low temperature properties due to association and blocking of ACN fragments (Musci, 1995).

Processability, a very general term, is reported to be very sensitive to structural features such as molecular weight, molecular weight distribution, short chain branching, long chain branching and gel content (Chang, 1981). With an increase in combined ACN content processability, thermoplasticity and stiffness increase.

A study into the effect of combined ACN content and molecular weight on the kinetics of sulphur based vulcanization concludes that cure rate and crosslink density are reduced with an increase in combined ACN content (Yehia and Stoll, 1982). Compounds based on higher molecular weight polymer vulcanize at a faster rate and form a network of higher crosslink density.

The mechanical properties of N.B.R. vulcanizates compounded with a standard carbon black loaded sulphur based formulation (ASTM D3187) are well documented (Bhattacharjee *et al.*, 1993). Shore A hardness is in the region of 67-70° for N.B.R. rubbers containing less than 35 weight % combined ACN content. Above 35 weight % hardness increases in an exponential manor with increasing combined ACN content.

Tensile strength is reported to be 16.6 MPa, 27.0 MPa and 24.5 MPa for grades containing 29 weight %, 34 weight % and 50.5 weight % combined ACN content, respectively. Stress at 100 % elongation is reported to be in the region of 7.9 MPa, 10.5 MPa and 15.7 MPa for grades containing 29 weight %, 34 weight % and 50.5 weight % combined ACN content, respectively. Elongation at break values of 450-600 % show little dependence on combined ACN content.

Chang (1981) reports that an increase in gel content causes an increase in compound green strength, modulus, tensile strength and tear strength. Elongation at break is reduced with an increase in gel content. Modulus, hardness and tear strength increase with an increase in molecular weight. Tensile strength increases up to a Mooney viscosity of 60 Mooney units followed by a reduction with further increase in Mooney viscosity.

Compression set increases with an increase in combined ACN content and decreases with an increase in molecular weight. Stollfuss and Warrach (1981) show compression set of sulphur cured N.B.R. vulcanizates of 18 and 39 weight % combined ACN, of 52 % and 64 %, respectively after 70 hours at 100°C. At -40°C, after 7 days the compression set of the equivalent compounds based on N.B.R. with

18 weight % combined ACN and 39 weight % combined ACN were found to be 55 % and 100 %, respectively.

N.B.R. is characterised by high resistance to gas permeability. The uptake of oxygen of N.B.R. with 30 weight % combined ACN at 130°C is quoted as 3.68×10^{-8} litre.$g^{-1}.s^{-1}$ (Dunn, 1981). Oxygen permeability increases with decreasing combined ACN content. A decrease in combined ACN content to 20 weight % results in a oxygen permeability at 130°C of 8.58×10^{-8} litre.$g^{-1}.s^{-1}$.

2.2. RUBBER VULCANIZATION

Although possessing some elasticity due to entanglements rubber in its raw state is simply a high viscosity fluid that can be highly deformed and made to flow by the application of a deforming force. If brought in contact with a thermodynamically good solvent rubber molecules simply dissociate and go into solution. N.B.R. in this form has little commercial application and is changed following shaping into a more useful elastic form by a process termed vulcanization. Vulcanization is a chemical process by which the individual polymer chains are tied together at a number of points by the introduction of chemical crosslinks.

2.2.1. PHYSICAL DESCRIPTION OF NETWORK STRUCTURE

Lightly crosslinked polymer chains form a three dimensional random network, made up of network chains, chemical crosslinks, physical crosslinks (chain entanglements) and chain ends. Such networks are characterised by three related terms of network chain density, crosslink density and molecular weight between crosslinks (Mark, 1982).

Network chain density (N_v) is expressed as the number of moles of network chains per unit volume. N_v is closely related to other terms which reflect the density of crosslinks, in particular the number of network chains per unit volume N and the average molecular weight between crosslinks M_c.

From elementary considerations it can be seen that,

$$N_v = N/N_a \qquad (2.1)$$

$$N_v = \rho/M_c \qquad (2.2)$$

where, N_a is Avogadro's number and ρ is the density of the rubber.

A second parameter which is directly related to network chain density is crosslink density which is defined as the number of moles of crosslink per unit volume. Crosslink density is calculated by considering crosslink functionality. Crosslink functionality, *f* is the number of network chains emanating from each crosslink. With a functionality of four, there are two network chains for each crosslink, (crosslink density = $0.5\ N_v$).

True functionality is invariably less than four because crosslinked networks contain chain ends and is dependent on molecular weight.

2.2.1.1. Introduction to Rubber Elasticity

The phenomenon of rubberlike elasticity, (the ability of materials to recover their original shape after being subjected to deformation of several hundred percent) is a fundamental property of rubber which gives these materials their commercial application.

The starting point for understanding such elastic behaviour in rubber is the kinetic theory of rubber like elasticity which has its origin in 19th century experimental observations of Gough and Joule that rubber held in tension under a constant load contracts on heating, (increases its modulus) and gives out heat when stretched (Mark, 1992; Treloar, 1975). This is in contrast to other materials where modulus is reduced with an increase in temperature. These early experiments gave some insight into the thermodynamics of rubber elasticity.

2.2.1.2. Thermo-Dynamic Aspects of Rubberlike Elasticity

According to the first and the second laws of thermodynamics the work done in stretching rubber at constant volume and pressure (W) is made up of an internal energy term (U) and a entropy term (S) (Treloar, 1975; Hamed, 1994; Mark, 1992).

$$dW = dU - TdS \qquad (2.3)$$

Deformation is associated with extension of polymer chains and a reduction in entropy. In the development of this model it is assumed that internal energy accompanying deformation is negligible, that rubberlike elasticity is independent of molecular interactions, that viscous effects have no effect and that network chain end to end distances follow a Gaussian distribution function. In the derivation of the statistical equation of rubber elasticity it is assumed that elasticity is primarily entropic in origin and that the retractive force on extension is caused by the system trying to attain its maximum entropy of the relaxed state.

According to this model the entropy of a single chain, (s) is related to its dimensions and structure. Central to the elastic theory is the 'freely jointed chain model' representation of a rubber molecule. The freely jointed chain model assumes rubber molecules to be constructed of a large number, (n) links of fixed length, (l), the links being free to rotate relative to their anchor points.

2.2.1.3. Entropy of a Single Chain

From Boltzman's principles of statistical thermodynamics, which describe the path of a diffusing gas molecule, the entropy of a single chain is proportional to the logarithm of the number of conformations available to the chain, such that,

$$s = k \ln \Omega \qquad (2.4)$$

where, k is Boltzman's constant and Ω in this treatment represents the number of possible chain conformations.

For a freely jointed chain with one end fixed at the origin the free chain end is described by the coordinates (x, y, z) and the mean square end to end distance r^2 is described by equation 2.5.

$$r^2 = x^2 + y^2 + z^2 \qquad (2.5)$$

In statistical treatment of polymer chain length it is assumed that network chain length follows the Gaussian probability density distribution function 2.6a. Since the

entropy of the freely jointed chain is proportional to the logarithm of the number of chain conformations equation 2.6a is reduced to 2.6b.

$$W(x, y, z) = (\beta/\pi^{1/2})^3 \exp(-\beta^2 r^2) \qquad (2.6a)$$

$$s = c - k\beta^2 r^2 \qquad (2.6b)$$

where, c is a constant and $\beta^2 = 3/(2nl^2)$.

The entropy change of a single chain upon stretching, (Δs) by λ is obtained by subtracting the entropy of the relaxed chain from that of the equivalent extended chain.

$$\Delta s = -k\beta^2[(\lambda_1^2-1)x^2 + (\lambda_2^2-1)y^2 + (\lambda_3^2-1)z^2] \qquad (2.7)$$

where, λ_1, λ_2 and λ_3 are the extension ratios in the x, y and z directions respectively.

2.2.1.4. Entropy of a Network

The total entropy change on stressing a network unit volume of N number of chains ΔS to (dx, dy, dz) is obtained by summing the entropy changes of all chains.

$$\Delta S = -1/3\ kN\beta^2 r^2 (\lambda_1^2 + \lambda_2^2 + \lambda_3^3 - 3) \qquad (2.8)$$

Since $r^2 = 3/2\ \beta^2$,

$$\Delta S = -1/2Nk (\lambda_1^2 + \lambda_2^2 + \lambda_3^2 - 3) \qquad (2.9)$$

In simple unidirectional elongation of a rubber network λ_2 and λ_3 are expressed in terms of λ_1 following an assumption that rubber deforms at constant volume, (V).

$$V = x\ y\ z = \lambda_1 x\ \lambda_2 y\ \lambda_3 z \qquad (2.10)$$

Therefore,

$$\lambda_1\lambda_2\lambda_3 = 1 \qquad (2.11a)$$

and,

$$\lambda_2 = \lambda_3 = \lambda_1^{1/2} \qquad (2.11b)$$

Substitution of terms from equation 2.11b into 2.9 gives equation 2.12.

$$\Delta S = -Nk/2[\lambda^2 + (2/\lambda) - 3] \qquad (2.12)$$

The elastic retractive force per unit area in tension, σ is the stored strain energy with respect to λ and is thus obtained by differentiating equation 2.12. The equation for compression is shown in the following section 2.2.1.5.

$$\sigma = (dW/dl) = NkT(\lambda - \lambda^{-2}) \qquad (2.13)$$

In many applications the constant NkT is written as $2C_1$. It was shown in equations 2.1 and 2.2 that the number of network chains per unit volume N is simply related to the average molecular weight between crosslinks.

$$NkT = \rho RT[M_c]^{-1} = 2C_1 \qquad (2.14)$$

2.2.1.5. Swollen Network Response to Applied Stress

Experimentally the statistical model is obeyed only under conditions of high swelling, in the region of V_r (volume fraction of rubber in the swollen system) 0.2 and moderate extension, ($\lambda \leq 2$) (Mark, 1982). This is thought to be because swelling causes separation of polymer chains leading to a reduction in chain interactions and a reduction in chain entanglements. The good agreement between experimental data and elastic theory exhibited by swollen networks has made this an important technique for determination of physical crosslink density (Brown, Porter and Thomas, 1985; Mark, 1982; Melley and Stuckey, 1970).

For swollen networks, in tension the statistical equation is modified by the inclusion of a $V_r^{-1/3}$ term to allow for the reduction in the number of network chains.

$$\sigma = 2(\lambda - \lambda^{-2})C_1 V_r^{-1/3} \qquad (2.15)$$

In compression equation 2.15 transforms to equation 2.16.

$$\sigma = 2(\lambda^{-2} - \lambda)C_1 V_r^{-1/3} \qquad (2.16)$$

2.2.1.6. Mooney-Rivlin Equation

Experimentally the behaviour of unswollen, (dry) rubber vulcanizates deviates from the statistical model (Hamed, 1994; Brown *et al.*, 1985). In the best known correction to experimental data Mooney-Rivlin quantified the extent of deviation by inserting an empirical C_2 term into the statistical equation. Such that,

$$\sigma = 2(\lambda-\lambda^{-2})\,(C_1+C_2\lambda^{-1}) \qquad (2.17)$$

Equation 2.17 shows good agreement with experimental stress-strain data at moderate extensions, (up to approximately $\lambda = 2$).

There have been many attempts at relating the C_2 parameter to specific molecular structures in rubber vulcanizates (Mullins and Thomas, 1963). These attempts have met with limited success and the origin of the C_2 term is still unclear. It is however well known that the C_2 parameter is reduced with increased swelling. Its value is effectively zero when rubber networks are swollen to V_r in the region of 0.2 or less.

The semi-empirical Mooney-Rivlin model has been applied to a range of rubber vulcanizates, and is frequently used for determination of physical crosslink density. Detailed study into the application of the Mooney-Rivlin equation to tensile data for C_1 determination has however highlighted practical uncertainties associated with the use of this technique. Campbell, Chapman, Goodchild and Fulton (1992) have reported that with an increase in test speed materials stiffen and C_1 increases. Distortion of sample in the region of the sample grips introduces uncertainties on sample length.

2.2.1.7. Swelling Behaviour of Networks

Experimentally it is observed that crosslinked networks absorb solvent and swell to equilibrium when immersed in thermodynamically good solvents. Fundamental understanding of such swelling behaviour is largely based on the work of Flory (1953). The treatment of Flory is based on the thermodynamics of solutions in which the free energy of mixing, ΔF_m is related to the enthalpy change, ΔH_m and entropy change, ΔS_m.

At equilibrium swelling $\Delta F_m = 0$ and the classical Flory-Rehner equation is obeyed.

$$-\ln[(1-V_r)+V_r+\chi V_r^2] = V_oN(V_r^{1/3}-V_r/2) \qquad (2.18)$$

In equation 2.18 the left hand term represents ΔH_m and the right hand term ΔS_m, V_o is the molar volume of swelling liquid and χ is a dimensionless parameter which is characteristic of polymer solvent interaction.

In measurement of crosslink density the value of χ, (which is known to change with a change in polymer and crosslink structure) is obtained by substituting for N, values obtained by an independent method of crosslink density determination, (such as stress-strain measurement). This need for an accurate value of χ is the major obstacle to wider application of equilibrium swelling in crosslink density determination, particularly for chemically probed samples where its value is known to change with probing (Saville and Watson, 1967).

2.2.1.8. Summary on Techniques of Crosslink Structure Determination

Application of the techniques of crosslink determination reviewed in preceeding sections is considered below.

Compression testing of swollen samples was thought to be the most suitable technique for determination of crosslink density in our samples because of its speed, applicability to low modulus samples and ability to study small samples (thickness 1 mm and area 16 mm^2). Another advantage is the reported improved approximation to the statistical model due to separation of network chains by solvent (Mark, 1982).

Tensile testing, and application of the Mooney-Rivlin equation was discounted due to experimental errors caused by sample deformation in the region of sample grips and dynamic effects (Campbell *et al.*, 1992). It was thought that the error will be significant for low modulus samples used in this study.

The Flory-Rehner technique was considered inappropriate because of the need for an accurate value of χ. This problem is particularly relevant to crosslink determination of probed samples because χ is known to change following probing of vulcanizates by the type of probe treatments used in this study (Saville and Watson, 1967).

2.2.2. CHEMISTRY OF VULCANIZATION

2.2.2.1. Introduction to Sulphur Based Vulcanization

The discovery of sulphur crosslinking of natural rubber, (caused by the insertion of sulphur between reactive sites) in the 19th century is credited to Goodyear of the U.S. and Hancock of England (Krejsa and Koenig, 1993a). Original vulcanization systems based on heating rubber with large additions of sulphur, were later modified by addition of metal oxides such as magnesium oxide and zinc oxide together with reductions in the concentration of sulphur. Organic accelerators were introduced into vulcanization systems at the beginning of the 20th century and the use of carboxylic acid to improve accelerator efficiency was introduced soon afterwards.

The range of chemical structures introduced into N.B.R. by heating in the presence of sulphur, as part of a conventional vulcanization system are illustrated in figure 2.1 (Lee and Morrell, 1973).

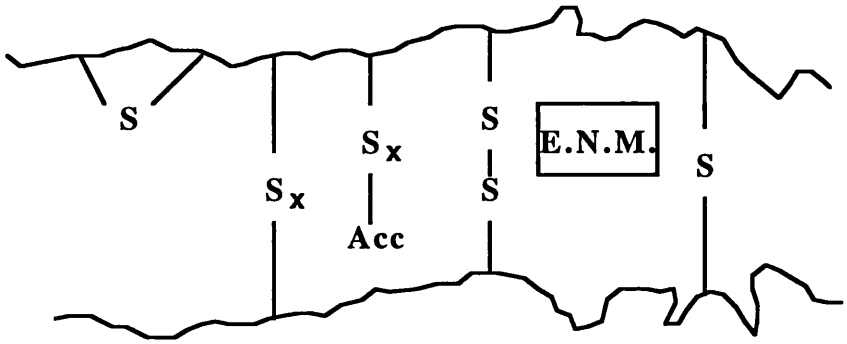

FIGURE 2.1. Simplified representation of a sulphur cured network, E.N.M.- extra network material; x = 3-6.

2.2.2.2. Vulcanization System

Commercial sulphur based N.B.R. vulcanization systems usually contain elemental sulphur, (which exists in the form of S_8 rings) or sulphur donor, zinc oxide, carboxylic acids and organic accelerators (Hertz, 1984).

In N.B.R., magnesium carbonate coated grades of elemental sulphur (typically 2.0 % $MgCO_3$ coated) are normally used because dispersion of elemental sulphur is found to be unsatisfactory (Bhattacharjee *et al.*, 1993). Sulphur dispersion in N.B.R. is further improved by adding sulphur at the beginning of mixing operations. The level of sulphur addition is highly variable within the range 0 phr to 1.5 phr (Zachoval and Brajko, 1989; Kotani and Teramoto, 1980). Addition levels above 1.5 phr are primarily employed in room temperature vulcanization systems.

Accelerators, (organothio nitrogen compounds) may be dithiocarbamate, thiuram, mercaptobenzothiazole, amine and sulphenamide type (Krejsa and Koenig, 1993a). The common feature of all these species is their ability to act as electron donors and acceptors. Usual addition levels fall within the range 0.4-5.0 phr.

Accelerator type, its addition level and accelerator:sulphur ratio have a strong influence on crosslink structure (Lee and Morrell, 1973). The effect of accelerator:sulphur ratio on crosslink structure is illustrated by considering the Moore efficiency parameter, E, (defined as the number of sulphur atoms per crosslink). A so called E.V. (efficient vulcanization) system comprising 3.0 phr tertamethyl thiuram disulphide (T.M.T.D.) and 0.2 phr sulphur is reported to have an E value of 1.0 whereas a system comprising 1.0 phr mercaptobenzothiazole, (M.B.T.) 0.25 phr diphenyl guanidine, (D.P.G.) and 1.5 phr sulphur is reported to have an E value of 3.5.

Zinc oxide and stearic acid are added as activators. The activating properties of zinc oxide, have been attributed to the ability of zinc to react with accelerator species. Zinc-accelerator salts are rendered soluble through coordination with added carboxylic acids and amines (Hertz, 1984). The addition of zinc oxide is usually 5 phr or 3 phr (Ridland and Pfisterer, 1983).

Carboxylic acids consist of a polar head which is capable of forming covalent and coordinate bonds and a non polar alkyl tail which makes the component soluble in rubber. Carboxylic acid, usually stearic or lauric acid is generally added at 0.5-1.0 phr.

2.2.2.3. Sulphur Only Vulcanization

Unaccelerated sulphur vulcanization is the oldest vulcanization system for rubber and as such it has been the system most extensively studied. This vulcanization system, although rarely used, forms the basis for understanding the chemistry of other

systems with commercial relevance. The bulk of work into the study of sulphur only vulcanization was undertaken by researchers working under the direction of Moore at the laboratories of M.R.P.R.A. (Malaysian Rubber Producers' Research Association) in the late 50's and early 60's (Bateman, Moore, Porter and Saville, 1963).

Much of this work studied the reaction of sulphur with low molecular weight compounds such as 2,6 dimethyl octadiene, 2-methyl-2-pentene and cyclohexene. The main products of these reactions are poly-sulphides of the form $2[RH_2]S_x$, x reducing with heating time to a limiting value of 1-2. Poly-sulphide reduction is accompanied by an increase in zinc sulphide, thiols and various sulphurated functional groups. These general findings have since been shown to be relevant to accelerated sulphur vulcanization systems (Lautenschlaeger, 1977).

The precise mechanism of sulphur only vulcanization, whether polar or free radical, has received considerable attention in published literature (Benerjee, 1989). Conflicting findings and the ability of the S_8 ring to undergo homolytic and heterolytic ring opening reactions have prevented unequivocal determination of the vulcanization pathway. Judging by the complexity and variety of reactions which occur during sulphur based vulcanization it seems reasonable to assume that both polar and free radical reactions occur. A summary of such work by Krejsa and Koening (1993a) concludes that the vulcanization system and to a lesser extent the base polymer determine the polar or radical nature of the vulcanization reactions. T.M.T.D. based systems react by a radical or mixed radical/polar mechanism while vulcanization in the presence of M.B.T., sulphur, zinc oxide and stearic acid proceeds by a mixed polar/radical or polar pathway.

2.2.2.3.1. Free Radical Reactions

The observation that homolytic cleavage of poly-sulphides occurs in the region of practical vulcanization temperatures to give persulphenyl radicals ($RS_{a}\cdot$) is used to support the free radical mechanism of sulphur only vulcanization (Parks, Parker and Chapman, 1971). Persulphenyl radicals are thought capable of both hydrogen abstraction and addition to a double bond. According to Chapman and Porter (1988), Markovnikov type addition of thiols to double bonds is also known to occur particularly in the presence of acidic protons. Reaction scheme III, published by Chapman and Porter (1988) summarises the postulated free radical reactions in sulphur only vulcanization.

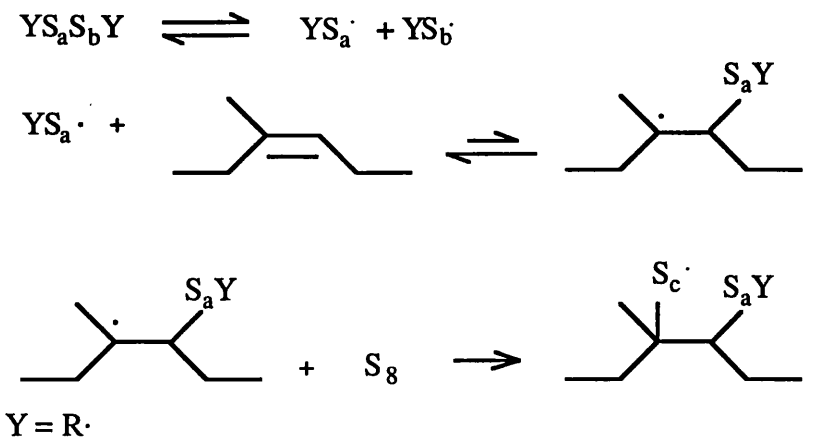

Y = R·

IIIa.

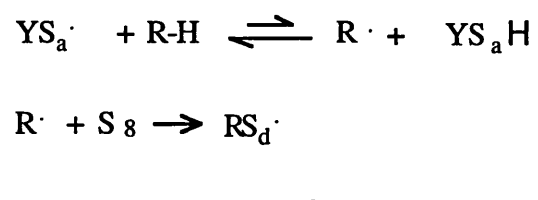

IIIb.

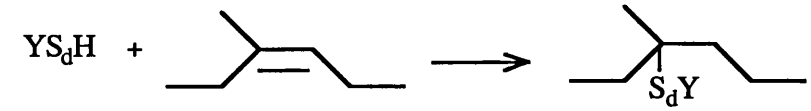

R· =

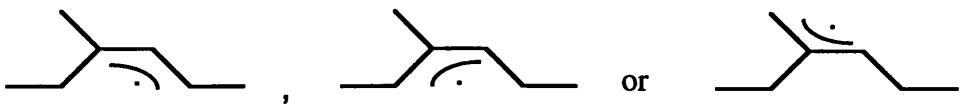

IIIc.

2.2.2.3.2. Polar Reactions

A polar pathway which is consistent with experimental observations of the reaction of sulphur with model olefins was published by Bateman *et al.* (1963), recently reviewed by Krejsa and Koenig (1993a) and also by Chapman and Porter

(1988). The polar mechanism involves heterolytic splitting of S_8 or poly-sulphide crosslinks into persulphonium cation, YS_a+ and persulphenyl anion YS_a-. Such heterolytic splitting occurs readily in the presence of nucleophiles or electrofiles. The postulated polar reactions of these species with double bonds are illustrated in reaction scheme IV.

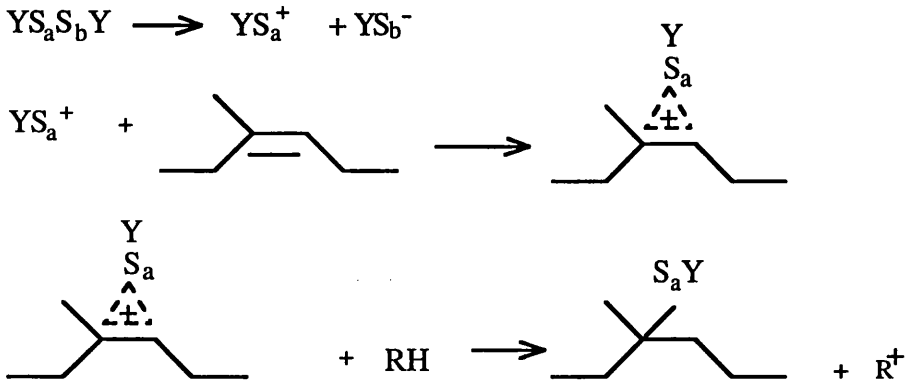

IVa.

$R^+ + S_8 \rightarrow RS_a^+$

$RS_a^+ + YS_b^- \longrightarrow RS_aS_bY$

$R^+ =$

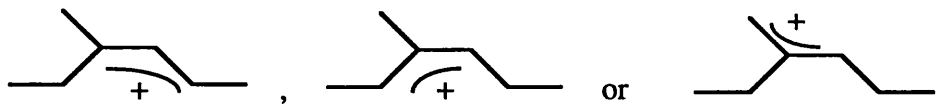

$Y = R \text{ or } RH_2$

IVb.

The site of crosslink attachment is thought to be primarily at the carbon in the allylic or tertiary position. The bond dissociation energy of the allylic hydrogen (355.6 $kJ.mole^{-1}$) is significantly lower than the bond dissociation energy of tertiary, secondary, primary and vinylic hydrogen (Hertz, 1984).

2.2.2.4. Accelerated Sulphur Vulcanization

Basic research into the chemistry of accelerated sulphur vulcanization of N.B.R. appears to have received little attention, however the mechanism of accelerated sulphur vulcanization of other diene rubbers has been widely reported. The interpretation of Bateman *et al.* (1963) on the reaction sequence of accelerated sulphur vulcanization of diene rubbers first published in the early sixties is universally accepted and has been reproduced in recent reviews on the subject (Krejsa and Koenig, 1993a; Chapman and Porter, 1988). An outline of the accepted mechanism of accelerated sulphur vulcanization is shown in figure 2.2.

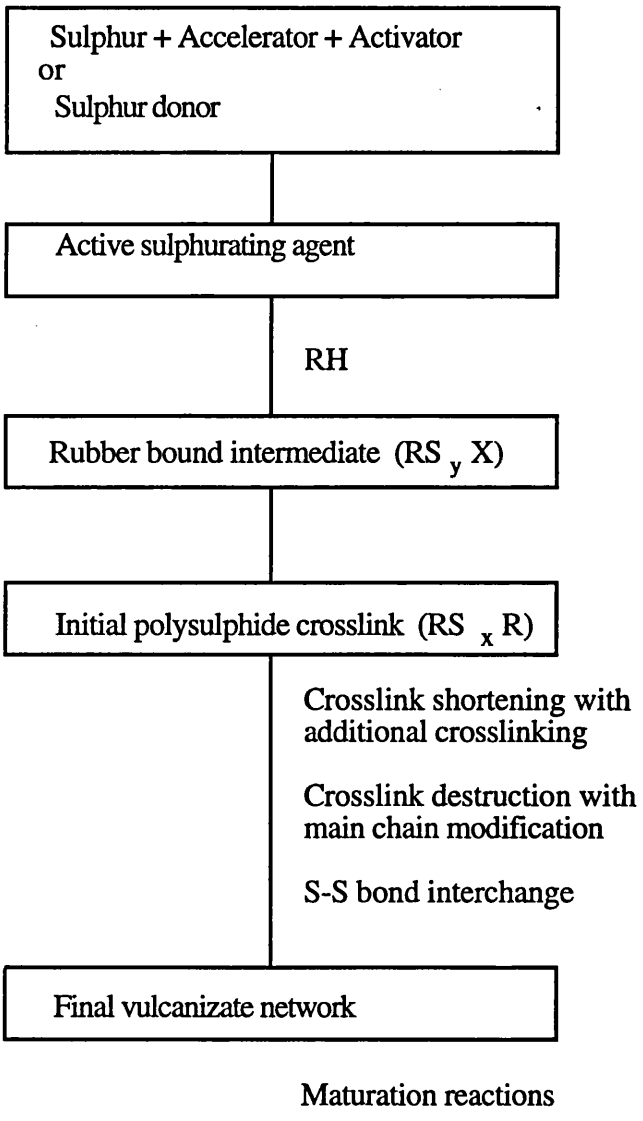

FIGURE 2.2. Reaction scheme for accelerated sulphur vulcanization.

2.2.2.4.1. The Nature of the Active Sulphurating Agent

During the vulcanization induction time of accelerated sulphur systems, sulphur and activators react to form zinc stearate and a variety of accelerator-zinc complexes (Butler and Freakley, 1992). In cyclohexyl benzothiazole sulphenamide, (C.B.S.) based systems the initial product is mercaptobenzothiazole, (M.B.T.). M.B.T. reacts further with C.B.S. to produce mercaptobenzothiazyl disulphide, (M.B.T.S.) and free amine. In M.B.T. accelerated N.R. sulphur compounds it is reported that there is a rapid increase in the concentration of soluble zinc species during the vulcanization induction period (Krejsa and Koenig, 1993a). This soluble zinc accelerator complex may be the active sulphurating agent. The concentration of soluble zinc complex reduces as vulcanization proceeds as does the concentration of unreacted accelerator and free sulphur.

There is contradictory evidence which suggests that the zinc-accelerator complex is not the active sulphurating agent. For example it has been reported that accelerators, such as tetramethyl thiuram disulphide (T.M.T.D.), tetramethyl thiuram mono-sulphide (T.M.T.M) and M.B.T.S. are essentially unreactive towards zinc oxide, zinc stearate and sulphur at practical vulcanization temperatures (Kruger and Mc Gill, 1991a; 1991b). Further studies of sulphur (9.46 phr) and T.M.T.D. (8.86 phr) interactions in cis-1,4-polyisoprene in the absence of zinc oxide showed that 30 % of T.M.T.D. became bound to the rubber after heating in D.S.C. to 143.2°C (Kruger and Mc Gill, 1992a). That zinc oxide is not required for the formation of crosslinks is powerful evidence for the postulate that zinc is not involved in the formation of the active sulphurating agent. The formation of rubber bound intermediates is slowed down however in the absence of zinc.

The situation is further complicated by observations that some accelerators such as M.B.T. form zinc complexes with zinc ion while others such as M.B.T.S. do not (Krejsa and Koenig, 1993a).

This type of conflicting experimental evidence has caused strong disagreement on the role of zinc in the formation of the active sulphurating agent. The involvement of zinc in the sulphurating agent appears to be more acceptable however because it explains the catalytic effect of zinc oxide, amines and carboxylic acids on vulcanization. Furthermore Chapman and Porter (1988) point out that zinc accelerator thiolate complexes have been observed to udergo reversible exchange with poly-sulphides and are capable of substituting sulphur for allylic hydrogen.

2.2.2.4.2. Crosslink Formation

In accelerated sulphur vulcanization there is sparse evidence on the mechanism of reaction between the active sulphurating agent and the rubber. It is thought however that the mechanism of accelerated sulphur vulcanization has many similarities with the mechanism of sulphur-only vulcanization. Rubber bound pendant groups consisting of poly-sulphidic sulphur and an accelerator fragment (R-S_x-Acc.) are undoubtedly the precursors of crosslinks (Rana and Koenig, 1993; Morrison and Ported, 1984; Parks *et al.*, 1971). The concentration of such groups increases during the initial part of vulcanization and falls rapidly as the reaction proceeds further. Accelerator and free sulphur becomes quickly bound to the network in the form of pendant groups. In C.B.S. accelerated sulphur based polybutadiene systems it has been reported that all accelerator is combined with the polymer at the end of the vulcanization process (Skinner, 1972).

Crosslinks are formed either by reaction of a pendant group with a second rubber molecule or alternatively through disproportionation with a rubber bound intermediate on a neighbouring molecule (Hertz, 1984). Cis-trans isomerisation occurs in the early stages of vulcanization during the reaction of the active sulphurating agent with the rubber hydrocarbon (Krejsa and Koenig, 1993b; Devlin, 1986). Cis-trans isomerisation is caused by double bond rearrangement. This is shown in reaction schemes III and IV. The concentration of sulphurated carbon atoms is related to the concentration of compounded-in sulphur and while free uncombined sulphur is present in the network the crosslinks formed are predominantly poly-sulphidic.

2.2.2.4.3. Crosslink Maturation

At advanced stages of cure almost all sulphur is present in crosslink structures, a significant concentration of such crosslinks being poly-sulphidic (Krejsa and Koenig, 1993b). Further heating is accompanied by maturation of poly-sulphide crosslinks. Maturation of poly-sulphide crosslinks involves mainly desulphuration of crosslinks to mono-sulphides. Published results show that maturation is not accompanied by any change in total crosslink density (Lee and Morrell, 1973). Additional crosslinks are therefore not formed during desulphurisation. Desulphurisation is accompanied by formation of cyclic sulphides, (this is shown by an increase in the Moore efficiency parameter) and formation of zinc-sulphur species, such as zinc sulphide (Deuri and Bhowmick, 1987).

Desulphurisation of poly-sulphide crosslinks is accelerated by zinc-accelerator complexes which may be present in vulcanized networks after vulcanization (Cunneen and Russel, 1969). The mechanism of equilibrium exchange reactions between poly-sulphide crosslinks and Zn-S_x-Acc complexes, proposed by Layer (1991) to explain recuring of vulcanizates is illustrated in reaction scheme V.

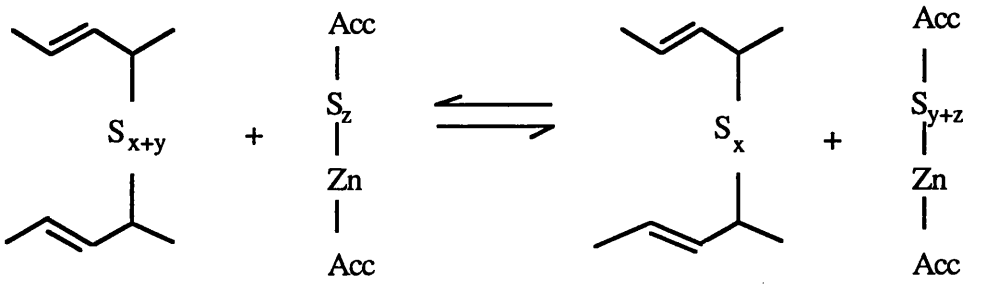

V.

The equilibrium of the exchange reaction in reaction scheme V is shifted to the right with a higher accelerator:sulphur ratio leading to more mono-sulphide crosslinks. According to this representation mono-sulphides form during extended vulcanization due to a reduction in the number of sulphur atoms in the complex. Study of desulphurisation of poly-sulphide crosslinks in 2-methyl-2-pentene based compounds shows that the position of crosslink attachment has an influence on the rate of desulphurisation (Morrison and Porter, 1984). Desulphurisation of pendant groups is thought to occur by a similar mechanism.

Poly-sulphide crosslinks also decompose thermally at temperatures in the region of 130°C, to form cyclic sulphide, conjugate diene and triene structures, and zinc sulphide (Kruger and McGill, 1992b). Mono-sulphide crosslinks are unlikely to undergo thermal decomposition at temperatures below 180°C (Morrison and Porter, 1984). The concentration and nature of the zinc-accelerator-thiolate complex influences the ratio of crosslink desulphurisation to crosslink decomposition, since such residues catalyse sulphur exchange reactions.

Amine species whose role in solubilising the zinc ion is well documented, has been shown to be capable of causing heterolytic cleavage of S_8 rings and poly-sulphides (Kruger and McGill, 1992b). The mechanism of this reaction, (reaction scheme VI) has been illustrated by Mayer, (1977).

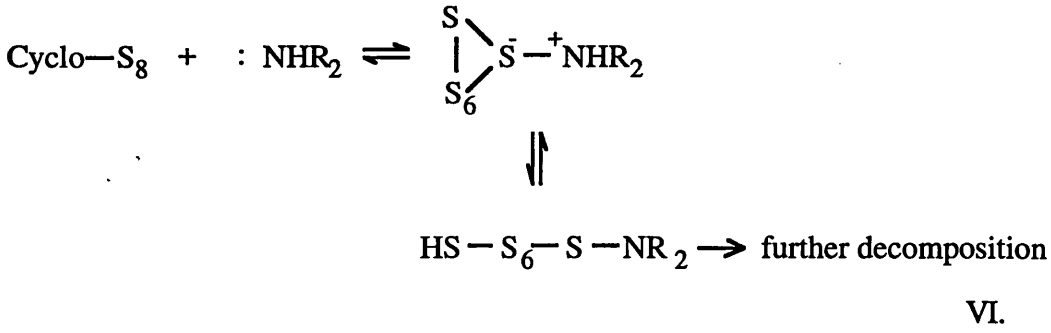

VI.

Other work suggets that amines do not catalyse poly-sulphide decomposition. Such work has recently been reported by Engels (1994) who found no difference in the poly-sulphide concentration of aged N.R. networks, containing p-phenylene diamine addition at 2 phr and 0 phr.

In N.B.R. the study of accelerated sulphur vulcanization has not received much attention. Lee and Morrell (1973) have however shown that the mechanism of crosslink maturation in sulphur crosslinked N.B.R. networks is similar to other rubbers. During N.B.R. vulcanization, compounded with 1 phr M.B.T., 0.25 phr D.P.G. and 1.5 phr sulphur in combination with zinc oxide and stearic acid, crosslinks are exclusively poly-sulphidic up to 15 minutes heating at 150°C. With further heating, up to 700 minutes at 150°C, total crosslink density is little affected. During this period the concentration of poly-suphide crosslinks is reduced to approximately 10 % of total crosslink density, while the concentration of mono-sulphide and di-sulphide crosslinks rises to 70 % and 20 % of total crosslink density, respectively. Crosslink shortening is accompanied by an increase in the concentration of zinc stearate, zinc oxide and zinc sulphide.

It has been suggested by Kirkham (1978) that in N.B.R. crosslink attachment is at the methylene allylic carbon of a butadiene unit adjacent to a cyanide group.

2.2.3. DETERMINATION OF CROSSLINK STRUCTURE

This study used established techniques of crosslink characterisation, based on chemical probe treatment in conjunction with measurement of crosslink density. Chemical probes are chemical reagents which are known to react with specific crosslink structures under controlled conditions. The main requirements for such chemical probes are high selectivity, (ability to react with specific structures) and solubility in the rubber network. When the reaction between chemical probe and crosslink causes crosslink

cleavage measurement of crosslink density before and subsequent to chemical treatment allows determination of the concentration of reactive crosslinks.

Previous development and use of chemical probes has enabled accurate determination of the concentration of mono-sulphide, di-sulphide and poly-sulphide crosslink structures in N.B.R. networks (Sims, 1988; Lee and Morrel, 1973).

Recently a valuable contribution to the determination of crosslink structure has also been made by the development of ^{13}C N.M.R. This technique, has provided useful information on the point of attachment of sulphur crosslinks in N.R. and B.R. networks but does not appear to have been applied to N.B.R..

2.2.3.1. Methyl Iodide Treatment

The use of methyl iodide in rubber network characterisation was first introduced by Meyer and Hohenemser (1935) in an attempt to estimate the concentration of mono-sulphide crosslinks in rubber.

The reaction between methyl iodide and organic sulphides is illustrated in reaction scheme VII.

$$RSR + 3[CH_3I] \longrightarrow 2[RI] + [(CH_3)S]^+ I^- \qquad \text{VII.}$$

Reaction of methyl iodide with n-propyl mono-sulphide, n-propyl di-sulphide and n-propyl mercaptide compounds was later studied in great detail by Selker and Kemp (1944). The reaction of methyl iodide and alkyl mono-sulphides could be driven to completion in 3 days at 24°C. The reaction with alkyl di-sulphides and alkyl mercaptans was found to be much slower while direct C-C bonds were found to be inert to methyl iodide treatment. The reaction was also demonstrated in sulphur cured vulcanizates of N.R. and S.B.R..

The finding of Selker and Kemp (1944) that allylic sulphide is more reactive to methyl iodide than other forms of sulphides was subsequently shown to be erroneous (Saville and Watson, 1967). It is now accepted that use of methyl iodide does not allow differentiation between allylic sulphides, cyclic mono-suphides and other sulphides.

Treatment with methyl iodide at 70°C in the absence of air for 10 days has been used successfully in N.B.R. vulcanizates, (free from di-sulphide and poly-sulphide crosslinks) to differentiate between mono-sulphide and C-C crosslinks (Lee and Morrell, 1973).

2.2.3.2. Thol-Amine Treatment

The use of thiol amine reagents was first suggested by Campbell and Saville (1967). Since then the thiol-amine probe reagents have been extensively applied to the study of crosslink structure particularly in natural rubber vulcanizates (Brown *et al.*, 1985; Brajko, Duchacek, Tauc and Tumova, 1980; Doyle, Humphreys and Russel, 1971).

The mechanism of thiol-amine reaction, (reaction scheme VIII) with di-sulphide and poly-sulphide crosslinks was illustrated by Saville and Watson (1967). Alkenethios react with di-sulphide and poly-sulphide crosslinks through a nucleophilic displacement reaction. The C-S bond is apparently unreactive to nucleophilic attack because of the difficulty of accomodating the unpaired electrons in the *p* orbitals of the carbon.

Campbell and Saville (1967) achieved cleavage of di-sulphides by using primary thiols, such as hexane-1-thiol at high concentrations and reaction times of 48 hours at room temperature. Cleavage of poly-sulphides only, was made by using secondary thiols such as propane-2-thiol, at reduced concentration and reaction times of 2 hours at room temperature.

$$R'SH + RSSR \rightleftharpoons RSSR' + RSH$$

VIII.

In reaction scheme VIII, the excess of thiol in comparison with crosslinks ensures that the equilibrium is pushed far to the right. Piperidine catalyses the reaction through the formation of a piperidinium propane-2-thiolate ion pair.

In an appendix to the paper by Campbell and Saville (1967) on 'current principles and practices in elucidating structure in sulphur-vulcanized elastomers' the

authors defended their work and expressed their belief that these probes are suitable for network characterisation of networks based on rubbers other than N.R.. Since then these probes have indeed been applied to many other rubber materials but perhaps unwisely the experimental conditions originally employed to characterise N.R. network structure have often been used in other rubbers.

2.2.3.2.1. Hexane-1-thiol (1M) in Piperidine Treatment

In the original paper of Campbell and Saville (1967) a solution of hexane-1-thiol (1M) in piperidine was shown to cleave bis-(2-methylpent-2-enyl) di-sulphide, bis-(1,3-dimethylbut-2-enyl) di-sulphide, di-isopropyl di-sulphide and t-butyl 1,3 dimethylbut-2-enyl di-sulphide after 20 hours at 25°C.

The application of these probes in the resolution of di-sulphide and poly-sulphide crosslink structures in N.R. networks was illustrated in the same paper. The authors recommended a reaction time of 48 hours at 25°C for hexane-1-thiol (1M) in piperidine treatment for 1 mm thick samples.

Hexane-1-thiol (1M) in piperidine treatment of N.B.R. has been reported on by Lee and Morrell (1973). In this study reaction conditions were similar to those recommended by Campbell and Saville (1967) however Lee and Morrell used a reaction time of 24 hours. Later work by Sims (1988) on optimising experimental conditions for hexane-1-thiol (1M) treatment of C.B.S. accelerated sulphur based N.B.R. vulcanizates recommended that reaction be carried out at room temperature for 72 hours.

2.2.3.2.2. Propane-2-thiol (0.4M) + Piperidine (0.4M) Treatment

Campbell and Saville (1967) also reported that a solution of propane-2-thiol (0.4M) + piperidine (0.4) in n-heptane cleaves bis-(2-methylpent-2enyl) tri-sulphide and bis-(1,3-dimethylbut-2-enyl) tri-sulphide in less than 1 hour at 25°C. Di-sulphides were not significantly cleaved under these conditions.

Probing vulcanized N.R. samples of thickness 1 mm with propane-2-thiol (0.4M) + piperidine (0.4M) in heptane required pre-swelling to equilibrium in n-heptane prior to probing. This step was necessary to facilitate rapid diffusion of chemical probe into the network.

An early study on structural characterisation of N.B.R. vulcanizates by Lee and Morrel (1973) used a treatment of propane-2-thiol (0.4M) + piperidine (0.4M) in benzene. Benzene was presumably used in preference to heptane because it swells N.B.R. to a greater degree. The reaction time used by Lee and Morrell was 3 hours. Later studies by Sims (1988) reported that a reaction time of 2 hours was more appropriate, to obtain cleavage of di-sulphide and poly-sulphide crosslinks only. The study of Sims used heptane as solvent, however. A reaction time of 2 hours has also been used by Brajko *et al.*, (1980) in chemical probing of N.R. vulcanizates with propane-2-thiol (0.4M) + piperidine (0.4M) in benzene.

2.2.3.3. Compression-Deflection Reticulometer

Compression stress-strain measurement on swollen networks has been previously applied to the study of the physical crosslink density of rubber vulcanizates (Sims, 1988; Melley and Stuckey, 1970). The compression technique is preferred to testing in tension because swollen samples are experimentally more difficult to handle in tension. When using swollen samples, equation 2.16 is written in the form of equation 2.21 to enable calculation of C_1 from compressive strain measurements on swollen samples.

The dimensions of the swollen sample are calculated from knowledge of unswollen dimensions and knowledge of the volume fraction of rubber in the swollen system, (V_r) by assuming isotropic swelling.

$$V_r = (h_o A_o)/(h_s A_s) \qquad (2.19)$$

where, h_o and h_s are the original and swollen heights, respectively while A_o and A_s are the original and swollen areas, respectively.

With isotropic swelling equations 2.20a and 2.20b are observed.

$$h_s = h_o V_r^{-1/3} \qquad (2.20a)$$

$$A_s = A_o V_r^{-2/3} \qquad (2.20b)$$

Compressive strain measurements, ($c = \Delta h_s/h_s$) can be expressed in terms of λ by the relationship $\lambda = 1-c$.

By substituting terms into equation 2.16 equation 2.21 is obtained.

$$C_1 = FV_r^{1/3}/2A_o\{\{1-[\Delta h_s/(h_o V_r^{-1/3})]\}^{-2}-\{1-[\Delta h_s/(h_o V_r^{-1/3})]\}\} \qquad (2.21)$$

Compression measurements on swollen samples were carried out on a Wallace-Smith compression deflection reticulometer. The compression-deflection reticulometer is a modification of a Wallace microhardness tester. It consists of a compression foot and a spindle which carries a load pan, (figure 2.3). The test piece is placed in a sample bath and immersed in the swelling solvent during testing. The vertical movement of the foot relative to the head is sensed by means of a plate attached to the head and is read off a dial gauge. The separation of two capacitor plates, one attached to the head and the other to the spindle, is controlled by the position of the compression foot. When the compression foot is just in contact with the sample the frequencies of the 2 circuits match and a null point is established.

The instrument is operated with a pre-load of 30 grammes this being necessary to overcome surface irregularities and flatten out the sample.

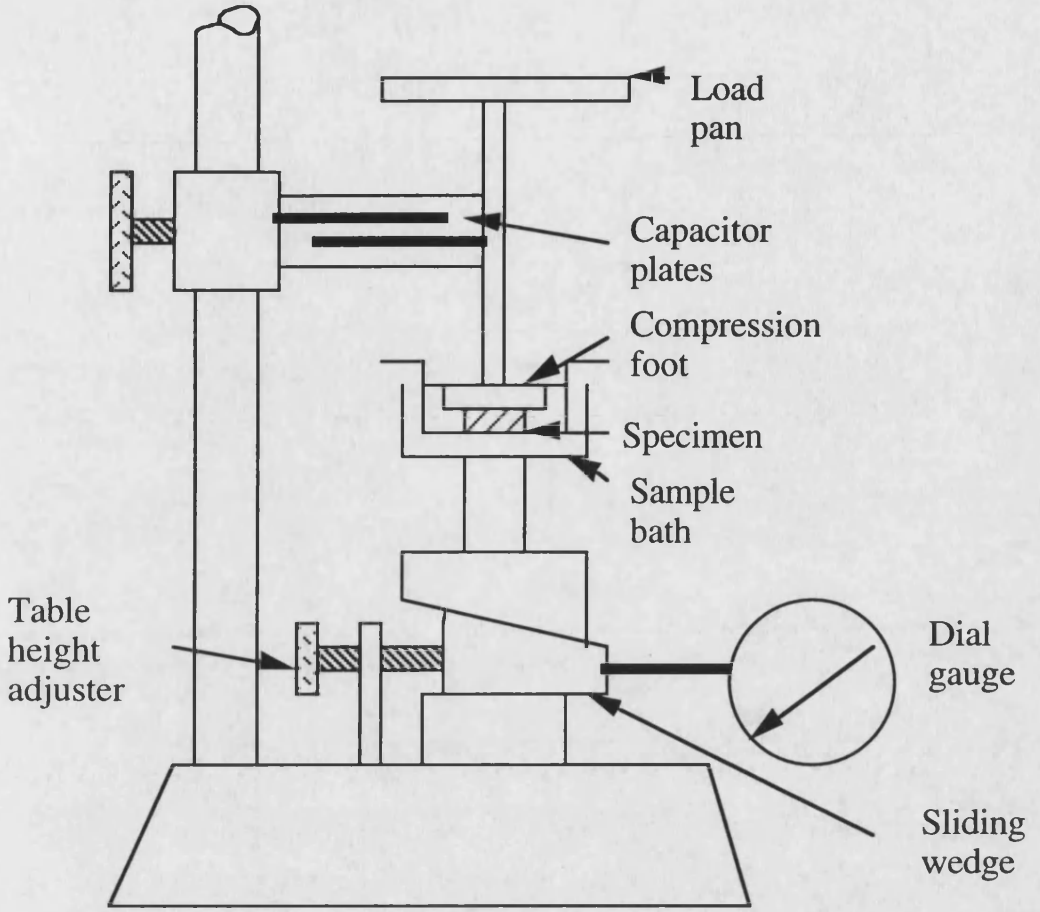

FIGURE 2.3. Schematic diagram of the Wallace-Smith compression-deflection reticulometer.

2.2.3.4. ^{13}C N.M.R. Spectroscopy

^{13}C nuclear magnetic resonance, (^{13}C N.M.R.) uses the magnetic moment displayed by the ^{13}C nuclei, and its ability to exist in two energy states in a magnetic field, to obtain information on its environment. In the standard ^{13}C N.M.R. technique application of an external magnetic field results in alignment of nuclei in line with the magnetic field in the low energy position. A change in alignment, to the high energy position, transverse to the magnetic field is caused by absorption of electromagnetic radiation in the radio frequency range. The frequency required to change the nuclei alignment is the resonance frequency.

The resonance frequency is highly sensitive to environment due to shielding and de-shielding by neighbouring electron donating and electron withdrawing groups, respectively.

The high sensitivity of the ^{13}C nuclei resonance towards changes in the mode of hybridisation and inductive effects has lead to the use of ^{13}C N.M.R. spectroscopy in network characterisation studies of sulphur cured vulcanizates. In sulphur crosslinked networks the resonance assignments of carbon nuclei at the point of crosslink attachment is made by referencing to model compounds. Such assignments have been reported by Krejsa and Koenig (1993b), Rana and Koenig (1993) and Koenig and Patterson (1986). The variability of such assignments is reported to be within ±1 ppm. The frequency assignments of sulphurated methylene groups in B.R. systems, reported by Rana and Koenig (1993) are shown in figure 2.4.

In the study of network structure ^{13}C N.M.R. was originally used with vulcanizates compounded with high levels of sulphur, however more recently the technique has been applied to practical vulcanization systems (Krejsa and Koenig, 1993b; Hoffman and Gronsky, 1992; Hoffman, Gronski, Simon and Wutzer, 1992). The technique has been used to give information on the point of crosslink attachment and the proportion of mono-sulphide and higher sulphide crosslinks. Quantitative measurement of the level of sulphuration and chemical crosslink density in vulcanizates, by integration of N.M.R. peaks has also been reported (Krejsa and Koenig, 1993b; Hoffman *et al.*, 1992; Gronski and Hoffman, 1992).

Most solid state ^{13}C N.M.R. studies into characterisation of network structure have investigated the effect of vulcanization system and vulcanization time in N.R. and B.R.. Characterisation of sulphur crosslinked vulcanizates based on N.B.R. by ^{13}C N.M.R. has not been reported. This may be due to the difficulty of assigning frequency shifts in random co-polymers where there are complications due to differences in ACN-butadiene sequence distribution.

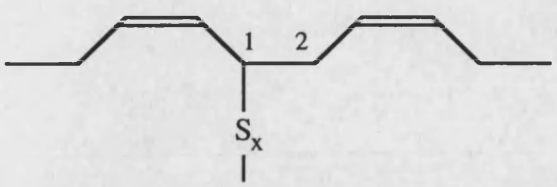

Shift (ppm)

C1=28
$C1S_1R$=44.7
$C1S_aR$=50.6
C1SH=36.7
C2=28
$C2S_1R$=35.2
$C2S_aR$=34.4
C2SH=40.0

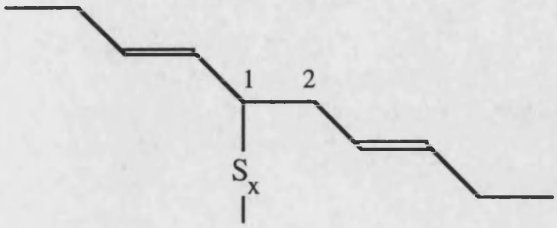

C1=32.4
$C1S_1R$=49.1
$C1S_aR$=55.0
C1SH=41.1
C2=32.4
$C2S_1R$=39.6
$C2S_aR$=38.8
C2SH=44.4

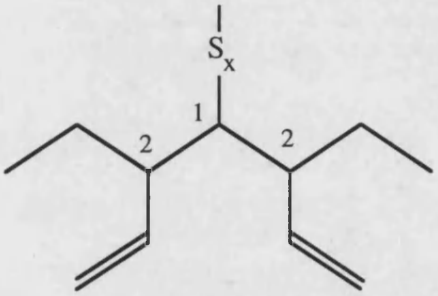

C1=34.4
$C1S_1R$=49.2
$C1S_aR$=57.0
C1SH=43.1
C2=43.7
$C2S_1R$=50.9
$C2S_aR$=52.3
C2SH=55.7

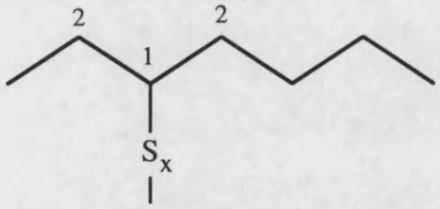

C1=29.1
$C1S_1R$=43.9
$C1S_aR$=51.7
C1SH=37.8
C2=29.1
$C2S_1R$=36.3
$C2S_aR$=35.2
C2SH=41.1

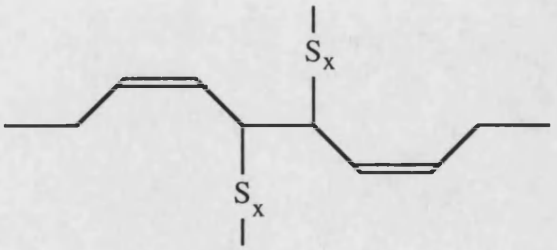

C1=27.6
$C1S_1R$=42.4
$C1S_aR$=51.3
C1SH=36.3

where, CS_1R = mono-sulphide, CS_aR = di- and poly-sulphide, CSH = thiol, x = 1-6.

FIGURE 2.4. Chemical ^{13}C N.M.R. shift assignments of Rana and Koenig (1993) of sulphurated carbons in B.R..

2.2.3.5. Influence of Crosslink Structure on Mechanical Properties

The effect of crosslink density on stress-strain properties and swelling is predicted by elasticity theory and the Flory-Rehner equation, (section 2.2.1).

An increase in the average number of sulphur atoms per crosslink causes an increase in tensile strength and tear strength (Hamed, 1994). This is explained by the ability of poly-sulphide crosslinks to break differentially under applied stress and thereby dissipate local stress concentrations through molecular rearrangement. A brittle fracture at low elongation is likely when chain motions become restricted and energy dissipation becomes more difficult.

Compression set percentage is higher in vulcanizates with a higher number of sulphur atoms per crosslink (Bhowmick and Sadham, 1980). The higher creep and stress relaxation in vulcanizate networks containing higher proportions of di-sulphide and poly-sulphide crosslinks is explained by their lower bond dissociation energy. Kotani and Teramoto (1980) report bond dissociation energies of 115.5 $kJ.mol^{-1}$, 229 $kJ.mol^{-1}$ and 261.6 $kJ.mol^{-1}$ for poly-sulphide, mono-sulphide and C-C crosslinks, respectively.

2.3. OXIDATIVE DEGRADATION

Hoffman (1984) has shown that N.B.R. polymer degrades readily when heated in oxygen at temperatures in the region of 100°C. Oxidation is accompanied by an increase in gel content and a reduction in molecular weight caused by crosslinking and scission, respectively.

2.3.1. OXIDATION OF THE BASE POLYMER

By analogy with the oxidation mechanism of simple olefins it is generally accepted that oxidation of N.B.R. polymer is accurately represented by the free radical chain mechanism, (reaction scheme IX) (Kotani and Teramoto, 1980). Oxidation is initiated by an outside factor such as heat, light, mechanical stress or high energy radiation, (generation of free radicals is very slow without initiation by one of these factors). The free radicals generated react with molecular oxygen to form peroxy radicals. Abstraction of hydrogen by peroxy radicals gives hydroperoxides. Hydroperoxide build up followed by hydroperoxide decomposition to secondary

oxidation products causes oxidation autoacceleration. Thermal analysis of N.B.R. thermo-oxidation shows that peroxide group formation and hydrogen abstraction is strongly exothermic (Slusarski, 1984). Propagation of the process continues with more hydroperoxide being formed. Oxygen absorption accompanies the propagation step (Budrugeac and Segal, 1991). Termination occurs through combination of free radicals. This process is also strongly exothermic.

Initiation

$$RH \xrightarrow{h\nu,\ stress,\ \gamma,\ \beta} R\cdot + H\cdot$$

Propagation

$$R\cdot + O_2 \longrightarrow RO_2\cdot$$
$$RO_2\cdot + RH \longrightarrow ROOH + R\cdot$$

Formation of secondary oxidation products

$$ROOH \longrightarrow RO\cdot + \cdot OH$$
$$2ROOH \longrightarrow RO\cdot + RO_2\cdot + H_2O$$

Termination

$$R\cdot + R\cdot \longrightarrow R\text{-}R$$
$$R\cdot + RO_2 \longrightarrow ROOR$$
$$RO_2\cdot + RO_2\cdot \longrightarrow \text{Non radical products}$$

IX.

In the chain reaction mechanism the rate of hydrogen abstraction by peroxy radicals is the rate determining step. The bond dissociation energies of allylic hydrogen, tertiary hydrogen, secondary hydrogen, primary hydrogen and vinylic hydrogen are stated to be 355.6 kJ.mole^{-1}, 380.7 kJ.mole^{-1}, 395.4 kJ.mole^{-1}, 410.0 kJ.mole^{-1} and 431.0 kJ.mole^{-1}, respectively (Hertz, 1984). In N.B.R. hydrogen abstraction at the point of a 1,2-vinyl branch is particularly favoured since it is tertiary and allylic.

The activating effect of the double bond is supported by experimental results showing that thermo-oxidative stability improves with an increase in combined A C N content (Bhattacherjee *et al.*, 1993). Partial saturation and hydrogenation of N.B.R. also results in improved thermo-oxidative stability (Milner, 1987).

Experimental results showing that N.B.R. has better thermo-oxidative stability than B.R. and N.R. have been associated with the electron withdrawing action of adjacent nitrile groups on the allylic hydrogen (Hoffman, 1984).

During thermo-oxidative degradation, N.B.R. polymer in the absence of added compounding ingredients exhibits a rapid change in mechanical properties. When heated in air at 60°C N.B.R. degrades and becomes extensively crosslinked and almost insoluble within 7 days (Hoffman, 1984). Bhattachajee *et al.* (1993) show crosslinking of N.B.R. during heating in air at temperatures in excess of 100°C to be accompanied by a reduction in viscosity average molecular weight, due to polymer chain scission and an increase in carboxyl and carbonyl structures.

Both crosslinking and chain scission reactions are thought to be associated with the termination step in the free radical chain oxidation process. Crosslink formation is though to occur either through combination of carbon free radicals or through the addition of a carbon free radicals onto vinyl-1,2- butadiene double bonds as shown in reaction scheme X. Evidence for the addition of radicals onto 1,2-double bonds is the reported reduction in 1,2-butadiene double bonds during oxidation of B.R. (Schneider, Doskocilova, Stork and Svoboda, 1993).

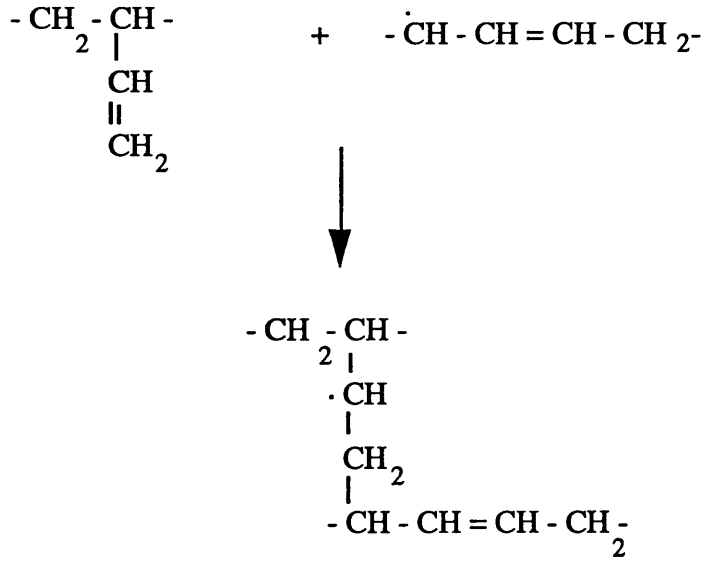

X.

A specific scission mechanism for N.B.R. has not been proposed, however the mechanism may be similar to the proposed scission mechanism for N.R. (reaction scheme XI) (Shelton, 1983). In N.R. scission is thought to occur by cleavage of cyclic

peroxide structures, which are formed by intramolecular addition of peroxy radicals to adjacent double bonds.

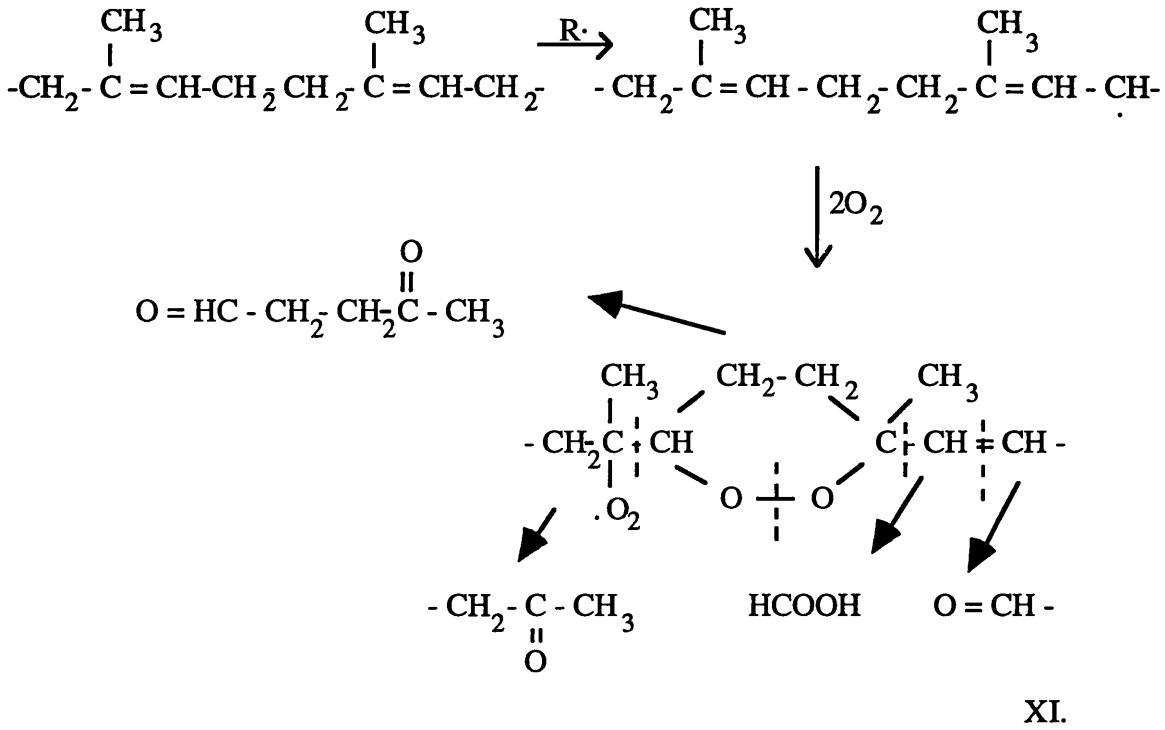

XI.

Until recently it had been thought that the nitrile group did not participate in oxidation within the service temperature of N.B.R. systems (Dunn, 1981), however it is well established that the nitrile group is vulnerable to hydrolysis (Frenkel, *et al.*, 1992). The view that the nitrile group is unreactive during oxidation has recently been challenged by Bhattacherjee, Bhowmick and Avasthi (1991), who have suggested intermolecular reaction of the nitrile group, (-CN) at temperatures in excess of 100°C with a tertiary carbon free radical of a neighbouring ACN unit. This is shown in reaction scheme XII.

The experimental evidence used to support this hypothesis is the observed shift in X.P.S. binding energy of the N_{1s} signal from 400.8 eV before oxidation to 406.0 eV subsequent to oxidation. According to these authors the shift in binding energy is caused by conversion of pendant R_1-CN groups to R_1R_2CNH structures. Infra-red measurements of the concentration of -CN in the samples showed no change with oxidation which suggests that the proposed reaction must be restricted to the first few atomic surface layers.

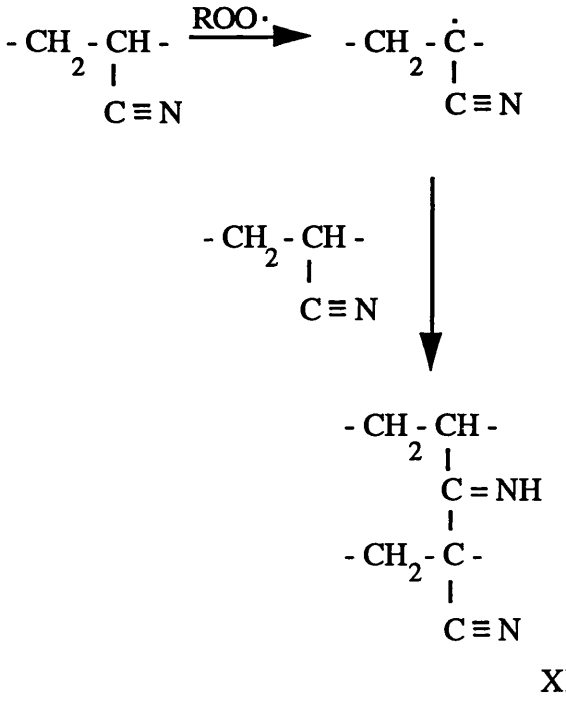

XII.

There is little published information on the effect of molecular microstructure on thermo-oxidation of N.B.R., however in S.B.R. it is reported that sequence distribution affects thermo-oxidative stability (Abu-Zeid, 1986).

2.3.1.1. Metal Catalysed Oxidation

It is generally recognised that metals of variable valency catalyse oxidation by the hydroperoxide decomposition mechanism illustrated in reaction scheme XIII.

$$M^{n+} + ROOH \longrightarrow M^{(n+1)} + RO\cdot + OH^-$$
$$M^{(n+1)} + ROOH \longrightarrow ROO\cdot + H^+ + M^{n+}$$

XIII.

In N.B.R. oxidation the effect of trace metals, which were shown to be present in N.B.R. as trace contaminants, has been studied by Lee, Stacy and Engel (1966a, 1966b). These studies reported on the oxidation induction time and rate of oxygen absorption after 0.1 weight % addition of stearates of caesium, cobalt, copper, iron, lead, manganese, nickel, sodium, tin and zinc.

The results of these studies showed that all stearates, apart from copper stearate and iron stearate act as mild pro-oxidants. The reduction in induction time after addition

of metal stearates, other than copper stearate and iron stearate of 10-20 % was equivalent for 0.1 weight % addition of stearic acid. This implies that these metals have no effect on oxidation of N.B.R. at these concentrations. Lee *et al.*, (1966b) also reported synergistic effects in oxidation catalysis between metal stearates and stearic acid, however they did not postulate as to how synergism occured.

The results of Lee et al. (1966a) show that iron stearate causes a reduction in oxidation induction time of 50 %. This implies that of the transition elements, cobalt, copper, iron, manganese and nickel only iron acts as a pro-oxidant in N.B.R.. Copper stearate acts as a powerful antioxidant resulting in a 300 % increase in oxidation induction time. The antioxidative properties of copper stearate were thought to be associated with the formation of a coordination complex between cupric ions and cyanide groups. These results indicate that the effect of variable valency metals in the oxidation of N.B.R. is not always adequately explained by reaction scheme XIII, possibly due to interaction of metal ions with the cyanide group.

In N.R. it is reported that treatment of the latex by divalent cations, such as $MgCl_2$, MgF_2, $Mg(NO_3)_2$, $MgSO_4$, $CaCl_2$ and $BaCl_2$, causes a reduction in storage hardening (Gan and Ting, 1993). In N.B.R. such chemicals may be present as coagulant residues. Treatment of latex with transition metal ions causes increased degradation (Gan and Ting, 1993).

2.3.2. OXIDATION OF CROSSLINKS

Vulcanizate oxidation is a highly complex chemical process involving simultaneous polymer oxidation, network maturation and network oxidation. Various chemicals which are introduced into rubber to enable vulcanization may act as catalysts or inhibitors to the oxidation process. The sulphur crosslinks introduced during vulcanization are themselves highly oxidisable and may undergo cleavage and interchange reactions. Oxidation products of organic sulphur compounds also exhibit pro-oxidative and anti-oxidative behaviour.

2.3.2.1. Oxidation of Dialkyl Mono-Sulphides

Mono-sulphide crosslinks have the general structure R_1SR_2, where R_1 and R_2 are the alkyl groups (polymer chains). Thermal S-C bond cleavage in simple di-alkyl

mono-sulphides is known to occur by a free radical mechanism, in the region of 170°C, to give a thiyl radical, (RS·) and an alkyl radical, (R·) (Hanthal, 1975; Martin, 1975).

There is little experimental work on the oxidation mechanism of mono-sulphide crosslinks in vulcanizates, however by analogy with low molecular weight compounds it is generally accepted that mono-sulphide crosslinks are rapidly converted to sulphoxides (Colclough, Cunneen and Higgins 1968; Shelton, 1983). The reaction in vulcanizates may be similar to reaction XIV which is utilised in the manufacture of dimethyl sulphoxide (Hanthal, 1975).

At 18°C, $(CH_3)_2S + 1/2\,O_2 \xrightarrow{ROOH} (CH_3)_2SO$ XIV.

The sulphur oxygen bond in sulphoxides is strongly polar and exhibits a large dipole moment. The high electron density on the oxygen induces a partial positive charge on the sulphur which causes a weak activation of the tertiary C-H bond, at the point of crosslink attachment. Due to the strong dipole moment sulphoxides form strong associations with 2 moles of water. Sulphoxides also form strong dipole-dipole complexes with cyanide groups.

2.3.2.2. Oxidation of Dialkyl Di-Sulphides

Di-sulphide bridges, introduced during sulphur vulcanization and also naturally occurring in proteins have the general structure R_1SSR_2. Thermally induced scission of di-sulphides has been reported to occur at temperatures in the region of 130-150°C to give two thiyl radicals (Kruger and Mc Gill, 1992b).

Di-sulphide are oxidised to thiolsulphinate in the presence of hydrogen peroxide (Shelton, 1983). Other oxidation structures, such as sulphonate, sulphenyl sulphone and αdi-sulphone, have also been isolated from the oxidation products of di-sulphides (Field, 1977).

2.3.2.3. Oxidation of Dialkyl Poly-Sulphides

Poly-sulphide crosslinks have the structure $R_1S_{(3-6)}R_2$. Thermal scission of poly-sulphides is highly likely at temperatures in the region of 130-150°C (Cunneen and Russel, 1969). The most important reaction of poly-sulphide crosslinks during heating appears to be crosslink desulphurisation. Crosslink desulphurisation is treated in section 2.2.2.4.3.

There is little published literature on the oxidation of poly-sulphide compounds, however the process is likely to be analogous to oxidation of mono-sulphide and di-sulphide bridges. This view is supported by the synthesis of oxidation compounds of the form $R_1SO_2S_{1-3}SO_2R_2$ (Field, 1977).

2.3.2.4. Oxidation of Crosslinks in Rubber Networks

Many technological studies into thermo-oxidation of N.B.R. have established that vulcanization system plays an important part in optimising ageing resistance (Hoffman, 1985; Dunn, 1984; Coulthard and Gunter, 1977; Lee and Morrell, 1973). However because networks with different crosslink structures are prepared by modification of vulcanization system there is doubt whether reported differences in ageing are always attributable to differences in crosslink structure or differences in antioxidative properties of accelerator complexes. For example the excellent thermo-oxidative stability of thiuram vulcanizing systems in N.B.R. is due not to the predominance of mono-sulphide crosslinks but to the formation of zinc dimethyl dithio carbamate, (Z.D.M.C.) (Lee and Morrel, 1973). Z.D.M.C. is known to be a powerful antioxidant.

N.B.R. systems consisting of sulphur at ≤0.25 phr concentration in combination with accelerators, (or mixtures of accelerators) added in excess of 5 phr give vulcanizates with a high proportion of mono-sulphide crosslinks and best 'retention of mechanical properties' during thermal ageing at temperatures in the region of 100°C.

In E.P.D.M. networks cured with 1.5 phr sulphur and 2.5 phr T.M.T.D./M.B.T. it is reported that crosslink desulphurisation of poly-sulphides is the dominant process during early stages of thermo-oxidation (Deuri and Bhowmick, 1987). At 100 °C poly-sulphide crosslink concentration is reduced from 54-70% to 24-34% after 72 hours heating in air at 100°C. Desulphurisation during early stages of

oxidation has also been reported in N.R. vulcanizates (Cunneen and Russel, 1969; Doyle *et al.*, 1971). Desulphurisation is catalysed by accelerator-zinc complexes and was treated in section 2.2.4.3. In literature it has always been assumed that the crosslinks which form during desulphurisation of poly-sulphides, during heating and oxidative ageing are exclusively mono-sulphidic. Published results show however that mono-sulphide crosslinks in N.R. systems are readily oxidised and cleaved during ageing (Colclough *et al.*, 1968). This implies that crosslinks other than mono-sulphides may be introduced during desulphurisation and oxidation.

There is much experimental data showing oxidative crosslink formation to be related to an increase in the proportion of poly-sulphide crosslinks. In a sulphur vulcanized S.B.R. it is reported that there is a direct correlation between the concentration of poly-sulphide crosslinks and the extent of hardening (Studebaker and Beaty, 1972). Crosslink formation is thought to be caused by persulphenyl radicals, (RSS·). Persulphenyl radicals are produced by homolytic cleavage of poly-sulphide crosslinks. It is reported that persulphenyl radicals, (similarly to peroxy radicals) are capable of hydrogen abstraction and addition to double bonds.

An additional source of persulphenyl radicals may be through reaction of poly-sulphide crosslinks with free radicals (reaction XV), as reported for E.P.D.M. systems by Deuri and Bhowmick (1987). Deuri and Bhowmick (1987) suggest that this is an antioxidative reaction because the concentration of free radical is reduced by this reaction but they also point out that this reaction explains poly-sulphide crosslink desulphurisation and crosslink formation.

$$R_1\cdot + R_2S_xR_3 \longrightarrow R_1S_{x-y}R_3 + R_2S_y\cdot \qquad \text{XV.}$$

In N.B.R. the rate of oxidative scission is not clearly identified with a change in crosslink structure (Lee and Morrell, 1973). In N.B.R. network cured by an efficient vulcanization type system based on T.M.T.D./sulphur only 40% of original crosslinks remain after 80 hours heating at 130°C in air compared to 90 % crosslinks remaining when heated in vacuum under these conditions. For a conventional M.B.T./D.P.G./sulphur system the percentage of crosslinks remaining after heating in air for 80 hours is also approximately 40 %. This is essentially the same level of crosslink scission as shown by the T.M.T.D./sulphur system. The M.B.T./D.P.G./sulphur system exhibits more crosslink scission than the

T.M.T.D./sulphur system when heated in vacuum, presumably due to desulphurisation and thermal dissociation of poly-sulphide crosslinks.

In N.R. and B.R. oxidative scission of mono-sulphide and disulphide crosslinks is thought to occur by reaction scheme XVI (Colclough et *al.*, 1968):

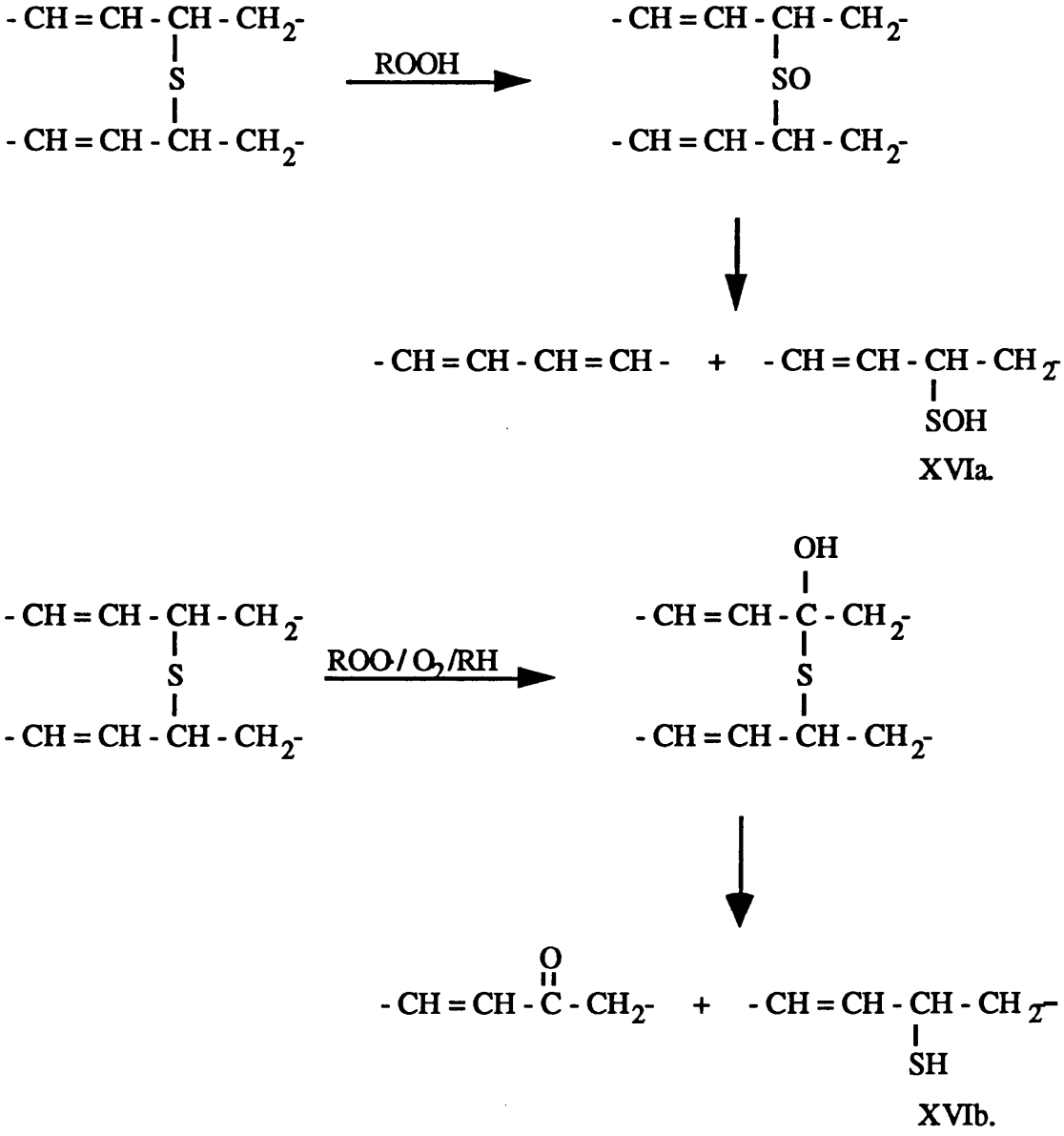

XVIa.

XVIb.

In low molecular weight compounds, it has been demonstrated that mono-sulphide crosslinks oxidise to sulphoxides and are converted to sulphenic acid (RSOH) by crosslink scission (Shelton, 1983). Di-sulphide crosslinks oxidise to thiolsulphinate and are converted to thiosulphoxylic acid (RSSOH) upon crosslink scission.

Further oxidation of the products of oxidative crosslink scission cause crosslink formation. Pendant thiols form crosslinks by oxidation. Sulphenic and thiosulphoxylic acid form crosslinks by condensation.

$$\begin{array}{lll} 2RSH \xrightarrow{[O]} & RSSR + H_2O \\ 2RSOH \xrightarrow{[-H_2O]} & RSSOR \end{array} \qquad \text{XVII.}$$

The review on network oxidation shows that most fundamental studies into the subject have been made on rubbers other than N.B.R., while work into N.B.R. has generally concentrated on technological improvements in ageing through variation in compound formulation.

2.3.2.5. Physical Aspects of Oxidation

During thermo-oxidative degradation of polymers the rate of oxidation away from the surface region is often limited or inhibited due to unavailability of oxygen. Published data on diffusion limited oxidation in E.P.D.M. have shown that uniform oxidation is dependent on sample thickness, rate of oxygen consumption, oxygen solubility, oxygen diffusion and atmospheric partial pressure (Gillen and Clough, 1992). Oxidised surface layers often have a lower permeability to oxygen than the original polymer and can further restrict the diffusion of oxygen into the bulk, thereby acting as a physical barrier to oxidation (Björk and Stenberg, 1985).

The dominance of thermal degradation away from surface regions has been confirmed in a recent investigation on the structure of a 100 year old N.R. bridge pad which showed oxidation to be restricted to a depth of 1.5 mm (Malek and Stevenson, 1992). Away from the oxidised surface region little deterioration of physical properties was found.

Frequently it is found that the depth of oxidation in polymers without added antioxidants is less than the depth of oxidation in the presence of powerful antioxidants. The oxidised surface layer has poor mechanical properties and has a deleterious effect on tensile properties. Dynamic properties of N.R. vulcanizates have been shown to be affected strongly by the presence of an oxidised surface layer (Björk and Stenberg, 1985).

It has been reported that oxidation is uniform below a limiting sample thickness of 1.02 mm, during ageing at 130°C (for a carbon black loaded N.R. tyre compound) (Brown, Morrell and Norman, 1973). Based upon such findings a sample thickness of 1 mm, for use in oxidation studies is specified in BS 903: part A52, (1986), equivalent international standard ISO 6914 (1985).

2.3.2.6. Effect of Oxidation on Mechanical Properties

The effect of long term atmospheric weathering in various environments on tensile properties of N.B.R. vulcanizates has been documented by Moakes (1975). This study reports that after 15 years ageing in temperate climate the change in the following properties of an N.B.R. compound P, (formulation not published) are as follows; tensile strength +20 %, elongation at break -6 %, modulus at 100 % +60 % and hardness +20 %. For a second compound, compound R, designed for optimum resistance, (formulation not published), the following results were reported; tensile strength +20 %, no change in elongation at break, modulus at 100 % +30 % and hardness +15 %.

Thermo-oxidative ageing in an oven at 82°C for a period of 28 days of compound P results in the following changes; tensile strength +25 %, elongation at break -30 %, modulus at 100 % +60 % and no change in hardness. For compound R the following results were given; tensile strength -60 %, elongation at break -70 %, modulus at 100 % +110 % and hardness +25 %.

The results clearly indicate that different properties are affected at different extents by a change in ageing environment.

The effects of ageing on dynamic properties and viscoelastic loss properties of N.B.R. have not been studied in much detail. In S.B.R. it is reported that peak tan δ is sensitive to ageing and it is shown that the reduction in peak tan δ is inversely related to the change in hardness, static modulus and swollen network density (Mifune, Nagai, Nishimoto and Ishimaru, 1991). A reduction in peak tan δ and a shift in peak tan δ temperature, (T_α) to higher temperature has also been reported in epoxidised natural rubber (E.N.R.) vulcanizates (Varughese and Tripathy, 1991). Tan δ may be particularly sensitive to ageing in these systems because the ageing process causes an increase in crosslink density and therefore an increase in storage modulus with a reduction in the viscous component.

$$\tan \delta = E''/E' \qquad (2.22)$$

where, E'' is the out of phase modulus and E' is the in phase modulus.

2.3.2.7. Oxidation Kinetics

Values for kinetics constants of N.B.R. and other polymer materials, obtained from modelling of tensile property data have been widely reported (Budrugeac, 1992; Dinzburg Keller and Bond, 1988; Boruta and Petrujova, 1987). Such measurements are obtained from modulus and elongation at break measurement because these properties show uniform dependence on ageing time. Modulus is reported to be less sensitive to ageing than elongation at break, therefore the majority of kinetic studies into N.B.R. ageing are based on measurement of elongation at break. Other measurements of degradation, such as tensile strength and hardness have been found unsuitable because they show non-uniform time dependence. Dynamic properties have not been fitted to kinetic ageing models. The kinetic expressions used in this context are reviewed in section 2.3.4.2.

Boruta and Petrujova (1987) have treated this subject in great detail and have reported values of apparent activation energy, (E_a) of degradation for a range of polymer materials. For N.B.R. vulcanizates samples (formulation and combined ACN content not given) E_a is reported to be in the region of 80-90 kJ.mole^{-1}. These values were obtained from measurement of elongation at break and stress at 200 % elongation data.

Budrugeac (1992) has reported on the values of E_a and pre-exponential factor of N.B.R. vulcanizates from study of residual deformation during ageing. The study into residual deformation identified an exponential decrease in residual deformation with time corresponding to a reaction order of 1. The values of E_a, obtained from the linear region, which was attributed to a chemical ageing process was reported to be 88.2 kJ.mole^{-1}, 69.4 kJ.mole^{-1} and 95.8 kJ.mole^{-1} for three vulcanizate samples, (formulation not given) containing 33 weight %, 33 weight % and 40 weight %, combined ACN content, respectively. The pre-exponential factor was reported to be 1.3×10^{11} s^{-1}, 4.4×10^{10} s^{-1} and 1.8×10^{12} s^{-1}, respectively.

The E_a derived from study of the change in Tg with temperature and time of ageing of N.B.R. containing 26 weight % combined ACN content, (compounded

with two sulphur based vulcanization system, termed A and B) is 77.0 kJ.mole^{-1} and 74.1 kJ.mole^{-1}, respectively (Wanyun, 1990).

There appear to have been few studies into the effect of compound formulation on the kinetics of N.B.R. thermo-oxidation. Study into the effect of compound formulation on thermo-oxidation of N.R. vulcanizates have reported values of E_a of 113.0 kJ.mole^{-1}, 102.6 kJ.mole^{-1} and 92.6 kJ.mole^{-1} for a conventional, semi E.V. and E.V. system, respectively (Barker and Tinker, 1989).

The effects of polymer structure and polymerisation residue composition on the kinetics of oxidation have not been studied, to the knowledge of the author.

2.3.3. STABILISATION

Because N.B.R. has inadequate thermo-oxidative stability for commercial application, it is usually protected from such degradation by addition of antioxidants (chemicals which retard the oxidation process). Antioxidants are added during manufacture and also during subsequent compounding. Often synergistic combinations of antioxidants are used. The chemistry of antioxidant action is briefly reviewed in sections 2.3.3.1. and 2.3.3.2.

2.3.3.1. Chain Breaking Antioxidants

The chemistry of antioxidant action of chain breaking antioxidants (aromatic amines and hindered phenols) has been studied extensively by Scott and co-workers (working at the University of Aston) and is fairly well established (Al-Malaika, 1991). The term chain breaking antioxidants, assigned by Scott describes antioxidants which act by removing propagating radicals of the oxidation process through donation of hydrogen or electron acceptance. Reaction scheme XVIII illustrates the hydrogen donating mechanism.

$$ROO\cdot + AH \longrightarrow ROOH + A\cdot \qquad \text{XVIII.}$$

AH represents an antioxidant molecule, A· is a stable radical.

The effectiveness of chain breaking antioxidants depend on the rate of reaction with free radicals and the reactivity of the generated radical A·. Regeneration of antioxidant is also likely since the stoichiometric coefficient of inhibition, f (the number of chains terminated per antioxidant molecule) is often in excess of the number of hydrogens involved in the process (Denisov, 1980). In polypropylene systems at atmospheric pressure, for butylated hydroxy toluene, f=1, for 2,2,-methylene bis-butylated hydroxy toluene, f=3 and for diphenyl amine, values for f of 10 have been reported.

Effectiveness of added antioxidants is also influenced by their volatility (Lustoñ, 1980). High volatility results in migration of antioxidant to the surface and optimum protection. At elevated temperatures antioxidants of high volatility are lost by evaporation. Antioxidants of low volatility exhibit low loss but their concentration at the surface is lower.

In addition to reacting with peroxy radicals antioxidants of this type, (such as diphenyl amine) are also observed to interact with other chemicals of the vulcanization process such as elemental sulphur and zinc ions (Porter, 1967). There is no information on the influence of such reactions on the antioxidative efficiency of diphenyl amine, however there may be synergism or antagonism. Interactions between diphenyl amine and other chemicals which are present in N.B.R., such as polymerisation residues have not been reported.

2.3.3.2. Sulphur Compounds as Preventive Antioxidants

The anti-oxidative properties of di-alkyl sulphides have been known since the early 1960s, when it was reported that the oxidation of peroxide vulcanized N.R. was strongly affected by the compounding-in of such chemicals (Cunneen and Lee, 1964). Di-alkyl di-sulphide compounds are reported to be more powerful antioxidants than the di-alkyl mono-sulphides. Tertiary sulphides are more active than secondary and primary sulphides. Di-alkyl sulphoxides and di-alkyl thiolsulphinate are more active antioxidants than equivalent di-alkyl mono-sulphides and di-alkyl di-sulphides, respectively.

Shelton (1981) has confirmed that the efficiency of sulphoxides and thiolsulphinates as preventive antioxidants is largely determined by their thermal instability. The instability required for their activity needs to be balanced against other factors such as persistence. Studies into the mechanism of inhibition have shown that

sulphenic and thiosulphoxylic acid, and their oxidation products inhibit oxidation through hydroperoxide decomposition, (preventive mechanism). Hydroperoxide decomposition is thought to occur by an acid catalysed reaction because addition of $CaCO_3$ base greatly slows down hydroperoxide decomposition.

Sulphoxide and thiolsulphinate decompose hydroperoxides only slowly and show an induction period which suggests that for the reaction to proceed they must first be converted into secondary oxidation products, such as sulphenic and thiosulphoxylic acids, respectively.

Shelton (1981) also observed that traces of sulphoxide reduce or eliminate hydroperoxide decomposition by thiolsulphinates. He postulated that sulphoxide is a sufficiently strong base to combine with acids which may be formed to form a stable complex.

SO_2 is also a very effective catalyst of hydroperoxide decomposition and is claimed to have radical trapping activity (Husbands and Scott, 1979).

2.3.4. TECHNIQUES OF ASSESSING OXIDATION

2.3.4.1. Circulating Air Oven Ageing

Published scientific and technical papers in the area of polymer thermo-oxidation show that air ageing at elevated temperatures, in circulating air ovens is the general method employed to accelerate the ageing process (Bille and Fendel, 1993). This type of accelerated ageing test is described in BS 903, part A19, (1986), equivalent international standard ISO 188, (1982).

During hot air ageing samples are affected by oxidation, bulk reactions and evaporation of volatile contents. Oven ageing in combination with measurement of mechanical properties, has been used extensively as a means of measuring the kinetics of oxidation.

2.3.4.2. Thermo-Oxidation Kinetic Expressions

There is much interest in literature on development of kinetic models for describing ageing behaviour of polymers due to the need to predict long term ageing behaviour from short term accelerated ageing experiments.

Kinetic models use the Arrhenius expression to obtain property change as a function of temperature (Budrugeac, 1992; Yongjin, 1989; Boruta and Petrujova, 1987). The application of the Arrhenius equation (equation 2.23) to property change during ageing of solid polymers has little theoretical justification however, since ageing is a highly complex process in which several chemical reactions, leading to scission and crosslinking occur simultaneously. Oxidation products may themselves exhibit pro-oxidative or antioxidative properties. The relative rate of crosslink formation with respect to scission may therefore change with temperature and affect the measured mechanical property. Because of these complications the Arrhenius model must be considered empirical and the activation energy derived from it, is an apparent activation energy, (E_a). The frequency factor, (A) is simply an arbitary pre-exponential constant.

By analogy with chemical reactions, the overall rate constant of the ageing process, (k) at ageing temperature, (T) is described in terms of the Arrhenius equation 2.23.

$$k = A \exp(-E_a/RT) \qquad (2.23)$$

where, R is the gas constant and T is test temperature.

For temperatures T_o and T,

$$k_o/k = \exp\{-(E_a/R)(1/T_o - 1/T)\} \qquad (2.24)$$

This is often written in terms of a shift factor.

$$a_T = k_o/k \qquad (2.25)$$

In treatment of ageing data the rate constant is considered to be inversely proportional to some characteristic time to equivalent degradation, τ.

$$\ln a_T = \ln k_o/k = \ln \tau/\tau_o = (E_a/R)(1/T - 1/T_o) \qquad (2.26)$$

Arrhenius plots of the temperature dependence of elongation at break change of N.B.R. in accordance have been shown to exhibit high linearity, (correlation coefficients > 0.99 have been quoted) and results obtained from such plots appear to be reproducible (Budrugeac, 1992). High linearity and reproducibility may be attributed partly however to the insensitivity of plots to moderate scatter.

The Arrhenius equation is nevertheless employed as a starting point for extrapolation of accelerated ageing results to experimentally inconvenient times. Substitution of E_a into equation 2.26 enables calculation of k or τ for any temperature.

Sometimes the property change vs. log time curves are found to have the same shape at different temperatures. They can then be superimposed as shown by Gillen and Clough (1989) by a shift along the log time axis to form a master curve at a reference temperature, (time temperature superposition). Alternatively such data are often shown as a single curve with a series of time axis corresponding to different temperatures (Barker and Tinker, 1989).

Different authors have employed various relations of a simple algebraic form to describe the rate of property change during thermo-oxidative ageing. These relationships have been found to fit limited ranges of experimental results for elongation at break, volume swell and continuous stress relaxation (Dinzburg Keller and Bond, 1988; Boruta and Petrujova, 1987).

$$P/P_o = kt \qquad (2.27)$$

$$P/P_o = A \exp(-kt) \qquad (2.28)$$

$$P/P_o = A \exp(-kt\alpha) \qquad (2.29)$$

where, t is the ageing time, P_o is unaged property, P is the property after ageing, while k is a measure of the rate of property change which may be positive or negative depending on whether the measured property shows an increase or decrease with ageing. In equation 2.29, α is a constant independent of temperature.

For equations 2.27-2.29 E_a is obtained by equations 2.23 and 2.24.

Boruta and Petrujova (1987) have shown that the values of E_a, which are obtained by fitting of elongation at break change and modulus change ageing data of

N.B.R.are influenced by the equation used. E_a values of aged N.B.R. vulcanizates obtained from fitting elongation at break data to equations 2.25 and 2.26 are reported to differ by 50 %. This variation in E_a values between different kinetic models implies a need for more detailed study of the application of these models to tensile property change ageing data.

2.3.5. ANALYTICAL TECHNIQUES

2.3.5.1. Infrared Spectroscopy

Infrared (I.R.) spectroscopy has been applied extensively to the study of vibrational structure of molecules (Ishida, 1987). For infrared active molecules energy absorption in the I.R. region causes a change in the mode of molecular vibration from a vibration of lower energy level to a vibration of higher level. The difference between energy levels corresponding to different molecular vibrations is characteristic of the atom, the type of bonding and the type of molecular vibration.

$$\nu = \Delta E / h \qquad (2.30)$$

where, ΔE is the energy difference, h is Planck's constant and ν is the frequency of radiation.

In conventional I.R. spectrometers the intensity of transmitted radiation is recorded as a function of frequency while in Fourier transform infrared spectroscopy (F.T.I.R.) instruments path length is measured and then converted to frequency (Ishida, 1987).

Various techniques of utilising I.R. spectroscopy have been developed for the study of surface oxidation of polymer samples. The most useful, and frequently used technique for study of polymer oxidation is attenuated total reflection (A.T.R.) spectroscopy. A.T.R. is also termed multiple internal reflection (M.I.R.). The simplified diagram of A.T.R. is illustrated in figure 2.5.

A.T.R. uses the concept of total reflection which occurs at the interface of two materials of different refractive index, (such as air and water). Usual internal reflection elements are thalium bromoiodide and germanium, refractive indices 2.4 and 4.0, respectively. The depth of radiant penetration is within the range of 1-20 μm and is

dependent on factors, such as the ratio of the refractive index of the crystal to the sample and the angle of reflection.

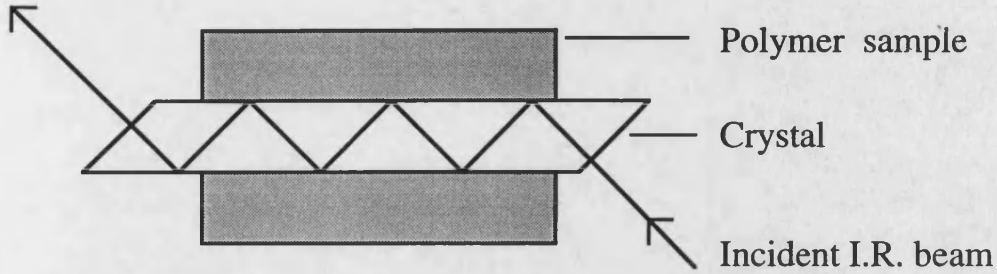

FIGURE 2.5. Simplified diagram of the principle of A.T.R..

The frequency assighnments of most use in the study of polymer oxidation are tabulated in table 2.1 (Cross, 1964; Haslam and Willis, 1972).

Structural feature	Aabsorption wavenumber (cm^{-1})
Acrylonitrile, (-CN)	~2250
Cis, 1-4, butadiene unsaturation	~740, 3010
Trans, 1-4, butadiene unsaturation	~975
Vinyl, 1-2, butadiene unsaturation	~910
Methhylene, ($-CH_2-$)	~1445
Free hydroperoxide	3580 - 3670
Hydrogen bonded hydroperoxide	3450 - 3550
Ketone	~1745
Peroxide, C-O	~1090

TABLE 2.1. I.R. absorption frequencies of structural features used in oxidation studies of polymers.

2.3.5.2. X-Ray Photoelectron Spectroscopy (X.P.S.)

X.P.S. involves the measurement of binding energies of electrons emitted from materials which are irradiated with soft X-rays (Seah and Briggs, 1990). The technique is highly surface specific (information being limited to 2 nm) due to inelastic collisions of emitted electrons. X.P.S. has high resolution, being able to detect elemental concentrations in the region of 0.1 atomic %. The principle of X.P.S. is shown in figure 2.6.

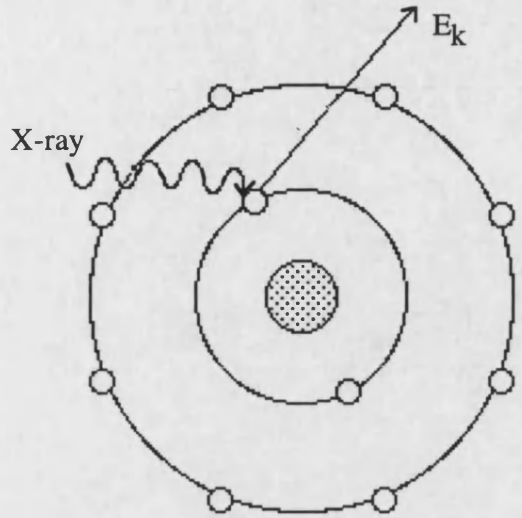

FIGURE 2.6. Schematic diagram of the principle of X.P.S..

Emitted core level electrons have a binding energy, E_b which is related to the kinetic energy of the emitted electron, E_k and the X-ray energy. Binding energy of emitted electrons is characteristic of each element and its orbital shell ($E_k = h\nu - E_b$).

Because the binding energy is further influenced by the electronegativity of substituent groups and the type of bonding it is found that the C_{1s} peak is useful for the study of polymer oxidation. The binding energies of various carbon oxidation structures published by Dilks (1983) are shown in table 2.2. Curve fitting of the C_{1s} peak has allowed quantitative determination of the concentration of oxidation structures. Binding energies of sulphur and zinc compounds are similarly influenced by the electronegativity of substituent groups.

Although expensive and specialised the technique has been shown to be particularly suited to elemental characterisation of polymer surfaces and the study of surface oxidation.

It appears that there has only been one publication into the use of X.P.S. for the study of N.B.R. oxidation (Bhattacharjee *et al.*, 1992). The study of crosslink network oxidation in N.B.R. vulcanizates, by X.P.S. has not been reported.

Chemical structure	C_{1s} binding energy (eV)
C-C, C-H	285.0
C-O	286.6
C=O	287.9
O-C-O	287.9
O=C-O	289.0
O=CO_2	290.6

TABLE 2.2. Published binding energy of C_{1s} in oxygen bonded structures, according to Dilks (1983).

2.3.5.3. Thermal Analysis

Thermal analysis techniques have been widely applied to the characterisation of polymers. The topic of thermal analysis includes a number of experimental techniques, in which a variety of properties are measured during programmed dynamic or static temperature treatment. These techniques are often used in combination because they give complimentary information.

2.3.5.3.1. Differential Scanning Calorimetry (D.S.C.)

Calorimetry is defined as a technique of measuring heat. Differential calorimetry (D.C.) measures the difference in heat between a sample and a reference, at constant temperature while differential scanning calorimetry (D.S.C.) involves heating or cooling at a controlled rate (Wunderlich, 1992). Both techniques measure heat change, between a sample, (mass 1-100 mg) and a reference, which are maintained at isothermal conditions during a controlled temperature programme. During endothermic reactions more heat has to be supplied to the sample in order to maintain isothermal conditions between sample and reference while during exothermic reactions less heat has to be supplied. The principle of D.S.C. is illustrated in figure 2.7.

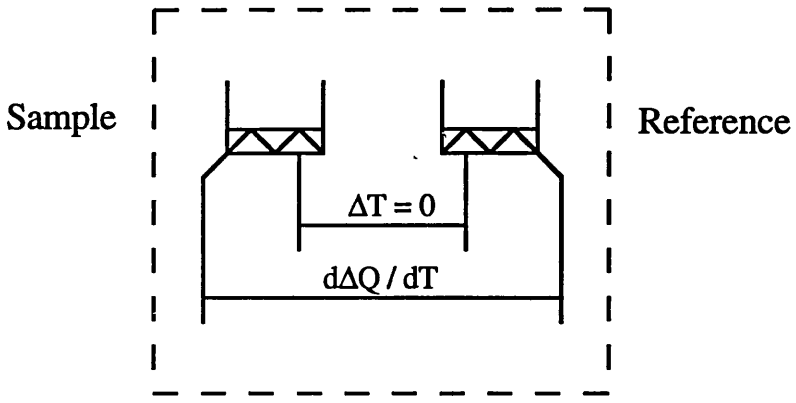

FIGURE 2.7. Schematic diagram of the principle of D.S.C..

There are several publications which report on the study of N.B.R. oxidation by D.S.C. (Budrugeac *et al.*, 1990; Budrugeac and Segal, 1990; Goh, 1986; Slusarski, 1984). All such studies have reported the observation of two overlapping exothermic peaks during non-isothermal controlled temperature ramp experiments. A peak in the region of 185°C is attributable to oxidation and a second peak in the region of 365°C is caused by thermal degradation. The magnitude of the oxidation peak is reported be 2.24 $kJ.g^{-1}$ and 0.29 $kJ.g^{-1}$ for N.B.R. polymers of 21 weight % and 45 weight %, respectively (Slusarski, 1984). D.S.C. peak temperature and peak area is strongly influenced by heating rate and surface area, therefore such figures are not absolute.

2.3.5.3.2. Differential Thermogravimetry (D.T.G.)

Thermogravimetry is based on the principle of measuring sample weight while applying a controlled temperature treatment (Dollimore, 1992). The instrument consists of a null point balance which is enclosed in a furnace. A simplified diagram of the technique is illustrated in figure 2.8.

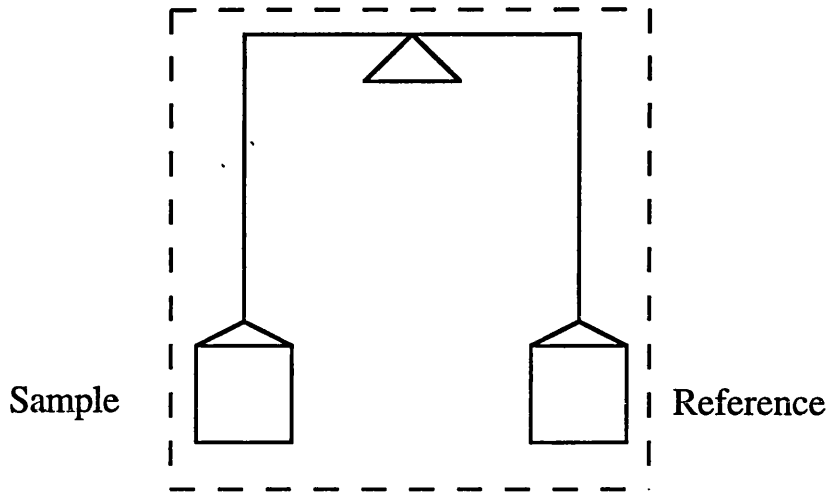

FIGURE 2.8. Schematic diagram of the principle of D.S.C..

T.G. has been applied to the study of degradation and composition of polymers (Budrugeac *et al.*, 1990; Budrugeac and Segal, 1990; Slusarski, 1984). Its application to the study of N.B.R. oxidation has shown that oxidation is accompanied by a weight gain. Thermal degradation which occurs at higher temperatures is accompanied by decomposition to volatile products and weight loss.

2.3.5.3.3. Differential Mechanical Themal Analysis (D.M.T.A.)

D.M.T.A. measures changes in mechanical properties, such as complex modulus at a test frequency during controlled heat treatment. In most instruments a sinusoidal tensile strain is applied to a sample, (in a bending or stretching mode of deformation) and the sinusoidal stress and phase angle, tan δ measured as a function of time and temperature (Reading, 1992). The sample is held under tension throughout, such that there is a restoring force keeping the sample in tension even at minimum strain. The complex modulus is separated into its individual components, via equation 2.22.

A Rheovibron DDV-II viscoelastometer was found to be suitable for measuring low stiffness rubber samples, (of dimensions 4 mm x 1 mm). This is a direct reading instrument in which the sample is subjected to stretching, type deformation. In this instrument a strain is applied to the sample and measured through a displacement

transducer. The resultant stress at the opposite end of the sample is measured by a stress transducer.

2.3.5.4. Stress Relaxation

The technique of stress relaxation, originally proposed by Tobolsky, Prettyman and Dilton (1944) has become a valuable tool for measuring network changes of vulcanizates during ageing and has been widely applied (Björk and Stenberg, 1990).

The principle of stress relaxation is based on the separation of elastically active and elastically inactive networks. In intermittent stress relaxation, samples are aged in a relaxed state, and extended at periodic time intervals to a moderate elongation, (such as 50 %). Since testing is at equivalent extension, volume and temperature all terms of the statistical equation 2.13 are eliminated and equation 2.31 is obeyed. Therefore normalised force is a measure of the change in network density. Real networks however contain a C_2 term of the Mooney-Rivlin equation (equation 2.17) and for equation 2.31 to be valid C_2 must remain constant during ageing.

$$F/F_0 = N/N_0 \qquad (2.31)$$

where, F and F_0 correspond to the retractive force of the aged and unaged samples and N and N_0 correspond to the number of network chains of the aged and unaged networks, respectively.

When samples are aged in the strained state it is postulated that newly formed crosslinks are elastically inactive and the decay in retractive force is a measure of the rate of scission. During initial stages of testing networks exhibit high stress relaxation which is attributed to physical relaxation caused by polymer chain rearrangement. In samples where extensive crosslinking occurs it has been shown that the measured stress in continuous stress relaxation is influenced by crosslink formation (Björk, Dickman and Stenberg, 1989). At early stages of oxidation physical relaxation, caused by conformational changes in polymer chains contributes to continuous stress relaxation.

According to this treatment the difference between the intermittent stress relaxation curve and continuous stress relaxaton curve is a measure of the concentration of newly formed crosslinks, (secondary network).

$$N / N_o = (F / F_o)_{int.} - (F / F_o)_{cont.} \qquad (2.32)$$

In light of the requirement for a constant value of C_2 it is surprising to see that previous stress relaxation studies have not reported on the change of C_2 with ageing (Björk and Stenberg, 1990).

CHAPTER III

3.0. CHARACTERISATION; EXPERIMENTAL PROCEDURE

3.1. MATERIALS

The work contained within this thesis is based on five equivalent specification commercial N.B.R. polymers which were supplied by different polymer manufacturers. The polymers selected for this work had combined ACN contents in the region of 25.5-30.8 weight % and Mooney (ML 1+4) viscosity in the region of 39-53 units.

Perbunan 2807 (lot number 202056) was supplied by Bayer P.L.C., Newbury, U.K.. Krynac 27.50, (lot number 0316) was obtained from Bayer, La Wantzenau, France. Chemigum N715B, (lot number not supplied) was obtained from Goodyear Chemicals Europe, Cedex, France through their agents Hubron Sales Limited, Manchester, U.K.. Nipol DN 300W45, (lot number not supplied) was procured from Zeon Chemical Europe Limited, Sully, U.K.. Europrene N28 45, (lot number not supplied) was obtained from Enichem Elastomers Ltd., Southampton, UK..

According to manufacturers' data all five polymers have been prepared by a cold emulsion polymerisation process and all contain a non-staining antioxidant.

These selected polymers were given designate names so as to simplify sample identification in following studies. Sample designations are shown in table 3.1. Structural and mechanical properties of polymers, supplied by their manufacturers are collated in table 3.2.

The compounding chemicals used in the study were procured from the Centre for Polymer Studies, Trowbridge Technical College, Trowbridge, U.K.. MC sulphur (2 % magnesium carbonate coated) was supplied to them by R.T.Z. chemicals, Manchester, U.K.. C.B.S., Z.D.M.C. and Z.D.E.C. (Rheogran-80 grades) were supplied by the Rheinchemie division of Bayer, Newbury, U.K.. Zinc oxide and Stearic acid (commercial purity grades) were supplied by Avon Industrial Polymers, Melksham, U.K.. Permanax B.L.W. antioxidant was obtained from the chemicals division of A.K.Z.O., Amersfoot, Holland. Zinc sulphide (laboratory reagent grade, 97.44 % purity) was obtained from B.D.H., Poole, U.K..

Various solvents were used in this study to treat vulcanized samples. Methanol (Analar grade), toluene (Analar grade), 1,1,1-trichloroethane (Analar grade), n-heptane

(Analar grade) and acetone (Analar grade) were obtained from B.D.H.. Propane-2-thiol (98 % purity), iodomethane (99 % purity), piperidine (99 % purity) and hexane-1-thiol (95 % purity) were obtained from Aldrich Chemicals, Gillingham, U.K.. Toluene (Analytical grade) was obtained from Fisons, Loughborough, U.K.. Calcium chloride hydrate (99.99+ % purity), oleic acid (technical grade, 90 % purity), sodium dodecyl sulphate (98 % purity) and sodium dodecane sulphonic acid (99+ % purity) were supplied by Aldrich Chemicals.

Manufacturer	Grade	Designation
Bayer	Perbunan 2807	B
Enichem	Europrene N28 45	E
Goodyear	Chemigum N715	G
Nippon / B.P.	Nipol DN 300W45	N
Bayer	Krynac 27.50	P

TABLE 3.1. Designation of the five commercial N.B.R. grades chosen for this work.

Parameter	Polymer				
	B	E	G	N	P
Combined ACN, weight %	28.2	28.0	27.9	28.0	26.9
Mooney viscosity, (ML 1+4 at 100°C)	47.0	45.0	46.0	45.0	52.0
Volatile matter, weight %	0.5	*	0.4	0.5	0.1
Ash content, weight %	0.1	*	0.45	0.4	0.7

*Data not supplied.

TABLE 3.2. Properties of raw N.B.R. samples determined by manufacturers' laboratories.

3.2. ELEMENTAL ANALYSIS

3.2.1. CHEMICAL ANALYSIS

Because it was felt that there would be little logic in investing time and resources in trying to replicate already established experimental procedures for determination of polymer elemental composition it was decided to use the expertise of a commercial analytical laboratory with a strong reputation in the field of elemental analysis. The company entrusted with this work was Butterworth Laboratories, Teddington, U.K..

Carbon, nitrogen and hydrogen concentrations were determined by them on a Perkin Elmer 2400 elemental analyser. Chlorine and sulphur levels were measured by ion chromatography. For metal residue analysis the polymer was first ashed at 500°C. Trace metal residue concentration was determined by atomic absorption spectroscopy.

3.2.2. X-RAY PHOTOELECTRON SPECTROSCOPY

All raw nitrile polymers were analysed on a V.G. Escalab mark II X.P.S., at the University of the West of England, Bristol, U.K.. The instrument was used with an aluminium anode operating at 12.5 kV and 40 mA. The analyser was set at a pass energy of 20 eV. Scan times of 30 minutes were used. The X.P.S. was operated under vacuum at 10^{-10} torr. Samples were first introduced into a secondary vacuum chamber where they underwent outgassing. After outgassing for 2 days, typically over a weekend, samples were introduced into the analysis chamber.

Curve fitting and data analysis was performed with software, written by R. Ewan of the University of the West of England. Elemental peak area data was converted into atomic area by use of Wagner sensitivity factors (Wagner, 1990).

The measurement of shifts in binding energy caused by surface charging, resulting from the non-conductivity of rubber, was assessed by referencing binding energies to the observed shift in the binding energy of C_{1s} at 285.0 eV, as shown by Seah and Smith (1990).

3.2.3. DETERMINATION OF CARBOXYLIC ACID RESIDUES AND ANTIOXIDANT RESIDUES

3.2.3.1. Extraction of Polymers

The method of carboxylic acid extraction employed in the present study is similar to the methods recommended in ISO 1407 and that used by Reeves and Packham (1992). Analar methanol was the extraction solvent used. Extraction was carried out in a Soxhlet extractor for a period of 16 hours.

Thin slithers of polymer (approximate diameter 1 mm) were wrapped in perforated aluminium foil to prevent adherence of polymer to the Soxhlet extractor thereby eliminating the need for pre-extraction of sample holder. To obtain sufficient extract for subsequent analysis a large scale extractor of approximately 800 ml pot volume was used. Sample weight was maintained at 25 g. A hot extraction process was used in preference to the cold process due to faster rates of extraction in the former process. Degradation of polymer during extraction was of no concern because the extracted polymer was of no further interest.

At the end of the extraction process the extraction solution was evaporated under vacuum at room temperature and the extracted material weighed on a Sartorius model A200S analytical microbalance. The concentration of methanol extracted material was expressed in terms of weight percent of original polymer weight.

The polymers were extracted for antioxidants by using conditions recommended by Haslam and Willis (1972). Experimental procedure entailed extraction of polymer sample, (of approximate weight 1 g) under reflux for 1 hour using 80 ml of Analar methanol. The polymer sample was first cut into thin slithers, of diameter below 1 mm. This was done to increase surface area. After 1 hour the extract solution was decanted into a separate flask and the sample extracted a second time under reflux using 80 ml of fresh solvent. The extract solution was cooled and combined with the extract from the first extraction. The extracted rubber and extraction flask were washed with solvent and the whole extract solution made up to 200 ml.

3.2.3.2. Gas Liquid Chromatography

Material extracted from raw nitrile polymers was analysed by gas liquid chromatography (G.L.C.) at Avon Tyres Limited with the assistance of A. Brodie.

Because hot methanol extract contains carboxylic acids and methyl esters and carboxylic acids and methyl esters have different G.L.C. retention times it was necessary to convert all remaining carboxylic acids in the methanol extract into their methyl ester form. Analysis of methyl ester was preferred to analysis of carboxylic acid because routine analysis has shown that carboxylic acids are normally too polar to give adequate retention times when injected into a G.L.C. column of the type (3 % SE-30). A 3 % SE-30 column was available for this work.

Carboxylic acids were converted into methyl esters through esterification with methanol. Experimental procedure was based on Avon Tyres Limited analytical laboratory method A20, (1993). Esterification was carried out by the addition of 1 ml of concentrated sulphuric acid to 75 ml of methanol into which 1 g of methanol extract was dissolved. The solution mixture was refluxed for 30 minutes in a reflux condenser and then allowed to cool. Once cooled 75 ml of distilled water was added to the solution. The methyl ester, which forms the top layer on cooling was separated from the solution with a separating funnel.

G.L.C. analysis was made on equal volume sample/chloroform solutions. 1 µl of solution was injected into the G.L.C. column (3 % SE-30, packed) using a calibrated syringe. The syringe was rinsed out with fresh methanol in between experiments. Methyl silicone formed the liquid phase in the column. An injection port temperature of 250°C was used to vaporise the solution rapidly. Column temperature was raised from 150°C to 250°C at a controlled heating rate of 6°C per minute after an initial temperature hold at 150°C of 5minutes. A flame ionisation detector (F.I.D.) was used, at a temperature of 275°C.

The F.I.D. was calibrated by running reference scans with methyl esters of stearic acid and palmitic acid using identical experimental conditions to sample runs.

3.2.3.3. Ultra-Violet Spectroscopy

Ultra-violet absorption of methanol extract solutions was measured on a Perkin Elmer Lambda 3 double-beam U.V.-visible spectrophotometer with methanol as the reference. Glass cells with a path length of 10 mm were used for all studies. U.V. cells and pipettes were washed by rinsing with methanol in between experiments. Scan speed was maintained at 120 nm throughout. U.V. absorption spectra were recorded within the range 190-390 nm.

Additional experiments were run with 0.1 alkali methanol extract solutions which were prepared by adding 2 ml of potassium hydroxide reagent and 1 ml of distilled water to 10 ml of methanol extract solutions. The potassium hydroxide reagent was made up by dissolving 10 g of Analar potassium hydroxide in 10 ml of distilled water and diluted with 60 ml of fresh methanol. The reference methanol blank was treated in an identical manner. This treatment is based on recommendations of Haslam and Willis (1972).

3.2.3.4. Mass Spectroscopy

Separation and analysis of individual trace antioxidants dissolved in the methanol extract was made by analysis on a solids / liquids mass spectrometer. The apparatus is located at the Structural Materials Centre of the D.R.A., Farnborough. The equipment was operated by Mr. C. Andrews working under the supervision of Dr. K. J. Timmins.

Experimental procedure involved injecting a 10 µl sample solution into column and heating at 1°C per second from ambient temperature to 800°C. Antioxidants were separated according to their volatility, and analysed by mass.

3.2.4. DETERMINATION OF FREE WATER CONTENT

Free water content was determined on a Metler DL 37 coulometer. This instrument determines water content in solutions by the Carl Fischer titration method, titration end point being determined electrometrically. The reaction of the Carl Fischer reagent which is illustrated in reaction scheme XIX is based on the reaction of iodine and sulphur dioxide, which takes place in the presence of water (Rosin, 1967).

$$H_2O + I_2 + SO_2 + 3C_5H_5N \longrightarrow 2C_5HN.HI + C_5H_5NSO_3$$

$$C_5H_5NSO_3 + CH_3OH \longrightarrow C_5H_5NH.SO_4CH_3$$

XIX.

For this analysis solutions of polymers were prepared by dissolving 0.1 g of rubber in 6 ml of Analar toluene. Testing involved injecting an accurately weighed sample solution, (weight in the region of 10 mg) into the instrument with the use of a calibrated syringe. The free water content of Analar toluene was determined separately

and later subtracted from the water content of the polymer solutions. These experiments were carried out in triplicate and a mean average value calculated.

3.3. ANALYSIS OF MACRO-STRUCTURE

3.3.1. DETERMINATION OF GEL CONTENT

Gel content (crosslinked material which does not dissolve when rubber is immersed for sufficiently long time in a thermodynamically good solvent) was determined in accordance with the procedures and conditions specified in A.S.T.M. D 3616, (1988). The method involved cutting a rubber sample into thin strips with cross sectional area of less than 1 mm and lengths of approximately 5 mm. Strips with a combined weight of approximately 0.4 g were then placed evenly on a 300 micron screen and immersed in 100 cm^3 of Analar M.E.K. (methyl ethyl ketone). In a modification to A.S.T.M. D 3616 one circular screen of 150 mm diameter was used, rather than 5 circular screens of 38 mm diameter arranged on a vertical rack as stated in the method. The rubber strips were left immersed in the solvent for 20 hours at 25°C in the dark. After 20 hours a fraction of solution was removed from the container filtered through cotton wool and the solvent allowed to evaporate. The weight of rubber which passed through the 300 micron screen is the fraction of the total soluble rubber content while the remainder is insoluble rubber. Percentage gel was calculated from the total weight of insoluble material as a percentage of the original sample weight.

It must be noted that no justification is given in the A.S.T.M. standard for the use of a 300 micron screen. Its specification would appear to be arbitrary.

3.3.2. DETERMINATION OF MOLECULAR WEIGHT

3.3.2.1. Gel Permeation Chromatography

Molecular weight distributions were initially determined by R.A.P.R.A., Shrewsbury. Later work was done at Bath University.

The R.A.P.R.A. instrument was a Viscotec, (combined G.P.C./viscometry instrument). The G.P.C./viscometry instrument was used in preference to conventional G.P.C. because the Viscotec instrument allows determination of true molecular weight through additional measurement of solution viscosity. Often G.P.C. calibration is

carried out with monodisperse polystyrene fractions and so only gives relative molecular weight distributions. N.B.R. calibration standards appear not to be available commercially.

Polymer solutions for G.P.C./viscometry work were prepared by dissolving polymer samples in tetrahydrofuran (T.H.F.), with added antioxidant. All experiments used solutions with polymer concentrations of 4 mg per ml. Before testing solutions were filtered through a 0.45 micron filter to remove crosslinked polymer. Under these conditions R.A.P.R.A. found that gel free solutions could not be obtained and the Viscotec, (viscosity measurement) attachment could not be used. This was the finding for all five polymers.

Calibration was made before testing by observing the molecular weight retention time relationship of monodisperse polystyrene fractions.

Later work at Bath University attempted to remove the gel fraction from solutions by filtering polymer-tetrahydrofuran solutions through a 0.2 micron filter. Polymer concentration was reduced to 1 mg per ml of solvent to facilitate filtration. Filtration was made with the use of a filtration syringe, into which the filter was inserted at the base of the piston. During filtration it was found that the 0.2 micron filter quickly became blocked by polymer and high hand pressures were required to filter sufficient quantities of sample for analysis. The filter was changed and the syringe rinsed with fresh T.H.F. in between changes in sample.

Molecular weight distributions of polymer-tetrahydrofuran solutions filtered through a 0.2 micron filter were investigated by a Bruker LC-41 chromatogram, with no viscosity measuring facility. Prepared solutions were injected into the G.P.C. column using a calibrated syringe. The G.P.C. column was packed with partially crosslinked microporous polystyrene beads with a distribution of pore sizes. The column was maintained at ambient temperature. Polymer concentration was determined by a refractive index detector. A flow rate of 1.0 ml per minute was used.

During experimental runs an increase in head pressure was observed which indicated that gelled material was present in these samples.

3.4. ANALYSIS OF MICROSTRUCTURE

3.4.1. ^{13}C N.M.R. SPECTROSCOPY

The experimental conditions employed in the present $^{13}CN.M.R.$ study are consistent with those employed by Willoughby (1989) in his structural study of N.B.R.. N.B.R. polymer samples were dissolved in deuterochloroform at concentrations in the region of 0.1 g per ml. T.M.S. (tetramethyl silane) formed the internal reference standard. Spectra were obtained at room temperature (22°C-23°C). The number of scans compiled per sample was approximately 12000. The spectrometer used was a (Jeol JNM ZX 270), of the N.M.R. service, University of Bath. The instrument was operated at 100.4 MHz. Integration of peak data was performed by manufacturer's software supplied with the instrument.

Sequence distribution in the N.B.R. samples was calculated in accordance with the $^{13}C.N.M.R.$ frequencies assignments of Willoughby (1989), who showed AAA, BAB, BBA, ABA, ABB and BBB tri-additions to appear at characteristic frequencies. In this representation A signifies an ACN unit and B signifies a butadiene unit.

Normalised tri-addition distribution was calculated by assuming that the sum of all tri-addition absorption is equal to unity. The fraction of ACN centred tri-addition is equvalent to the mole fraction of combined ACN and the fraction of butadiene centred groups is representative of the mole fraction of combined butadiene.

3.4.2. INFRA-RED SPECTROSCOPY

Polymer samples were analysed on a Perkin Elmer, Fourier Transform infra-red spectrometer, model 1720 using the attenuated reflection spectroscopy (A.T.R.) technique, (section 2.3.5.1, figure 2.5). A thallium bromo-iodide (KRS-5) crystal of refractive index 2.4, formed the internal reflection element. The critical angle of reflection was maintained at 60° throughout. Thin sheet samples (10 mm x 10 mm) were used for all F.T.I.R. analysis. Resolution was maintained at 2 cm^{-1}. 100 scans were performed for each sample to obtain sufficient spectral resolution.

Background spectra were periodically recorded by scanning with the crystal, clamped in the A.T.R. attachment, in the absence of sample. For background spectra resolution was maintained at 2 cm^{-1} and the number of scans used was 50.

3.4.3. DIFFERENTIAL SCANNING CALORIMETRY

Raw nitrile rubber samples of weight in the region of 10-15 mg were scanned on a differential scanning calorimeter, DuPont 9900 instrument. Samples were cooled from room temperature to -80°C at a controlled cooling rate of 5°C per minute using a DuPont L.N.C.A. II cooling accessory. Upon reaching -80°C samples were immediately re-heated at specific heating rates of 2°C per minute, 5°C per minute, 7°C per minute, 10°C per minute, 15°C per minute, and 20°C per minute.

A two point temperature calibration was performed at each heating rate with ice (melting point, 0°C) and indium (melting point 156.6°C). Integration of area was made by D.S.C. version 2.2 software supplied with the instrument. The cell calibration constant was obtained by calibrating with respect to the experimentally observed endothermic melting peak of indium (heat of fusion 28.4 J/g).

The onset and end of glass transition was determined by fitting tangents to measured profiles in the temperature region where a step change in heat flow occurred. The temperature difference between onset and the end of the glass transition represents the width of transition $\Delta T_{(Tg)}$. The change in heat capacity at the glass transition is calculated from the heat flow change ($\Delta Cp_{(Tg)}$) between the onset and end of the glass transition. These experimental terms are illustrated in figure 3.1.

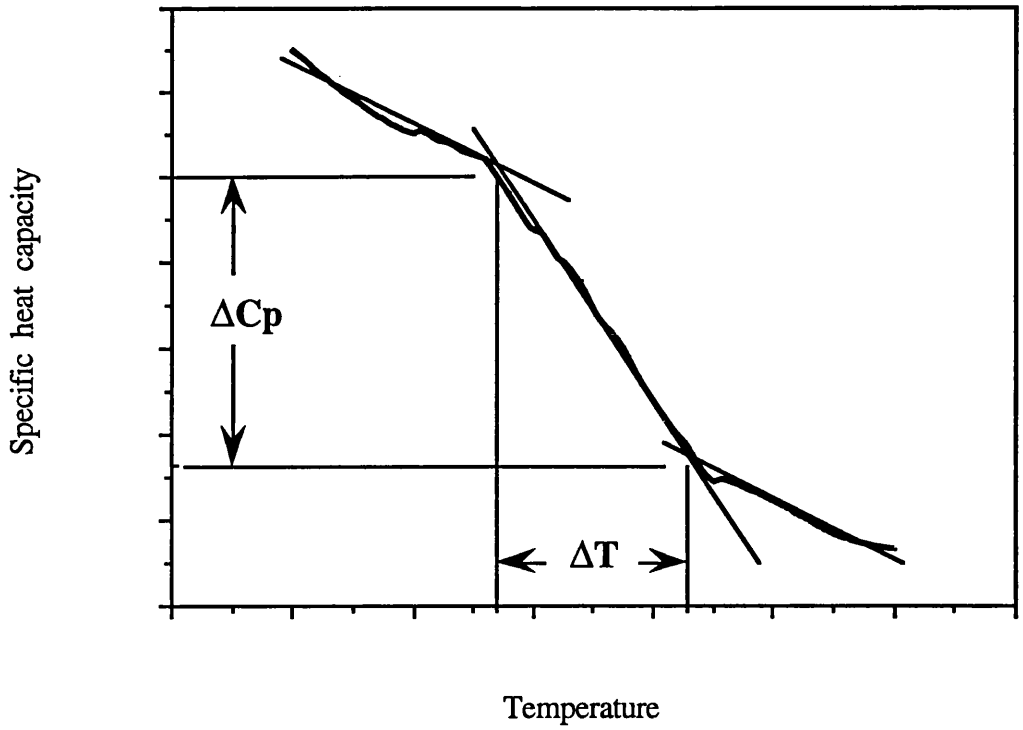

FIGURE 3.1. Illustration of terms used to characterise D.S.C., glass transition data.

3.5. DETERMINATION OF RAW POLYMER VISCOSITY

3.5.1. T.M.S. RHEOMETRY

Viscosity measurements in the region of 1-20 s^{-1} were carried out on a 'cone and plate' type T.M.S. (Turner, Moore and Smith) rheometer. The instrument is located at the Centre for Polymer Studies. The instrument used is an early design which was manufactured by S.P.R.I. of Dorking, U.K.. A commercial T.M.S. instrument developed from this early design is marketed by Negretti Automation of Aylesbury, U.K..

In this instrument sample is injected from a transfer chamber and moulded around a smooth biconical rotor (cone angle 6°) which is then rotated enabling measurement of shear stress and shear rate.

All measurements were made at a test temperature of 120°C with an injection time of 30 seconds and an injection pressure of 80 psi. This test temperature is

representative of practical processing temperatures. After injection of raw polymer the shear stress on the rotor was increased in incremental steps of 10 kPa between 30 kPa and 190 kPa. Rotor speed was recorded on an Advanced Bryans chart recorder.

Shear stress calibration was performed before testing by applying a known shear stress to a calibration rotor by means of a calibration frame and weights.

3.5.2. CAPILLARY RHEOMETRY

A capillary rheometer, Instron model 3211, located at the Centre for Polymer Studies, was used to determine the rheological properties of N.B.R. polymers at rates of shear which are inaccessible to the T.M.S. rheometer (in excess of 40 s^{-1}). High rates of shear in the region of 2000 s^{-1} are encountered in practical processing such as injection moulding and in new generation, more capable mixing type extruders with shear heads and cavity add on transfer mixers. Shear stress and shear rate were determined from capillary rheometry by measuring the pressure drop across the capillary and applying Poiseuille's equation (Brydson, 1981).

$$\Delta P = \pi R^3 2L(\eta 4 \dot{Q})^{-1} \qquad (3.1)$$

where, ΔP represents the pressure drop across the capillary, R is the capillary radius, L is the capillary length, η is the apparent viscosity and $\dot{Q}$ is the volumetric flow rate.

Experiments were carried out at 120°C with two capillary dies of different dimensions. Die 1 was of diameter 1.27 mm and length 25.4 mm. Die 2 was of diameter 1.277 mm and length 50.8 mm.

Experimental procedure involved feeding raw polymer into the heated rheometer barrel taking care to exclude air from the barrel. In the next step the rheometer extrusion ram was brought down via the motorised drive to compress the polymer melt. Compression was deemed sufficient when polymer began extruding from the die orifice. After compression the ram was stopped and the material allowed to equilibrate at the test temperature for a period of 1 minute. At the end of the warm up time the ram was brought down at several pre-set speeds, available to the instrument, starting from the lowest. Extrusion pressure (pressure on the ram) was monitored by means of an Advanced Bryans chart recorder. When the pressure reading at a pre-set extrusion speed

reached a plateau value the speed of extrusion was increased to the next available speed setting.

The raw data obtained from the capillary rheometer were corrected to overcome entrance and end effects by application of the Couette-Hagenbach correction, (Brydson, 1981).

$$\tau_w = (P_1-P_2)\, R[2(L_1-L_2)]^{-1} \qquad (3.2)$$

where, τ_w is the wall shear stress, P represents the pressure drop across the capillary ($P_1>P_2$), L and R are the length and radius of the capillary, respectively ($L_1>L_2$).

Due to the non-Newtonian nature of polymer melts an additional non parabolic shear rate, γ correction was made (Rabinowitsch correction).

$$\dot{\gamma}_w = 4\,\dot{Q}/(\pi\, R^3)\,(3n + 1)/4n \qquad (3.3)$$

where n is the melt flow index.

3.6. COMPOUNDING

Polymers were formulated with two simple sulphur based gumstock formulations (table 3.3). The formulations used are based on a previous research project by Sims (1988) on the relationship between composition and density of crosslinks and dynamic mechanical properties of accelerated sulphur vulcanizates of N.B.R.

Compounds were prepared by mixing formulation components of table 3.3 on a laboratory size 2-roll mill. Mixing was carried out at room temperature, with water cooling on throughout the mixing process. A two stage mixing procedure was used to ensure good dispersion of sulphur and minimise the risk of pre-vulcanization. The activator and crosslinking agent were mixed into N.B.R. in the first mixing stage. Accelerator and antioxidant were added into the stage one mix in a second mixing stage. Mixing procedures used for compound preparation are tabulated in tables 3.4 and 3.5.

	Formulation	
Ingredient	A	B
Base polymer	100	100
Zinc oxide	5	5
Stearic acid	1	1
C.B.S.	1.5	1.5
M.C. Sulphur	1.5	1.5
Permanax BLW*	0	2

*Permanax BLW = diphenyl amine antioxidant, addition is in weight parts.

TABLE 3.3. N.B.R. compound mix formulations.

Time, minutes	Addition
0	Base polymer
3.5	Vulcanizing agent
5.5	Activator system
12	Compound sheeted off

TABLE 3.4. First stage, N.B.R. mixing schedule.

Time, minutes		Addition
A	B	
0	0	Stage one mix
-	1	Antioxidant
1	4	Accelerator
5	7	Compound sheeted off

TABLE 3.5. Second stage, N.B.R. mixing schedule.

3.7. DETERMINATION OF CURE CHARACTERISTICS

3.7.1. MONSANTO RHEOMETER

Compounded samples were tested on the Monsanto Tm_{100} rheometer which is located at the Centre for Polymer Studies. The vulcanization temperature used for these experiments was maintained at 150°C for all compounds. The arc of oscillation was 1°.

3.7.2. DIFFERENTIAL SCANNING CALORIMETER

3.7.2.1. Differential Calorimetry Technique

Differential calorimetry (D.C.) experiments involved equilibrating the D.S.C., (DuPont, model 9900) instrument at 150°C, without sample. For all experiments the cell was continuously purged with nitrogen at a flow rate of 2 ml per minute.

Compound samples, typically 20 mg, were crimped in aluminium pans and introduced into the D.S.C. sample cell, once equilibriated. The temperature was found to initially drop from the set point, as sample is introduced into the instrument but quickly recovers and is within thermal equilibrium in approximately 2 minutes of sample introduction. Experiments were conducted at 140°C, 150°C, 160°C and 170°C.

The small sample size used in these studies necessitates adequate dispersion of compounding ingredients. Reproducibility was checked by repeating experiments.

3.7.2.2. Differential Scanning Calorimetry Technique

Under non-isothermal, scanning mode conditions samples, typically 20 mg were crimped in aluminium pans and introduced into the D.S.C. at room temperature. Samples were then subjecting to a continuous temperature increase at a controlled heating rate. Continuous nitrogen purge was maintained throughout the heating process at 2 ml per minute. Experiments were stopped when the sample reached 350°C.

Samples were scanned at heating rates of 5°C per minute, 7°C per minute, 10°C per minute and 15°C per minute. Calibration was performed at each heating rate with tin, (melting point 231.9°C) and indium, (melting point 156.6°C, heat of fusion 28.4 J/g).

3.7.2.2.1. D.S.C. Study of Compounding Chemicals Interactions

Compounding ingredients and mixtures of compounding ingredients were heated in calibrated D.S.C. at a heating rate of 5°C per minute. Mixtures of compounding ingredients were prepared by combining and mixing accurately weighed amounts in aluminium sample pans with tweezers. For these studies continuous nitrogen flow was maintained throughout heating at flow rate of 2 ml per minute.

3.8. PREPARATION OF VULCANIZATE SHEETS

Vulcanized test sheet samples (127 mm x 127 mm x 1 mm) were prepared by compression moulding rubber compounds at 150°C in a laboratory size Moore compression press, with reconditioned electrically heated platens controlled by CAL 9900 temperature controllers. Compound sample moulding blanks of approximate weight 20 g were introduced into the compression mould, preheated to the vulcanization temperature. The mould was maintained under pressure of (250 Bar) and the moulding temperature for the duration of vulcanization.

Cure times (time to 95 % conversion) were determined from Monsanto rheometer rheographs. At the completion of cure the vulcanized sheets were removed from the compression mould and immediately submerged in water maintained at room temperature to stop further reaction.

3.9. CHARACTERISATION OF VULCANIZED POLYMERS

3.9.1. NETWORK EXTRACTION

This study used network extraction conditions established by Sims (1988) in the study of N.B.R. network structure. The study uses a cold (room temperature) Soxhlet extraction technique to reduce the possibility of network maturation during extraction.

Experimental procedure involved extracting accurately pre-weighed vulcanized rubber sheets (80 mm x 80 mm x 1 mm) for a continuous period of 48 hours. The extraction apparatus used is illustrated in figure 3.2. An azeotropic mixture of acetone 110 pbv (parts by volume), 1,1,1-trichloroethane 60 pbv and methanol 42 pbv was the extraction solvent used. After extraction the vulcanizates were desorbed under vacuum at room temperature until constant weight.

The difference in weight between unextracted and extracted vulcanizates was used to calculate the weight percentage of extra network material.

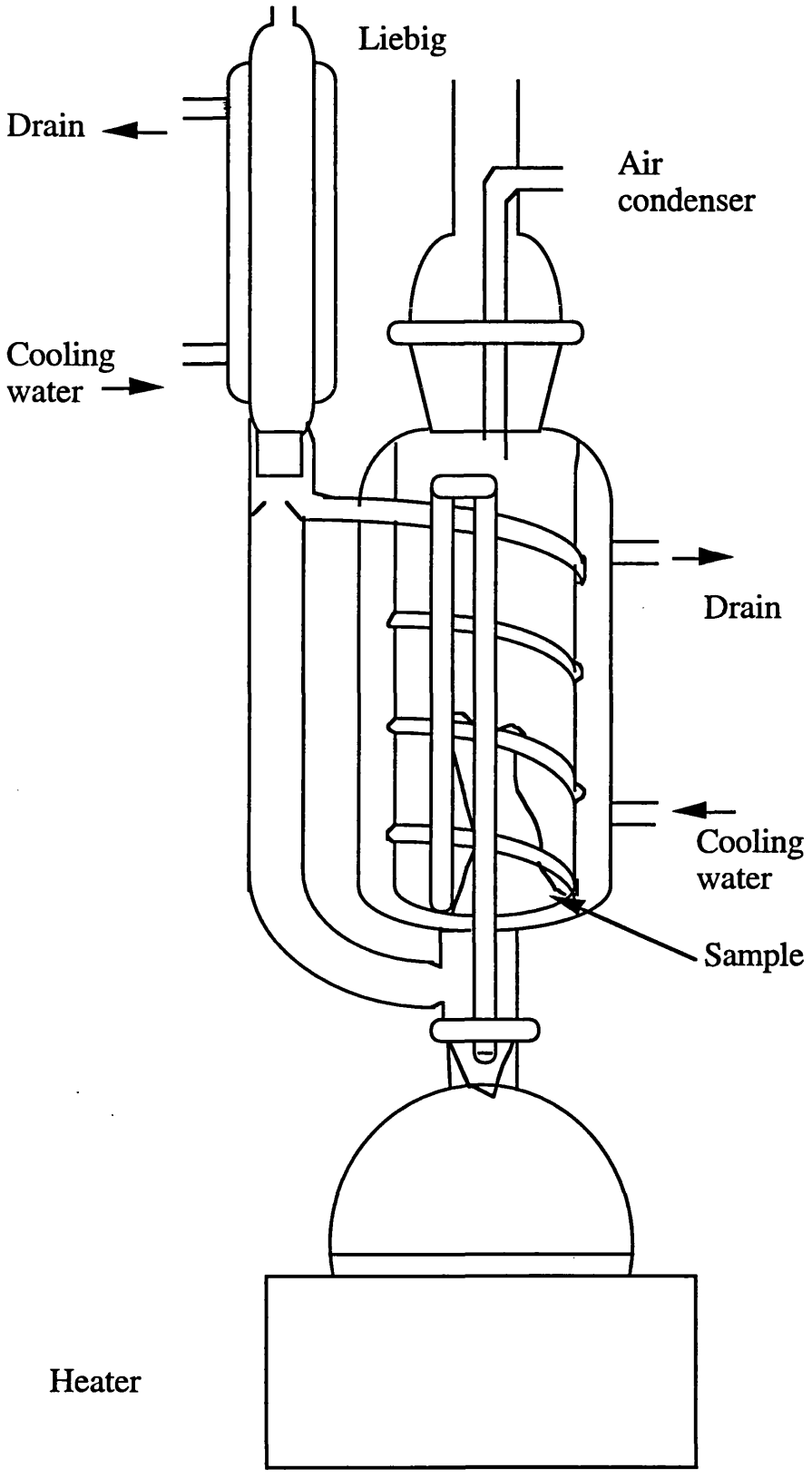

FIGURE 3.2. Cold extraction apparatus used in extraction of vulcanized samples.

3.9.2. DETERMINATION OF CROSSLINK DENSITY

3.9.2.1. Tensile Stress-Strain Measurement on Dry Networks

Tensile stress-strain measurements were conducted on an Instron 1195 tensile testing machine with a 50 kg load cell. Calibration was performed before testing and chart recorder full scale adjusted to 10 % of load cell capacity.

Work was carried out on parallel sided test samples (4 mm x 1 mm x 127 mm). Sample dimensions were accurately measured with Mitutoyo Digimatic calipers. Test samples were clamped in the grips of the tensometer at a gauge length of 50 mm. Initial gauge length was set by accurately setting the crosshead travel stops.

Prior to tensile testing, samples were conditioned using conditions of Sims (1988) by extending to 160 % elongation ($\lambda = 2.6$), at a grip separation rate of 20 mm per minute. Samples were held in the extended form for 15 minutes then released and allowed to relax for 45 minutes. Such conditioning reduces polymer hysteresis effects.

Testing involved extending samples at a grip separation rate of 20 mm per minute. Three experiments with separate testpieces were performed for each vulcanizate.

3.9.2.2. Compression-Deflection Measurement on Swollen Networks

3.9.2.2.1. Swelling of Networks

Rubber samples (3 testpieces for each sample) were punched out of pre-extracted vulcanized sheets and immersed in Analar toluene. The samples of dimensions 6 mm x 6 mm x 1 mm were subjected to swelling at room temperature in the dark. All 3 samples were cut from the same vulcanized sheet. Individual samples were contained in separate sample bottles. Swollen samples were periodically removed from toluene and weighed in a closed pre-weighed sample bottle. Before weighing, excess solvent present on the surfaces of samples was absorbed by blotting with Whattman filter paper. Swollen samples were always handled with flat nose tweezers. Swelling experiments were stopped when samples reached equilibrium weight.

3.9.2.2.2. Compression Deflection Reticulometer Testing

Compression measurements on samples swollen to equilibrium in Analar toluene were carried out on a Wallace-Smith compression deflection reticulometer, located at the Centre for Polymer Studies. The instrument is illustrated in figure 2.3.

Network extracted samples swollen to equilibrium in Analar toluene were immersed in the solvent bath of the compression-deflection reticulometer, (containing Analar toluene) and the compression foot was brought down until submerged in the solvent. At this stage the null point was brought to zero by adjustment of the null adjuster. The compression foot was then brought down further until contact with the sample was established, this being made apparent by a movement of the null indicator. The compression foot is locked into this position and the pre-load of 30 g applied to the sample. The null point was brought back to zero after application of the pre-load. A pre-load of 30 g was applied to overcome surface irregularities. A calibration load of 100 g was then applied and the deflection necessary to bring the null indicator back to zero was noted. The deformation produced by a 100 g load was used to calculate the compressive load necessary to produce a 15 % deflection (excess load). The sample which was used to calculate the excess load was discarded.

The calculated excess load is applied onto a fresh swollen sample and quickly removed. This step flattens the sample and overcomes problems with sample barrelling. After an adequate relaxation time incremental loads of 10 % of the calculated excess load were added and the deflection noted. Deflection measurements were made for increasing and decreasing loads. Only decreasing loads were used to calculate C_1 because under these conditions entanglement and polymer chain interaction effects are reduced. The attainment of equilibrium stress also occurs within a shorter time during decreasing loading. Compression measurements at low deflections (below 5 %) were ignored.

3.9.2.3. Chemical Probing of Vulcanizates

Network characterisation studies were conducted by treating network extracted nitrile rubber vulcanizates with established thiol-amine chemical probe reagents.

3.9.2.3.1. Treatment with Hexane-1-thiol (1M) in Piperidine

In order to cleave di-sulphide and poly-sulphide crosslinks samples were treated with hexane-1-thiol (1M) in piperidine solution. Treatment was carried out in sample bottles under nitrogen for 72 hours at 23°C using an excess of probe reagent.

3.9.2.3.2. Treatment with Propane-2-thiol (0.4M) + Piperidine (0.4M) in Solvent

The following two treatments were used to cleave poly-sulphide crosslinks while not affecting mono-sulphide and di-sulphide crosslinks:

Network extracted samples which were pre-swelled in toluene for 16 hours at room temperature under nitrogen were treated with propane-2-thiol (0.4M) + piperidine (0.4M) in toluene solution for 2 hours at 23°C in the dark under nitrogen.

Network extracted samples were also treated by pre-swelling in n-heptane for 16 hours under nitrogen followed by probing with propane-2-thiol (0.4M) + piperidine (0.4M) in n-heptane solution at 23°C under nitrogen for 2 hours.

3.9.2.3.3. Extraction of Probe Reagent from Treated Networks

Imbibed chemical probe solution was removed from treated networks by liquid liquid extraction with petroleum ether. Experimental procedure involved decanting the chemical probe solution, at the end of the reaction time and replacing with petroleum ether. The petroleum ether was decanted after 1 hour and fresh petroleum added. This washing procedure was repeated a further 4 times. At the end of the washing process the samples were left under vacuum at room temperature, in the dark until constant weight was achieved and the percentage of extracted material was recorded.

3.9.2.3.4. Treatment with Excess Methyl Iodide

Further treatment of several hexane-1-thiol (1M) in piperidine probed samples was by reaction with an excess of methyl iodide in the dark and absence of air at a temperature of 70°C for 10 days. Methyl iodide was removed from networks after treatment by washing with light petroleum ether. The washing procedure was identical to that of section 3.9.2.3.3.

3.9.2.4. Determination of Network Extracted Material

Material extracted from vulcanizates during chemical probe treatment and treatment with piperidine alone for 72 hours was analysed by F.T.I.R.. Analysis was made by the specular reflection technique. Samples were prepared by spreading a few drops of solutions on aluminium sheet and allowing solvent to evaporate at room temperature.

The F.T.I.R. instrument was operated at a resolution of 2 cm^{-1}. The number of scans compiled per sample was 100. Background scans were made on polished aluminium sheet using a resolution of 2 cm^{-1} and 50 scans.

3.9.2.5. Solid State ^{13}C N.M.R. Spectroscopy Study of Vulcanizates

Selected vulcanizates were analysed by solid state ^{13}CN.M.R. spectroscopy in order to obtain further information on crosslink structure in vulcanizates. Because time and resources did not allow for the study of all vulcanizate samples it was decided to work with the two polymers which elemental and structural analysis indicated would be of greatest interest. Work was with vulcanizates of EA, EB, PA and PB. Vulcanizates which were analysed by ^{13}C N.M.R. were subjected to network extraction, (described in section 3.9.1.).

The instrument used in this study is based at the solid-state N.M.R. Service, University of Durham, U.K. and was operated by Dr. D. Apperley. Samples were converted into powder form by grinding vulcanizates cooled to below Tg with a facility available to Dr. Apperley.

Experimental conditions used for ^{13}C N.M.R. spectroscopy were based on previous studies of Gronski and Hoffman (1992) and Krejsa and Koenig (1993b).

The spectrometer was operated at 75.43 MHz, with a spectral width of 7.5 Hz. The number of scans per sample was 8000 with an acquisition time of 40.5 ms. The experiments used gated decoupling with a pulse angle of 90° and spin rate of 7500 Hz. All experiments were performed at room temperature.

3.9.2.6. X.P.S. Study of Vulcanizates

The chemical structure of sulphur and zinc species and the role of polymerisation residues in vulcanization were examined by X.P.S.. Analysis was made on untreated vulcanizates of EA, EB, PA and PB. Work was based on these samples to complement results from ^{13}C N.M.R. spectroscopy. The X.P.S. was operated at 12.5 kV and 40 mA with an Al anode. The analyser pass energy was maintained at 50 eV throughout.

Sample surfaces were prepared by cutting into vulcanizates, thereby exposing the sample surface to the atmosphere immediately before insertion into the X.P.S. chamber.

All samples were inserted into the X.P.S. chamber at the same time and outgassed under vacuum at room temperature for 2 days.

3.9.2.6.1. Mass Spectroscopy

Molecular fragments released from samples by X-ray bombardment during X.P.S. analysis were analysed by an attached mass spectrometer, (HAL 320 gas analyser). The concentrations of the ten most abundant fragments were measured by change in partial pressure.

3.9.2.6.2. Model Compound Studies

Because there appers to be no published literature on the binding energies of zinc and sulphur in zinc accelerator species and some dispute on the binding energies of other zinc-sulphur chemical species, it was decided to conduct model compound studies on several such species. Model compounds were prepared by mixing into N.B.R. polymer zinc oxide, zinc sulphide, zinc di-methyl dithiocarbamate, zinc di-ethyl dithiocarbamate and zinc stearate. Mixing was carried out on a 2-roll mill which was maintained at room temperature.

X.P.S. analysis of model compounds was made using the conditions employed for X.P.S. study of N.B.R. vulcanizates, (section 3.9.2.6).

3.10. MECHANICAL PROPERTIES

3.10.1. DETERMINATION OF STATIC TENSILE PROPERTIES

The tensile properties of N.B.R. vulcanizates were determined in accordance with recommendations and conditions specified in BS903, part A2, (1989). Tensile test samples, (dumbbells) type 2, punched out of vulcanized sheet were tested on an Instron 1195 tensometer at a crosshead speed of 500 mm per minute. Extension of samples was followed with the use of an attached Wallace optical extensometer. Six testpieces were tested for each sample. Sample dimensions were measured with Mitutoyo Digimatic calipers.

3.10.2. DETERMINATION OF TEAR PROPERTIES

Tear strength was measured in accordance with BS 903, part A3 method A, (1982) using trouser tear samples. Testpieces (six for each sample) were tested at a crosshead speed of 100 mm per minute. Testpiece thickness was measured with Mitutoyo Digital calipers.

3.10.3. DETERMINATION OF HARDNESS

Hardness measurements were made by a Wallace I.R.H.D. (international rubber hardness degrees) tester on samples of approximate thickness 3 mm. Testpieces were prepared by plying up three vulcanizate sheets of nominal thickness 1 mm. Measurements were made in accordance with testing instructions recommended by its manufacturer and BS 903 part A26, (1982). The instrument is calibrated to the international rubber hardness scale and values obtained are quoted as international rubber hardness degrees. For each sample three hardness readings were obtained.

3.10.4. DETERMINATION OF DYNAMIC PROPERTIES

A Rheovibron DDV-II manual reading instrument was used to determine the dynamic properties of the rubber vulcanizates. The instrument uses an inline stretching arrangement which is convenient for testing low modulus materials and testpieces of dimensions which are obtained from the parrallel side portion of tensile dumbell type testpieces.

The Rheovibron DDV-II was operated according to the instructions of the manual using a frequency of 11 Hz. The rubber samples were in the form of 1 mm thick, 4 mm wide strips. The distance between the sample grips was maintained at 20 mm. Samples were cooled rapidly to temperatures in the region of -25°C followed by heating at an approximate heating rate of 2°C per minute. Tan δ values were read directly, during the heating cycle.

Stress and strain gauges were calibrated before experimental measurements.

Experiments were repeated on a Polymer Labs. D.M.T.A. instrument, located at D.R.A., Holton Heath. This instrument used a dual cantilever 3 point bend arrangement to deform the sample. The rubber strips (7 mm x 1 mm x 20 mm) were clamped in the frame in a slightly strained form and rapidly cooled to -40°C. At -40°C the clamps holding the sample in place were tightened and a test run was commenced. A controlled heating rate of 2°C per minute was used in combination with a frequency of 10 Hz.

CHAPTER IV

4.0. CHARACTERISATION; RESULTS AND DISCUSSION

This chapter presents results on characterisation of the five polymers and ten vulcanizates used in this study. The results discussed here are of importance because they show the range of structures and residues that may be encountered in equivalent N.B.R.s and their vulcanizates. They also establish the foundation for understanding results on the thermo-oxidation of vulcanizates presented in chapter six.

The chapter is arranged into five sections. Data on elemental composition and structural composition of polymers are presented and discussed in sections 4.1 and 4.2, respectively. Rheological behaviour of polymers is also presented in section 4.2. Sections 4.3 and 4.4 discuss vulcanization behaviour of polymers and characterisation of vulcanizate network structure, respectively. Section 4.5 presents results on static and dynamic properties, of vulcanizates.

4.1. ELEMENTAL COMPOSITION

Atomic concentrations of carbon, hydrogen and nitrogen of N.B.R. determined by chemical analysis are given in table 4.1. The reproducibility of measured values presented in table 4.1 is ±0.9 %.

Theoretical concentrations of carbon, hydrogen and nitrogen which are calculated from manufacturers' data of combined ACN content, (table 3.2) are shown in table 4.2. Table 4.3 shows the concentration of trace residues not shown in tables 4.1 and 4.2. The reproducibility of results shown in table 4.3 is better than ±10 %.

The concentration of carbon, hydrogen and nitrogen in N.B.R. is little affected by a change in base polymer. This is consistent with the similar combined ACN content of these polymers, (section 3.1, table 3.2).

The concentration of elemental nitrogen found on the surface of N.B.R. by X.P.S. is shown in table 4.4. Table 4.4 shows large variation in nitrogen between polymers. The concentration of nitrogen is approximately 2.9 times higher in polymer E than it is in polymer P. This implies that polymer E contains a nitrogen rich surface

layer, possibly caused by migration of nitrogen rich species. These differences in surface nitrogen between polymers are discussed in detail in section 4.4.3.2.

Element weight %	B	E	G	N	P
Carbon	82.14	83.05	82.40	82.95	83.41
Hydrogen	9.63	9.68	10.02	9.65	10.11
Nitrogen	7.26	7.67	7.45	7.67	6.84

TABLE 4.1. Experimentally determined elemental composition of N.B.R..

Element weight %	B	E	G	N	P
Carbon	82.90	82.94	82.96	82.94	83.17
Hydrogen	9.55	9.56	9.57	9.56	9.62
Nitrogen	7.55	7.50	7.47	7.50	7.20

TABLE 4.2. Theoretical elemental composition of N.B.R., calculated from combined ACN determined by manufacturers.

Element mol./g x10^6	B	E	G	N	P
Sulphur	37.31	70.31	37.19	67.50	49.53
Sodium	5.40	1.23	0.68	1.00	4.32
Calcium	4.95	2.40	0.95	22.60	75.30
Magnesium	6.08	28.00	~	0.63	~
Chlorine	4.22	1.18	~	6.18	12.50
Iron	0.01	0.46	0.54	0.29	0.02
*Water, wt%	0.69	0.78	0.81	0.61	0.64

~None detected. *Water in hydrated salts not included.

TABLE 4.3. Trace elemental residue composition of N.B.R..

Element atomic %	B	E	G	N	P
C_{1s}	94.5	92.7	95.9	94.5	96.9
N_{1s}	4.9	7.0	3.9	4.9	2.4
$S_{2p(164eV)}$	~	0.1	0.1	0.2	~
$S_{2p(169eV)}$	0.6	0.1	0.1	0.4	0.6

~None detected.

TABLE 4.4. Atomic percentage of carbon, nitrogen and sulphur found on the surface of raw N.B.R. by X.P.S..

Chemical analysis, (table 4.3) shows that all polymers contain sulphur in excess of 37.0 moles x 10^{-6} per gramme of polymer. The sulphur level of polymer E (70.3 moles x 10^{-6} per gramme of polymer) is particularly high. Sulphate/sulphonate emulsifiers and alkyl mercaptan modifiers which are introduced into N.B.R. during its polymerisation, as discussed in sections 2.1.2.1 and 2.1.2.4 are likely to be the origin of this sulphur. This matter is further considered in section 4.1.1 below.

Sodium which is present in all the polymers is associated with emulsifier and also coagulant residues (Reeves and Packham, 1992; Reeves, Kiroski and Packham, 1993; Lotfipour et *al.*, 1994). This is discussed in sections 2.1.2.1. and 2.1.2.4.

Other elements such as Mg and Ca are thought to be coagulant residues, (sections 2.1.2.1 and 2.1.2.4). Polymer E and polymer B appear to have been coagulated with magnesium salts, (such as $MgCl_2$). Elemental analysis would indicate that polymer P and N are coagulated by calcium salts, (such as $CaCl_2$). Polymer G is the cleanest polymer, (as determined by elemental analysis) and contains the lowest concentration of polymerisation residues. Iron which is present in all polymers may be residue from the Redox initiator systems. Iron has been used as a co-agent in such systems (section 2.1.2.1). Alternatively it may simply be contamination, since much of the polymerisation equipment is fabricated from stainless steel, (section 2.1.2.2).

For all polymers simple addition shows that there is a considerable excess of cations (Mg, Ca and Na) compared to the concentration of anions. This suggests that a high proportion of the cations must be combined with chemical species not shown in table 4.3 such as carboxylic acids residues. The proportion of carboxylic acid emulsifier residue of polymers which is in the salt form may be low because formation

of soap from fatty acid, during early stages of coagulation is reversed during final stages of coagulation, by the addition of dilute sulphuric acid, (section 2.1.2.3).

4.1.1. NATURE OF SULPHUR RESIDUES

Elemental results presented in table 4.3 show that sulphur species are present in all polymers at significant concentrations.

Information on the chemical structure of sulphur species (whether likely to be emulsifier residues or transfer agent residues), determined by X.P.S. is given in table 4.4. Use of X.P.S. for determination of chemical bonding of sulphur is possible because different sulphur species emit electrons of different binding energy, (refer to section 2.3.5.2). Sulphur which is bonded to sulphur, hydrogen, carbon, such as mercaptan transfer agent residue has been shown to emit electrons with a characteristic binding energy in the region of 164 eV (Lotfipour *et al.*, 1994). Emulsifier sulphur species in the form of sulphate or sulphonate occur at a binding energy in the region of 169 eV.

The X.P.S. technique is highly surface sensitive, (section 2.3.5.2) therefore results of table 4.4 should be viewed with caution since chemical composition of surface regions is often different from that of the bulk polymer due to migration of chemical species from the bulk polymer to the surface (Lotfipour *et al.*, 1991; Reeves *et al.*, 1995).

X.P.S. results in table 4.4 show that all sulphur in P and B occurs at 169 eV. It is postulated, therefore that all sulphur present in polymers P and B is associated with sodium alkyl/aryl sulphate and sodium alkyl/aryl sulphonate emulsifier residues (such as sodium lauryl sulphate and sodium dodecyl benzene sulphonate). This postulate is supported by elemental analysis results presented in table 4.3 which show that polymers P and B contain over three times more sodium than the other polymers.

Polymer N shows a similar total sulphur concentration as polymers P and B. However in polymer N both oxygen bonded and carbon, hydrogen, sulphur bonded sulphur is detected. Also found in the hot methanol extract of polymer N were trace levels of elemental sulphur (S_8). There seems to be no recent reference to the use of elemental sulphur in the polymerisation of N.B.R., however a detailed monograph into emulsion polymerisation, published in the 1950's by Bovey, Kolthoff, Medalia and Meehan (1955), suggests that elemental sulphur has a very strong retarding effect in the

polymerisation of styrene and is also a fairly effective chain terminator. It is therefore likely that detected elemental sulphur is uncombined residue from the polymerisation process.

In polymers E and G approximately 50% of the total sulphur detected is oxygen bonded and the remainder bonded to carbon, hydrogen, sulphur. Some of the oxygen bonded sulphur of polymer E is in the form of dinaphthyl sulphone. Dinaphthyl sulphone was extracted from polymer E by hot methanol extraction. This is treated further in section 4.1.3.

X.P.S. results show polymer E to have a lower sulphur concentration in comparison with other polymers, (table 4.4) than shown by chemical elemental analysis, (table 4.3). The relatively low level of total sulphur, found on the surface of polymer E compared to the bulk and other polymers is likely to be associated with differences in mobility and migration of such species. Transfer agent sulphur residues which are inferred in polymer E, from table 4.4 will not migrate to the surface because they are combined with the polymer.

Aluminium, which may be associated with aluminium sulphate coagulants, (Reeves *et al.*, 1993) such as $(Al)_2(SO_4)_3$ could not be detected in any polymer by X.P.S..

4.1.2. CARBOXYLIC ACID RESIDUES

There are significant differences in total concentration of hot methanol extractable materials between the polymers, (table 4.5). The concentration of such material differs considerably with polymer. Similar results for commercial N.B.R. of 34 weight % combined ACN content have been reported by Reeves and Packham (1992).

Polymer G, (at 5.39 %) has a much higher level of methanol extractable material, than polymers B, E, N and P. A high proportion of methanol extractable material is likely to be carboxylic acid emulsifier. Carboxylic acid salts and sulphate/sulphonate salts are not soluble in methanol and therefore not extracted (Reeves and Packham, 1992). Polymers B, E, N and P while having a lower concentration of methanol extractable residue have much higher concentrations of calcium and magnesium residue. This may imply that some carboxylic residues in polymers B, E, N and P are in the form of insoluble carboxylic acid salts.

Elemental analysis results presented in tables 4.3 and 4.4 showing polymer G to have a low concentration of sodium and sulphur may suggest that the manufacturers of polymer G use mostly carboxylic acids as emulsifier.

The composition of methanol extract (table 4.6) differs considerably with polymers. All the polymers contain a range of saturated carboxylic acids of various molecular weights. Polymer B contains species of lowest molecular weight, (mainly lauric acid, $C_{11}H_{23}COOH$). Polymers N and P contain mostly erucic acid, ($C_{21}H_{43}COOH$). Polymers G and E contain a mixture of stearic acid, ($C_{17}H_{35}COOH$) and palmitic acid, ($C_{15}H_{31}COOH$). Polymer E also contains lauric acid. Polymer G, in contrast to other polymers contains unsaturated oleic acid, (cis-9-octadecanoic).

Polymer	Weight %
B	1.97
E	2.08
G	5.39
N	2.49
P	3.12

TABLE 4.5. Weight of material extracted from N.B.R. polymer by continuous hot methanol extraction.

Acid type weight %	B	E	G	N	P
Lauric	62.6	35.8	~	~	~
Myristic	13.3	1.2	9.7	~	8.0
Palmitic	8.3	16.9	24.2	~	3.3
Oleic	~	~	19.3	~	~
Stearic	10.8	43.8	42.1	14.5	20.9
Eicosanoic	4.8	0.7	1.9	~	~
Erucic	~	1.7	2.6	82.7	67.9

~None detected.

TABLE 4.6. Composition of material extracted from N.B.R. polymer by hot methanol extraction.

4.1.3. ANTIOXIDANT RESIDUES

U.V. spectroscopy studies have shown that all five polymers used in this study contain methanol extractable chemical species whose U.V. absorption spectra are characteristic of antioxidant U.V. spectra published by Hummel and Scholl (1981). The U.V. spectra of the methanol extract solutions are shown in figures 4.1 and 4.2. The presence of antioxidant residues was expected since it is usual commercial practice to add antioxidants to N.B.R. polymers during the latter stages of manufacture, (refer to section 2.1.2.3). Antioxidants are added for the purpose of protecting polymer from degradation during hot air drying and storage. U.V. spectroscopy indicated that the five N.B.R. polymers contain different antioxidant species however comparison of spectra with reference U.V. spectra did not enable quantitative identification of antioxidant types.

Separation and identification of individual antioxidant types was made by mass spectroscopy. The chemical structures of the antioxidants found are shown in figure 4.3.

The methanol extract of polymers B and P contains predominantly 2,2-methylene bis-[6-(1,1-dimethylethyl)-4-methyl-phenol]. N-Octadecyl-3-(3',5'-di-tertiary butyl-4'-hydroxyphenyl) propionate is present at lower concentration.

The methanol extract of polymer E contains mainly 2,6-di-tertiary butyl-p-cresol and low levels of n-octadecyl-3-(3',5'-di-tertiary butyl-4'-hydroxyphenyl) propionate. A minor component tentatively identified as di-naphthyl sulphone is also found.

The methanol extract of polymer G contains octadecyl-3-(3',5'-di-tertiary butyl-4'-hydroxyphenyl) propionate as a minor component. The major antioxidant type is highly substituted butylated phenol. Also found were traces of oleic acid. The presence of oleic acid in the methanol extract of polymer G has also been determined by G.L.C., (section 4.1.2, table 4.6).

The methanol extract from polymer N does not contain substituted phenol type antioxidants. The major species extracted from polymer N was found to be the dioctyl ester of hexanedioic acid, ($(CH_2)_8$-O-C(=O)-O-$(CH_2)_8$). Rosin soap (abietic acid) was present at lower levels.

Analysis for antioxidants shows the complexity and wide diversity of antioxidants which are used by N.B.R. manufacturers.

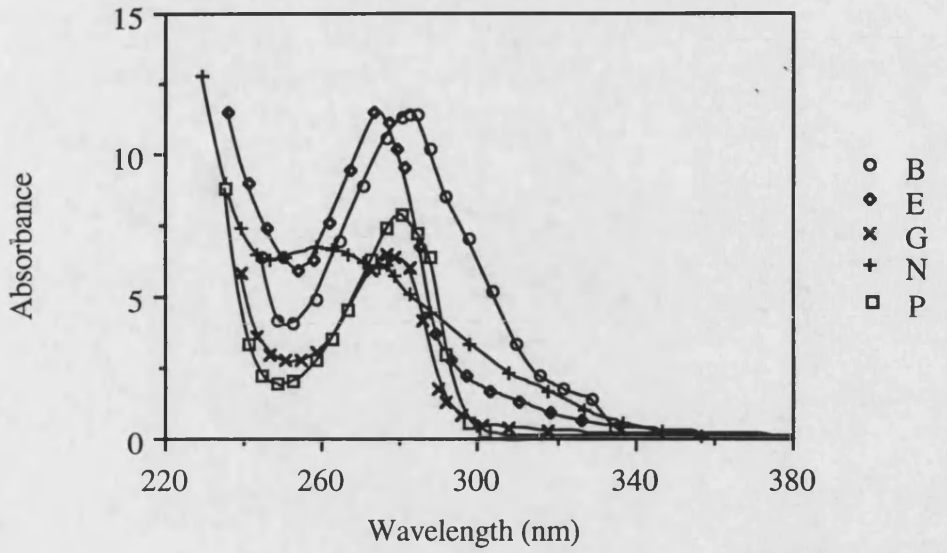

FIGURE 4.1. U.V. absorbance spectra of methanol extract solutions of N.B.R..

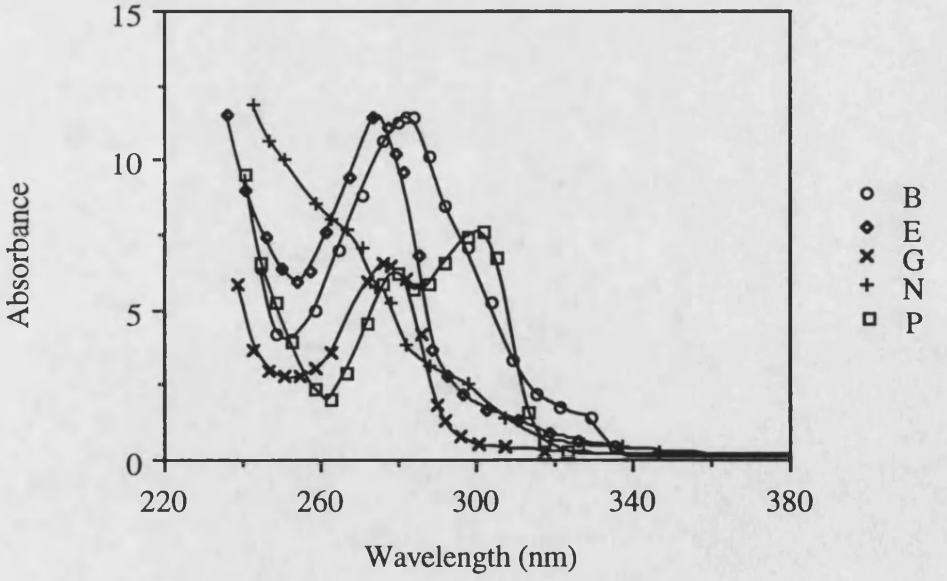

FIGURE 4.2. U.V. absorbance spectra of 0.1 alkali methanol extract solutions of N.B.R..

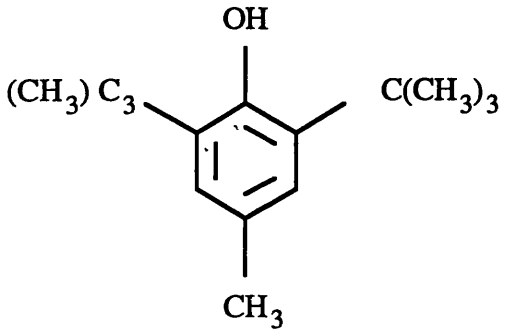

a. 2,6-Di-tertiary butyl-p-cresol.

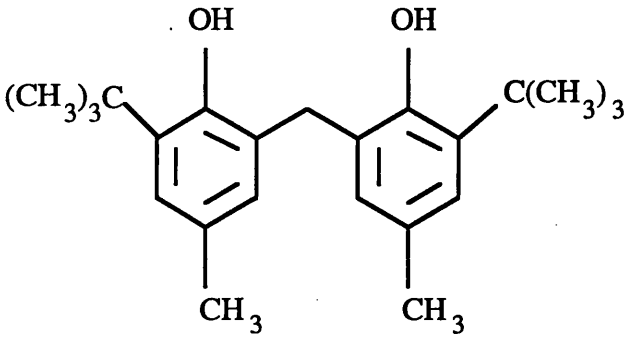

b. 2,2-Methylene bis-(4-methyl-6-tertiary butyl phenol).

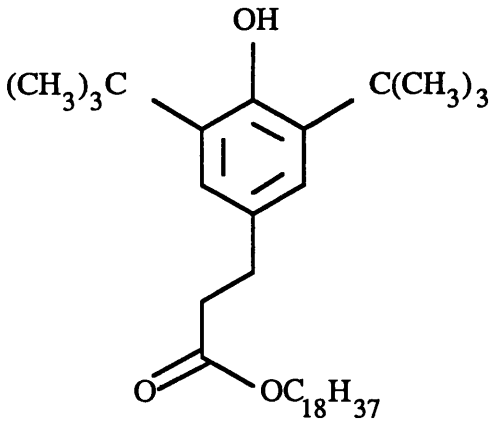

c. Octadecyl-3-(3',5'-di-tertiary butyl-4'-hydroxyphenyl) propionate.

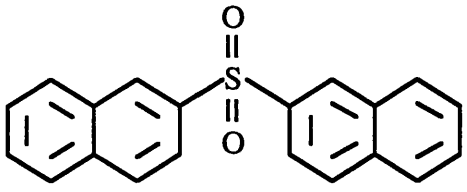

d. Di-naphthyl sulphone.

FIGURE 4.3. Chemical structure of antioxidant residues extracted from N.B.R. by hot methanol extraction.

4.1.4. SUMMARY ON ELEMENTAL COMPOSITION

Elemental analysis results of section 4.1 have shown that the total concentration of carbon, hydrogen and nitrogen is similar for all polymers of equivalent combined ACN content. On the surface of N.B.R. the concentration of nitrogen differs with base polymer, (refer to table 4.4) while the concentration of carbon is independent of base polymer. This implies that nitrogen rich species migrate to the surface. Variation in elemental nitrogen on polymer surfaces will be treated further in section 4.4.3.2.

The most significant polymerisation residues found in N.B.R. are emulsifiers, coagulants, modifiers and antioxidants. The effect of such residues on oxidative stability of N.B.R. will be considered in chapter six.

Emulsifier residues are sulphate/sulphonate species, and carboxylic acid species. The concentration and the chemical structure of emulsifier residues is specific to each polymer. Results to note are the high concentration of sulphate/sulphonate emulsifier in polymers P and B, (tables 4.3 and 4.4).

Polymer G contains a higher concentration of methanol extractable component than other polymers, (table 4.5). A significant proportion of such residue is free carboxylic acid emulsifier. The composition of carboxylic acid residue is specific to each polymer, (table 4.6). Polymer G contains a significant concentration of unsaturated carboxylic acid (oleic acid) in addition to saturated species.

Calcium, magnesium, sodium and chlorine are thought to be coagulant residues. Coagulants are inorganic salts of the form calcium chloride, magnesium chloride and sodium chloride. In the polymer such residues may be in the hydrated form since drying temperatures outlined in section 2.1.2.3 are insufficiently high to remove all hydrated water. Results of table 4.3 show that some polymers are coagulated mostly with calcium chloride while others are coagulated with magnesium chloride, or combinations of calcium chloride, magnesium chloride and sodium chloride. The combined concentration of sodium, calcium and magnesium is 11.25, 31.65, 1.63, 24.23 and 79.6 $mol.g^{-1} \times 10^{-6}$ in polymers B, E, G, N and P, respectively. Polymer G which contains the lowest concentration of sodium, calcium and magnesium also contains the lowest concentration of chlorine.

In polymers B, E, N and P there is an excess of cation species compared to the concentration of chlorine. This suggests that a high proportion of cations in polymers B, E, N and P may be combined with chemicals other than chlorine, such as carboxylic

acids in the form of carboxylic acid salts. Association between coagulant cations and carboxylic acids is supported by results of table 4.5 where it is shown that these polymers contain a low concentration of methanol extractable residue. Carboxylic acid salts are insoluble in methanol and therefore not extracted by it. Polymer G contains a very low concentration of calcium and magnesium and it is therefore more likely that carboxylic acid emulsifier residues in this polymer will be in the carboxylic acid form.

Polymers B, E, G and P contain mixtures of antioxidants of the non-staining phenol type, such as butylated hydroxy toluene and other substituted butylated phenols, such as 2,2-methylene bis-(-4-methyl-6-tertiary butyl phenol) and n-octadecyl-3-(3',5'-di-tertiary butyl-4'-hydroxyphenyl) propionate. Polymer E also contains dinaphthyl sulphone antioxidant. Polymer N contains rosin soap and dioctyl ester of hexanedioic acid but does not contain phenol type antioxidants.

All polymers are stabilised by different antioxidant combinations, with the exception of polymers B and P.

Alkyl mercaptan modifier residues are detected in polymers E, G and N. Such residues will be combined with the polymer. Polymer N also contains uncombined elemental sulphur residue. The concentration of elemental sulphur in this polymer would be 0.07 weight % if the assumption is made that all sulphur with a binding energy of 164 eV in this polymer is elemental sulphur. This will have practical implications in compounding and vulcanization.

4.2. STRUCTURAL CHARACTERISATION

4.2.1. GEL CONTENT

Gel is caused by crosslinking and as such may occur during polymerisation by free radical chain addition across vinyl-1,2 double bonds of butadiene units and also during degradation of N.B.R (Hoffman, 1984; Mazzeo, 1995). In section 2.1.3.3 it was pointed out that such gel influences processing properties and some mechanical properties of N.B.R.. The relationship between gel content and properties is however not well documented and its effect on properties, such as the viscoelastic loss angle and ageing behaviour seems not to have been studied.

The gel content of the polymers is shown in table 4.7. The large variation in gel content (crosslinked polymer) between polymer samples suggests differences in

microstructure or extent of degradation. Results on microstructural characterisation of the polymer samples are discussed in following sections 4.2.3 and 4.2.4. Polymer degradation is discussed in detail in chapter six.

Polymer	M.E.K. gel content, %
B	7.2
E	8.8
G	7.5
N	2.4
P	None detected

TABLE 4.7. Percentage of M.E.K. gel content of polymers.

4.2.2. MOLECULAR WEIGHT DISTRIBUTION

4.2.2.1. Gel Permeation Chromatography (G.P.C.)

Work on determination of molecular weight illustrates the difficulty of determining absolute values of molecular weight parameters of N.B.R. polymers. The difficulty arises because of the absence of monodisperse N.B.R. calibration standards and the presence of crosslinks and gel in commercial polymers. In G.P.C. work on nitrile polymers more accurate calibration has been made by additional measurement of solution viscosity and universal calibration through the Mark-Houwink relation (Kenyon and Mottus, 1974).

Universal calibration and measurement of true molecular weight data by G.P.C./viscosity (at R.A.P.R.A.) could not be made because all polymers used in this study contained gel when dissolved in T.H.F.. Gel was not removed upon filtration through a 0.45 micron filter. Gel permeation chromatography values obtained by R.A.P.R.A. are polystyrene equivalent molecular weight distributions, representative of the soluble polymer fraction in each sample.

G.P.C. results from R.A.P.R.A., presented in table 4.8, show polymer B to have a significantly higher weight average molecular weight and broader molecular weight distribution than the other polymer samples. The molecular weight distribution curves of solutions which were filtered through a 0.45 micron filter are shown in figure

4.4. Polymer E has the lowest weight average molecular weight. Other differences in molecular weight between the polymers are not significant.

The molecular weight parameters of the polymers solutions filtered through a 0.2 micron filter are much more uniform than those obtained by R.A.P.R.A., (refer to table 4.9 and figure 4.5). Filtration through a 0.2 micron filter was an attempt to obtain gel free solutions. Results from solutions filtered through a 0.2 micron, (table 4.9) would suggest that there are no significant differences in molecular weight distributions between the polymer samples. Weight average molecular weight values of samples filtered through a 0.45 micron filter are higher than the values of the polymers when filtered through a 0.2 micron filter. Number average molecular weight values are lower. This is particularly noticeable with polymer B.

Results of tables 4.8 and 4.9 and figures 4.4 and 4.5 indicate removal of high molecular weight material in solutions filtered through 0.2 micron filter. $\bar{M}_W$ falls with a reduction in the concentration of high molecular weight material. $\bar{M}_n$ is greatly influenced by the concentration of low molecular weight material. The molecular weight distribution curves sample presented in figures 4.4 and 4.5 support the view that in addition to gel, high molecular weight material has also been removed from solutions which are filtered through a 0.2 micron filter.

To test the validity of this hypothesis the molecular weight of an unperturbed nitrile rubber chain, (dissolved in T.H.F. solution) with mean end to end distance, ($\bar{r}_o$) in the region of 0.2 micron was calculated based upon the knowledge of polymer structure and bond length. This was attempted in order to calculate an approximate $\bar{M}_W$ of an unperturbed N.B.R. polymer chain that can pass through a 0.2 micron filter.

Molecular weight of a model N.B.R. chain was calculated by using the freely jointed chain model in which the mean end to end chain length, ($\bar{r}$) is assumed to be proportional to the square root of the number of bond links, (n) in the chain backbone (Flory, 1953).

$$\bar{r}^2 = nl^2 \qquad (4.1)$$

where, l is the bond length.

The C-C bond length l was taken as 0.153 nm while that of C=C as 0.134 nm (Morrison and Boyd, 1987). For purposes of calculation a single average bond length of 0.1493 nm was calculated from the ratio of C-C bonds to C=C bonds in the main

chain backbone. Calculation was based on N.B.R. with combined ACN content of 28 % and 9:1 ratio of 1,4-butadiene to 1,2-butadiene addition. This is shown to be a good approximation for N.B.R., (section 4.2.4).

The relationship between $\bar{r}_0$ and $\bar{r}$ was assumed to be $(\bar{r}^2)_0 = 2\,\bar{r}^2$ (Slusarski, 1984). This relationship was reported for 26 weight % combined ACN content N.B.R. in a solvent at the theta temperature, (precipitation temperature). The front factor of 2 is a product of the expansion in length of the freely jointed chain caused by bond angle constraints and steric hindrances, (at the theta temperature the solvent does not cause chain expansion).

According to this relation the total number of links, n in a unperturbed chain (of 28 weight % combined ACN content) of mean end to end distance 0.2 microns, at the theta temperature is 89725 of which 15253 are attributable to ACN addition and 74472 to butadiene addition. Division of the total number of links by the average number of links per monomer unit (2 for ACN, 3.8 for butadiene) gives the degree of polymerisation. According to this treatment the average molecular weight of an unperturbed chain, $\bar{r}_0 = 0.2$ microns in solution at the theta temperature is 14.6×10^5 g.mole^{-1}. This calculated cut-off value is shown in figure 4.5.

The calculated cut-off value shows good agreement with the experimentally observed cut-off point, however there is uncertainty in using the relationship $(\bar{r}_0^2) = 2\bar{r}^2$, because the theta temperature for N.B.R./T.H.F. is not known. Visual observation confirmed that N.B.R. was completely dissolved in T.H.F. at the test temperature and it is therefore possible that the experiment was made above the theta temperature. Above the theta temperature there is additional expansion of polymer chains by the solvent. If the experiment was well above the theta temperature, the calculated cut-off value shown in figure 4.5 would be an over estimate.

Molecular weight distributions of solutions which are filtered through a 0.45 microns filter contain molecules of $\overline{M}_W$ in excess of 14.6 g.mol^{-1} x 10^5, (refer to figure 4.4). As a result lower average molecular weight values and molecular weight distributions are observed for polymers filtered through a 0.2 micron filter. This is to be expected if high molecular weight material is removed.

These results show that the conventional G.P.C. technique is limited in its application to molecular weight characterisation of N.B.R. due to the un-availability of appropriate monodisperse N.B.R. calibration standards. Viscosity/G.P.C. measurement is also unsuitable due to the inability to filter 'gel free' N.B.R. solutions.

Gel being rather an arbitrary term which is difficult to distinguish from high molecular weight polymer.

Polymer	M_W	M_n	M_W/M_n
B	6.18×10^5	0.70×10^5	8.89
E	2.55×10^5	0.69×10^5	3.72
G	3.67×10^5	0.72×10^5	5.07
N	3.30×10^5	0.84×10^5	3.93
P	3.70×10^5	0.80×10^5	4.65

TABLE 4.8. Relative polystyrene equivalent G.P.C. molecular weight values of N.B.R. solutions filtered through a 0.45 micron filter.

Polymer	M_W	M_n	M_W/M_n
B	2.70×10^5	0.95×10^5	2.84
E	2.84×10^5	1.08×10^5	2.63
G	2.95×10^5	0.97×10^5	3.03
N	3.56×10^5	1.32×10^5	2.70
P	3.21×10^5	1.09×10^5	2.94

TABLE 4.9. Relative polystyrene equivalent G.P.C. molecular weight values of N.B.R. solutions filtered through a 0.2 micron filter.

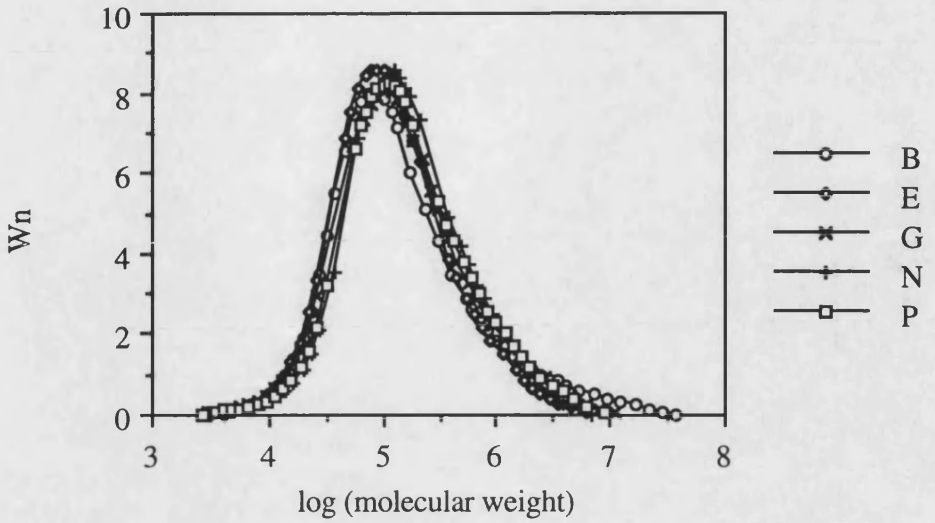

FIGURE 4.4. Relative polystyrene equivalent G.P.C. molecular weight distribution curves of N.B.R. solutions filtered through a 0.45 micron filter.

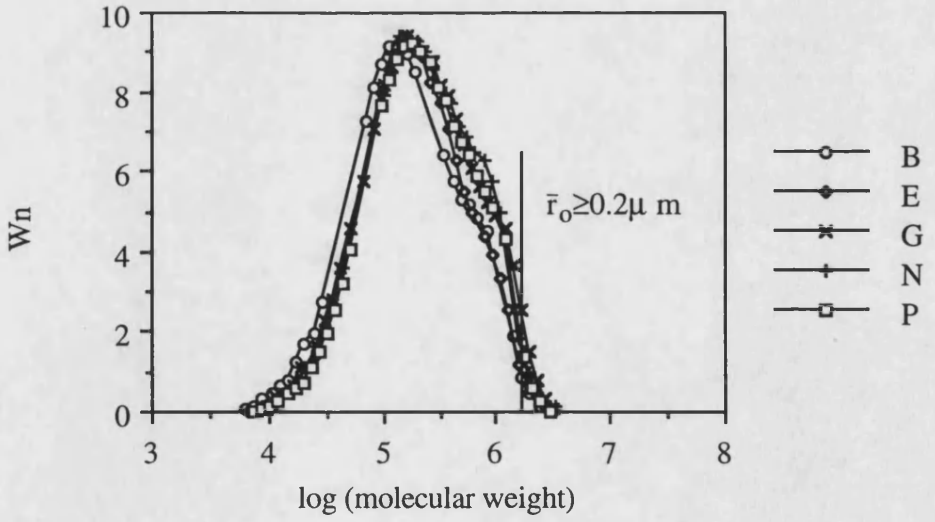

FIGURE 4.5. Relative polystyrene equivalent G.P.C. molecular weight distribution curves of N.B.R. solutions filtered through a 0.2 micron filter.

4.2.3. MONOMER SEQUENCE DISTRIBUTION

Results on monomer sequence distribution obtained by ^{13}C N.M.R. are tabulated in table 4.10. Results which are expressed as tri-additions are based on the frequency assignments of Willoughby (1989).

With all polymers only one ACN (A) centred tri-addition structure, (BAB) was detected. In the absence of other ACN centred species the fraction of BAB tri-addition is equivalent to the mole fraction of combined ACN.

A high degree of alternation is shown for all polymers. The high alternation is associated with the co-polymerisation ratios of ACN and butadiene which are both less than 1, (refer to section 2.1.3.2). The results show that polymer P has a lower combined ACN content than the other polymers. This is also shown in previous results, (tables 4.1 and 4.2). Because polymer P contains a lower level of combined ACN content there is a higher concentration of butadiene tri-addition (BBB). Polymer E which has the highest combined ACN content contains the lowest fraction of butadiene tri-addition.

^{13}C N.M.R. does not allow estimation of the length of butadiene blocks, however inhomogeneity in sequence distribution of low molecular weight polymer is suggested in section 4.4.3.2.

All polymers exhibit similar monomer sequence distributions. This suggests good control of polymer composition in all polymers.

Polymer	ABA	ABB	BBB	BAB	BAA
B	0.09	0.34	0.31	0.26	~
E	0.13	0.33	0.25	0.29	~
G	0.11	0.33	0.29	0.27	~
N	0.10	0.35	0.27	0.28	~
P	0.08	0.35	0.32	0.25	~

~None detected. A - ACN, B - butadiene.

TABLE 4.10. Mole fraction of tri-additions in N.B.R., obtained by ^{13}C N.M.R..

4.2.4. STRUCTURAL ANALYSIS BY F.T.I.R.

F.T.I.R. results of the micro-structural composition of the butadiene fractions in N.B.R. are presented in tables 4.11. Calculation was made by the Beer Lambert method using absorbance measurement at peak maxima and the extinction coefficients of Haslam and Willis (1972).

The values of table 4.11 differ little with polymer and are in good agreement with previously published data on structural composition of the butadiene units in nitrile rubbers of similar weight percent combined ACN content, (Willoughby, 1989).

Polymer	Trans-1,4 %	Cis-1,4 %	Vinyl-1,2 %
B	74.5±2.6	14.7±2.2	10.8±0.9
E	78.7±2.8	11.5±1.7	9.9±1.1
G	76.0±0.6	14.9±0.7	9.1±0.8
N	77.0±1.1	13.5±1.0	9.5±0.8
P	75.5±2.9	14.4±3.5	9.9±0.5

TABLE 4.11. Micro-structural composition of the butadiene fraction in N.B.R. determined from I.R. peak maxima absorptions of table 2.2.

4.2.5. THE GLASS TRANSITION

4.2.5.1. Glass Transition Temperatures of Polymers

The use of D.S.C. for determination of glass transition temperatures was discussed in section 3.4.3. Glass transition temperatures of raw polymers at various heating rates are tabulated in table 4.12.

Glass transition temperatures are similar for all polymers however different polymers show a different dependence of glass transition temperature on heating rate. The dependence of glass transition on heating rate is treated further in section 4.2.5.2.

Values representing the width and magnitude of glass transition are reported in table 4.13. These terms are illustrated in section 3.4.3. The results of table 4.13 are

mean average values of all heating rates. These glass transition parameters should be compared to glass transition parameters of vulcanizates, shown in section 4.5.2.1.

All D.S.C. scans of raw polymers exhibit a relatively pronounced step change in heat flow in the region of the glass transition at all heating rates, (refer to figure 4.6), apart from the G polymer which exhibits a gradual decrease in heat flow over a wide temperature range. The slope of the curve changing sharply near the high temperature end of the transition region. This is reflected in a high value of width of transition, ($\Delta T_{(Tg)}$) in table 4.13. This type of transition may be associated with heterogeneous materials which contain structurally different molecules with different relaxation times (Schaefer, 1995). The molecular structure of polymer G is not significantly different from the molecular structure of other polymers however this polymer contains a high concentration of methanol extractable residue, (table 4.5). Much of the residue of table 4.5 is carboxylic acid, (table 4.6). Such residues, acting as internal lubricants may be the cause of the observed wider glass transition in polymer G. Polymer E exhibits transition over a much narrower temperature range than other polymers. This behaviour could have its origin in the low molecular weight distribution and high gel content of polymer E.

	Heating rate (°C/min)					
Polymer	5	7	10	15	20	30
B	-34.0	-32.5	-31.0	-30.5	-29.8	-28.5
E	-32.0	-31.8	-29.5	-28.7	-28.0	-27.5
G	-35.0	-32.5	-29.8	-27.5	-24.0	-20.5
N	-32.0	-33.0	-32.3	-32.0	-28.0	-27.0
P	-32.6	-33.0	-32.5	-31.7	-30.1	-28.2

TABLE 4.12. Glass transition temperatures of N.B.R. polymers, obtained by D.S.C. at various heating rates.

Polymer	$\Delta Cp_{(Tg)}$, J/g	$\Delta T_{(Tg)}$, °C
B	0.82±0.2	18.1±1.8
E	0.66±0.1	7.6±1.3
G	0.98±0.2	36.0±2.5
N	0.77±0.2	18.9±2.1
P	0.74±0.1	19.5±1.9

$\Delta Cp_{(Tg)}$-change in specific heat capacity at Tg, $\Delta T_{(Tg)}$-width of transition.

TABLE 4.13. The average change in specific heat capacity and the width of transition of N.B.R. polymers, obtained by D.S.C. at various heating rates, (95 % confidence limits are given).

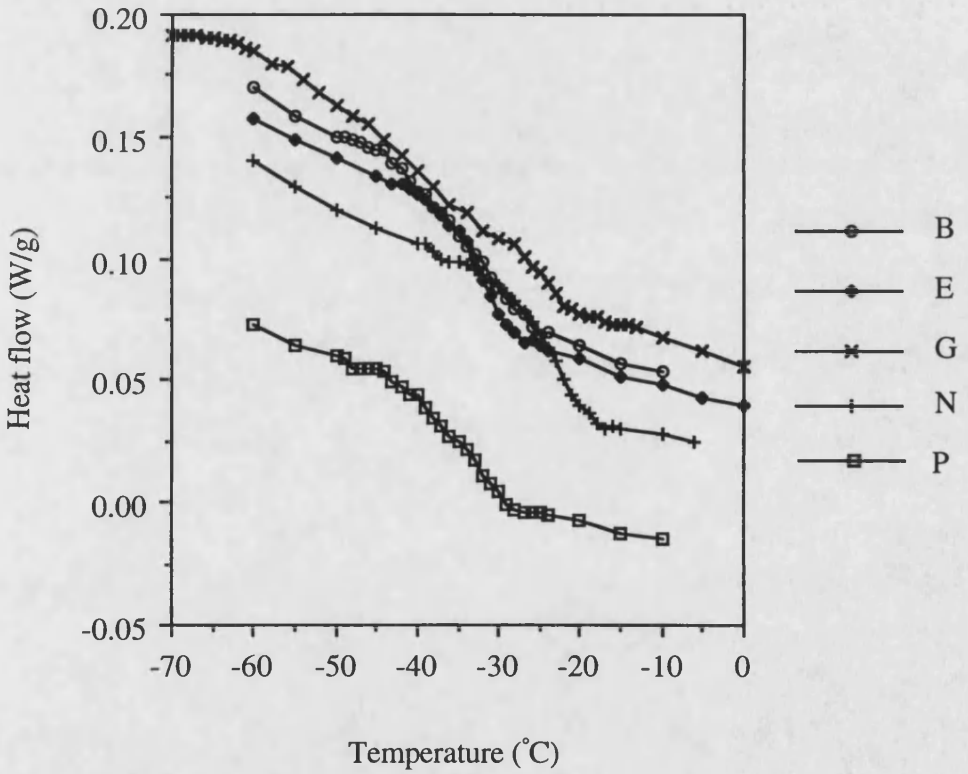

FIGURE 4.6. D.S.C. curves of N.B.R. polymers, obtained during heating at 5°C/minute.

4.2.5.2. Relaxation Behaviour

In table 4.12 it is shown that glass transition increases with an increase in heating rate. Such behaviour, has not been studied in rubbers, but has been reported in inorganic glass materials.

Analysis of heating rate dependence of glass transition is based on the treatment of Moynihan, Eastal, DeBolt and Tucker (1976) of fictive temperature, (T_f) in glasses during cooling at a controlled rate, (q-). Dependence of T_f on available relaxation time, Δt, ($\Delta t = \Delta T^{-}/q$-), where ΔT^{-} is a temperature step, implies that Δt is proportional to the relaxation time τ_r of the glass and therefore inversely related to q-. In this treatment the slope of Arrhenius type plots of the natural log of cooling rate against reciprocal T_f temperature is assumed to be related to the apparent activation energy of structural relaxation.

Scherer (1986) also studied the effects of cooling rate (q-) on the fictive temperature of a glass and found that the variation of T_f with cooling rate closely paralleled the change of shear viscosity with temperature for the same glass. This implied:

$$\{d(1/T_f)\} / \{d\ln [q-]\} = -\Delta H/R \qquad (4.2)$$

where, R is the gas constant, and ΔH is an 'apparent activation energy' of structural relaxation.

An Arrhenius plot of relaxation time usually shows two portions which are approximately linear, the change of slope occurring at the glass transition. The slope below T_g corresponding to a lower apparent activation energy. Narayanaswamy (1986) expressed this as:

$$\tau_r = \tau_o \exp [\, x\Delta H/RT + (1-x)\, \Delta H/RT_f] \qquad (4.3)$$

where τ_o is a constant and T is the absolute temperature. x is a constant between 0 and 1.

Although there appears to be no theoretical justification for the Narayanaswamy equation, Scherer (1986) quotes work where results for the temperature variation of

viscosity above and below T_g have been analysed according to the equation with fair success.

Avramov, Grantscharova and Gutzow (1986) have extended this treatment by studying the effects of heating from below T_g, as well as cooling from above Tg on the value of transition temperature. When natural logarithm of heating or cooling rate was plotted against reciprocal of the transition temperature, fairly good straight lines were obtained. The gradient of the line for different cooling rates implied a similar activation energy for that found for equilibrium viscosity, but that for heating rate gave a lower activation energy. They interpreted this according to the Narayanaswamy equation with activation energies ΔH and $x\Delta H$ respectively. They found $x = 0.6$.

Activation energies of structural relaxation obtained by Arrhenius type treatment of glass transition temperatures found in this work at different heating rates are tabulated in table 4.14. Due to high scatter in Arrhenius plots of samples B, E, P and N, (±30kJ/mole) differences in activation energies between these polymers were considered not to be significant. The scatter was less in polymer G, (figure 4.7) possibly because of its wider transition.

Polymer G exhibits a greater glass transition dependence on heating rate than other polymers. This is reflected in a lower apparent activation energy of structural relaxation. Polymer G also exhibits the widest distribution of relaxation times, (see figure 4.6). Later results of figure 4.8 will show that polymer G also exhibits lower viscosity than other polymers. The molecular structure of polymer G is not significantly different to other polymers. It is therefore likely that the lower apparent activation energy of structural relaxation of polymer G is associated with the higher concentration of methanol soluble residue of table 4.5.

Polymer	$-x\Delta H$, kJ/mole
B	135
E	142
G	60
N	106
P	142

TABLE 4.14. Apparent activation energies of structural relaxation, (ΔH) of N.B.R. polymers, determined from glass transition data at different heating rates.

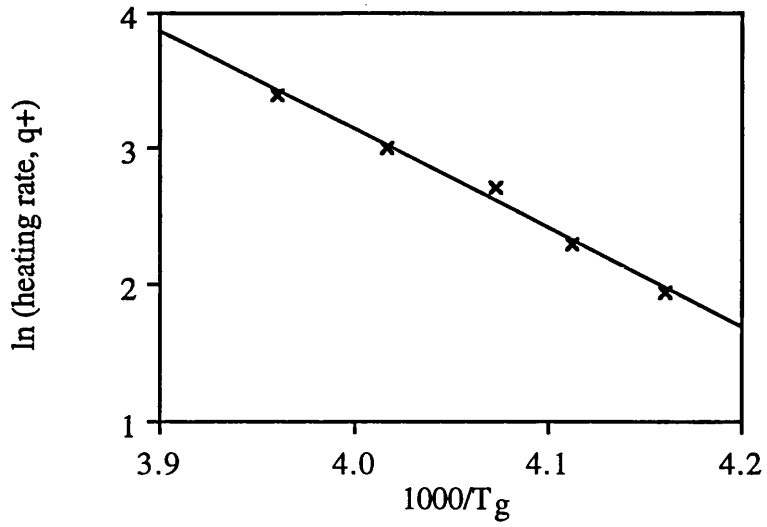

FIGURE 4.7. Arrhenius plot of the dependence of the natural logarithm of heating rate on reciprocal glass transition temperature of polymer G, obtained by D.S.C..

4.2.6. RHEOLOGICAL BEHAVIOUR

4.2.6.1. Mooney Viscosity

The Mooney viscosity values of the raw polymers are tabulated in table 4.15.

Polymer B exhibits the highest Mooney viscosity. G.P.C. results of table 4. show that this polymer is of highest weight average molecular weight. The two results are mutually supportive since it is well known that Mooney viscosity is related to molecular weight (Chang, 1981).

Polymer	ML 1+4 at 100°C
B	50.0
E	45.0
G	45.2
N	45.5
P	45.0

TABLE 4.15. Mooney viscosity of raw N.B.R. polymers at 100°C.

4.2.6.2. Shear Rate-Shear Stress Dependence

The flow properties of the raw polymers over a wide shear rate range at 120°C are shown in figure 4.8. The flow curves below 15 s^{-1} obtained by a T.M.S. rheometer, (cone and plate type rheometer) show excellent agreement with flow curves above 15 s^{-1} which are measured on a capillary rheometer.

Polymer B and P exhibit the highest apparent viscosity at the lowest rates of shear. These low shear rates are primarily associated with viscous effects. The high apparent viscosity of polymer B obtained by T.M.S. is consistent with results of Mooney viscosity at 100°C and molecular weight, however the high viscosity of polymer P is not consistent with its Mooney viscosity. Relative Mooney and T.M.S. values may be different due to the differences in rotor and cavity design.

Polymers G exhibits similar viscosity to polymers E and N at low shear rates, however the melt flow index, n of polymer G is lower, (for clarification of n, see section 3.5.2). Polymer G therefore shows a greater reduction in apparent viscosity with an increase in shear rate in comparison with other polymers. The reduction in viscosity is particularly apparent at shear rates above 300 s^{-1}. The low viscosity of polymer G is likely to be associated with its high concentration of emulsifier residue, such as carboxylic acid, (table 4.5). The reduction in shear stress at high shear rates may also be caused by exudation of carboxylic acid to the interface causing wall slip (George, 1980).

For all samples the respective order of apparent viscosity at the high shear rates is similar to that observed at low shear rates.

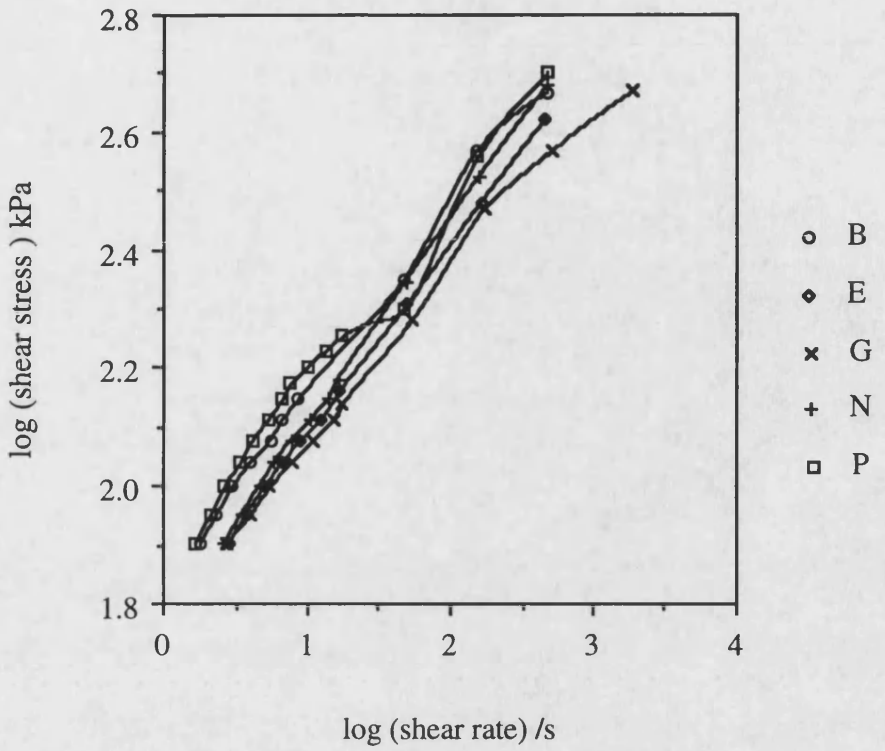

FIGURE 4.8. Flow curves of raw polymers at 120°C, obtained by cone and plate and capillary rheometers.

4.2.7. SUMMARY ON STRUCTURAL ANALYSIS

The major differences in structure which were found between samples in section 4.2 are summarised and outlined below.

Gel content shown in table 4.7 is high, (7.2-8.8 %) for polymers B, E and G. Polymer P has no gel content while polymer N contains 2.4 % gel. Differences in gel content may be a result of differences in polymerisation conditions or they may be associated with storage ageing. This will be treated further in the chapter on polymer oxidation, (chapter 6). These results are of practical interest since gel content influences processing properties and mechanical properties, (section 2.1.3.3).

Molecular weight parameters obtained by G.P.C. reported in tables 4.8 and 4.9 and figures 4.4 and 4.5 illustrate the difficulty of using G.P.C. for determination of

molecular weight of N.B.R.. Limitations arise due to the unavailability of N.B.R. calibration standards and the inability to separate high molecular weight material from gel. This implies a need for further development of the technique.

Relative, polystyrene equivalent G.P.C. results indicate that $\bar{M}_W$ of polymer B of table 4.8, (6.18×10^5 g.mole^{-1}) is higher than for other polymers. $\bar{M}_W$ of polymer E, (2.55×10^5 g.mole^{-1}) is lower. $\bar{M}_n$ does not vary significantly with polymer. The width of distribution, ($\bar{M}_W/\bar{M}_n$) is 8.89 for polymer B and 3.72-5.07 for polymers E, G, N and P.

The high molecular weight of polymer B is reflected in a high Mooney viscosity value. Polymer G exhibits low Mooney viscosity and low shear viscosity, particularly at high shear rates. The low viscosity of polymer G may be associated with its high concentration of methanol extractable residue of table 4.5, a high proportion of which is carboxylic acid, (table 4.6). These results have practical implications for processing behaviour.

Glass transition behaviour is strongly affected by polymer sample, the main difference being in the width of transition. In sample G transition occurs over a wide temperature range and in sample E over a narrow temperature range, (table 4.13). The difference in width of transition between these two samples, (x 7) is highly significant. These findings have practical implications for properties which are associated with the glass transition such as the viscoelastic loss angle.

With all samples the temperature of glass transition is increased with a reduction in available relaxation time, (increase in heating rate). This glass transition dependence on available relaxation time is lower for polymer G. The higher temperature dependence of T_g on available relaxation time is shown by a lower apparent activation energy of structural relaxation, (table 4.14). The implications of these results are that, in applications where the position of T_g is critical, (such as for acoustic applications), testing should be carried out at service conditions.

The characteristic behaviour of polymer G in the glass transition region may be associated with its high concentration of methanol extractable species, (table 4.5). The narrow glass transition of polymer E may perhaps be associated with its lower molecular weight distribution and high gel content.

4.3. VULCANIZATION BEHAVIOUR

Differences in elemental and structural composition of polymers summarised in sections 4.1.4 and 4.2.7, respectively are important in understanding raw polymer behaviour, but of even greater practical interest is the effect of these differences on network structure of vulcanizates.

Two simple sulphur based gumstock compounds, (A and B) were studied for each base polymer. Compounds A and B are identical except that compound B contains 2 phr diphenyl amine antioxidant, (refer to table 3.3).

4.3.1. TORQUE RHEOMETER STUDIES

Compounds formulated with different base polymers exhibit widely varying cure times and torque maxima, as measured by a Monsanto rheometer (table 4.16).

Compounds of polymer G exhibit longer cure times and a significantly lower torque modulus than compounds which are based on other polymers. Compounds of polymer B and N exhibit higher torque modulus than other polymers.

The reader is reminded that polymer G contains significant quantities of unsaturated fatty acid residues, in the form of oleic acid, (see table 4.6). It was considered that the presence of this unsaturated residue was associated with the unusual cure behaviour as in literature where crosslinking of unsaturated carboxylic acid species during sulphur based vulcanization of N.R. has been implied by the inability to extract such residues after vulcanization (Crowther, Lewis and Metherell, 1988). In order to test this hypothesis oleic acid was compounded into NA and the vulcanization behaviour studied. The effect of oleic acid addition on the torque modulus of NA compound is shown in figure 4.9.

Addition of oleic acid to compound NA at 1 phr, (3.54×10^{-5} mol.g^{-1} of rubber) causes a large reduction in torque modulus, (approximately 20 %). This implies that the active sulphurating agent reacts preferentially with the double bond of the oleic acid. The high reactivity of oleic acid double bond in comparison with the butadiene double bond is likely to be associated with the high mobility of oleic acid.

Addition of antioxidant to the formulations results in a consistent reduction in cure time and a small but consistent increase in torque maximum. This accelerating

effect of Permanax B.L.W. antioxidant on sulphur based N.B.R. oxidation has also been observed in previous work (Sims, 1988). It is worth noting that the extent of acceleration is dependent on base polymer.

Torque rheometer studies of vulcanization should be compared with D.S.C. results which are presented in the following section, (section 4.3.2). Information on crosslink density and crosslink structure is presented in section 4.4.

Compound	Cure time (T_c95), mins.	Torque at T_c95, Nm
BA	29.0	53
BB	28.0	55
EA	35.0	47
EB	23.0	48
GA	36.5	35
GB	34.0	36
NA	31.5	53
NB	25.5	53
PA	30.0	48
PB	24.0	49

TABLE 4.16. Vulcanization parameters of N.B.R. compounds determined by Monsanto rheometry at 150°C.

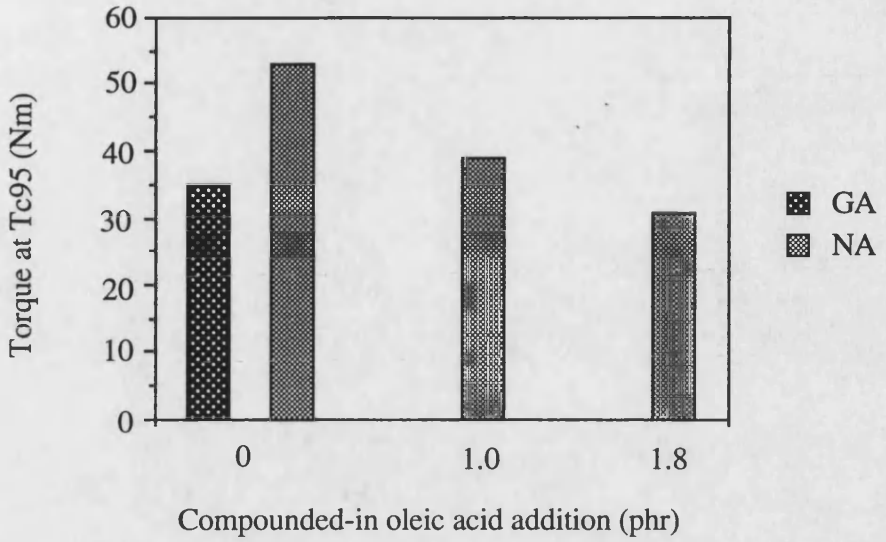

FIGURE 4.9. Effect of compounded-in oleic acid on torque modulus of NA compound at 150°C

4.3.2. DIFFERENTIAL CALORIMETRY STUDIES

Differential calorimetry, (D.C.) was used to gain further information on vulcanization. The studies involved heating compounds at isothermal conditions of 140°C, 150°C, 160°C and 170°C, under nitrogen and measuring the enthalpy change of vulcanization.

D.C. studies showed that the sum of all vulcanization reactions is exothermic. Vulcanization exotherms were characterised by the time required for exothermic peak maximum, (t_{max}) to be reached and overall enthalpic heat change of vulcanization, (ΔH_c). These parameters for isothermal heating at 150°C are tabulated in table 4.17. The reproducibility of (t_{max}), obtained by running several experiments on one compound was ±0.3 minutes, (expressed to 95 % confidence). The reproducibility of ΔH_c was ±1.0 J/g.

Compounds based on different polymers show little difference in (t_{max}). Addition of diphenyl amine results in reduction in (t_{max}). This is consistent with Monsanto results of table 4.16. Vulcanization times which are determined by D.C. are generally lower than rheometer values because of improved temperature control due to the use of smaller sample.

ΔH_c values of compounds BA, EA, PA and NA are not significantly different, but GA exhibits a lower ΔH_c, (table 4.17). This is consistent with results of table 4.16 where it is shown that torque modulus, (an indirect measure of crosslink density) is much lower for compounds of polymer G. Compounding-in of diphenyl amine causes a reduction in ΔH_c in all compounds, except BA. This reduction in ΔH_c is accompanied by a small increase in torque modulus, (table 4.16). The effect of diphenyl amine on cure exotherm has not been reported in literature, but in the D.C. study of sulphur based N.R., S.B.R. and B.R. vulcanization a similar effect is found when increasing accelerator:sulphur ratio at constant sulphur loading (Brazier, Nickel and Szentgyorgyi, 1980).

Combined D.C. and Monsanto study of vulcanization is more informative than using one technique alone because D.C. gives information on all enthalpic reactions while Monsanto gives information on crosslinking and scission reactions.

Apparent activation energies of vulcanization are in the range of 89.0-98.0 kJ/mole for compound A and 85.5-90.0 kJ/mole for compound B. These values were determined from logarithmic plots of the temperature dependence of (t_{max}), (Arrhenius treatment in the context of ageing kinetics is shown in section 2.3.4.2). These results show that diphenyl amine catalyses vulcanization. The scatter of results is such that differences in activation energies between polymers are not considered significant.

Compound	ΔH_c, J/g	t_{max}, mins.
BA	9.8	9.7
BB	10.4	8.8
EA	10.8	11.7
EB	9.0	7.5
GA	7.9	9.0
GB	5.6	7.9
NA	10.7	11.5
NB	10.6	8.9
PA	10.6	11.0
PB	9.2	8.2

TABLE 4.17. Differential calorimetry cure exotherm, ΔH_c and time to maximum reaction rate, t_{max} of N.B.R. compounds at 150°C.

4.3.3. CONTROLLED HEATING RATE D.S.C. STUDIES

Measurement of D.S.C. vulcanization at isothermal temperature reported in the previous section 4.3.2 was supplemented by study of vulcanization by heating at various heating rates. These controlled heating rate experiments were made to obtain information on network maturation, this being possible because the composite exothermic peak obtained under these conditions is made up of vulcanization, crosslink maturation and crosslink decomposition reactions (Brazier *et al.*, 1980).

The data obtained from the instrument in the scanning mode at a heating rate of 10°C/minute is tabulated in table 4.18. The D.S.C. curves of GA, GB, BA and BB compounds are shown in figures 4.10 and 4.11. D.S.C. vulcanization curves of compounds formulated with polymer B are similar to D.S.C. vulcanization curves of compounds formulated with polymers E, N and P.

All samples heated under non-isothermal controlled heating rate conditions exhibit a very broad exothermic peak between approximately 150°C and 250°C. The shoulder on D.S.C. scans, at the high temperature side has previously been identified with maturing and degradation reactions (Brazier *et al*, 1980). This shoulder is much more prominent in compounds formulated with polymer G. The onset peak temperature, (T_i) is lower for vulcanizates compounded with polymer G but the overall width of the exothermic reaction peak is greater than for other polymers. The value of the cure exotherm obtained under controlled heating rate conditions is lower with G.

Compounding-in of diphenyl amine causes a shift in D.S.C. vulcanization peak to lower temperatures.

The magnitude of cure exotherm under scanning conditions is higher by a factor of two than the cure exotherm obtained under isothermal conditions. The cure exotherm under scanning conditions is higher because crosslink maturation and decomposition reactions contribute to the measured exotherm.

Experiments with different heating rates showed that the peak maxima progressively shift to higher temperatures with an increase in heating rate. The shape of the exothermic peak also changes suggesting an increase in the ratio of degradation to cross-linking reactions. However the peak exotherm values remain constant. Compounds based on polymer G consistently exhibit lower exotherm values than compounds based on other polymers.

Compound	T_i, °C	T_{max}, °C	ΔH_s, J/g
BA	182.8	187.8	19.2
BB	179.2	183.5	20.5
EA	180.2	185.7	21.8
EB	174.9	180.1	19.3
GA	177.3	183.9	14.8
GB	173.4	179.4	15.9
NA	181.6	186.4	20.4
NB	179.2	183.2	18.7
PA	183.2	186.8	20.6
PB	177.5	181.6	18.8

TABLE 4.18. D.S.C. cure exotherm, ΔH_s, peak onset temperature, T_i and temperature at peak maximum, T_{max} of N.B.R. compounds heated at 10°C/minute.

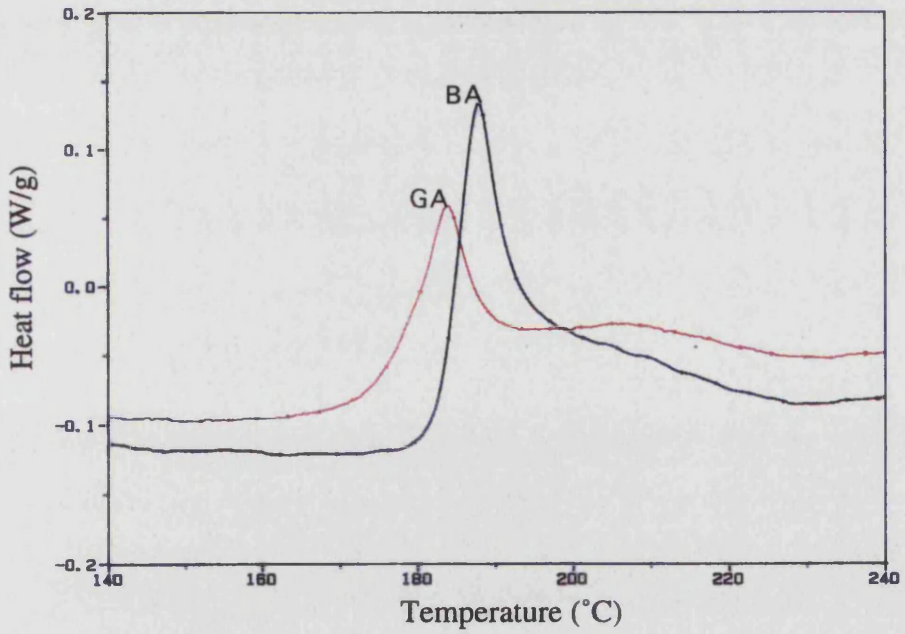

FIGURE 4.10. D.S.C. vulcanization scans of compounds BA and GA obtained during heating at 10°C/minute.

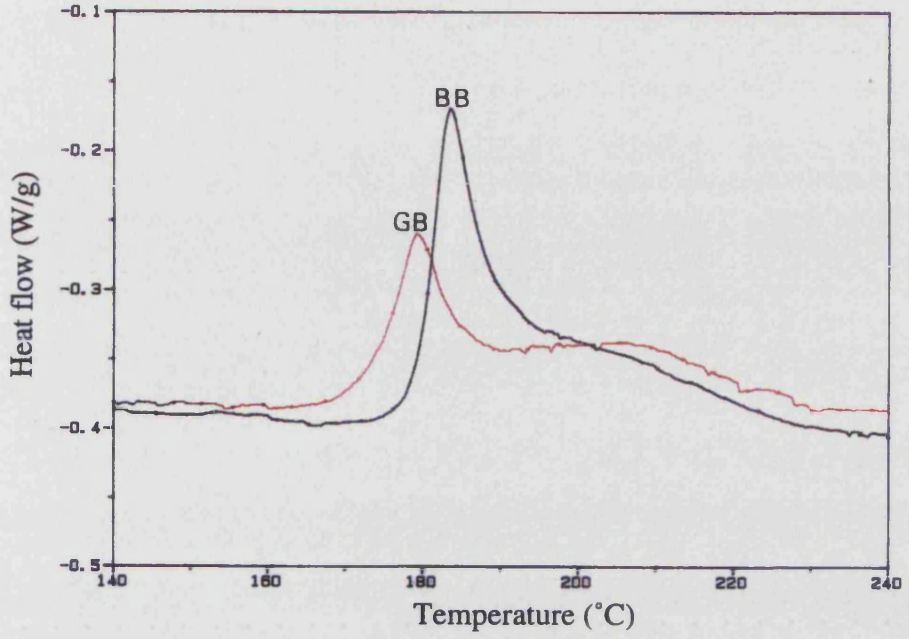

FIGURE 4.11. D.S.C. vulcanization scans of compounds BB and GB obtained during heating at 10°C/minute.

4.3.3.1. D.S.C. Interactions of Compounding Ingredients

Information on reactions between compound ingredients was obtained by controlled heating rate D.S.C. experiments on individual compound ingredients and compound mixtures. Of particular interest were interactions between diphenyl amine and components of the vulcanization system, to explain the accelerating effect of diphenyl amine on vulcanization, (tables 4.16-4.18).

Figure 4.12 shows D.S.C. scans of zinc oxide, stearic acid, zinc stearate and an equal weight mixture of zinc oxide-stearic acid. Figures 4.13 shows D.S.C. scans of sulphur, diphenyl amine and an equal weight mixture of sulphur-diphenyl amine. Figure 4.14 shows scans of sulphur-C.B.S. and sulphur-diphenyl amine-C.B.S. mixtures.

From figure 4.12 it can be seen that reaction of zinc oxide and stearic acid to form zinc stearate is exothermic and occurs at 80-90°C.

The scans of elemental sulphur contain two endothermic peaks at approximately 104°C and 118°C. The endothermic peak at 104°C may be associated with phase transition of sulphur from orthorhombic to monoclinic structure, (this transition is known to occur above 95.5°C) (Miller, 1984). The second endothermic peak at 118°C is likely to be associated with melting of the monoclinic system, (according to Miller (1984) melting of monoclinic sulphur occurs at 119°C). The addition of diphenyl amine causes a reduction in the melting point of monoclinic sulphur but does not affect the magnitude of the endothermic peak. There is also an appearance of an additional endothermic peak at approximately 109.5°C. This additional peak may be associated with melting of some transitionary S_8 structure.

A reaction mechanism for secondary amine and elemental sulphur reaction is illustrated in section 2.2.2.4.3, reaction scheme VI.

Heating sulphur in the presence of C.B.S. accelerator causes a reduction in the melting point of monoclinic sulphur, (compare with the D.S.C. scan of sulphur alone, figure 4.13). A similar effect was shown in figure 4.13, in the presence of diphenyl amine, however the reduction in melting point was less. C.B.S. has no effect on the temperature of the orthorhombic to monoclinic phase transition. Addition of diphenyl amine to sulphur-C.B.S. mixture has no effect on the melting of C.B.S. but as in figure 4.13 it introduces an additional phase transition peak in sulphur.

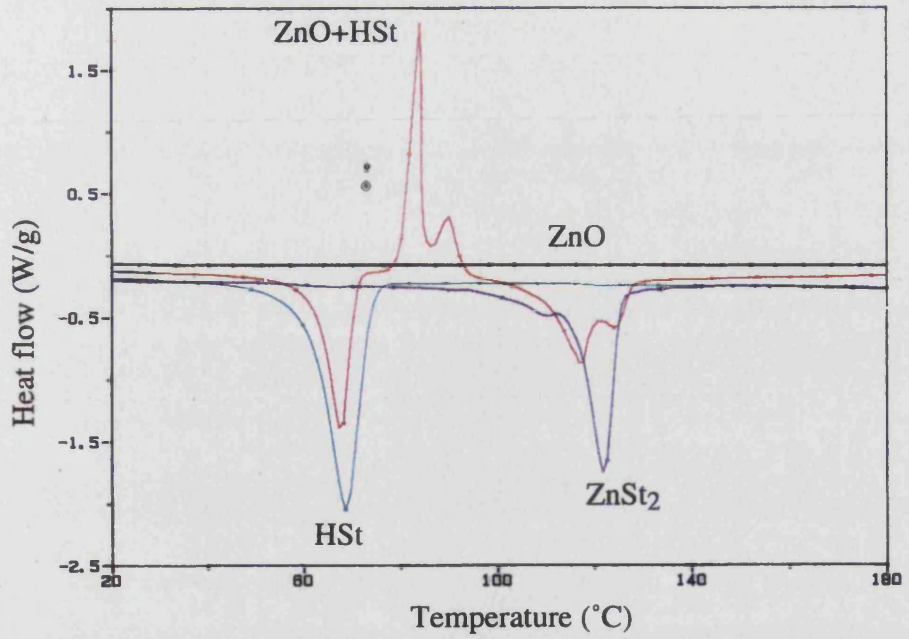

FIGURE 4.12. D.S.C. scans of ZnO, HSt, $ZnSt_2$ and a mixture of ZnO-HSt, heated at 5°C per minute.

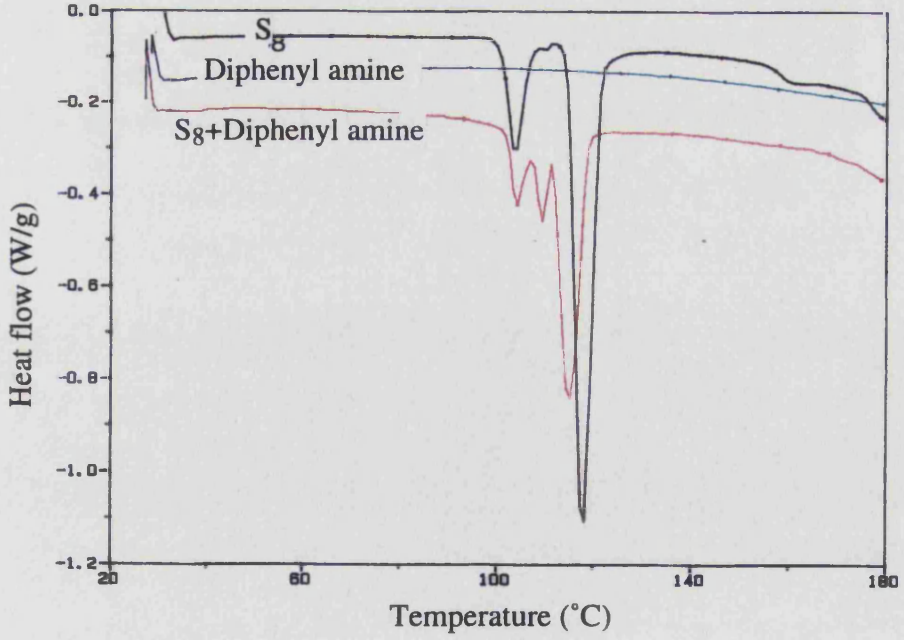

FIGURE 4.13. D.S.C. scans of S_8, diphenyl amine and a mixture of S_8-diphenyl amine, heated at 5°C per minute.

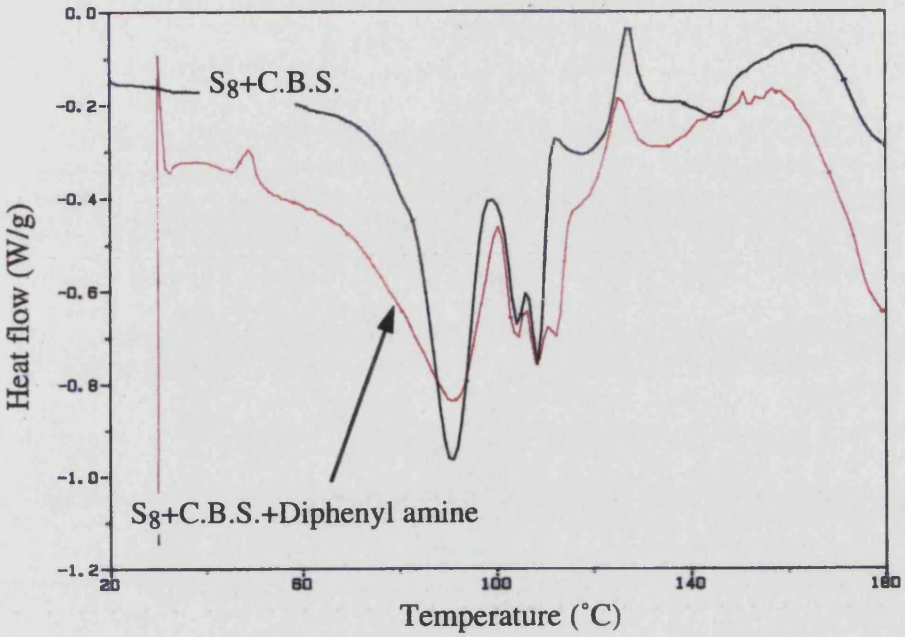

FIGURE 4.14. D.S.C. scans of S_8-C.B.S. and S_8-C.B.S.-diphenyl amine, heated at 5°C per minute.

4.3.4. SUMMARY ON VULCANIZATION BEHAVIOUR

Vulcanization of N.B.R. was studied by measurement of torque modulus and measurement of reaction enthalpy. The techniques give complementary information. Measurement of torque modulus during isothermal heating of compounds gives an indication of crosslink formation. Enthalpic measurement during isothermal heating of compounds gives information on the total enthalpy of vulcanization reactions. The peak exotherm obtained under controlled heating rate measurement is a composite peak made up of vulcanization and network degradation reactions. The magnitude of the peak exotherm obtained under controlled heating rate conditions is higher than the peak exotherm obtained under isothermal conditions by a factor of two for all compounds, due to additional network maturation reactions.

Measurement of vulcanization shows that base polymer and compound formulation affect vulcanization characteristics, (tables 4.16, 4.17 and 4.18).

Compounds formulated with polymer G show significant differences in vulcanization behaviour in comparison with other polymers. The D.S.C. vulcanization exotherm of G compounds during isothermal heating occurs at shorter times and the temperature of the vulcanization peak exotherm during heating at a controlled heating rate is lower than for compounds of other polymers. Compounds of polymer G attain a much lower torque modulus, (approximately 30 % lower) on vulcanization than compounds based on other polymers (table 4.16). This suggests a lower crosslink density. The reduction in torque modulus in compounds of polymer G is caused by preferential reaction of curatives with unsaturated carboxylic acid, (oleic acid) species. Oleic acid is found in polymer G as polymerisation residue at significant concentration, (tables 4.5 and 4.6). Reaction of oleic acid was demonstrated in compound NA, where it was shown that compounding-in of 1 phr oleic acid causes a reduction in torque modulus of approximately 20 %.

The effect of oleic acid has major implications for compounding and design of formulation recipes. In the same context addition of oleic acid to sulphur based compounds is a means of reducing crosslink density and introducing carboxylic acid terminated short chain branching.

Compounding in diphenyl amine causes a reduction in vulcanization enthalpy and a reduction in the time and temperature of vulcanization, (tables 4.16, 4.17 and 4.18). Figures 4.13 and 4.14 show that diphenyl amine interferes with phase transition and melting point of sulphur. Further results on the influence of diphenyl amine on crosslink structure and its effect will be presented in section 4.4. The extent of acceleration of the vulcanization process by diphenyl amine is largely influenced by base polymer. This may suggest synergism and antagonism between diphenyl amine and base polymer. Interactions between diphenyl amine and polymerisation residues are discussed in section 6.3. The greatest acceleration after addition of diphenyl amine occurs in compounds based on polymer E.

4.4. CROSSLINK NETWORK STRUCTURE

4.4.1. NETWORK EXTRACTION

Cold extraction of vulcanized rubber sheets with an azeotropic solution of acetone, 1,1,1,-trichloroethane and methanol was used to remove uncombined extra-network material from samples, prior to swelling measurement. This type of treatment has previously been applied by Sims (1988) for network extraction of sulphur based N.B.R. vulcanizates.

The percentage of material removed during this network extraction was found to differ little with base polymer. In vulcanizates which were compounded with formulation A approximately 3% of material was extracted. This value is similar to the concentration of material which is extracted from polymers by methanol, (table 4.5), however much higher concentrations of material were extracted from polymer G than vulcanizate GA. The concentration of extractable residue may be reduced in compound GA after vulcanization because oleic acid residue of polymer G is tied into the network during vulcanization.

In vulcanizates compounded with formulation B approximately 6 weight % was extracted for all polymers. The difference in the weight of network extract between vulcanizates of compound A and compound B of 3 weight % is higher than would be expected, from the compound formulation. Compound B differs from compound A only in the addition of 2 phr diphenyl amine. The higher than expected weight loss difference between compounds A and B would suggest involvement of diphenyl amine in vulcanization and formation of extractable chemical species. Reactions between diphenyl amine and vulcanization ingredients are outlined in section 2.2.2.4.3 and studied in 4.3.3.1.

4.4.2. ELASTIC CONSTANTS OF VULCANIZATE NETWORKS

Determination of the elastic constant, C_1, (for definition see section 2.2.1.4, equation 2.14) by stress-strain measurements on dry networks was found to be unsatisfactory because of theoretical and practical uncertainties. Theoretically dry networks conform less well to the statistical model, C_1 being obtained by extrapolation. Practically there are uncertainties about the contribution of dynamic effects and viscous effects during testing. All reported C_1 values of pre-extracted rubber networks were therefore obtained by compression-deflection measurement on networks swollen to

equilibrium in toluene. The theory behind the measurement is discussed in sections 2.2.3.3.

Values of the elastic constant, C_1 network chain density, N_v and volume fraction of rubber in the swollen network, V_r are presented in table 4.19. These results show that the differences in C_1, V_r and N_v values between compounds formulated with different base polymers are greater than differences in compounds formulated with different formulation. In the extreme there is a 30 % difference in C_1 and N_v between vulcanizates based on different polymers: this is highly significant.

Vulcanizates compounded with polymer G exhibit a lower network chain density than other vulcanizates. This result is consistent with Monsanto rheometer and D.S.C. studies of vulcanization where it was shown that compounds of polymer G exhibit low cure exotherms and low torque modulus in comparison with other compounds, (table 4.16-4.18). The lower network chain density of compounds formulated with polymer G is caused by reaction of crosslinking agent with its unsaturated oleic acid residue, (tables 4.5 and 4.6). Network chains which are introduced by crosslinking of oleic acid will be elastically inactive.

The relatively low network chain density of compounds based on polymer E may be due to its low molecular weight, (table 4.8). A reduction in molecular weight causes a reduction in the ratio of elastically active network chains (chains terminated by crosslinks at both ends) to elastically inactive network chains (chain ends).

Compounds formulated with polymer B and N exhibit higher network chain density than other polymers. In polymer B this effect may be associated with its higher average molecular weight, (table 4.8). Polymer N has a similar molecular weight to polymers G and P, but contains elemental sulphur residue at concentrations in the region of 0.07 phr, (section 4.1.1).

Vulcanizate	V_r	C_1, $x10^{-5}$, (N/m^2)	N_V $x10^4$, ($mol./cm^3$)
BA	0.238	2.47±0.07	2.10
BB	0.227	2.30±0.05	1.97
EA	0.223	1.90±0.03	1.61
EB	0.226	1.90±0.06	1.64
GA	0.218	1.75±0.07	1.48
GB	0.220	1.72±0.04	1.47
NA	0.235	2.22±0.05	1.90
NB	0.230	2.24±0.05	2.02
PA	0.207	1.90±0.05	1.60
PB	0.210	2.14±0.06	1.83

TABLE 4.19. C_1, V_r and N_v values evaluated using equation 2.21 for pre-extracted vulcanizates swollen in toluene, (also given are 95 % confidence limits).

4.4.3. CHEMICALLY PROBED NETWORKS

4.4.3.1. Weight Change During Chemical Probing

During chemical probing it was found that rubber networks exhibit a significant weight loss. The nature of this residue is treated in the following section 4.4.3.2. The percentage weight loss during probing with various probe solutions is shown in table 4.20.

The percent weight change during treatment with thiol-amine chemical probes differs little with change in formulation and appears to be primarily associated with base polymer. Compounds based on polymer N exhibit the lowest weight loss during probing. Compounds based on polymers B and P also exhibit relatively low weight loss. Vulcanizates based on polymer G exhibit the highest weight loss during probing. Vulcanizates based on polymer E also exhibit high weight loss. This weight loss appears to be inversely related to network chain density, which implies that material extracted during treatment may be low molecular weight polymer.

The weight change subsequent to treatment with chemical probes can not be caused by extraction of previously un-extracted extra network material because the percent weight change is simply too high. Later results of section 4.4.3.2 confirm that the network extracted material is N.B.R.. Extraction of polymer chains occurs because

individual polymer chains break free from the network during probing (thus constituting extra network material). This may occur through cleavage of sufficient number of crosslinks.

After treatment with propane-2-thiol (0.4M) + piperidene (0.4M) in toluene solution the network chain density of the polymers is reduced to 0.70-1.08 x 10^{-4} moles/cm^3, (table 4.22). This translates to an average molecular weight between crosslinks (via equation 2.2) of 14368-9217 $g.mol.^{-1}$. Referring to G.P.C. curves, (figure 4.4) it can be seen that all polymers contain chains with molecular weight below this value. Networks treated with the more active hexane-1-thiol probe exhibit lower network chain density and higher average molecular weight between crosslinks, (table 4.23). The number of chains which break free from the network increases as does the percentage of material extracted during probing.

These results indicate that the weight change in probed samples is caused by extraction of polymer chains with molecular weight below M_c.

The finding that polymer chains are extracted during swelling has very important practical implications for determination of crosslink density, by swelling techniques. For networks of low N_v, (high M_c) where there is high weight loss the volume element which is lost during swelling should be included in calculation of crosslink density. For the effect of this volume element on network chain density compare tables 4.22 and 4.23 with table 4.24.

N.B.R. networks which were probed with propane-2-thiol (0.4M) + piperidine (0.4M) in n-heptane did not exhibit a weight loss although polymer chains with molecular weight below M_c were present. This is because n-heptane is a poor solvent for N.B.R. and does not swell the network, therefore extraction does not occur.

Vulcanizate Weight loss, %	Hexane-1-thiol (1M) in piperidine	Propane-2-thiol (0.4M) + piperidine (0.4M) in toluene
BA	12.8	0.7
BB	11.4	0.7
EA	15.0	0.5
EB	21.3	0.3
GA	29.5	3.6
GB	24.3	3.8
NA	9.9	0.5
NB	8.8	0.8
PA	12.7	1.2
PB	15.2	1.2

TABLE 4.20. Weight percentage of material extracted from pre-extracted N.B.R. vulcanizates during chemical probing.

4.4.3.2. Analysis of Network Extract

The presence of N.B.R. polymer in hexane-1-thiol piperidine probe solution of vulcanizates of compound A was confirmed by F.T.I.R. spectroscopy using the specular reflection technique. The spectrum of B compounds was not used for sample identification because of interference from extracted diphenyl amine.

Material removed during propane-2-thiol (0.4M) + piperidine (0.4M) was also found to be N.B.R. as was material extracted during swelling in piperidine alone. F.T.I.R. analysis of piperidine extract represents molecular weight material of $M_c \leq 6803\text{-}4762$ g.mole^{-1}, (from table 4.19).

F.T.I.R. spectra of material extracted from EA and PA vulcanizates during swelling in piperidine are shown in figure 4.15. The spectra of extracts from BA, GA and NA were very similar to that of PA shown in figure 4.15. The extract from EA, (figure 4.15) shows some significant differences, particularly in the region of -CN absorption (~2250cm^{-1}). This implies that the low molecular weight material of polymer E contains a higher fraction of combined A C N content. In section 4.1, (table 4.1 and 4.2) it was shown that polymer E contains a similar concentration of total nitrogen concentration to polymer P, however the concentration of nitrogen on the surface of polymer E is much higher, (table 4.4). A much higher concentration of nitrogen is also found on the surface of vulcanizates of polymer E than vulcanizates of polymer P, (see later section 4.4.4.2, table 4.28). The increased concentration of

nitrogen found on the surface of polymer E may be associated with migration of high A C N content low molecular weight material to surface regions.

High A C N content low molecular weight polymer is likely to be produced at low degrees of conversion, where the kinetics of the co-polymerisation favour preferential A C N addition, (see section 2.1.3.2).

Analysis of piperidine extract of polymers EA, EB, PA and PB by mass spectroscopy failed to detect accelerator and sulphur residue. This suggests that in N.B.R. all such residues are combined with the network. Complete combination of accelerator has been reported by Skinner (1972) for sulphur based C.B.S. accelerated B.R. networks.

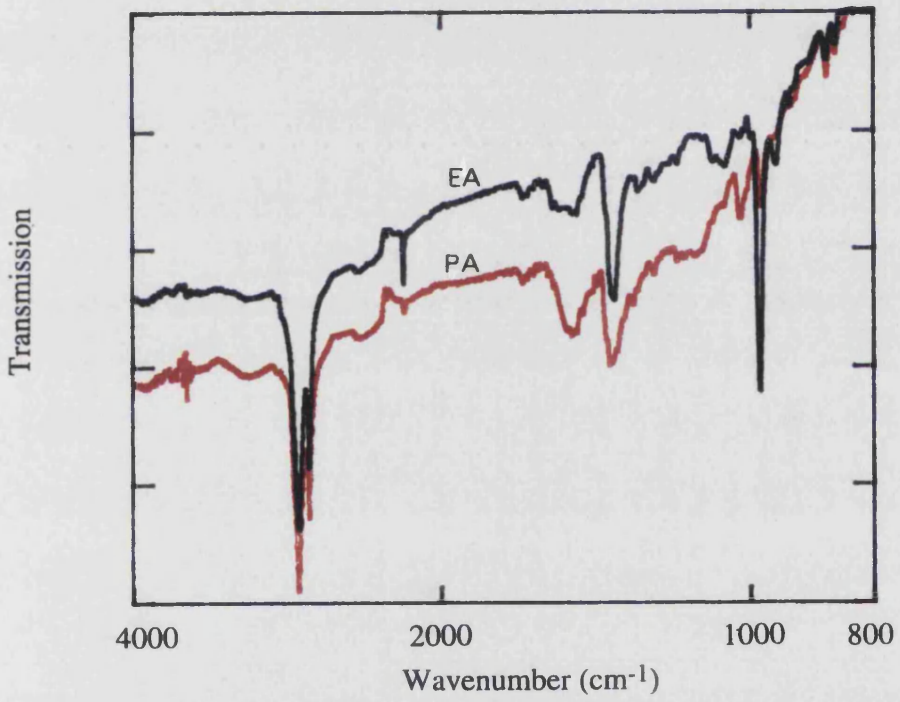

FIGURE 4.15. F.T.I.R. spectra of material extracted from N.B.R. vulcanizates by piperidine.

4.4.3.3. Chemical Probing of Peroxide Crosslinked Networks

In N.B.R. characterisation of network structure by thiol-amine and methyl iodide, it has been assumed that the base polymer is unreactive. In order to assess

whether this is so additional measurements were made by treating peroxide crosslinked networks, containing direct carbon to carbon crosslinks. The peroxide compound (polymer E 100 weight parts, dicumyl peroxide 1.9 phr) was prepared using previously established mixing and curing procedures (sections 3.6 and 3.8).

Measurement of crosslink density before and after probing of peroxide vulcanized samples with hexane-1-thiol (1M) in piperidine and methyl iodide confirmed that N.B.R. network polymer chains are unreactive towards these treatments.

4.4.3.4. Elastic Constants of Chemically Probed Networks

The network density subsequent to treatment with probes is reduced drastically (this is seen in tables 4.21-4.23). Reduction in crosslink density is caused by cleavage of selective crosslink structures. Propane-2-thiol (0.4M) in piperidine (0.4M) solutions react with and cleave almost exclusively poly-sulphide crosslinks. Hexane-1-thiol (1M) in piperidine cleaves poly-sulphide crosslinks and di-sulphide crosslinks so that only mono-sulphide crosslinks remain.

Treatment of several networks subsequent to hexane-1-thiol (1M) in piperidine with methyl iodide resulted in complete removal of crosslinks. Removal of all crosslinks with methyl iodide treatment suggests that C-C crosslinks have not been introduced in N.B.R. during vulcanization.

Comparison of propane-2-thiol (0.4M) + piperidine (0.4M) in heptane treatment and propane-2-thiol (0.4M) + piperidine (0.4M) in toluene treatment illustrate the effect of solvent on crosslink cleavage, (tables 4.21 and 4.22). The treatment was applied in heptane and toluene solvent because similar treatments have been used in literature for chemical probing of N.B.R. networks (Sims, 1988; Lee and Morrell, 1973). Both treatments result in a reduction in network chain density, (compare with table 4.19) and an increase in swelling. The reduction in network density is higher when treatment is applied in toluene rather than heptane, presumably because toluene is a better solvent for N.B.R. and introduces the probe reagent more rapidly and uniformly into the network. This implies that results of table 4.22 are more appropriate.

Network chain density results of propane-2-thiol (0.4M) + piperidine (0.4M) in toluene treated samples adjusted for the volume loss during swelling are shown in table 4.24. Differences in network chain density values between table 4.22 and 4.24 are not significant for this treatment because the weight of polymer extract was low.

After propane-2-thiol (0.4M) + piperidine (0.4M) in toluene treatment the network density of vulcanizates compounded with polymer G is lower than with other polymers. A similar relationship was observed in measurement of total crosslink density, (table 4.19).

Vulcanizate	V_r	C_1, $x10^{-5}$, (N/m^2)	$N_V x10^4$, ($mol./cm^3$)
BA	0.199	1.39±0.07	1.18
BB	0.204	1.57±0.08	1.36
EA	0.205	1.56±0.13	1.32
EB	0.210	1.63±0.08	1.39
GA	0.188	1.18±0.03	1.10
GB	0.189	1.03±0.02	1.00
NA	0.212	1.60±0.05	1.36
NB	0.214	1.50±0.08	1.30
PA	0.171	1.25±0.06	1.06
PB	0.175	1.28±0.06	1.09

TABLE 4.21. C_1, V_r, and N_V values of pre-extracted N.B.R. vulcanizates subsequent to treatment with propane-2-thiol (0.4M) + piperidine (0.4M) in n-heptane, (95% confidence limits given).

Vulcanizate	V_r	C_1, $x10^{-5}$, (N/m^2)	$N_V x10^4$, ($mol./cm^3$)
BA	0.174	1.13±0.02	0.96
BB	0.182	1.27±0.04	1.08
EA	0.178	1.10±0.04	0.93
EB	0.170	1.06±0.02	0.90
GA	0.181	0.84±0.03	0.71
GB	0.178	0.81±0.02	0.70
NA	0.186	1.25±0.04	1.06
NB	0.193	1.26±0.03	1.08
PA	0.159	0.93±0.02	0.79
PB	0.162	1.08±0.03	0.92

TABLE 4.22. C_1, V_r, and N_V values of pre-extracted N.B.R. vulcanizates subsequent to treatment with propane-2-thiol (0.4M) + piperidine (0.4M) in toluene, (95 % confidence limits given).

Vulcanizate	V_r	C_1, $x10^{-5}$, (N/m^2)	$N_V x10^4$, ($mol./cm^3$)
BA	0.177	0.45±0.07	0.38
BB	0.179	0.47±0.07	0.40
EA	0.178	0.32±0.09	0.28
EB	0.180	0.59±0.02	0.46
GA	0.185	0.52±0.03	0.44
GB	0.199	0.59±0.02	0.50
NA	0.180	0.32±0.04	0.27
NB	0.213	0.62±0.04	0.53
PA	0.171	0.32±0.05	0.27
PB	0.170	0.54±0.07	0.46

TABLE 4.23. C_1, V_r, and N_V values of pre-extracted N.B.R. vulcanizates subsequent to treatment with hexane-1-thiol (1M) in piperidine, (95 % confidence limits given).

There seems to be no published work, on treatment of the extracted volume element in swollen compression-deflection measurement of crosslink density. It appears that previous workers have not taken account of the extracted volume element, assuming it to be extra network material. These experimental results show extracted material to be uncombined polymer and therefore should be included in calculation of network density. Reduced network density values which are adjusted to take account of the volume element lost during probing and swelling are shown in table 4.24. Values of table 4.24 were calculated by incresing the volume element of N_V of tables 4.22 and 4.23 by the extracted volume element. This correction assumes that the extracted uncombined polymer would not have affected the values of C_1 used in the determination of N_V of tables 4.22 and 4.23.

Ignoring the polymer fraction lost during swelling does not affect calculations of network chain density significantly in vulcanizates of high network density where weight loss during swelling is low. At low crosslink density network density values are erroneously too high when the volume loss is not incorporated into the calculation, (compare network density values of tables 4.22 and 4.23 with 4.24).

Vulcanizate N_V x10^4, mol./cm^3	Propane-2-thiol (0.4M) + piperidine (0.4M) in toluene	Hexane-1-thiol (1M) in piperidine
BA	0.95	0.33
BB	1.07	0.35
EA	0.92	0.23
EB	0.89	0.36
GA	0.68	0.31
GB	0.67	0.38
NA	1.06	0.24
NB	1.08	0.49
PA	0.78	0.24
PB	0.91	0.39

TABLE 4.24. Network chain density of probed samples after correction for the volume fraction of polymer lost during probing.

The concentration of mono-sulphide, di-sulphide and poly-sulphide crosslinks in N.B.R. vulcanizates derived from tables 4.19, 4.22 and 4.23 are tabulated in table 4.25 and illustrated graphically in figure 4.16. Crosslink distributions calculated from tables 4.19 and 4.24 are shown in table 4.26 and figure 4.17.

Results of tables 4.25, 4.26 and figures 4.16, 4.17 show that there are many differences in crosslink distribution between polymers, but few trends except for the high mono-sulphide concentration and low di-sulphide concentration in G vulcanizates (when values are not corrected for polymer loss during extraction). Reducing N_V by the volume percentage of polymer which is lost during extraction has an effect of reducing mono-sulphide concentrations, most drastically in vulcanizates based on polymer G. This is because the volume fraction of polymer lost during probing with G was particularly high, (see table 4.20).

All vulcanizates compounded with formulation B have a higher percentage of mono-sulphidic crosslinks than vulcanizates based on formulation A. The overall concentration of crosslinks was not affected significantly by the addition of diphenyl amine. This would imply higher concentration of sulphur which is not in the form of crosslinks in B compounds. This is consistent with the observation that in compounds B more extra network material is extracted, compared to compounds A than can be accounted for by the presence of diphenyl amine, (section 4.4.1).

Vulcanizate	Mono-sulphide	Di-sulphide	Poly-sulphide
BA	18.3	27.3	54.4
BB	20.2	34.6	45.2
EA	17.1	41.7	42.2
EB	28.2	26.6	45.1
GA	29.9	18.1	52.0
GB	34.1	13.2	52.6
NA	14.3	41.5	44.2
NB	26.3	27.5	46.2
PA	17.0	32.6	50.4
PB	25.2	25.6	49.5

TABLE 4.25. Distribution of crosslinks in N.B.R. vulcanizates expressed as percentage of total crosslinks, from tables 4.19, 4.22 and 4.23.

Vulcanizate	Mono-sulphide	Di-sulphide	Poly-sulphide
BA	15.9	29.4	54.7
BB	18.0	36.4	45.6
EA	14.6	42.9	42.5
EB	21.8	32.6	45.3
GA	21.1	25.2	53.7
GB	25.9	19.7	54.4
NA	12.9	42.7	44.4
NB	24.1	29.3	46.6
PA	14.8	34.2	51.0
PB	21.4	28.5	50.1

TABLE 4.26. Distribution of crosslinks in N.B.R. vulcanizates, correcting for volume fraction of polymer lost during extraction, expressed as percentage of total crosslinks, from tables 4.19 and 4.24.

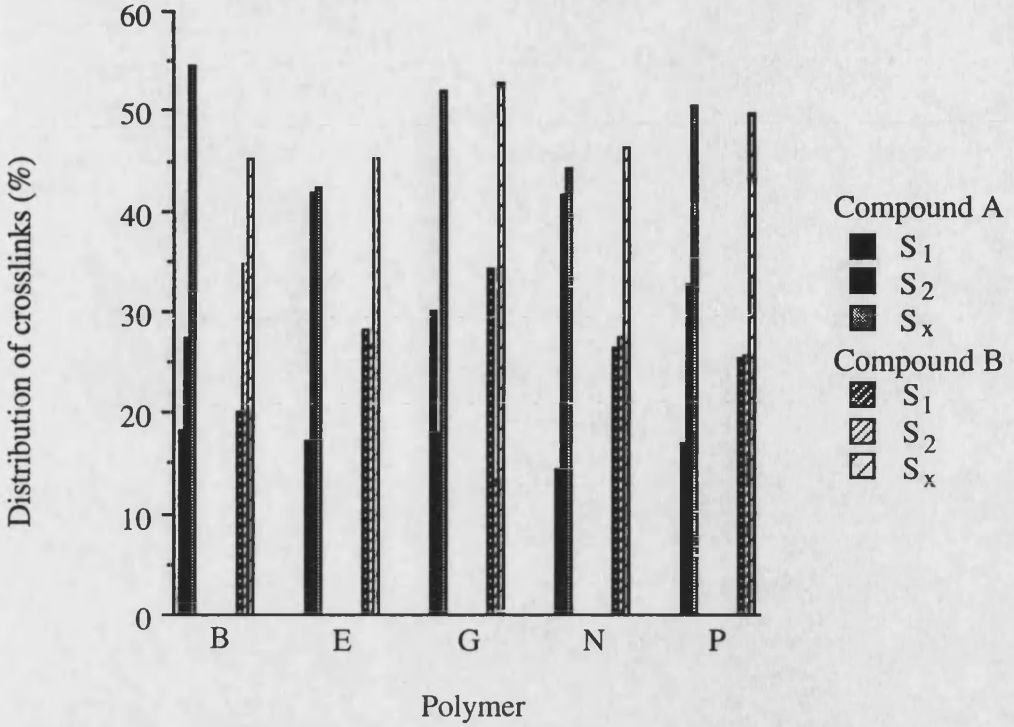

FIGURE 4.16. Distribution of crosslinks in N.B.R. vulcanizates, calculated from tables 4.19, 4.22 and 4.23, (extracted volume element not included in calculation).

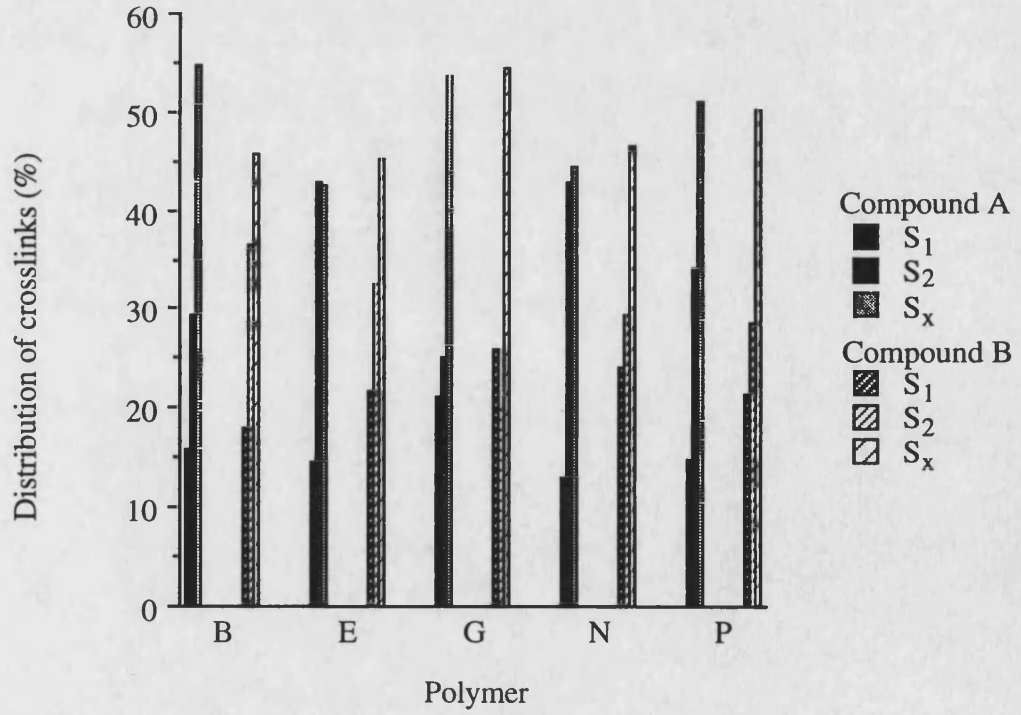

FIGURE 4.17. Distribution of crosslinks in N.B.R. vulcanizates, calculated from tables 4.19 and 4.24, (extracted volume element included in calculation).

4.4.3.5. Determination of Crosslink Density from Network Extraction

The observation that material removed during probing is polymer of molecular weight below M_c, gave rise to the possibility of calculating M_c and N_v from weight loss results of table 4.20 and molecular weight distribution curves of figure 4.4. The calculation was made by integrating G.P.C. molecular weight distribution curves and calculating the fractional area of curves corresponding to equivalent percentage weight loss at the low molecular weight end. Integration of area was made by printing molecular weight distribution curves on graph paper and counting squares.

Calculation of M_c from extraction weight loss and molecular weight distribution is illustrated in figure 4.18 and 4.19. The results of this calculation are tabulated in table 4.27.

The values of N_v obtained from weight loss data agree reasonably well with values which were obtained from compression deflection measurement, tables 4.22, 4.23 and 4.24. In vulcanizates of low network density, (subsequent to hexane-1-thiol (1M) in piperidine treatment) N_v values obtained from network extraction are significantly lower than N_v values obtained by compression deflection measurement. This is because N_v values obtained from compression deflection measurements include contributions from physical entanglements whereas network extraction measurements do not. Determination of N_v from network extraction is more representative of chemical crosslink density, therefore G.P.C.-extraction is a more accurate technique of calculating M_c and N_v. The determination of M_c and N_v by extraction of vulcanizates in which the molecular weight distribution of the polymer has been established is experimentally simpler and less time consuming to perform particularly in studies where the base polymer is a constant, and crosslink structure is investigated as function of other variables.

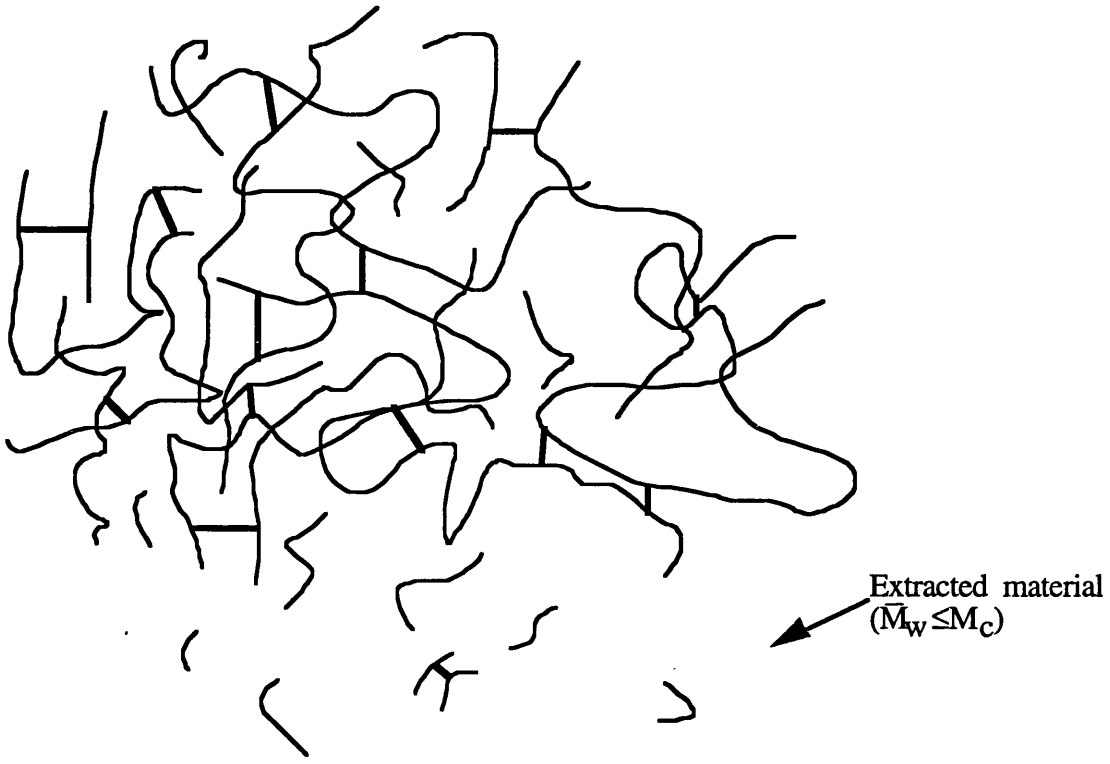

FIGURE 4.18. Illustration of the extraction of low molecular weight polymer material during network swelling.

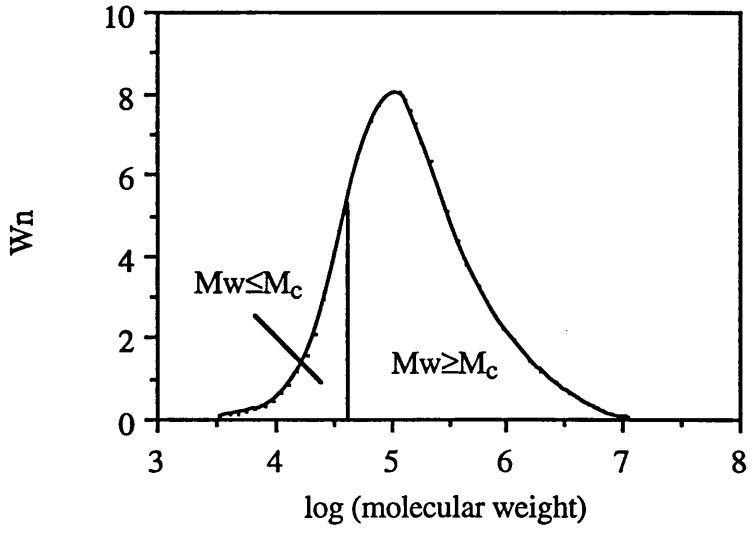

FIGURE 4.19. Illustration of calculation of M_c from extraction of uncombined polymer and molecular weight measurement.

	Propane-2-thiol (0.4M) + piperidine (0.4M) in toluene		Hexane-1-thiol (1M) in piperidine	
Vulcanizate	M_c, (g.mole^{-1})	$N_v x10^4$, (mol./cm^3)	M_c (g.mole^{-1})	$N_v x10^4$, (mol./cm^3)
BA	7727	1.29	35645	0.28
BB	7727	1.29	33420	0.30
EA	8851	1.13	38726	0.26
EB	7244	1.38	48417	0.21
GA	17701	0.57	70469	0.14
GB	17865	0.56	63826	0.16
NA	7079	1.41	39355	0.25
NB	9120	1.10	35481	0.28
PA	11885	0.84	43351	0.23
PB	11885	0.84	48753	0.21

TABLE 4.27. M_c and N_v values of pre-extracted N.B.R. vulcanizates determined from weight fraction of polymer removed during swelling, (from table 4.20).

4.4.4. SPECTROSCOPIC ANALYSIS OF NETWORK STRUCTURE

4.4.4.1. ^{13}C N.M.R. Spectroscopy

Solid state ^{13}C N.M.R. analysis was used as a complimentary technique to chemical probe-crosslink density experiments. There were insufficient resources to study all compounds and study was restricted to compounds EA, EB, PA and PB because these were deemed to be of particular interest based on their large differences in oxidative stability reported on in chapter six.

The expanded, (vertical and horizontal) ^{13}C N.M.R. spectra of these samples, within the resonance of interest in the study of sulphurated carbon structures are shown in figures 4.20 and 4.21.

The strong peak at a resonance of 25-40 ppm is caused by methylene carbon. The strong intensity of this peak and peak overlap prevented quantification of low intensity peaks.

For the purposes of interpreting spectra we have used the chemical shift assignments of sulphurated carbon structures in B.R. vulcanizates reported by Rana and Koenig (1993). The chemical shift assignments of Rana and Koenig are illustrated

in section 2.2.3.4, figure 2.4. In B.R. vulcanizates sulphurated structures are found upfield of the methylene peak.

It is pointed out there is some uncertainty in the use of these chemical shifts for N.B.R. vulcanizates because it is not known whether the point of sulphurisation is adjacent to a butadiene unit. Assignments of B.R. networks will only be valid for sulphurated carbons which are adjacent to a butadiene unit. Where the sulphurated carbon is adjacent to an ACN unit the chemical shift will be influenced by the inductive effect of the -CN group. The chemical shift of sulphurated carbons which are adjacent to ACN units is further influenced by the position of the ACN group relative to the sulphurated carbon. The tertiary carbon at the point of the -CN group may be α or β to a sulphurated allylic carbon of a butadiene unit.

The sample spectra of figures 4.20 and 4.21 show several, low intensity signals which have been assigned to various sulphurated carbon structures. The sharp peak at approximately 46 ppm is seen to occur only in vulcanizates based on polymer P. Measurement of physical crosslink density and crosslink type by chemical probe treatment shows that crosslink density and structure of vulcanizates of polymers E and P is not significantly different. This implies that this resonance is not associated with a crosslink structure. In B.R. networks Rana and Koenig (1993) have assigned this resonance to one of several structures. Specific assignment to one particular structure is not possible because there are several structures with chemical shifts in the vicinity of 46 ppm and accuracy of binding energy assignment is reported to be ± 1 ppm.

The carbon at the point of attachment in a saturated R-SX pendant group occurs at 45.8 ppm. X may be an accelerator fragment. In cyclic sulphur structures of the form RSR, resonance occurs in the region 46.4-46.8 ppm.

The observation that this resonance is not present in vulcanizates based on polymer E may imply that at the end of vulcanization a higher concentration of sulphur and accelerator fragments are combined with the polymer in P vulcanizates. Later results of table 4.28 indicate accelerator-sulphur-zinc species are more mobile in vulcanizates EA and EB than vulcanizates PA and PB.

The resonance at approximately 43.9 ppm which is present in all vulcanizates may be an R-S-R type structure in a saturated fragment, R-SX type structure in a cis-1,4-butadiene unit or R-SH in a vinyl-1,2-butadiene unit or a trans-1,4-butadiene unit.

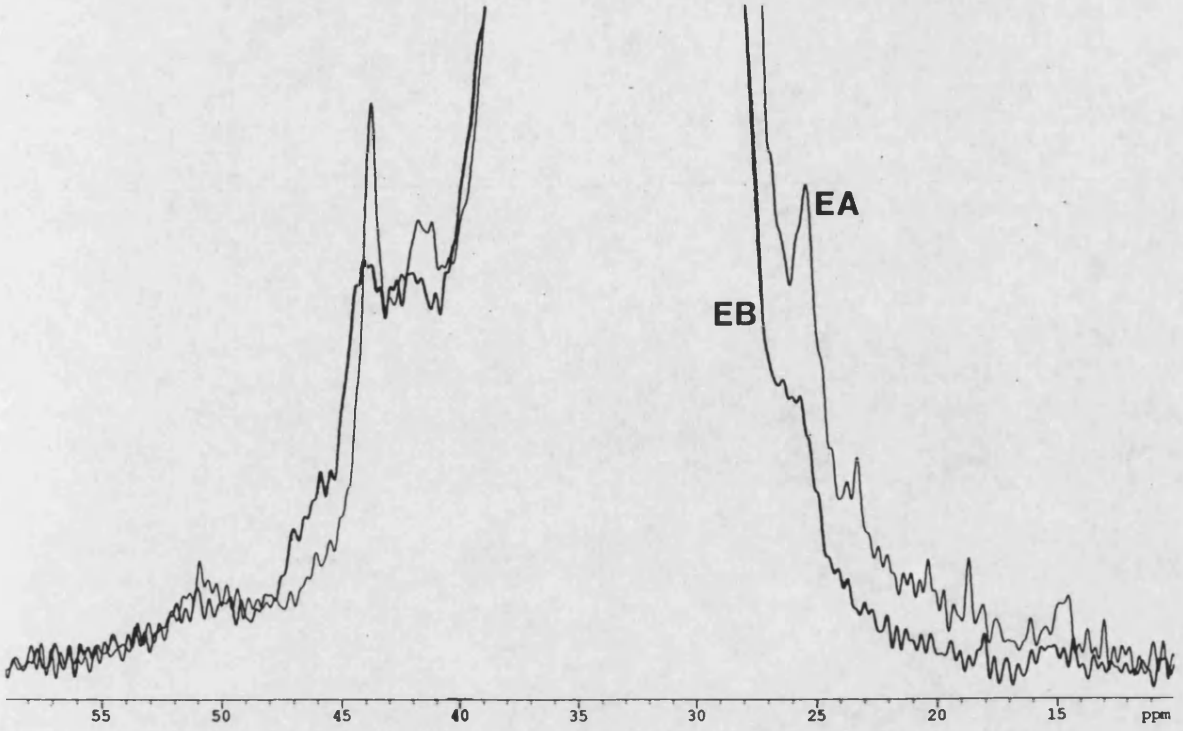

FIGURE 4.20. ^{13}C N.M.R. spectra of N.B.R. vulcanizates compounded with polymer E.

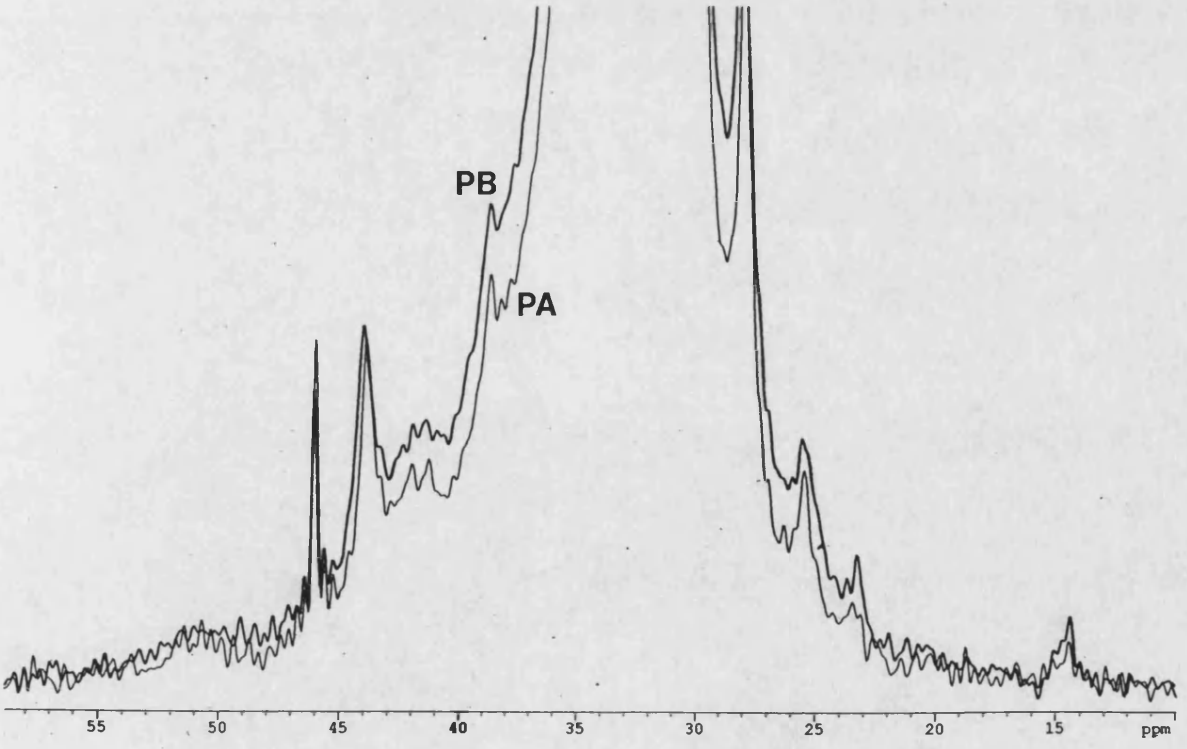

FIGURE 4.21. ^{13}C N.M.R. spectra of N.B.R. vulcanizates compounded with polymer P.

4.4.4.2. X-Ray Photoelectron Spectroscopy

X.P.S. analysis was carried out on vulcanized surfaces of EA, EB, PA and PB in order to obtain information on the structure of sulphur and zinc species.

Results from this study are presented in table 4.28. Results are expressed in terms of ratios to enable direct comparison between samples.

The S_{169ev} species present on the surface of P vulcanizates are associated with sulphate/sulphonate emulsifier residues. Such residues, which are present at very much lower concentrations in E polymer, (table 4.4) could not be detected in E vulcanizates. The higher oxygen concentration on the surfaces of P vulcanizates may also be associated with sulphate/sulphonate emulsifiers. The nitrogen concentration is much higher on the surfaces of vulcanizates of polymer E than those of polymer P. This effect was also reported in table 4.4 for raw polymer surfaces. The high nitrogen concentration on surfaces of E vulcanizates is thought to be associated with migration of low molecular weight polymer of high combined ACN content, (see section 4.4.3.2).

Compared to the surfaces of polymers all vulcanizates contain additional S_{164eV} and zinc due to the compounding in of ZnO, C.B.S. and elemental sulphur, (compare with table 4.4). The concentration and ratio of zinc and sulphur on the surfaces of vulcanizates is shown to be affected by a change in formulation and a change in base polymer. It appears that the Zn and S_{164eV} are associated in some sort of complex, (compare compounds EA with PA and EB with PB). Vulcanizates of polymer E contain a much higher concentration of S_{164eV} and zinc residue than vulcanizates of polymer P. The higher concentration of S_{164eV} and Zn on the surface of E vulcanizates may be associated with a different concentration of such species in the polymer or alternatively with higher mobility of zinc-sulphur species.

Information on the structure of zinc-sulphur species was obtained by referencing the binding energies of sulphur and zinc in vulcanizates with the binding energy of sulphur and zinc in ZnO, $ZnSt_2$, ZnS, zinc dimethyl dithiocarbamate, (Z.D.M.C). and zinc dibutyl dithiocarbamate (Z.D.B.C.). Z.D.M.C. and Z.D.B.C. were used as chemical approximations to represent the chemical bonding of zinc in the zinc-accelerator complex of section 2.2.2.4.1. The measured binding energies of sulphur and zinc found in vulcanizates and model compounds are shown in table 4.29. The binding energy of the zinc species on the surfaces of E vulcanizates are somewhat higher than the binding energies of zinc on PA surfaces and in $ZnSt_2$, Z.D.M.C. and

Z.D.B.C., however not significantly so. The binding energies of zinc on the surface of P vulcanizates, ZnO and ZnS although only slightly lower than the binding energies of zinc in Z.D.M.C. and Z.D.B.C., are significantly different from the binding energies of zinc species which are found on the surface of E vulcanizates. This implies that zinc-sulphur associated species which are found on the surface of E vulcanizates are not in the form of zinc sulphide whereas in P they may be. The difference in binding energy of zinc species on the surface of E and P vulcanizates suggest differences in the structure of such species.

The binding energy of sulphur in vulcanizates is less useful for characterising the structure of zinc-sulphur species because the sulphur peak, in the region of 164 eV is made up of contributions from crosslink structures as well as zinc-sulphur species.

The compounding-in of diphenyl amine antioxidant reduces the ratio S_{164eV}:Zn_{2p} in vulcanizates, irrespective of base polymer. This implies that the concentration of sulphur in the zinc-sulphur complex, (thought to be zinc-accelerator-thiolate) is reduced. A reduction in the concentration of sulphur in the active sulphurating agent of section 2.2.2.4.3 would cause a reduction in the number of sulphur atoms per crosslink due to increased rate of exchange reactions with poly-sulphide crosslinks and pendant groups (reaction scheme V). Practically, the compounding-in of diphenyl amine antioxidant reduces vulcanization time, (tables 4.16 and 4.17), increases overall crosslink density and increases the concentration of mono-sulphide crosslinks, (tables 4.19, 4.25 and 4.26).

Atomic ratio	PA	PB	EA	EB
O_{1s}:C_{1s}	$147.3x10^{-3}$	$134.6x10^{-3}$	$90.0x10^{-3}$	$89.0x10^{-3}$
N_{1s}:C_{1s}	$19.0x10^{-3}$	$29.5x10^{-3}$	$52.3x10^{-3}$	$46.8x10^{-3}$
*S_{164eV}:C_{1s}	$6.8x10^{-3}$	$2.9x10^{-3}$	$40.7x10^{-3}$	$16.3x10^{-3}$
^S_{169eV}:C_{1s}	$15.2x10^{-3}$	$11.1x10^{-3}$	~	~
Zn_{2p}:C_{1s}	$2.9x10^{-3}$	$4.6x10^{-3}$	$9.5x10^{-3}$	$10.1x10^{-3}$
S_{164eV}:Zn_{2p}	2.3	0.6	4.3	1.6

~None detected. *Bonded to S, C or H, ^bonded to O.

TABLE. 4.28. Mole ratios of N:C, O:C, S:C, Zn:C and S:Zn found on the surface of N.B.R. vulcanizates by X.P.S.

	Binding energy, eV	
Compound	Zn_{2p}	S_{2p}
EA	1022.90	163.70
EB	1022.75	163.15
PA	1022.35	162.95
PB	1022.45	163.25
ZnS	1022.20	163.55
Z.D.M.C./Z.D.B.C.	1022.50/1022.50	162.50/162.60
ZnO	1022.30	-
$ZnSt_2$	1022.60	-

TABLE 4.29. X.P.S. Binding energies of sulphur and zinc in N.B.R. vulcanizates and model compounds.

4.4.5. SUMMARY ON NETWORK STRUCTURE

Section 4.4 has elucidated significant differences in network density and network structure between polymers and compounds. In all vulcanizates it was found that direct carbon to carbon crosslinks are not introduced during vulcanization.

Overall network chain density is significantly lower for vulcanizates of polymer G. The lower network chain density, in vulcanizates of polymer G is thought to be caused by reaction of sulphur with oleic acid emulsifier residue, (see table 4.6 and figure 4.9). Network chains which may be introduced by reaction with oleic acid will not be stress supporting and will not contribute to measured network chain density. The low network chain density of vulcanizates of polymer E may be associated with the low molecular weight of polymer E, (table 4.8). The high network chain density of vulcanizates of polymer B may be associated with the high molecular weight of polymer B, (table 4.8). The high network chain density of vulcanizates of polymer N is thought to be caused by the presence of elemental sulphur residue in polymer N, (section 4.1.1).

At the end of vulcanization vulcanizates contain a distribution of crosslink structures. Tables 4.26 and 4.27 show that 40-55 % of all crosslinks are poly-sulphide, 20-40 % are di-sulphide and 10-25 % are mono-sulphide. In all vulcanizates it was found that polymer chains of $\bar{M}_W$ below M_c are extracted during swelling, (figure 4.15). The treatment of the extracted volume element during calculation of network density, (whether included in total volume or not) has a large influence on calculated

values of network density, (see tables 4.22, 4.23 and 4.24). This is particularly true for low network density vulcanizates where there is high weight loss during swelling.

Calculation of network density from weight loss during swelling and integration of molecular weight distribution curves, (table 4.27) gives lower values of network chain density than compression-deflection measurement and application of elastic theory, (compare with tables 4.22 and 4.23). The extraction technique is a simpler and faster method of crosslink density determination.

Vulcanizates with compounded-in diphenyl amine antioxidant exhibit a higher concentration of mono-sulphide crosslinks with all polymers, (tables 4.25 and 4.26, figures 4.16 and 4.17). X.P.S. results of vulcanizates EA, EB, PA and PB show that addition of diphenyl amine reduces the ratio of sulphur:zinc on the surfaces of vulcanizates. This may imply that the effect of diphenyl amine is attributed to increased desulphurisation of poly-sulphide crosslinks by the mechanism described by Layer (1990), (section 2.2.2.4.3, reaction scheme V).

Surfaces of vulcanizates EA and EB contain a higher concentration of sulphur and zinc than surfaces of PA and PB. This suggests that zinc-sulphur species are more mobile in vulcanizates of polymer E. This result is supported by ^{13}C N.M.R. results which show that in vulcanizates PA and PB sulphur accelerator pendant groups, or cyclic sulphur groups in saturated heptane chain fractions are present, whereas in vulcanizates EA and EB they are not. Mass spectroscopy failed to detect sulphur and accelerator fragments in the piperidine extract of vulcanizates EA, EB, PA and PB. This means that all sulphur and accelerator is combined with the network or with zinc in a insoluble zinc salt form which is not extracted by piperidine.

4.5. VULCANIZATE PROPERTIES

4.5.1. STATIC TENSILE PROPERTIES

Tensile properties of vulcanizates are tabulated in tables 4.30 and 4.31. The values agree well with previous tensile measurements on sulphur crosslinked N.B.R. gumstock compounds reported by Sims (1988).

Vulcanizates of polymer G exhibit significantly higher tensile strength and tear strength than other samples for both compound formulations. In

the absence of significant differences in molecular structure between G and other polymers the higher tensile strength and tear strength of vulcanizates based on this polymer are likely to be associated with the lower network chain density. It is well documented that in sulphur vulcanized N.R. the dependence of tensile strength on crosslink density assumes a parabolic function. Up to a limiting value of crosslink density tensile strength increases while with further increase in crosslink density tensile strength is reduced (Brown *et al.*, 1985). Tear strength follows a similar relationship but the increase and fall in strength is more dramatic.

The addition of diphenyl amine to compounds causes an increase in tensile stress, ultimate tensile strength and tear strength. This increase will be associated with the higher network chain density of vulcanizates of compound B, (these are reported in table 4.19). The effect of ageing on tensile properties is reported in chapter six.

Property	BA	EA	GA	NA	PA
σ at 100 % elongation	1.13±0.02	0.99±0.03	1.00±0.03	1.04±0.08	1.03±0.06
σ at 200 % elongation	1.57±0.04	1.30±0.05	1.43±0.09	1.39±0.08	1.37±0.07
σ at 300 % elongation	2.00±0.05	1.56±0.08	1.84±0.12	1.66±0.99	1.63±0.11
σ at break	2.39±0.42	2.42±0.22	2.92±0.36	2.40±0.24	2.14±0.11
elongation at break, %	380±34	489±37	461±41	467±60	427±48
Hardness (I.R.H.D.)	55	54	52	55	53
Tear strength	1.72±0.17	1.79±0.24	2.42±0.48	1.52±0.13	1.72±0.36

σ is in units of MPa and tear strength in units of kN/m, (95 % confidence limits are given).

TABLE 4.30. Mechanical properties of N.B.R. gum vulcanizates of compound A.

Property	BB	EB	GB	NB	PB
σ at 100 % elongation	1.07±0.01	0.98±0.05	1.04±0.04	1.04±0.02	1.04±0.06
σ at 200 % elongation	1.44±0.04	1.30±0.03	1.56±0.16	1.37±0.02	1.42±0.04
σ at 300 % elongation	1.81±0.08	2.54±0.07	2.10±0.22	1.68±0.03	1.75±0.05
σ at break	2.61±0.28	2.48±0.10	3.47±0.38	2.57±0.29	2.50±0.15
elongation at break, %	439±26	489±32	458±35	465±38	431±21
Hardness (I.R.H.D.)	53	52	53	53	53
Tear strength	1.81±0.26	2.00±0.27	2.08±0.30	1.79±0.12	1.84±0.18

σ is in units of MPa and tear strength in units of kN/m, (95 % confidence limits are given).

TABLE 4.31. Mechanical properties of N.B.R. gum vulcanizates of compound B.

4.5.2. GLASS TRANSITION

4.5.2.1. Differential Scanning Calorimetry

Glass transition parameters of vulcanizates obtained by D.S.C. at a heating rate of 5°C/minute are tabulated in table 4.32. These values should be compared with the glass transition parameters of the base polymers obtained under equivalent conditions, (tables 4.12 and 4.13). An increase in glass transition temperature is observed with all vulcanizates, particularly sample G, in comparison with the corresponding polymers, (table 4.12).

The increase in glass transition temperature may be associated with a reduction in chain mobility caused by the introduction of crosslinks between polymer chains.

The width of glass transition in vulcanizates is strongly influenced by the width of transition in the corresponding polymers. Vulcanizates of polymer E exhibit a narrow transition while vulcanizates of polymer G exhibit a wide transition. Glass transition in vulcanizate samples occurs over a narrower temperature range than in the corresponding raw polymers, (compare with table 4.13). The reduction in the width of transition is particularly large in vulcanizates of polymer G. This is consistent with the theory that unsaturated low molecular weight material of polymer G, (tables 4.5 and 4.6) is crosslinked into the polymer during vulcanization. A narrower temperature of glass transition suggests a narrower distribution of relaxation times.

Vulcanizate	Tg, °C	$\Delta Cp_{(Tg)}$, J/g	$\Delta T_{(Tg)}$, °C
BA	-29.4	0.98	15.6
BB	-29.1	1.00	14.5
EA	-26.4	0.75	7.0
EB	-27.7	0.92	7.0
GA	-27.0	1.27	19.5
GB	-27.5	1.25	18.0
NA	-27.6	1.06	16.8
NB	-27.1	1.16	15.8
PA	-30.3	0.69	10.7
PB	-28.7	0.71	10.6

TABLE 4.32. Glass transition temperature, change in specific heat capacity and the width of transition of N.B.R. vulcanizates, determined from D.S.C. at a heating rate of 5°C/minute.

4.5.2.2. Dynamic Properties in the Glass Transition Region

For all polymers dynamic modulus changes in the transition region from a glassy value of $1.34 \pm 0.04 \times 10^6$ kPa to a room temperature value of $2.57 \pm 0.12 \times 10^3$ kPa.

The relationship between E' and E" of compounds based on polymers E and G illustrated by viscoelastic loss angle is shown in figure 4.22 and 4.23. Viscoelastic loss properties are tabulated in table 4.33.

The peak tan δ temperature, (T_α) is related to D.S.C. glass transition temperature of vulcanizates, with high degree of scatter. The width of the viscoelastic loss peak at its base, (table 4.33) is related to the width of glass transition measured by D.S.C., (table 4.32). The viscoelastic peak of GA and GB are characterised by a broad shoulder at the low temperature end, (figures 4.22 and 4.23). A wide glass transition was also found in vulcanizates of polymer G by D.S.C., (table 4.32). Vulcanizates based on polymer G also exhibit lower tan δ values.

It is thought that differences in relaxation behaviour and viscoelastic loss characteristics between vulcanizates based on polymer G and other polymers are caused by the presence of a higher concentration of methanol extractable residue in polymer G, (table 4.5). The width of glass transition is reduced after vulcanization due to crosslinking of low molecular weight material into the network.

The viscoelastic peak in vulcanizates of polymer E is narrower at its base than the viscoelastic peaks of other polymers. A narrow glass transition region was also found by D.S.C. measurement, (table 4.32). The narrower viscoelastic loss peak of vulcanizates of polymer E could be associated with its narrow molecular weight distribution.

Vulcanizate	Tan δ maximum	Tα, (°C)	Width of tan δ at base, (°C)
BA	1.57	-16.2	47.2
BB	1.50	-15.3	47.2
EA	1.84	-14.5	40.5
EB	1.94	-15.0	40.0
GA	1.38	-14.5	49.5
GB	1.38	-13.4	49.5
NA	1.48	-15.4	47.2
NB	1.53	-15.2	47.0
PA	1.55	-17.7	46.9
PB	1.78	-16.4	47.5

TABLE 4.33. Viscoelastic loss peak parameters of N.B.R. vulcanizates, obtained at a test frequency of 10 Hz.

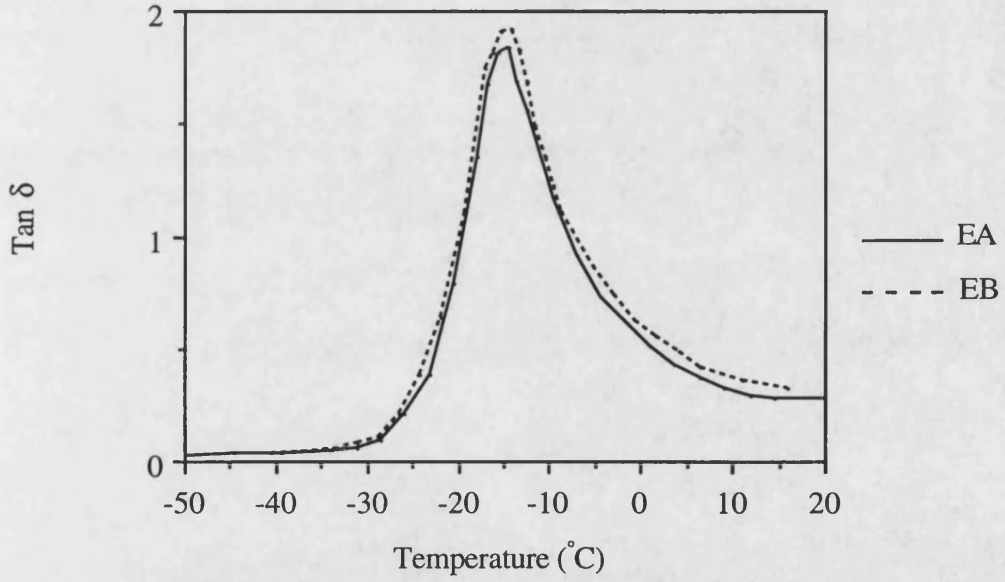

FIGURE 4.22. Viscoelastic loss angle, (tan δ) in the glass transition region of EA and EB compounds, obtained at a test frequency of 10 Hz.

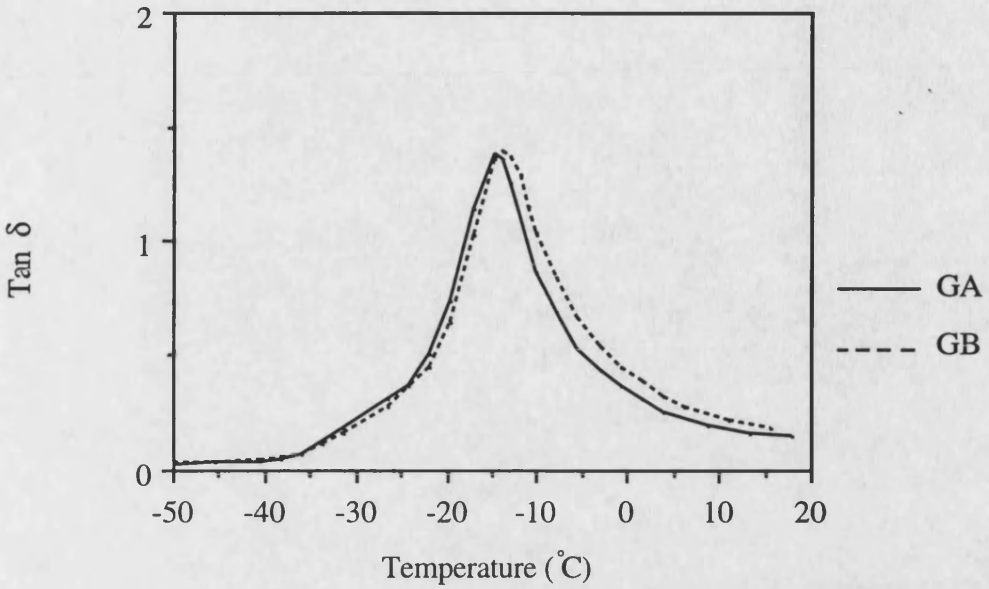

FIGURE 4.23. Viscoelastic loss angle, (tan δ) in the glass transition region of GA and GB compounds, obtained at a test frequency of 10 Hz.

4.5.3. SUMMARY ON VULCANIZATE PROPERTIES

Section 4.5 shows there to be differences in tensile and viscoelastic loss properties in the glass transition region between polymers.

Vulcanizates of polymer G exhibit a significantly higher modulus, tensile strength and tear strength than other polymers, (see tables 4.30 and 4.31). These differences in properties between vulcanizates of polymer G and other vulcanizates may be caused by the lower crosslink density found in vulcanizates GA and GB, (see table 4.19). This is a consequence of unsaturated carboxylic acid residues of polymer G.

The viscoelastic response of vulcanizates in the glass transition region is sensitive to a change in base polymer. This has important implications for applications where viscoelastic loss properties are important, such as dynamic applications. Vulcanizates of polymer G exhibit a significantly lower tan δ maximum and a wider glass transition region. A wider glass transition region was also measured in polymer G in comparison with other polymers, (table 4.13). The wider structural relaxation region appears to be associated with methanol extractable residues, such as carboxylic acid

emulsifier residue. It is thought that the width of transition in vulcanizates based on polymer G is greatly reduced after vulcanization due to crosslinking of unsaturated carboxylic acid residue, (compare table 4.13 and 4.33).

Vulcanizates of polymer E exhibit a higher tan δ maximum and a narrower glass transition region. A narrower glass transition region is also noted in E polymer (table 4.13). This could be associated with the low molecular weight distribution and high gel content of polymer E.

4.6. CONCLUDING REMARKS ON MATERIAL CHARACTERISATION

This concluding section briefly reviews the results and discussion of the preceding sections into material characterisation and highlights results which will be of interest in the study of N.B.R. oxidation of chapter six.

Detailed differences in molecular structure and elemental composition have been demonstrated between commercial N.B.R. samples of identical specification. It is shown that these differences are important in understanding structural relaxation behaviour and vulcanization behaviour of polymers and vulcanizates. It is likely that such differences in structure and composition will also influence and help to understand the oxidation of N.B.R. vulcanizates, treated in chapter six.

Structural characterisation of the raw polymer has elucidated differences in gel content, molecular weight distribution and sequence distribution between polymer samples. Elemental characterisation has shown that commercial N.B.R. polymers contain emulsifier and coagulant residues which are found to vary with manufacturer. Emulsifier residues are in the form of alkyl/aryl sulphate/sulphonate surfactants and saturated/unsaturated carboxylic acid/salt species. Coagulant residues are calcium chloride and magnesium chloride. In the polymer such residues will be hydrated. Other polymerisation residues such as alkyl mercaptan modifier and elemental sulphur are found in some polymers at low concentrations.

All polymers contain different mixtures of commercial antioxidants. The differences in antioxidant residues will be important in the study of N.B.R. oxidation, (chapter six).

Work on structural relaxation behaviour in the glass transition region shows that the width of relaxation is high in polymer G. Polymer G also exhibits lower viscosity, particularly at high shear rates than other polymers. Both effects are associated with the high methanol extractable residue of polymer G, a high proportion of which is carboxylic acid emulsifier residue.

Study of N.B.R. vulcanization shows that total vulcanization behaviour and network chain density is strongly affected by base polymer. Network chain density is low in vulcanizates of polymer G due to preferential reaction of crosslinking agent with unsaturated oleic acid residue of polymer G. A reduction in torque modulus was demonstrated in a separate compound by compounding in oleic acid.

Network chain density is sensitive to molecular weight. Polymer B has high molecular weight and its vulcanizates have high network chain density, while polymer E has low molecular weight and its vulcanizates have low network chain density. Elemental sulphur residue is associated with increased crosslink density.

Vulcanization is accelerated by diphenyl amine antioxidant and the concentration of mono-sulphide crosslinks is increased, probably due to reduction in the sulphur:zinc ratio in the active sulphurating agent. The extent of acceleration is influenced by base polymer. This implies antagonism between base polymer and polymerisation residues. The effect will be studied further in section 6.4, by compounding in individual polymerisation residues.

The study of network structure of N.B.R. by compression-deflection measurement of swollen networks shows that significant extraction of uncrosslinked polymer chains occurs during swelling of networks with low crosslink density. Measurement of the weight of extracted material and molecular weight distribution of the base polymer allows determination of chemical molecular weight between crosslinks, (M_c) by assuming that extracted material is uncombined polymer of average molecular weight in the region of M_c. In the measurement of physical crosslink density the volume element which is removed from the network during swelling should therefore be included in the total sample volume.

CHAPTER V

5.0. THERMO-OXIDATION; EXPERIMENTAL PROCEDURE

5.1. THERMO-OXIDATIVE AGEING OF VULCANIZATES

This chapter describes experimental procedures used in study of N.B.R. oxidation. Where experimental procedures are identical to those used in material characterisation, described in chapter three, the reader is referred to that chapter.

5.1.1. CIRCULATING AIR OVEN AGEING

Tensile dumbbell testpieces type 2 and trouser tear strength testpieces of nominal thickness 1 mm, cut from vulcanized sheets of section 3.8 were suspended and aged in a circulating air oven, Gallenkamp, model 300 series. Oven, air temperature, measured by a mercury thermometer was seen to vary by approximately ±1°C. Ageing was in accordance with BS 903, part A19, (1986), equivalent international standard ISO 188, (1982)

Samples were aged at temperatures of 70°C, 85°C, 100°C, 115°C and 130°C. At each temperature six testpieces from each sample were removed after periods of 1 day, 3 days, 7 days, 14 days and multiples of 7 days thereafter. The multiple was adjusted for test temperature such that at high temperatures samples were removed more frequently than at low temperatures.

Samples based on different compounds were aged in separate ageing ovens, to prevent cross contamination from compounded-in antioxidant.

5.1.1.1. Measurement of Mechanical Properties

Tensile testing of samples subsequent to ageing and conditioning at room temperature for 24 hours are consistent with testing procedures outlined in section 3.10.1.

Dynamic testing of aged samples was carried out on a Rheovibron DDV II manual reading instrument, in accordance with experimental conditions outlined in

section 3.10.4. Samples for these studies were cut from the parallel section of aged dumbbell testpieces (width 4 mm and nominal thickness 1 mm).

5.1.1.2. Weight Change of Samples During Ageing

The weight change of vulcanizates during circulating air oven ageing at 100°C was monitoring by removing dumbbell testpiece samples (thickness of 1 mm), at periodic intervals and weighing immediately on a Sartorius A200S analytical microbalance. After weighing samples were returned to the ageing oven.

5.1.1.3. Measurement of Density

The relative density of vulcanizate samples, (approximate thickness 1 mm) before and subsequent to air oven ageing at 100°C was determined by test method BS 903, part A1, (1980), equivalent international standard ISO 2781, (1975). Density is determined by weighing samples in air and in solvent. Density determination is based on the principle that the reduction in weight when weighing in solvent is equal to the weight of solvent displaced, (this allows measurement of sample volume). The solvent used was methanol of relative density 0.7915.

5.2. NETWORK OXIDATION

5.2.1. STRESS RELAXATION

5.2.1.1. Intermittent Stress Relaxation

Parallel side test samples of width 10 mm and nominal thickness 1 mm, cut from vulcanized rubber sheets were aged in a circulating air ageing oven, Gallenkamp model 300 at a temperature of 100°C. Aged samples (3 from each vulcanizate) were removed at periodic time intervals and conditioned for 1 hour at room temperature before testing. Samples were tested on an Instron 1195 tensometer in accordance with conditions specified in BS 903, part A52 C, (1986), equivalent international standard ISO 6914, (1985).

Samples were conditioned by cycling between the relaxed state and 50 % elongation at a uniform crosshead speed of 50 mm per minute. The force which

produced a 50 % elongation on the fifth cycle was used for subsequent calculations. After testing intermittent stress relaxation samples were immediately transferred to the ageing oven. The time the samples were outside the ageing oven was not included in determination of ageing time.

5.2.1.2. Continuous Stress Relaxation

Continuous stress relaxation of vulcanized samples at 100°C was measured on a non-commercial continuous stress relaxation in tension instrument, built by the author to meet the requirements of this work and BS 903, part A52A, (1986), equivalent international standard ISO 6914, (1985). The instrument was based on a development of A. L. Gregory from the Centre for Polymer Studies.

The relaxometer (shown in figure 5.1) consists of parallel face sample grips which hold a sample, without slippage. The stationary upper sample grip is connected to a load cell type BAB-7.5M supplied by Graham and White Instruments of St. Albans, U.K.. Each load cell is connected to a separate 8000 series load indicator, (also supplied by Graham and White). Load resolution is specified at 0.05 % of full scale (full scale 7.5 kg), repeatability is specified at 0.03 % of full scale. The movable lower grip is connected to a dial gauge, type 258A, supplied by Mercer of England, to allow measurement of extension.

Sample and sample grips are enclosed in insulated aluminium tubes with openings to atmosphere to allow sufficient circulation of air. Temperature control is provided by band heaters with a power rating of 750 W, connected to Omega CN9000A series P.I.D. temperature controllers supplied by Omega Engineering, Broughton Astley, U.K.. Test temperature, (air temperature approximately 5 mm away from sample surface) was within ±1°C at 100°C.

Continuous stress relaxation testing involved extending parallel sided samples, cut from vulcanized sheet, (width 40 mm and approximate thickness 1 mm) to 50 % elongation. A test piece width of 40 mm was found to be suitable after initial experiments with narrower samples. Samples were introduced into the instrument, after pre-heating to 100°C, and the load reading zeroed. After stabilisation of test temperature at 100°C the samples were extended and the load readings recorded manually as a function of time.

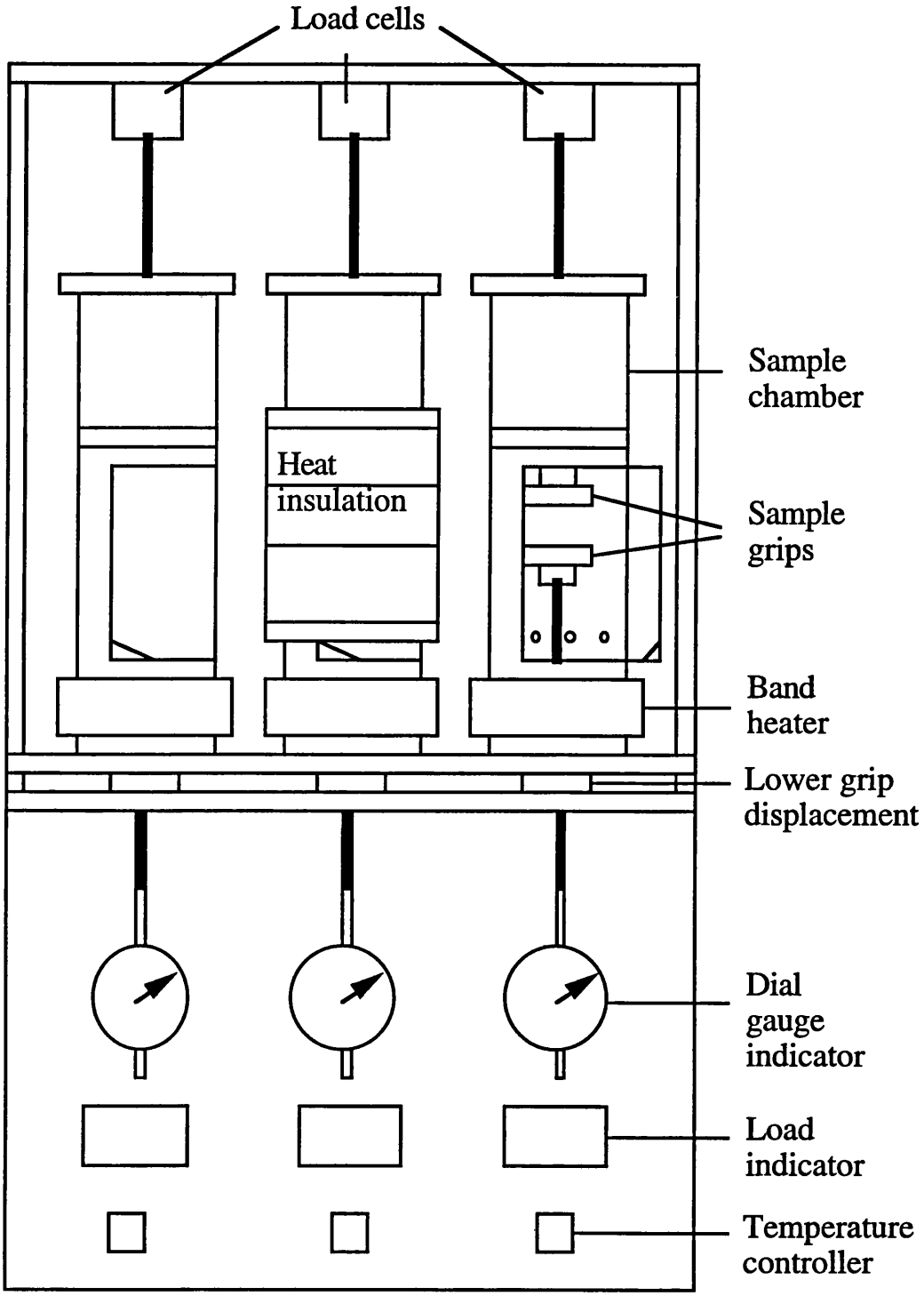

FIGURE 5.1. Simplified diagram of the continuous stress relaxation in tension apparatus.

5.2.2. CHARACTERISATION OF OXIDISED NETWORK STRUCTURE

5.2.2.1. Chemical Probe Treatment

Chemical probing of vulcanizate samples which have been aged at 100°C for periods of 7 days, 14 days, 42 days and 84 days was carried out by experimental procedures outlined in section 3.9.2.3. Aged samples were extracted before probing using conditions of section 3.9.1.

5.2.2.2. Measurement of Crosslink Density

Determination of swelling behaviour in toluene and determination of elastic constants of vulcanizates which have been aged at 100°C for periods of 7 days, 14 days, 42 days and 84 days used experimental procedures developed in the study of network structure of unaged vulcanizates. Experimental conditions were outlined in section 3.9.2.2.2.

5.2.2.3. Oxidation of Chemically Probed Networks

5.2.2.3.1. Preparation of Samples

Sample networks containing mono-sulphide crosslinks only were prepared by probing vulcanizates of compound A with hexane-1-thiol (1M) in piperidine. Work was based on compound A because it is likely that much of compounded in antioxidant would be extracted during probing. The conditions used in probing and washing probed samples have been outlined in section 3.9.2.3.

Further samples were prepared by treating vulcanizates compounded with formulation A with piperidine alone for 72 hours at 23°C under nitrogen. The piperidine solvent was removed from vulcanizates by the washing and drying procedures of section 3.9.2.3.3.

5.2.2.3.2. Weight Change of Probed Samples During Ageing

Network samples of known crosslink structure, (thickness 1 mm), prepared by chemical probe treatment of section 5.2.2.3.1 were aged at 100°C in a circulating air

oven using conditions outlined in section 5.1.1 and their weight measured using conditions of section 5.1.1.2.

5.2.2.3.3. Study of Oxidation by D.S.C.

Chemically probed network samples were heated in a calibrated DuPont 9900 D.S.C. at a controlled heating rate of 5°C per minute in static air. Samples were heated in open aluminium pans, the D.S.C. cell being open to the atmosphere. For these studies sample weight was maintained at 0.2 mg.

5.2.2.3.4. Intermittent Stress Relaxation

Intermittent stress relaxation testpieces (width 10 mm, thickness 1 mm) were cut out of chemically probed samples and aged at 100°C using conditions of section 5.2.1.1.

5.2.2.3.5. Continuous Stress Relaxation

Continuous stress relaxation testpieces (width 40 mm, thickness 1 mm) were cut out of probed samples and tested at 100°C using conditions outlined in section 5.2.1.2. Chemically probed samples were only extended to 25 % elongation because these samples failed rapidly by rupture when extended to 50 %.

5.3. ANALYTICAL STUDY OF THERMO-OXIDATION

5.3.1. F.T.I.R. SPECTROSCOPY

N.B.R. vulcanizates of thickness 1 mm which had been aged at 100°C using conditions of section 5.1.1, for periods of 1 day, 3 days, 7 days, 14 days and 42 days were analysed by F.T.I.R. spectroscopy using the A.T.R. technique with thallium bromoiodide crystal as the internal reflection element. The surface area of samples was maintained at 1 cm^2 (combined surface area, for both sides of crystal = 2 cm^2). Resolution was maintained at 2 cm^{-1} for all such work. The critical angle of reflection was set at 60° and the number of scans used 100.

A background scan was made before sample scanning. Background scanning was repeated when peak absorbances which are associated with background absorbance such as CO_2 and N_2 began to appear in sample spectra.

5.3.2. X-RAY PHOTOELECTRON SPECTROSCOPY

Vulcanizates of PA, PB, EA and EB after oxidation at 100°C for 14 days using conditions of 5.1.1 were analysed on a V.G. Escalab mark II X.P.S. Work was based on these samples in order to compare results from oxidised surfaces with results from unoxidised samples. Because of the need for consistency the instrument was operated according to conditions used for analysing unoxidised samples, (section 3.9.2.6).

5.3.2.1. Mass Spectroscopy

Molecular fragments released from oxidised samples by X-ray bombardment during X.P.S. analysis were analysed by an attached mass spectrometer, (HAL 320 gas analyser) as for unoxidised samples, (section 3.9.2.6.1).

5.3.3. DIFFERENTIAL THERMAL ANALYSIS

5.3.3.1. Differential Scanning Calorimetry

5.3.3.1.1. Heating in Air

Raw polymer samples and vulcanized samples were heated in a DuPont 9900 D.S.C. instrument from ambient to 500°C at a heating rate of 5°C per minute. Samples were heated in open aluminium pans in static air. The reference was an empty aluminium pan. The D.S.C. sample cell was open to atmosphere. Initial studies used sample weight of 8 mg. Later studies used samples of weight in the region of 0.2 mg, in order to overcome diffusion effects. The surface area of 0.2 mg samples was maximised by subdividing samples in five smaller weight fractions.

The heating rate of 5°C per minute was chosen from preliminary study into the effect of heating rate on oxidation of polymer B samples (weight 6 mg) using heating rates of 1°C per minute, 2°C per minute, 5°C per minute and 20°C per minute. Heating at a rate of 5°C per minute reduced the time base of the experiments, and

increased resolution in comparison with experiments at lower heating rates. Use of a heating rate of 20°C per minute was discounted due to an increase in dynamic temperature effects.

Calibration was made prior to sample analysis by running experiments with tin and indium, (see section 3.7.2.2).

5.3.3.1.2. Heating in Nitrogen

Thermal D.S.C. degradation was measured by heating vulcanized samples in open aluminium pans under flowing nitrogen (flow rate 2 ml per minute). Samples were heated from ambient to 500°C at a heating rate of 5°C per minute. Samples weight was maintained at 6 mg.

5.3.3.2. Combined Differential Thermal Analysis and Thermogravimetric Analysis

Combined differential thermal analysis and thermo-gravimetric analysis was made on a Stanton Redcroft simultaneous thermal analyser model 785, located at D.R.A., Holton Heath, U.K.. Vulcanizate samples were heated from ambient to 600°C in open aluminium pans at a heating rate of 10°C per minute in flowing air. The reference was an aluminium pan containing a similar weight of aluminium powder to the sample. A sample size of approximately 0.7 mg ($7.0 \text{ g} \times 10^{-4}$) was used for this study because the instrument could not operate efficiently with lower sample weight. Maximum resolution of the instrument is 1×10^{-5} g. Samples were sub-divided into several smaller weight fractions, to obtain an increase in surface area.

The instrument was calibrated prior to running sample experiments.

5.4. MEASUREMENT OF OXYGEN DIFFUSION

5.4.0.1. Preparation of Membranes

Vulcanizate membranes (of thickness in the region of 0.1 mm) were prepared by pressing rubber compounds between two sheets of melinex film at 150°C. The rubber compound of weight in the region of 1 g was divided into smaller fractions and

spread over an area of 100 cm^3 to eliminate membrane thickness variation. Vulcanization times of table 4.16 were used for preparation of membranes.

Diffusion experiment test pieces were made by cutting out circular sections (diameter 50 mm) from moulded sheet membranes. Variation in membrane thickness was checked with Mitutoyo digital callipers. Sample thickness was calculated from measurement of membrane weight, density and area.

5.4.0.2. Isobaric Measurement of Diffusion

The isobaric diffusion apparatus set up to measure oxygen diffusion through polymer films uses design principles established by Yasuda and Rosengren (1970). The apparatus consists of two cavities which are separated by the membrane. One side of the membrane was connected to a sweep gas, (this being helium) whilst the other side was connected to the permeant gas, (this being oxygen). Diffusion of gas through the membrane was measured by a thermal conductivity detector. The differential thermal conductivity detector was connected to the sweep gas on the low concentration side of the membrane and to a reference gas stream, (this being helium).

Initial experiments utilising a differential measurement arrangement, in which one side of the membrane is open to the permeant gas whilst the other was continuously purged with the sweep gas proved unsuccessful because the detector was insufficiently sensitive to detect the low concentration of diffusing gas.

Subsequent experiments used a integral arrangement (figure 5.2) in which the cavity which is connected to the detector is sealed. The detector used for these experiments was a Pye series 104 chromatograph. Sweep gas and permeant gas flow was 100 cm^3 per minute. The column oven temperature was the same as detector oven temperature.

The permeation of the gas on the high concentration side of the membrane is characterised by a time lag corresponding to the time required for permeant gas to break through the film and steady state permeation conditions to be established. The value of the time lag L, obtained by extrapolating the linear part of permeation curves to zero concentration on the time scale is related to diffusion constant, D by equation 5.1.

$$D = l^2/6L \qquad (5.1)$$

where, l is the thickness of the membrane.

The time required for oxygen to reach the sample cavity after opening of the gas cylinder was checked in preliminary experiments. Prior to running diffusion experiments both sides of the membrane were purged with helium until a constant baseline was established.

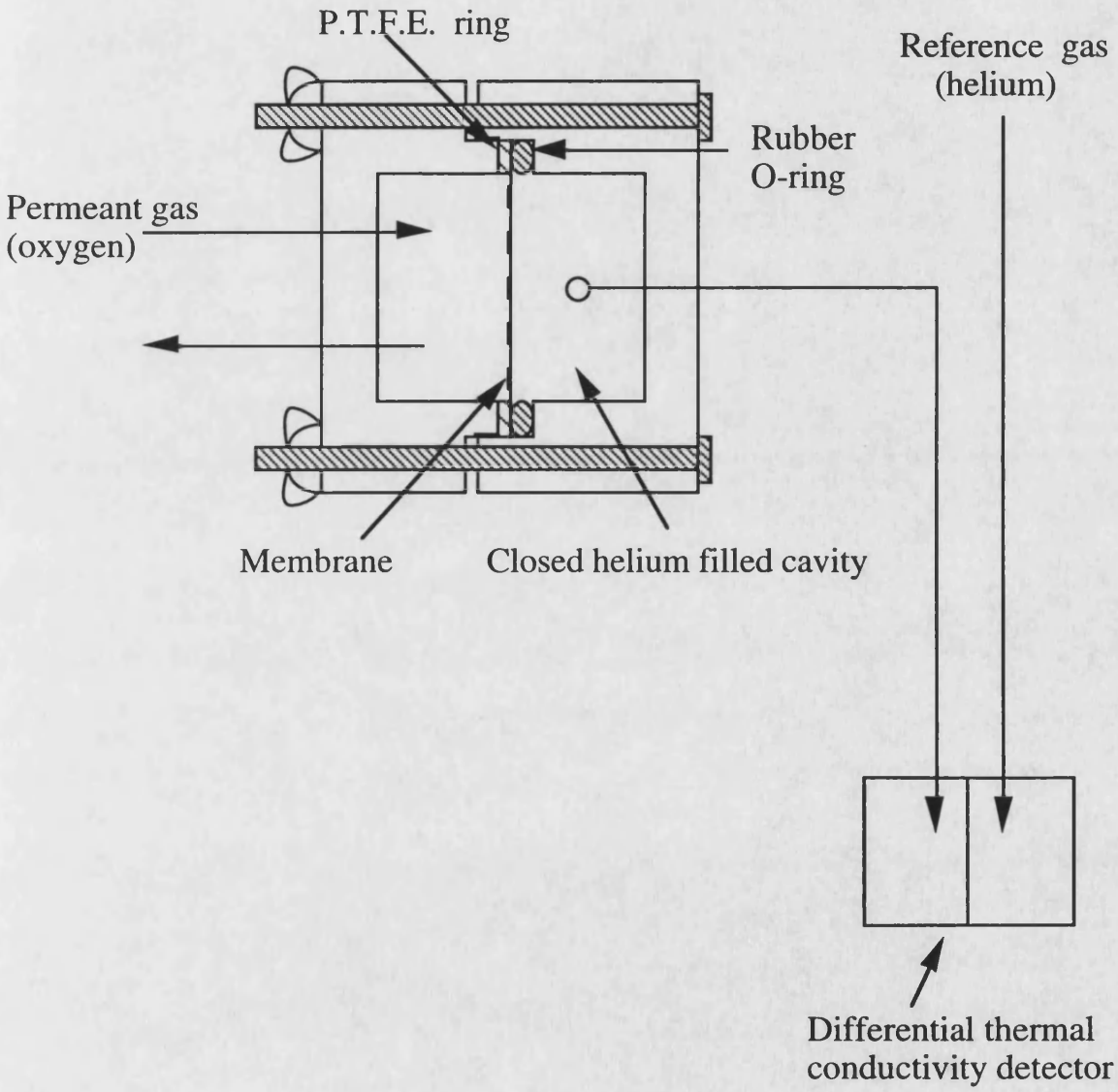

FIGURE 5.2. Simplified diagram of the apparatus set up to measure oxygen diffusion.

5.5. INFLUENCE OF POLYMERISATION RESIDUES ON OXIDATION

5.5.1. COMPOUNDING-IN OF POLYMERISATION CHEMICALS

The effects on thermo-oxidative ageing of N.B.R. of calcium chloride coagulant residues, sodium dodecyl sulphate emulsifier and sodium dodecane sulphonic acid emulsifier, (shown in table 4.3) were assessed by compounding in such chemicals into compounds EA and EB. Polymer E was chosen for these studies because it contains lower concentrations of calcium, chlorine and oxygen bonded sulphur than polymer P. Calcium chloride was added in the hydrate form because calcium chloride polymerisation residues of table 4.3 are likely to be in this form. Sodium dodecyl sulphate and sodium dodecane sulphonic acid were added at the same molar concentration. These compounds are illustrated in tables 5.1 and 5.2.

Compounds of tables 5.1 and 5.2 were mixed on a water cooled two-roll mill for 2 minutes, then sheeted off.

The vulcanization behaviour of prepared compounds was measured on a Monsanto Tm_{100} rheometer at 150°C, using conditions of section 3.7.1. Vulcanized compression sheets were moulded in accordance with experimental conditions described in section 3.8.

Ingredient	EACACL	EADS	EADSA
Compound EA	109	109	109
Calcium chloride hydrate	0.4	0	0
Sodium dodecyl sulphate	0	0.85	0
Sodium dodecane sulphonic acid	0	0	0.90

Table 5.1. N.B.R. formulations of EA compound.

Ingredient	EBCACL	EBDS	EBDSA
Compound EB	111	111	111
Calcium chloride hydrate	0.4	0	0
Sodium dodecyl sulphate	0	0.85	0
Sodium dodecane sulphonic acid	0	0	0.90

Table 5.2. N.B.R. formulations of EB compound.

5.5.1.1. Polymerisation Additives-Curative Interactions

Interactions between calcium chloride hydrate, sodium dodecyl sulphate and sodium dodecane sulphonic acid and compounding chemicals were examined in a D.S.C. using conditions outlined in section 3.7.2.2.1.

5.5.2. THERMO-OXIDATIVE AGEING

5.5.2.1. Tensile Property Change on Ageing

Tensile dumbbell samples of thickness 1 mm, containing polymerisation additives were aged at 100°C in a circulating air oven and tensile tested using conditions described in section 5.1.1.

5.5.2.2. Weight Change on Ageing

Weight measurement of samples of nominal thickness 1 mm during oven ageing is described in section 5.1.1.2.

5.5.2.3. Stress Relaxation

Intermittent and continuous stress relaxation studies of compounds containing polymerisation additives used experimental conditions outlined in section 5.2.1.

CHAPTER VI

6.0 THERMO-OXIDATIVE AGEING; RESULTS AND DISCUSSION

This chapter presents results on the oxidation of N.B.R. vulcanizates and discusses the effect of base polymer and compound formulation on the process.

The first section (section 6.1) illustrates the effect of oxidation on static and dynamic tensile properties of all ten compounds used in this study, but as the chapter unfolds greater attention is given to the two polymers (four compounds) which exhibit the most significant differences in oxidative stability. The temperature dependence of the rate of property change is included in section 6.1. Section 6.2. reports on network oxidation and section 6.3 presents further information obtained by spectroscopic techniques on the mechanism of oxidation. The final section 6.4 looks at raw polymer effects on oxidative stability by compounding in polymerisation residues.

6.1. PHYSICAL PROPERTY CHANGE DURING AGEING

6.1.1. STATIC TENSILE PROPERTIES

Ageing of N.B.R. under aerobic conditions is accompanied by change in mechanical properties, caused by oxidative scission and crosslinking reactions. The study of mechanical properties is therefore a useful means of measuring oxidative stability of rubber vulcanizates.

Results of this section show the effect of ageing on static and dynamic tensile properties and the effect of base polymer and compound formulation on the rate of property change. Retention of elongation at break values of vulcanizates of compound A and B, are shown in figures 6.1 and 6.2, respectively. The change in stress at 100 % elongation is shown in figures 6.3 and 6.4, and the change in tensile strength in figures 6.5 and 6.6.

For all compounds ageing causes a reduction in elongation at break and an increase in modulus and tensile strength. Such property change of N.B.R. during ageing has been associated with an increase in crosslink density (Kotani and Teramoto, 1980).

The rate of tensile property change is shown to be influenced by base polymer and compound formulation. In compound A vulcanizates of polymer P show best oxidative stability while vulcanizates of polymer E show worst stability, (figures 6.1-6.6). After 14 days ageing at 100°C, the change in elongation at break, stress at 100 % elongation and tensile strength, of PA are -101 %, +0.18 MPa and +0.04 MPa, respectively. After 14 days ageing at 100°C of EA, the change in elongation at break, stress at 100 % elongation and tensile strength are -323 %, +0.84 MPa and +0.51 MPa, respectively.

Addition of diphenyl amine antioxidant reduces the rate of tensile property change during ageing. Diphenyl amine, however appears to increase the rate of property change in the first week of ageing at 100°C. This effect may be associated with crosslink network modification. Network oxidation is treated in section 6.2.

The influence of base polymer on tensile property change in compound B is different to that of compound A. While the compound based on polymer E, (EB) again shows poor relative stability, the high relative stability exhibited by PA is not repeated in the behaviour of PB. The stability associated with polymer P is negated after diphenyl amine addition. This implies antagonism between polymer P and diphenyl amine antioxidant. For this reason interactions between diphenyl amine and polymerisation residues were studied. The results are described in section 6.4.

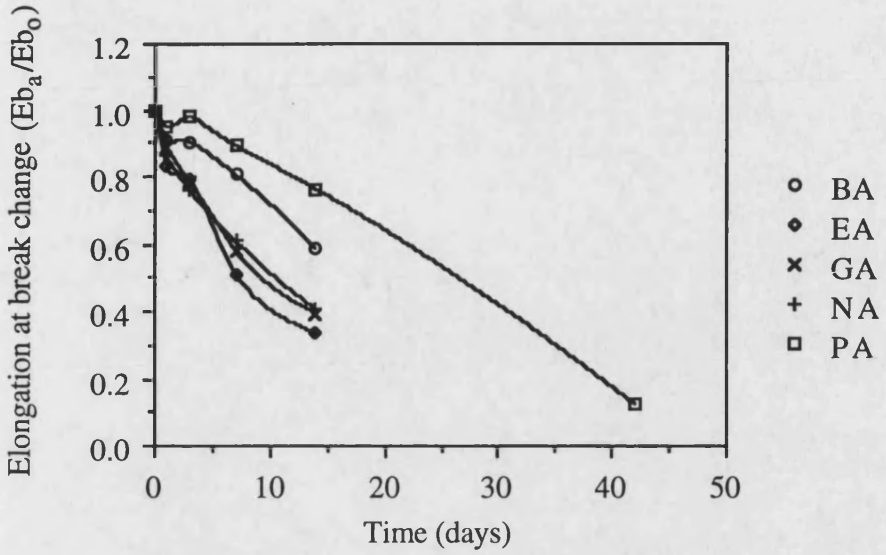

FIGURE 6.1. Change in elongation at break, (Eb), in vulcanizates of compound A during circulating air oven ageing at 100°C.

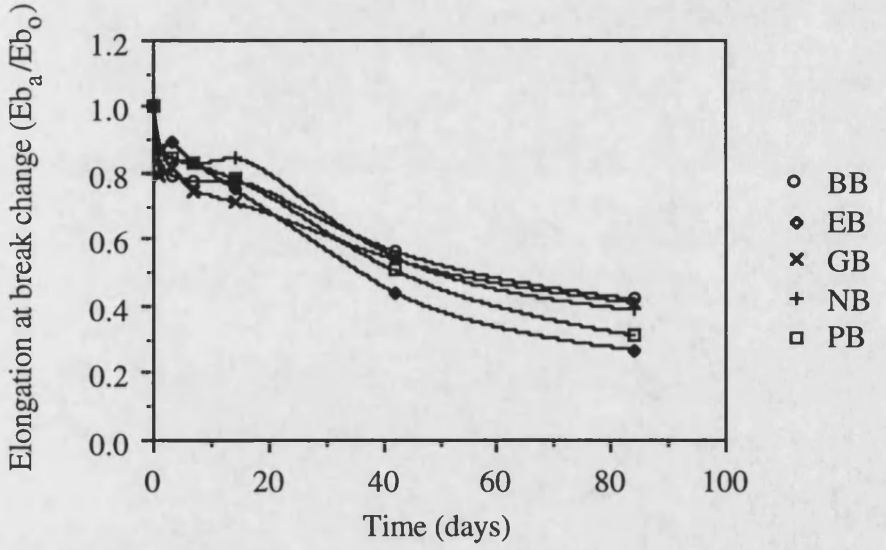

FIGURE 6.2. Change in elongation at break, (Eb), in vulcanizates of compound B during circulating air oven ageing at 100°C.

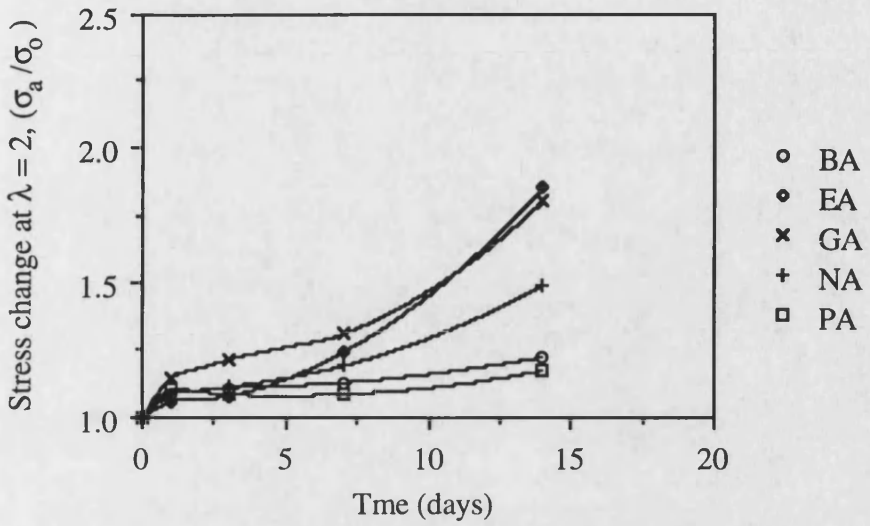

FIGURE 6.3. Change in stress, (σ) at extension ratio λ = 2, in vulcanizates of compound A during circulating air oven ageing at 100°C.

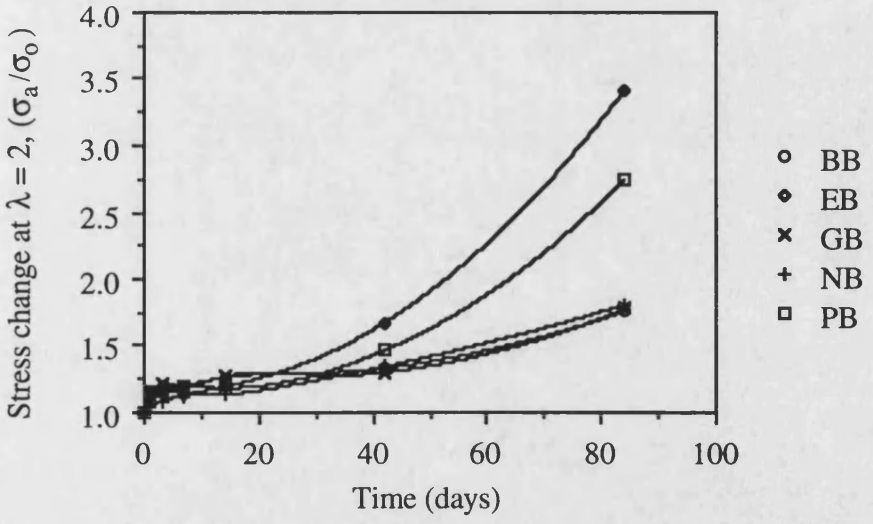

FIGURE 6.4. Change in stress, (σ) at extension ratio λ = 2, in vulcanizates of compound B during circulating air oven ageing at 100°C.

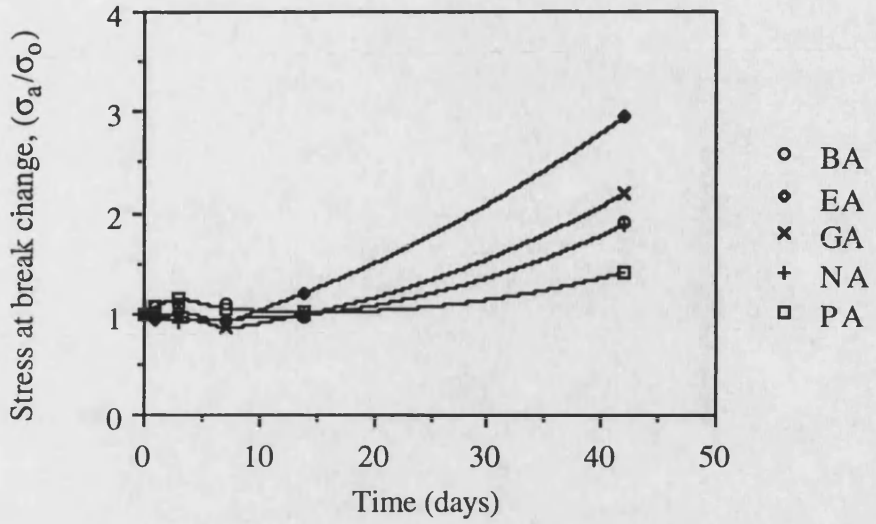

FIGURE 6.5. Change in stress, (σ) at break, in vulcanizates of compound A during circulating air oven ageing at 100°C.

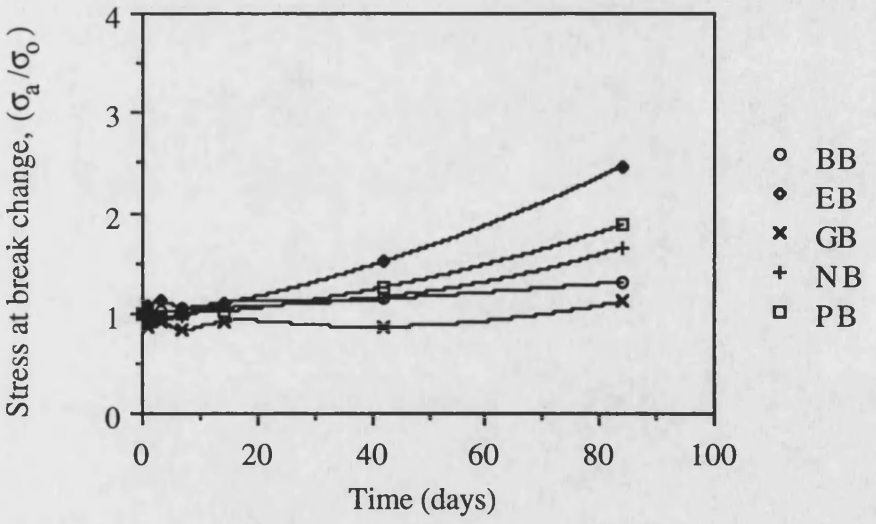

FIGURE 6.6. Change in stress, (σ) at break, in vulcanizates of compound B during circulating air oven ageing at 100°C.

6.1.2. GRAVIMETRIC MEASUREMENT

6.1.2.1. Weight Change on Ageing

In addition to property change aerobic ageing is also accompanied by weight and density change due to reaction of the polymer with oxygen and loss of volatile components, such as hydrogen, carbon dioxide, water, methane and antioxidant. There is also reduction in volume. Weight change plots of vulcanizates during ageing at 100°C are shown in figures 6.7 and 6.8.

In all curves four distinct processes are identified.

During the first day of heating at 100°C, vulcanizates show rapid weight loss. Compounds of polymer G exhibit higher weight loss than other polymers. The higher weight loss of compounds based on polymer G may be associated with the higher concentration of methanol extractable residue of polymer G, (refer to table 4.5). Vulcanizates of compound B exhibit approximately 1 % more weight loss than vulcanizates of compound A. This would imply that 50 % of compounded-in diphenyl amine is lost during early stages of oxidation. Heating of diphenyl amine alone at 100°C for 24 hours resulted in a weight loss of 43 %. This similarity in diphenyl amine weight loss shows that migration of diphenyl amine to the surface of N.B.R. is rapid and its evaporation in vulcanizates is not diffusion controlled.

Initial weight loss is followed by an apparent oxidation induction period during which there is little weight change. During this period weight gain due to oxygen absorption is balanced by weight loss due to loss of volatiles, such as water, (see section 6.3.2.1). This apparent induction time is longer than for property change. Vulcanizates of polymer E show a shorter induction time, irrespective of compound. This shorter induction time is consistent with more rapid property change, (figures 6.1-6.6). In compound A the gravimetric induction period is longer for vulcanizates which are based on polymer P, however compound PB exhibits a similar induction period to EB, BB and NB. The poor improvement in the oxygen absorption induction period of vulcanizates based on polymer P after diphenyl amine addition further suggest antagonism between diphenyl amine and polymer P. Antagonism between diphenyl amine and polymerisation residues of polymer P is treated in section 6.4.

The apparent induction period is followed by rapid weight increase. This step is associated with rapid oxygen absorption. The rate of weight increase appears to be

independent of base polymer and compound formulation. The final step in the process is reduced oxygen absorption, caused by a reduction in the concentration of reactant.

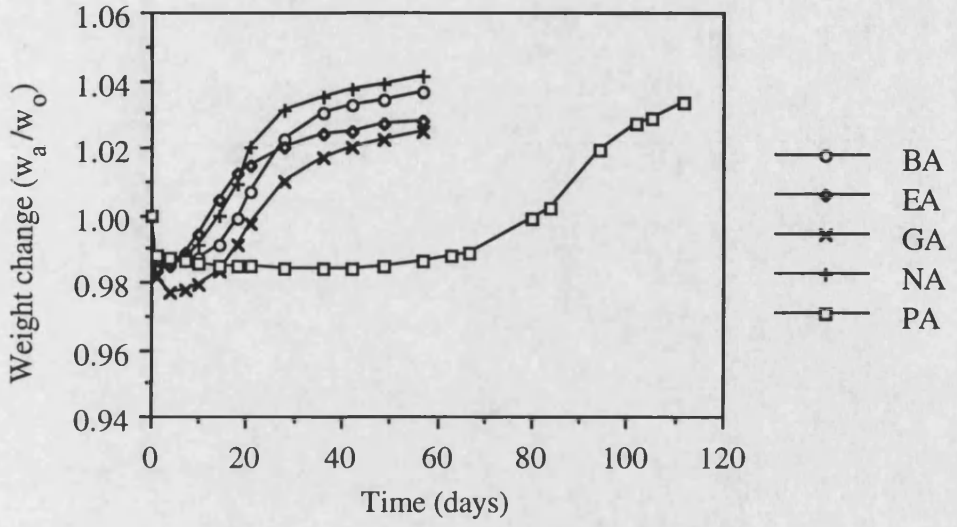

FIGURE 6.7. Weight change plots of vulcanizates of compound A during circulating air oven ageing at 100°C.

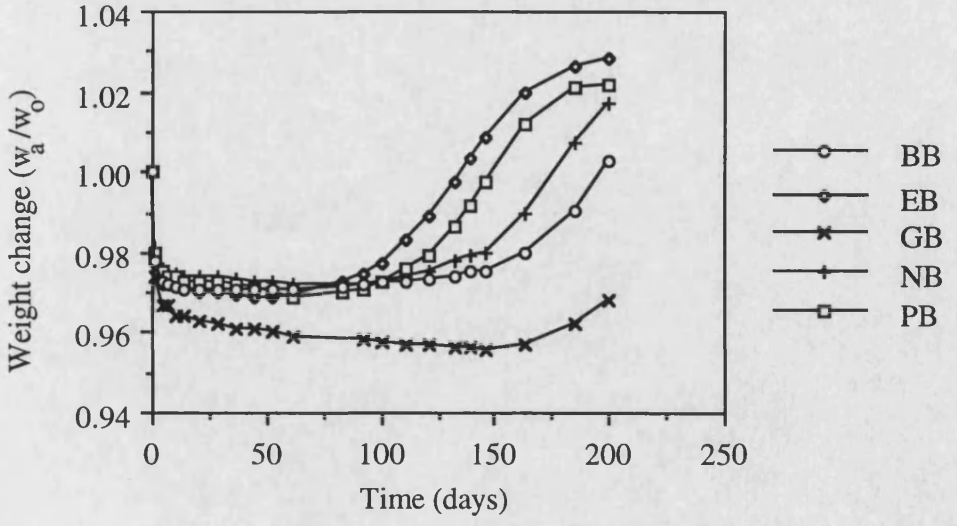

FIGURE 6.8. Weight change plots of vulcanizates of compound B during circulating air oven ageing at 100°C.

6.1.2.2. Density Change on Ageing

Density change on ageing gives different information to weight change because, whereas weight change is independent of volume change density change is not. A reduction in volume and increase in density can occur in the absence of weight change through crosslinking. Such a density increase has been demonstrated during radiation induced thermal crosslinking of polyethylene (Gillen, Clough and Dhooge, 1986). The change in density of vulcanizates of compounds A and B, during thermo-oxidation is shown in figures 6.9 and 6.10.

As with tensile property change of figures 6.1 to 6.6 vulcanizates based on compound B show lower rate of change than vulcanizates of compound A.

Vulcanizates of polymer E show higher density increase than other polymers in both compounds. In compound A vulcanizates of polymer P show lowest density increase while in compound B vulcanizates of polymer P show high density increase, in comparison with other polymers.

Figures 6.9 and 6.10 show that density change is more rapid than tensile property change and weight change because density is influenced by crosslinking and oxygen absorption processess. Unlike weight change plots of figures 6.7 and 6.8, density change plots show little induction time and almost linear dependence on ageing time in many instances. Density increases within the first few days of heating due to more rapid reduction in volume, (volume reduction may be through crosslink formation) than weight. Elongation at break is also highly sensitive to crosslink formation and the change in elongation at break shows little induction time. An almost linear dependence of density change, noted by Gillen *et al.* (1986) in polyethylene, during radiation induced degradation has been associated with crosslink formation and volume reduction.

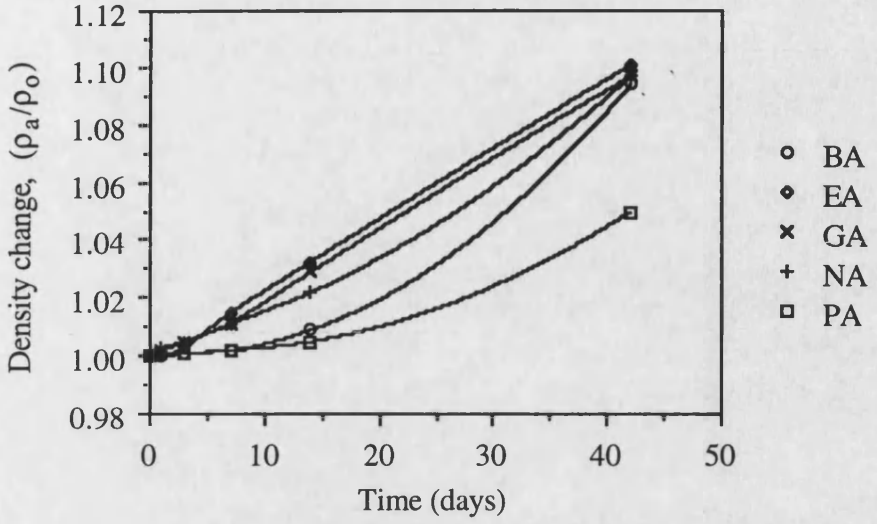

FIGURE 6.9. Change in density, (ρ) in vulcanizates of compound A during circulating air oven ageing at 100°C.

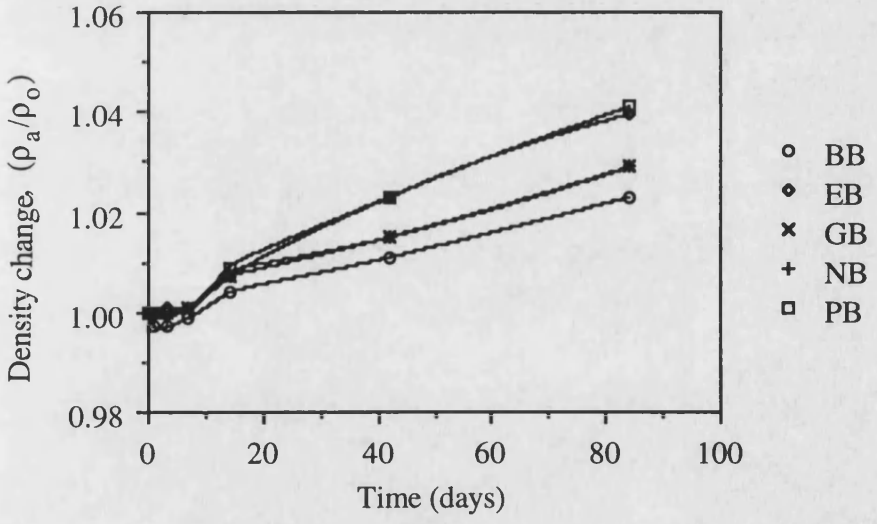

FIGURE 6.10. Change in density, (ρ) in vulcanizates of compound B during circulating air oven ageing at 100°C.

6.1.3. DYNAMIC PROPERTIES

The study of tensile property change during ageing was supplemented by the study of dynamic and viscoelastic loss properties. This was done because dynamic and viscoelastic properties, although less frequently studied, may be more informative than static tensile properties due to the ability of separating the complex modulus into its viscous and elastic components, (section 2.3.2.6, equation 2.22). The effect of ageing of N.B.R. vulcanizates on the viscoelastic properties of N.B.R. vulcanizates is illustrated in figures 6.11 and 6.12.

In figure 6.11 it is shown that ageing of EA vulcanizate is accompanied by reduction in the viscoelastic loss peak maximum and its shift to higher temperatures. Similar behaviour was observed for other compounds although the change in the character of the viscoelastic loss peak was less. The reduction in the viscoelastic loss peak may be a result of reduction in loss modulus and a increase in storage modulus. Cole-Cole type plots, (figure 6.12) of the relationship between in phase modulus, (E') and out of phase modulus, (E") show that reduction in tan δ is associated with reduction in E". This implies a reduction in the viscoelastic loss component during ageing. These results are of practical interest in applications where N.B.R. is used for energy absorption, such as acoustic insulation. Ageing causes a deterioration in energy absorbing properties.

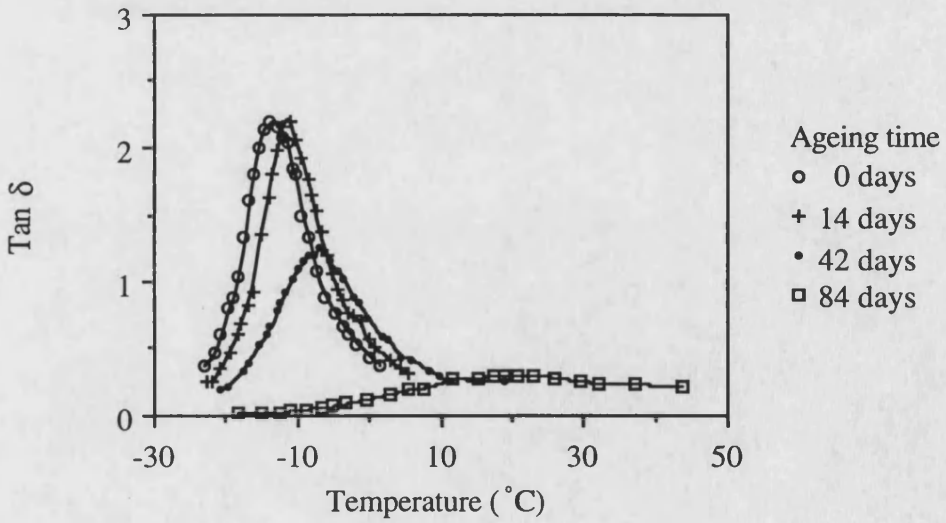

FIGURE 6.11. Change in viscoelastic loss angle, (tan δ) of EA vulcanizate during circulating air oven ageing at 85°C.

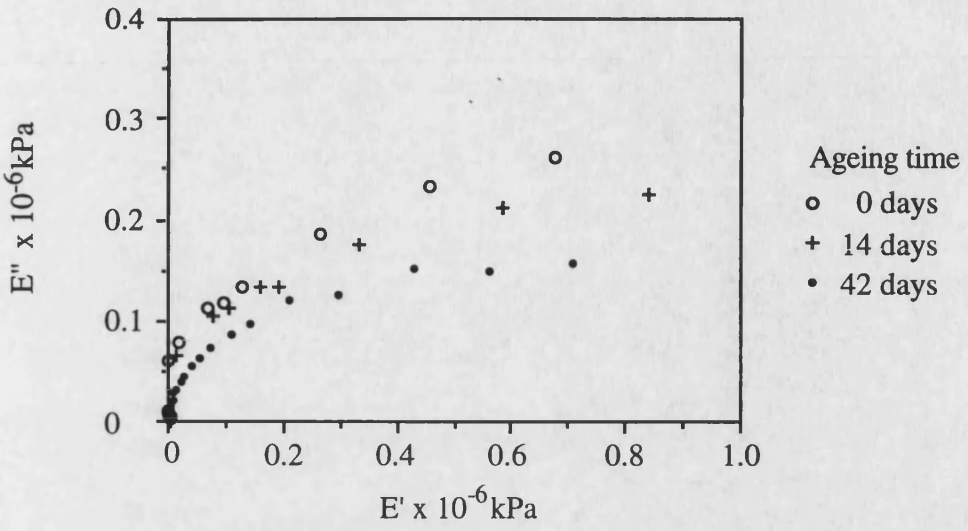

FIGURE 6.12. Cole-Cole type plots of the relationship between storage modulus, (E') and loss modulus, (E'') of EA vulcanizate during circulating air oven ageing at 85°C.

6.1.3.1. Curve Fitting of Viscoelastic Loss Peaks

It is clear from visual inspection that the viscoelastic loss peak undergoes subtle changes in shape and position as a consequence of ageing (figure 6.11). The extent of deviation in the character and shape of the tan δ peak during ageing is influenced by base polymer and compound formulation. As with tensile properties the change in tan δ characteristics during ageing was greater in vulcanizates which have no compounded-in antioxidant. EA vulcanizates exhibited greatest change in tan δ and PA vulcanizates the least change.

In an attempt to present viscoelastic loss peak data in a more concise tabulated form viscoelastic loss peak data of aged vulcanizates were characterised by curve fitting viscoelastic loss peaks using a mathematical function developed by Harris, Braddell, Almond, Lefebvre and Verbist (1993) for fitting loss peak data of plain and treated epoxy resin fibre composite systems.

This function takes the following form:

$$\tan \delta = A/\{[\omega\tau_o(1-T_o/T)^{-\alpha}]^{-m}+[\omega\tau_o(1-T_o/T)^{-\alpha}]^{1-n}\} \qquad (6.1)$$

where, ω is the test frequency, τ_o is a characteristic relaxation time, T is temperature and α is an empirical fitting parameter. A is a scaling factor which is related to peak height, T_o is a temperature at which the left hand side of the tan δ curve falls to zero, (A = 0) and *m* and *n* are related to the gradients of the right and left hand sides of the tan δ curve respectively. With A, α and T_o remaining constant, raising *m* steepens the right hand high temperature side of the curve while raising *n* decreases the gradient of the left hand low temperature side of the curve. At constant α, τ_o T_o and tan δ an increase in *m* also causes an increase in A while a change in *n* has little affect.

The values of A, *m* and *n* are very sensitive to changes in the value of τ_o and for this reason the value for τ_o was kept constant. For τ_o a value of 1.1 $x10^{-11}$ s was adopted from the work of Harris *et al.* (1993) who used this value in preference to other experimentally determined values because it is consistent with values of atomic vibrational frequency. The value of α was found to have little effect on fitting parameters, (α = 9 was based upon the work of Harris et al. (1993)). Curve fitting of experimental data was carried out with a graphing package Fig. P marketed by Biosoft of Cambridge. A fitted curve of experimental Rheovibron tan δ data is shown in figure 6.13. This exercise was carried out to see whether this curve fitting approach gives any additional information on visually observed differences in the change of the viscoelastic loss peak during ageing and the influence of base polymer. The parameters A, T_o, *m* and *n* were obtained by refitting repeatedly using different values of T_o until obtaining the best fit to experimental data. In such a way curve fits with correlation coefficients greater than 0.99 were obtained. The tan δ peaks of extensively aged samples could not be fitted by this function.

The effect of thermo-oxidative ageing at 85°C on the Rheovibron tan δ fitting parameters in E and P vulcanizates is shown in tables 6.1 to 6.3.

The results presented in tables 6.1 to 6.3 show that during early stages of oxidation there is a shift in the position of the loss angle to higher temperature, as shown by an increase in peak tan δ temperature, T_α and fitting parameter T_o. There is also a reduction in peak height maximum, tan δ and the related fitting parameter A and a reduction in the gradient of the right hand side of the tan δ peak, *m*. In some instances, however the high value of A may be influenced by a high value of *m*. This appears to be the case in sample EB after 42 days ageing at 100°C, (table 6.2). Fitting parameters

of tables 6.2 and 6.3 agree with visual observations of tan δ curves of more heavily degraded samples, (figure 6.11).

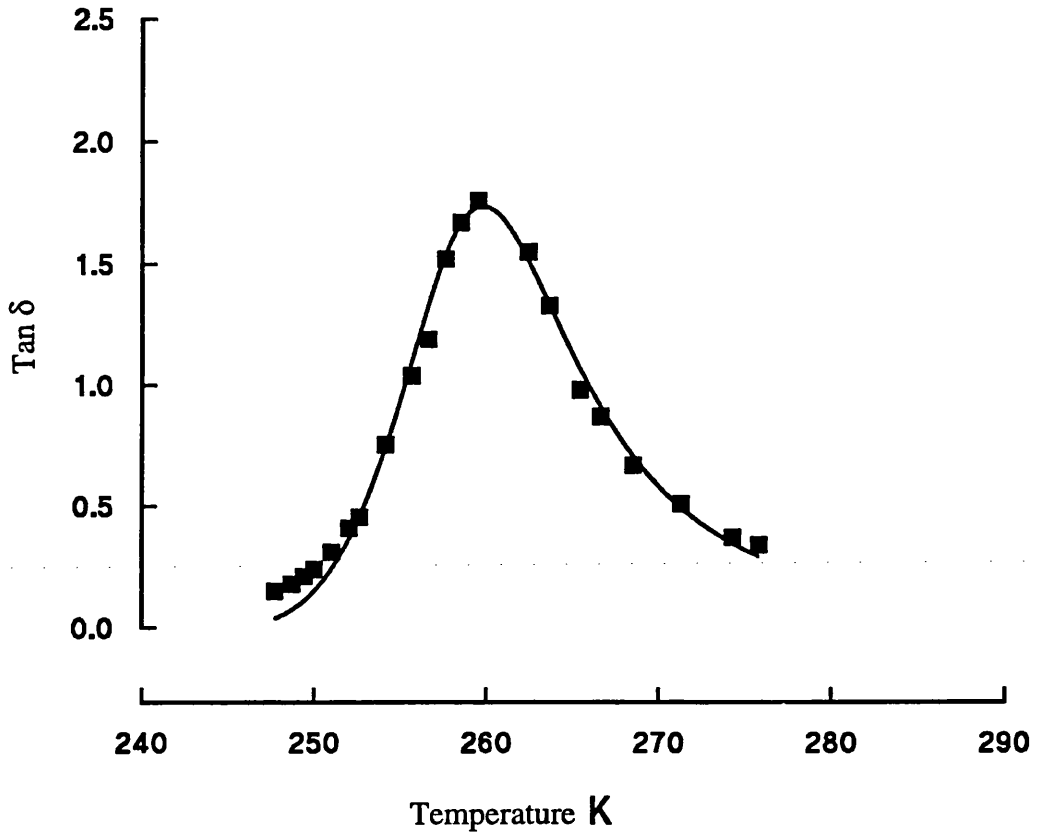

FIGURE 6.13. Fitted tan δ curve using equation 6.1 of aged PA vulcanizate, (sample aged in a circulating air oven at 85°C for 84 days).

Vulcanizate	Peak tan δ	T_α (K)	A	T_o(K)	*m*	*n*
EA	2.3	260.3	4.1	242.0	0.45	0.58
EB	2.1	259.3	4.0	242.2	0.45	0.60
PA	2.3	257.5	4.2	240.3	0.50	0.57
PB	2.0	258.0	4.0	240.3	0.44	0.58

TABLE 6.1. Summary of peak tan δ, the temperature at peak tan δ, (T_α(K)) and curve fitting parameters of Rheovibron viscoelastic loss peak data of unaged vulcanizates.

Vulcanizate	Peak tan δ	T_α (K)	A	T_o(K)	*m*	*n*
EA	1.3	266.8	2.4	246.9	0.33	0.68
EB	2.1	261.8	4.0	245.0	0.52	0.57
PA	1.9	259.8	3.7	242.3	0.49	0.61
PB	2.1	261.2	3.6	243.6	0.47	0.59

TABLE 6.2. Summary of peak tan δ, the temperature at peak tan δ, (T_α(K)) and curve fitting parameters of Rheovibron viscoelastic loss peak data of vulcanizates aged in a circulating air oven at 85°C for 42 days.

Vulcanizate	Peak tan δ	T_α (K)	A	T_o(K)	*m*	*n*
EB	1.9	263.9	3.7	245.6	0.43	0.57
PA*	0.7	261.8	-	-	-	-
PB	1.7	262.4	3.2	244.7	0.44	0.65

*Tan δ data of this sample could not be fitted.

TABLE 6.3. Summary of peak tan δ, the temperature at peak tan δ, (T_α(K)) and curve fitting parameters of Rheovibron viscoelastic loss peak data of vulcanizates aged in a circulating air oven at 85°C for 126 days.

6.1.4. TEMPERATURE DEPENDENCE OF PROPERTY CHANGE

In order to study the temperature dependence of the rate of tensile and viscoelastic property change, ageing experiments were carried out at several ageing temperatures. The theoretical discussion behind this type of analysis is discussed in section 2.3.4.2. The analysis is of prognostic value for assessment of service performance of vulcanizates. The temperature dependence of the change in viscoelastic loss peak maximum, (tan δ) and the temperature of viscoelastic loss peak maximum, (T_α) for compound EA are illustrated in figure 6.14. Compound EA was chosen arbitrarily for this illustration. The temperature dependence of the rate of change in modulus and elongation at break of EA are illustrated in figure 6.15.

It is apparent from figures 6.14 and 6.15 that equation 2.27 which represents a constant rate of property change poorly represents them. In order to obtain estimates of overall apparent activation energies for the degradation process results were analysed in three ways.

The simplest numerically was based on the recognition that the 'time to equivalent degradation', τ is inversely proportional to the rate constant, (equation 2.26). Values for τ were taken from property change curves and the activation energies calculated, (equations 2.23 and 2.26). The values of apparent activation energies are given in tables 6.4-6.6. The regression coefficient, R is also given to indicate the goodness of fit of the points to a straight line.

Apparent activation energies were also calculated from equation 2.28 by estimating the rate constants from the best linear fit to a curve of logarithm of relative elongation at break against time. Results are tabulated in table 6.4 and 6.5.

For some degradation conditions, such as elongation at break of compound A shapes of the property change curves at different temperatures were essentially the same when plotted against the logarithm of time, (figure 6.16). This enabled a reference temperature to be selected and a shift factor, (ln a_T) to be calculated for other temperatures. Apparent activation energies, derived from equation 2.26 are also included in table 6.4.

Curve fitting was performed by Cricket graph software. The properties studied were the viscoelastic loss peak maximum, the temperature of viscoelastic loss peak maximum, elongation at break and stress at 100 % elongation. Study of viscoelastic properties was of interest because there is no published information on the temperature

dependence of viscoelastic property change during ageing. Elongation at break and modulus change, the usual properties used in ageing studies were measured in order to study the effect of kinetic model on apparent activation energy, (E_a) values and to complement viscoelastic property studies.

When using the time to equivalent degradation for determination of E_a the following changes in properties were used:
a) in the study of the change in peak tan δ the time to 30 % reduction of the initial unaged value,
b) for the change in T_α, (in K) the time to 1 % increase,
c) elongation at break measurements were based on the time to 30 % reduction,
d) modulus measurements used the time to 30 % increase.

Arrhenius type plots of elongation at break change of EA compound are shown in figure 6.17. Apparent activation energies obtained from fitting elongation at break data and correlation coefficients, (R) are tabulated in table 6.4. Values from Modulus change are tabulated in table 6.5. Data from viscoelastic loss properties T.E.D. values are tabulated in table 6.6.

Table 6.4 compares the influence of kinetic model and compound on apparent activation energy and correlation coefficient, obtained from elongation at break data. These results show that the apparent activation energy values which are obtained from time to equivalent degradation, (T.E.D.), fitting property change to $e^{(kt)}$ and shifting property change curves by ln a_T are comparable. These values show good agreement with literature values reviewed in section 2.3.2.7. Values from ln a_T for vulcanizates of compound B could not be obtained because in such cases elongation at break change data at different temperatures could not be superimposed by a horizontal shift. This was a function of the more complex time dependence of elongation at break change data in compound B, (see figure 6.2). All three techniques give high correlation coefficients, when Arrhenius type plots are made, however correlation coefficients of the T.E.D. method are somewhat lower because in such treatment a single point property measurement is used in their construction.

Apparent activation energy values for different compounds may be considered comparable, although showing a high degree of scatter. The high degree of scatter is caused by the inherent high scatter in tensile property values, (see tables 4.31 and 4.32). The low apparent activation energy of compound PA in table 6.4 may not be significant since it is not consistent with later values of tables 6.5 and 6.6. The low

apparent activation energy of PB obtained from T.E.D. measurement of table 6.4 is unreliable due to its low correlation coefficient.

Values obtained from fitting stress at 100 % elongation results, (table 6.5) are similar to those obtained from fitting elongation at break data, (table 6.4) and also show high correlation.

Apparent activation energies obtained from fitting T.E.D. viscoelastic loss properties, (table 6.6) are also comparable to results obtained from static tensile property change, (tables 6.4 and 6.5) and give similar correlation coefficients.

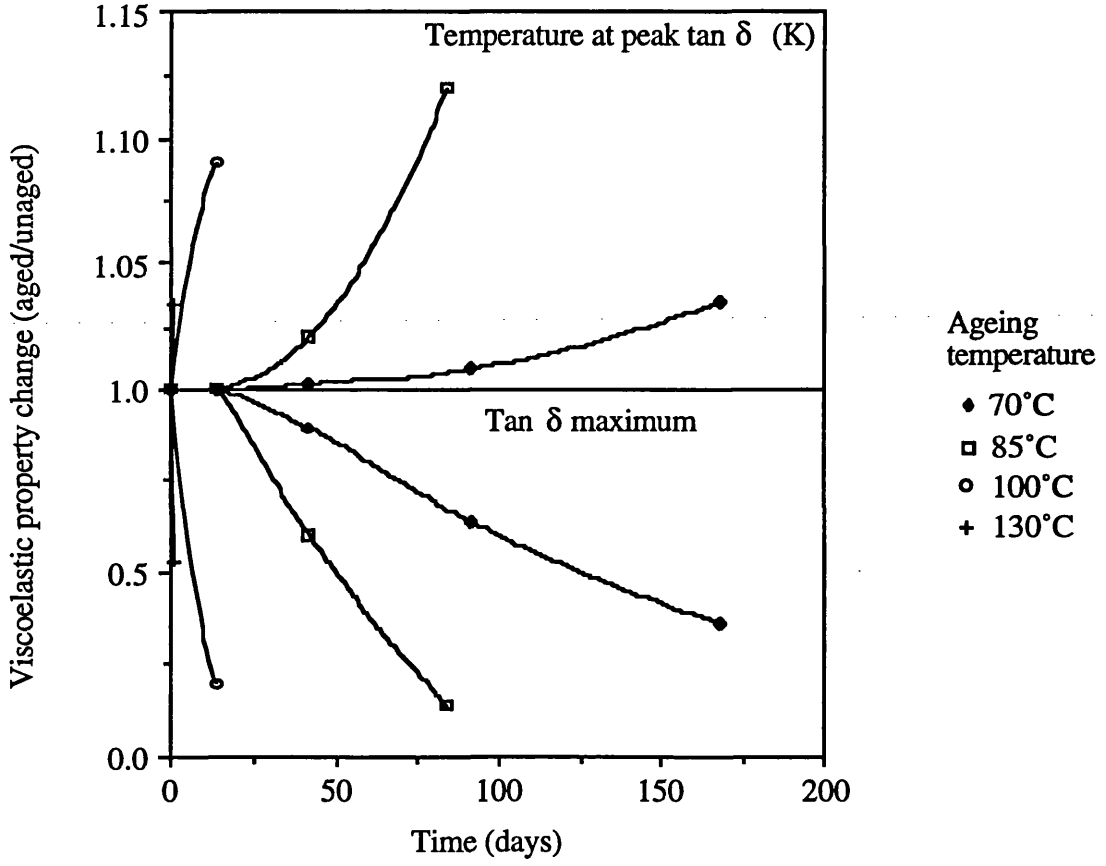

FIGURE 6.14. Change in viscoelastic loss peak maximum and temperature of peak maximum values of EA compound during circulating air oven ageing.

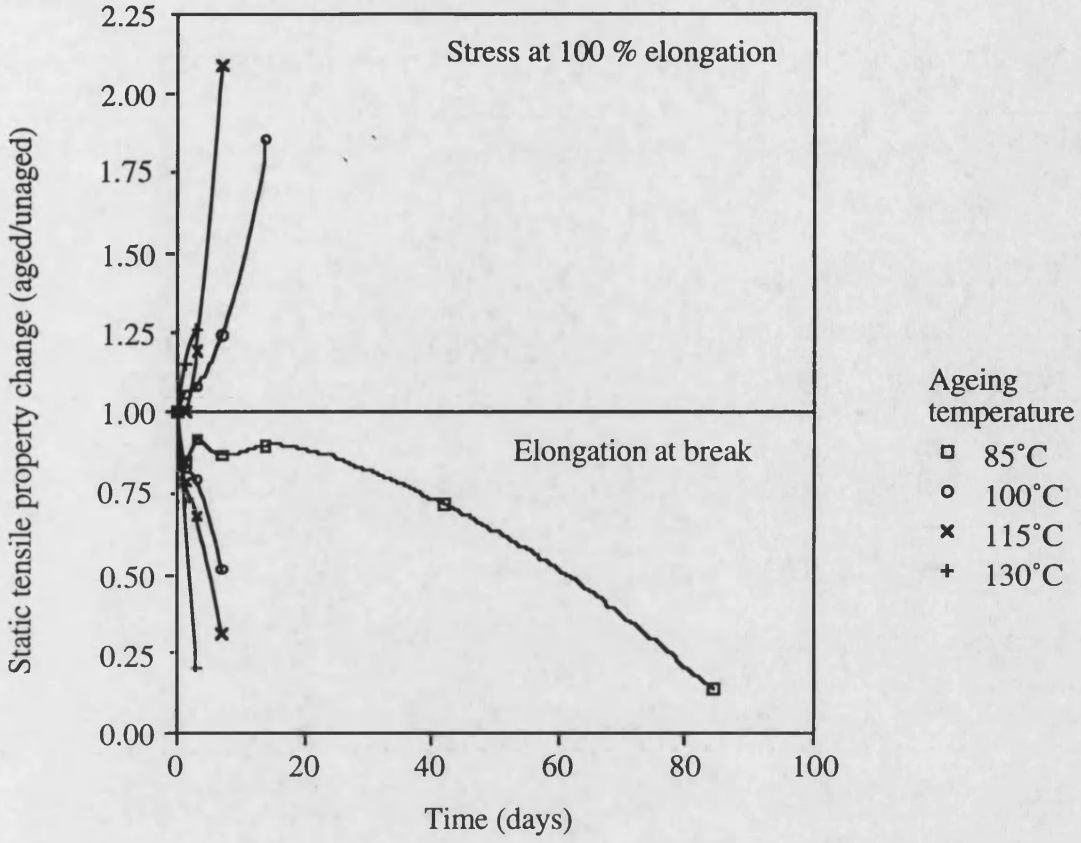

FIGURE 6.15. Change in elongation at break and stress at 100 % elongation values of EA compound during circulating oven air ageing.

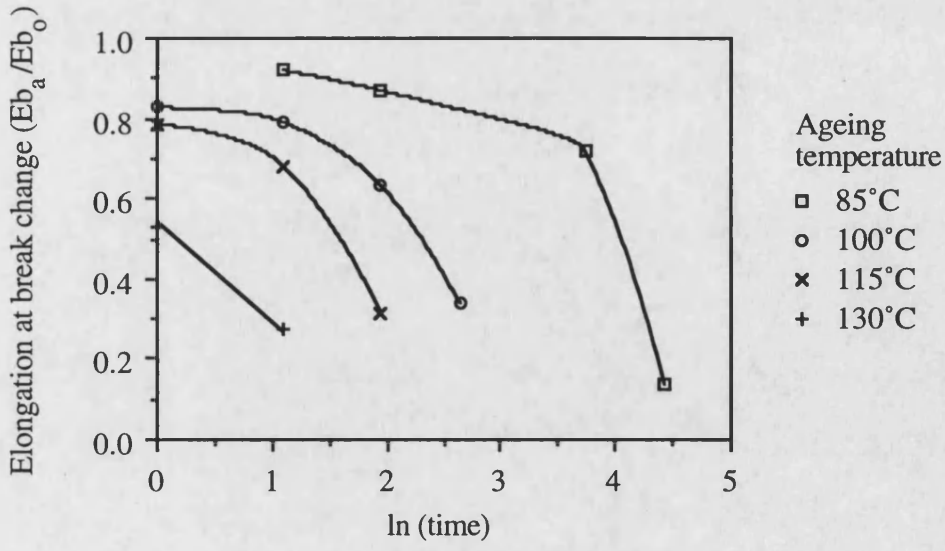

FIGURE 6.16. Change in elongation at break, (Eb) of EA plotted on a logarithmic time scale.

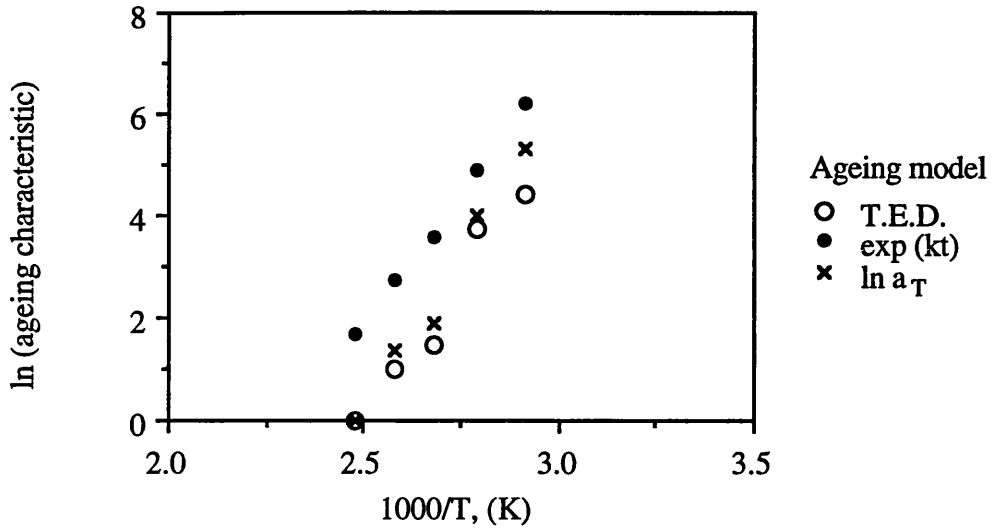

FIGURE 6.17. Arrhenius type plots of EA elongation at break, based on measurement of time to equivalent degradation, (T.E.D.), fitting property change to $e^{(kt)}$ and shifting property change curves by ln a_T.

Vulcanizate	T.E.D.	R	$e^{(kt)}$	R	ln a_T	R
BA	102	0.97	105	0.99	89	0.99
BB	115	0.96	87	1.00	-	-
EA	89	0.95	89	0.99	80	0.99
EB	82	0.89	109	0.98	-	-
GA	112	1.00	88	1.00	79	0.99
GB	94	0.91	98	0.98	-	-
NA	78	0.89	88	0.93	75	0.91
NB	96	0.89	99	0.96	-	-
PA	72	0.95	68	0.93	63	0.97
PB	68	0.50	88	0.96		-

TABLE 6.4. Apparent activation energies in kJ/mole, of N.B.R. vulcanizates obtained from the temperature dependence of elongation at break data, over the temperature range 70°C-130°C, based on time to equivalent degradation, (T.E.D.), fitting property change to $e^{(kt)}$ and shifting property change curves by ln a_T.

Vulcanizate	T.E.D.	R	$e^{(kt)}$	R
BA	-	-	85	0.98
BB	76	0.99	88	0.99
EA	-	-	104	0.98
EB	88	0.99	109	0.98
GA	84	0.97	88	0.95
GB	93	0.95	99	0.98
NA	-	-	114	0.97
NB	91	0.98	99	0.96
PA	-	-	-	-
PB	87	0.98	88	0.96

TABLE 6.5. Apparent activation energies in kJ/mole, of N.B.R. vulcanizates obtained from the temperature dependence of stress at 100 % elongation data, over the temperature range 70°C-130°C, based on time to equivalent degradation, (T.E.D.) and fitting property change to $e^{(kt)}$.

Vulcanizate	Peak tan δ	R	Temp. at peak tan δ	R
BA	105	1.00	104	1.00
BB	-	-	-	-
EA	107	0.98	122	0.91
EB	-	-	-	-
GA	96	0.97	116	1.00
GB	-	-	-	-
NA	100	1.00	88	1.00
NB		-	82	0.99
PA	94	0.91	99	1.00
PB	-	-	85	0.99

TABLE 6.6. Apparent activation energies in kJ/mole, of N.B.R. vulcanizates obtained from the temperature dependence of time to equivalent degradation of viscoelastic loss properties, over the temperature range 70°C-130°C.

6.1.5. SUMMARY ON PROPERTY CHANGE ON AGEING

The oxidation of N.B.R. is characterised by an increase in elastic modulus and a reduction in viscous modulus, (figure 6.12). This is consistent with crosslink formation. Ageing is accompanied by a reduction in elongation at break, (figures 6.1

and 6.2), a reduction in tan δ maximum, (tables 6.1-6.3, figure 6.11), a shift in tan δ maximum to higher temperatures, an increase in modulus, (figures 6.3 and 6.4) and an increase in tensile strength, (figures 6.5 and 6.6). The change in the shape of viscoelastic loss peaks is described by fitting peaks to equation 6.1, (tables 6.1 to 6.3). Oxidation is also accompanied by weight increase, (following an initial weight loss due to volatile loss), (figures 6.7 and 6.8) and density increase, (6.9 and 6.10). Weight increase does not occur until latter stages of oxidation by which time property change is extensive. Density change occurs during early stages of ageing. This indicates volume reduction, thought to be caused by crosslink formation.

Mechanical property change is influenced by base polymer and compound formulation. Compounds of polymer E show more rapid change in static and dynamic tensile properties than compounds of other polymers, particularly in the absence of compounded-in antioxidant, (compound A). Polymer P shows less rapid property change and a much longer induction time than other polymers when compounded with formulation A. Differences in the extent of degradation between polymers E and P are suggested in section 4.2.1, table 4.7 where it is shown that polymer E contains 8.8 % gel content while polymer P contains no gel. Differences in oxidative stability between polymers may be caused by differences in polymerisation residues of section 4.1, (particularly antioxidant residues of section 4.1.3).

The addition of diphenyl amine antioxidant (compound B) reduces the rate of property change in all polymers of compound A, although not equally. When compounded with compound B polymer P shows more rapid property change than other polymers, except polymer E. This implies antagonism between diphenyl amine and polymer P. This effect is similar to that reported in the vulcanization of N.B.R., (section 4.3.1, table 4.16) where the accelerating effect of diphenyl amine was less in polymer P than polymer E. Interactions between diphenyl amine and polymerisation residues are studied in section 6.4. Vulcanizates of compound B show more rapid reduction in elongation at break in the first few days of ageing at 100°C than vulcanizates of compound A, (figures 6.1 and 6.2). This may be due to catalysis of poly-sulphide crosslink desulphurisation by diphenyl amine, suggested in section 4.4.3.4. Network degradation is treated further in the following section 6.2.

Tensile and viscoelastic property dependence on ageing temperature is similar for all polymers and compounds. Apparent activation energies obtained from elongation at break, stress at 100 % elongation, tan δ maximum and the temperature of tan δ maximum are generally in the range 80-110 kJ/mole, (tables 6.4-6.6), with the exception of a few values which are thought not to be significant due to the high scatter

of tensile property values, (tables 4.30 and 4.31). The three models used to describe the time dependence of property change, namely the time to equivalent degradation, the shift factor superposition and the exponential fitting function give comparable results of apparent activation energy and correlation coefficients in excess of 0.9, when fitted to the Arrhenius model. The shift factor method could not be used to superimpose elongation at break change data of compounds B due to the complex time dependence of such plots. Arrhenius plots from time to equivalent degradation give lower correlation coefficients than Arrhenius plots from the other two methods because only single point measurements at each ageing temperature are used in their construction.

6.2. MECHANISM OF NETWORK OXIDATION

6.2.1. STRESS RELAXATION

6.2.1.1. Intermittent Stress Relaxation

Ageing of vulcanizates was also studied by stress relaxation so as to separate oxidative crosslinking and scission reactions. In intermittent stress relaxation studies samples are aged in the relaxed form and then extended to constant strain at constant temperature. The normalised retractive force in stress relaxation studies approximates to relative network chain density via equation 2.31, (refer to section 2.3.5.4).

Intermittent stress relaxation curves of vulcanizates compounded with formulation A and B, which were aged at 100°C are presented in figures 6.18 and 6.19, respectively. Figure 6.20 shows the relationship between the C_2 elastic term of the Mooney-Rivlin equation and ageing time at 100°C, for compound GB. The effect of ageing on the C_2 term for other vulcanizates and compounds was as for GB.

From figure 6.20 it is evident that C_2 remains unaffected by ageing time and it is therefore valid to approximate the ratio F_a/F_o of figures 6.18 and 6.19 to the ratio N_a/N_o.

Intermittent stress relaxation results of figures 6.18 and 6.19 show an initial increase in retractive force, (F) this being slightly higher for vulcanizates of compound B. Over the same test period vulcanizates of compound B show a more rapid reduction in elongation at break than vulcanizates of compound A, (figures 6.1 and 6.2). A similar reduction in elongation at break of sulphur cured E.P.D.M. systems during the first few hours of oxidative ageing at temperatures of 100°C, 120°C, 150°C and 180°C

has been reported by Deuri and Bhowmick (1987). In E.P.D.M. the initial reduction in elongation at break is thought to be associated with crosslink modification, such as desulphurisation of poly-sulphide crosslinks. Results of section 4.4.3.4, (tables 4.25, 4.26 and figures 4.16, 4.17) showing that diphenyl amine increases the concentration of mono-sulphide crosslinks during vulcanization are consistent with this theory. The effect of diphenyl amine on network ageing is treated further in section 6.2.2.

After the initial rise in retractive force stress relaxation curves show an induction period. The induction period is followed by rapid crosslink formation. In N.B.R. oxidation crosslink formation is thought to be caused by free radical chain termination reactions, (section 2.3.1).

Crosslink formation in compound A is greatly influenced by base polymer. Vulcanizates of compound EA exhibit greatest crosslink formation and could not be extended to 50% elongation beyond an ageing time of 164 hours. This compound exhibits the greatest rate of tensile property change, (section 6.1). Compound GA also exhibits rapid crosslink formation. Compound PA exhibits the lowest rate of crosslink formation. This compound showed the lowest rate of tensile property change, (section 6.1).

The compounding-in of diphenyl amine antioxidant reduces crosslink formation, beyond 5 days, ageing at 100°C for all polymers. In compound B polymer E exhibits most rapid crosslink formation while polymers G and B exhibit less crosslink formation. Compound PB displays a higher rate of crosslink formation than compounds BB, GB and NB. The poor improvement in thermo-oxidative stability of polymer P by addition of diphenyl amine antioxidant is consistent with previous results, (section 6.1). Diphenyl amine-base polymer interactions are reported in section 6.4.

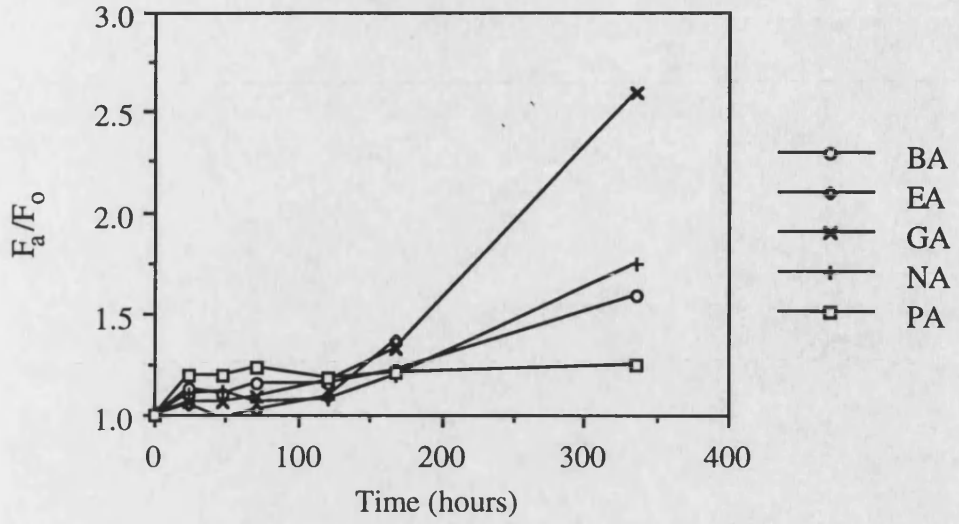

FIGURE 6.18. Intermittent stress relaxation in vulcanizates of compound A during heating in a circulating air ageing oven at 100°C.

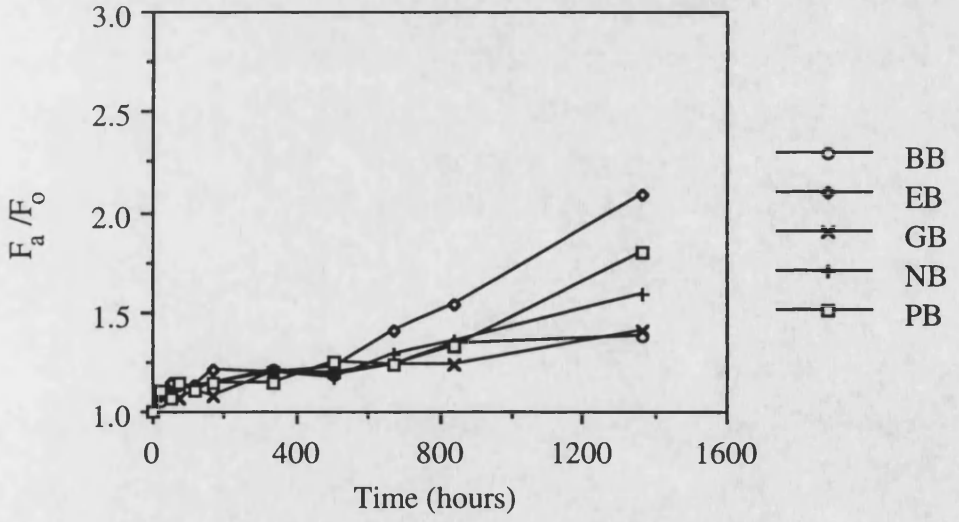

FIGURE 6.19. Intermittent stress relaxation in vulcanizates of compound B during heating in a circulating air oven at 100°C.

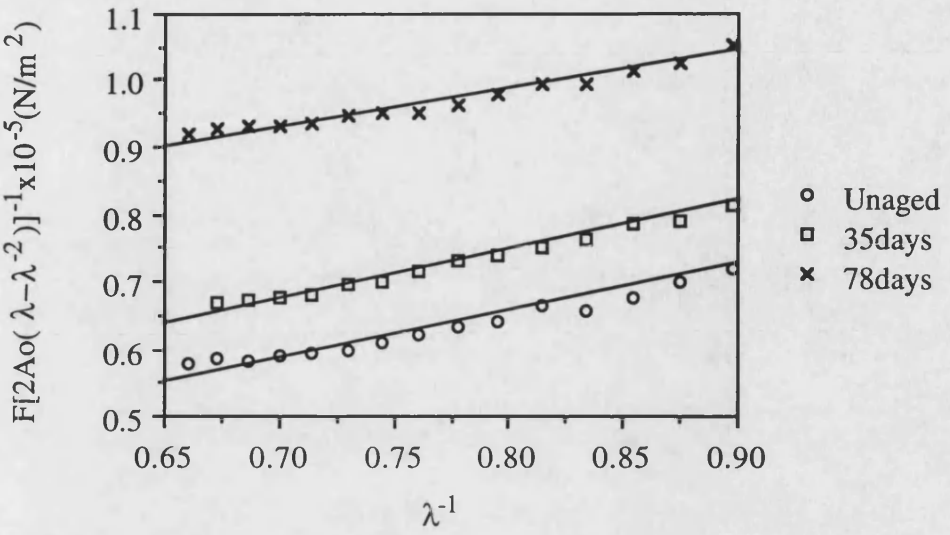

FIGURE 6.20. Dependence on C_2 on ageing time of GB vulcanizate aged in a circulating air oven at 100°C.

6.2.1.2. Continuous Stress Relaxation

Continuous stress relaxation studies were made to supplement intermittent stress relaxation studies. In continuous stress relaxation studies samples are aged in the extended form and measured retractive force is mainly independent of crosslink formation, (see section 2.3.5.4). Measurements were made on a instrument which was built for this purpose, (described in section 5.2.1.2).

Continuous stress relaxation curves of compounds A and B at 100°C are shown in figures 6.21 and 6.22, respectively.

In all continuous stress relaxation curves there is an initial rapid drop in retractive force. This initial drop in retractive force, F of continuous stress relaxation curves has usually been associated with physical relaxation, (conformational changes and alignment of polymer chains), (Bjork *et al.*, 1989). Other publications suggest that chemical reactions, such as poly-sulphide desulphurisation as observed in E.P.D.M. networks by Deuri and Bhowmick (1987) and polymer chain scission reported by Bhattacharjee *et al.* (1991) within the first hour of heating of N.B.R. polymer at 100°C

in air contribute to the reduction in retractive force. Results presented in sections 6.2.2 and 6.2.3 show that chemical reactions occur during this inital period of rapid stress relaxation. Following this initial period of rapid relaxation there is further relaxation which may be caused by crosslink scission, crosslink desulphurisation and network chain scission.

Vulcanizates of compound A show large differences in the rate of continuous stress relaxation between polymers. Compound EA shows the greatest rate of oxidative scission while compound PA exhibits the lowest rate of scission. In figure 6.18 it was shown that crosslink formation is greatest in EA and lowest in PA. Network oxidation mechanisms are shown in section 2.3.2.4, (reaction scheme XV, XVI and XVII).

Compounding-in of diphenyl amine reduces the rate of scission beyond the first few hours for compounds of polymer E, but does not reduce much the rate of scission in other polymers. Compound GB exhibits the lowest rate of scission after the initial rapid relaxation. For all vulcanizates the presence of diphenyl amine increases the magnitude of relaxation within the first few hours of heating. Previously it was shown that diphenyl amine causes more rapid reduction in elongation at break of vulcanizates within the first day of heating, (figures 6.1 and 6.2) and greater increase in retractive force in intermittent stress relaxation studies within the first day of heating, (figures 6.18 and 6.19). These results are discussed further with reference to network oxidation in section 6.2.2.

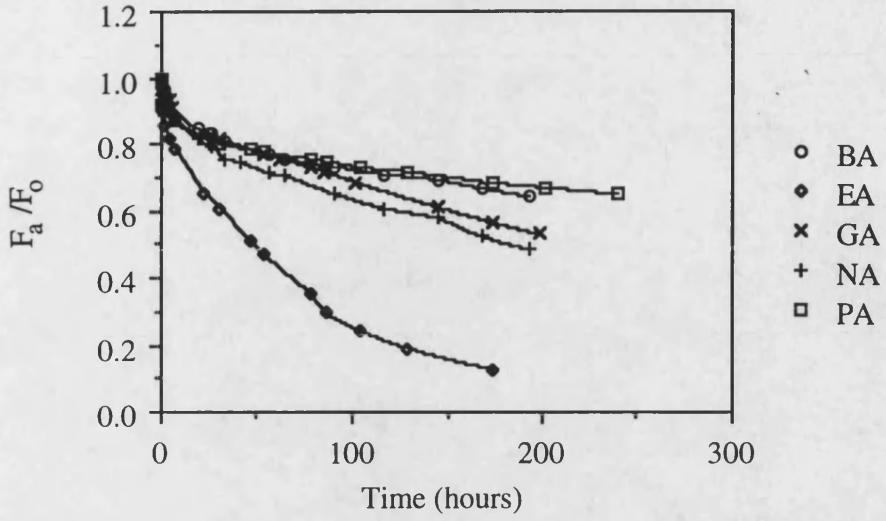

FIGURE 6.21. Continuous stress relaxation in vulcanizates of compound A during heating in air at 100°C.

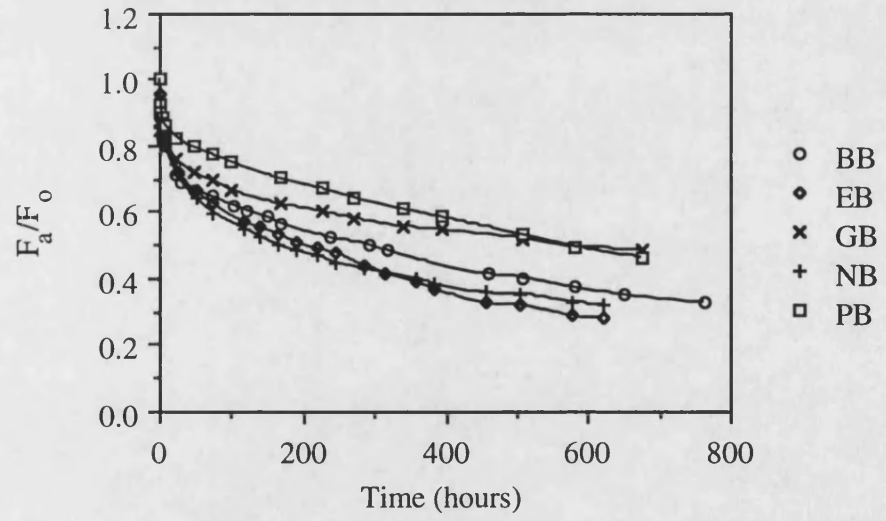

FIGURE 6.22. Continuous stress relaxation in vulcanizates of compound B during heating in air at 100°C.

6.2.2. CHARACTERISATION OF AGED NETWORKS BY CHEMICAL PROBE TREATMENT

6.2.2.1. Thiol-Amine Treatment of Compound A

The network structure of vulcanizates after ageing at 100°C was determined by treating samples with thiol-amine chemical probes, described in sections 2.2.3.2, using experimental procedure of 3.9.2.2.2 and 3.9.2.3. In aged samples weight loss during swelling was negligible and it was unnecessary to adjust values for the extracted volume element, (see section 4.4.3.4). Network characterisation was made on all samples but only the results of compounds based on polymer E and P have been reported because these polymers exhibit the two extremes in thermo-oxidative stability.

The change in network density and network structure during thermo-oxidative ageing at 100°C of EA and PA samples is shown in figures 6.23 and 6.24. Aged samples of EA could not be characterised beyond 14 days because they were excessively crosslinked and as a result cracked and fragmented during swelling. The same problem occurred with vulcanizates of PA beyond 42 days. Network characterisation results of vulcanizates BA, GA and NA are not shown because they are intermediate to those of EA and PA and do not give further information of interest other than to confirm the reproducibility of network density measurements.

For all samples ageing at 100°C is accompanied by an increase in overall crosslink density, the increase being much more rapid in compounds of polymer E than P. The concentration of di-sulphide crosslinks is reduced slightly. The concentration of poly-sulphide crosslinks appears to be little affected by ageing at 100°C. In literature it is reported that the concentration of poly-sulphides crosslinks is reduced during thermal heating of sulphur cured vulcanizates based on N.B.R. and other rubbers at temperatures in excess of 140°C, (Hoffman, 1985; Brajko *et al.*, 1980; Doyle *et al.*, 1971), however there appears to be no available information on network oxidation of N.B.R. systems at temperatures in the region of 100°C.

In both vulcanizates there is an increase in the concentration of crosslink structures which are resistant to cleavage by hexane-1-thiol (1M) in piperidine treatment, the increase being more rapid in vulcanizates of polymer E than P. There is little published experimental work into the structure of these vulcanizates, however there is a widely held belief that such crosslinks are mono-sulphide (Deuri and Bhowmick, 1987; Lee and Morrell, 1973). Suggestion that such structures are sulphoxides must be viewed with caution since it is reported by Colclough *et al.* (1968)

that mono-sulphide crosslinks in N.R. rubber once oxidised to sulphoxide are rapidly cleaved at temperatures of 75°C. Crosslinks which form during oxidation and are resistant to hexane-1-thiol treatment are unlikely to be mono-sulphide or sulphoxide because of the poor oxidative stability of mono-sulphides and sulphoxides. Information on the structure of crosslinks which are resistant to hexane-1-thiol (1M) in piperidine treatment is given in sections 6.2.2.3 and 6.2.3.

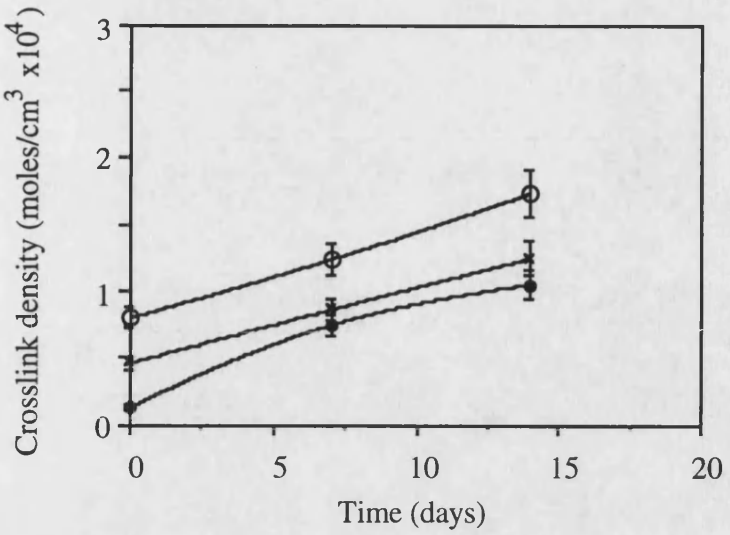

FIGURE 6.23. Crosslink structure of EA vulcanizate after ageing at 100°C in air;
(a) o total crosslink density,
(b) × crosslink density after propane-2-thiol treatment (cleaves poly-sulphides),
(c) • crosslink density after hexanethiol treatment (cleaves di-sulphides and poly-sulphides).

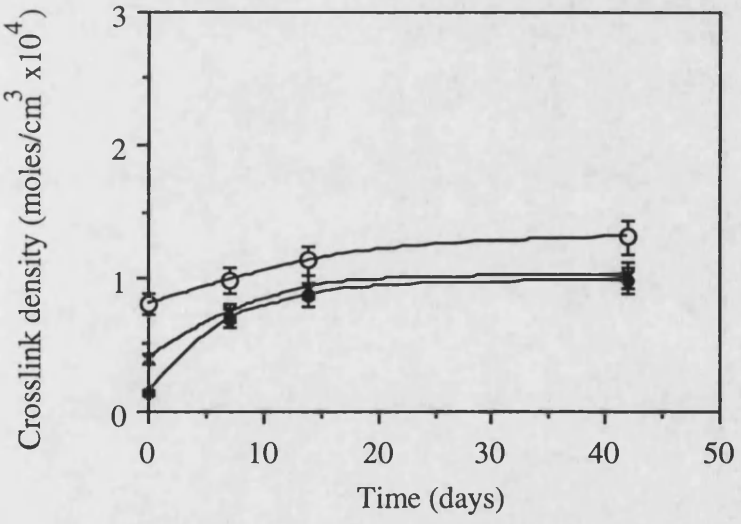

FIGURE 6.24. Crosslink structure of PA vulcanizate after ageing at 100°C in air;
(a) o total crosslink density,
(b) × crosslink density after propane-2-thiol treatment (cleaves poly-sulphides),
(c) • crosslink density after hexanethiol treatment (cleaves di-sulphides and poly-sulphides).

6.2.2.2. Thiol-Amine Treatment of Compound B

The effect of oxidative ageing at 100°C on crosslink structure of vulcanizates EB and PB is shown in figures 6.25 and 6.26. Crosslink structure in vulcanizates BB, GB and NB was similarly affected by ageing at 100°C.

In vulcanizates of compound B there is an increase in total crosslink density. This increase in crosslink density which is more rapid in compound EB than PB follows an induction period. The induction period of change in total crosslink density is similar to the induction period shown in stress change, (figures 6.4 and 6.18). The induction period in vulcanizates of compound A, notably EA, (figures 6.23 and 6.24) is less apparent because the increase in crosslink density in vulcanizates of compound A is more rapid.

For all vulcanizates of compound B there is a significant reduction in total crosslink density after 7 days heating at 100°C. The reduction in total crosslink density is accompanied by elimination of poly-sulphide crosslinks and di-sulphide crosslinks. In compound A, poly-sulphide crosslinks and di-sulphide crosslinks were found to be stable under these conditions. These results are consistent with the postulate that diphenyl amine acts as a catalyst for poly-sulphide and di-sulphide desulphurisation or decomposition and may explain the rapid change in tensile properties and stress relaxation seen in vulcanizates of compound B. In literature it is well documented that amine can initiate heterolytic cleavage of elemental sulphur, (see section 2.2.2.4.3, reaction scheme VI). Published information on the effect of diphenyl amine on poly-sulphide desulphurisation in rubber networks is however contradictory. For example it has been reported by Kruger and McGill (1992b) that poly-sulphide crosslinks in B.R. networks undergo enhanced decomposition in the presence of tertiary amines, while more recently Engels (1994) reported no effect of p-phenylene diamine addition on poly-sulphide decomposition in N.R. and S.B.R. networks during ageing at 70°C, up to a period of 21 days.

Figures 6.25 and 6.26 show that during heating at 100°C there is an increase in the concentration of crosslinks which are resistant to hexane-1-thiol (1M) in piperidine treatment. This was also seen in vulcanizates of compound A, (figures 6.23 and 6.24). Further information on the structure of these crosslinks is given in section 6.2.2.3. At extended periods of ageing crosslink density increases further. Most of the newly formed crosslinks are resistant to hexane-1-thiol treatment. Crosslinks which are cleaved by hexane-1-thiol treatment are di-sulphides. Di-sulphides may form by oxidation of pendant thiols and condensation reactions between sulphenic acids and

thiols. The mechanisms of thiol and sulphenic acid formation and their further oxidation is illustrated in section 2.3.2.4.

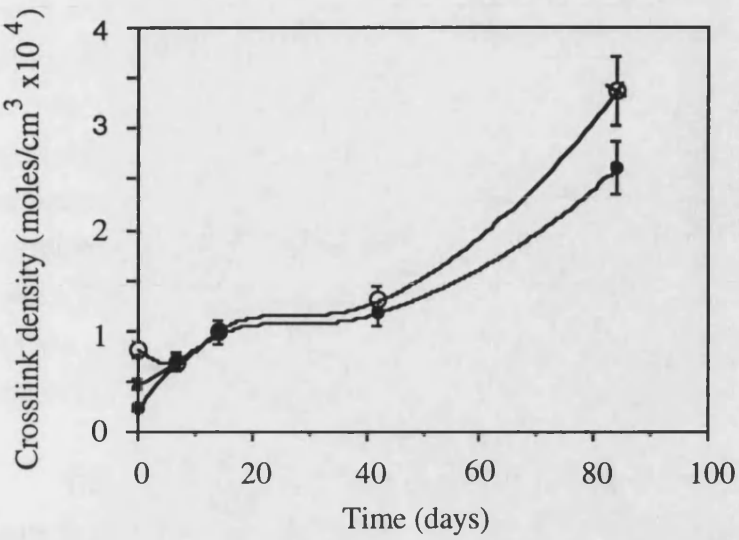

FIGURE 6.25. Crosslink structure of EB vulcanizate after ageing at 100°C in air;
(a) o total crosslink density,
(b) × crosslink density after propane-2-thiol treatment (cleaves poly-sulphides),
(c) ● crosslink density after hexanethiol treatment (cleaves di-sulphides and poly-sulphides).

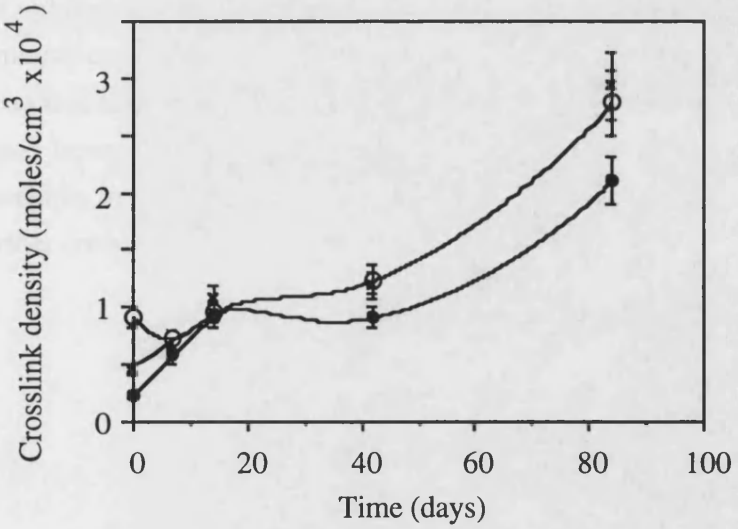

FIGURE 6.26. Crosslink structure of PB vulcanizate after ageing at 100°C in air;
(a) o total crosslink density,
(b) × crosslink density after propane-2-thiol treatment (cleaves poly-sulphides),
(c) ● crosslink density after hexanethiol treatment (cleaves di-sulphides and poly-sulphides).

6.2.2.3. Structure of Crosslinks Resistant to Thiol-Amine Treatment

For all vulcanizates oxidation at 100°C was accompanied by a rapid increase in overall crosslink density and an increase in the concentration of crosslinks which are unreactive towards hexane-1-thiol (1M) in piperidine treatment, (sections 6.2.2.1 and 6.2.2.2). The increase in total crosslink density and hexane-1-thiol unreactive crosslinks was faster in compounds of polymer E than compounds of polymer P. The crosslinks of networks which were unreactive towards hexane-1-thiol (1M) in piperidine were further treated with methyl iodide using experimental conditions of sections 3.9.2.2.2 and 3.9.2.3.4. This was done so as to differentiate between mono-sulphide and C-C crosslinks, (refer to section 2.2.3.1). The crosslink densities of samples treated in this way are shown in figure 6.27.

The lack of reactivity of hexane-1-thiol treated networks towards methyl iodide, (figure 6.27) strongly suggests that the majority of crosslinks introduced into N.B.R. networks during thermo-oxidative are C-C. The mechanism by which C-C crosslinks are introduced is not associated with poly-sulphide and di-sulphide decomposition, since it occurs in samples where there is little change in poly-sulphide and di-sulphide crosslink concentration, (figures 6.23 and 6.24). In a slightly different context, rapid crosslink formation, (M.E.K. gel > 50 %) has been reported in N.B.R. polymers containing no antioxidant and 1.25 phr tertiary alkyl-p-cresol during hot air ageing at 60°C by Hoffman (1984). It should be noted that Lee and Morrell (1973) considered that sulphoxides which are formed by oxidation of mono-sulphidic crosslinks are the dominant crosslink structure upon oxidation. The suggestion that crosslinks which are unreactive towards methyl iodide are sulphoxides cannot be excluded completely at this stage, however the poor oxidative stability of sulphoxides and the formation of crosslinks in N.B.R. polymer during ageing makes this unlikely, (see section 2.3.2.4). Further consideration of this point is given in the following section 6.2.3.

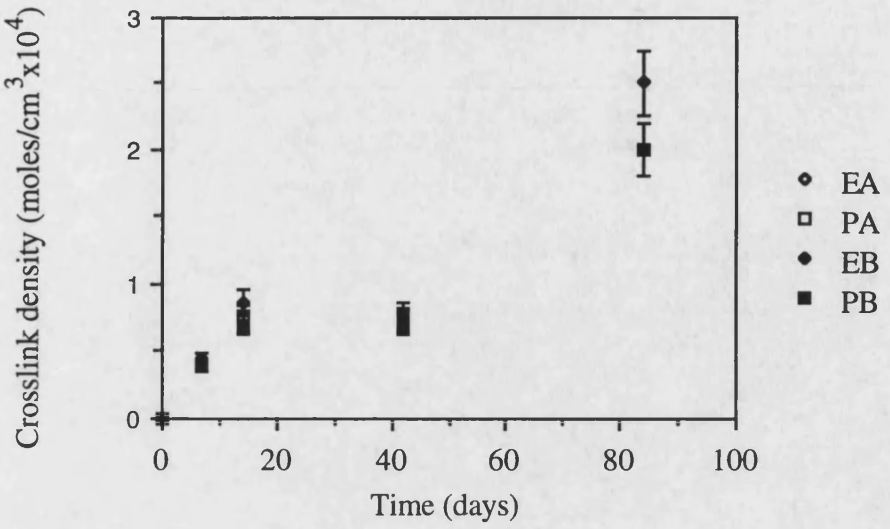

FIGURE 6.27. C-C crosslink density of N.B.R. vulcanizates after ageing at 100°C, (hexane-1-thiol and methyl iodide treatment).

6.2.3. OXIDATION OF CHEMICALLY PROBED SAMPLES

6.2.3.1. Stress Relaxation of Chemically Probed Samples

In order to obtain information on the oxidation of specific crosslink structures, additional samples of known network structure were aged. These samples were prepared by chemically probing vulcanizates of compound EA and PA, the probe solution being removed from samples after probing, (see section 3.9.2.3.3). Vulcanizates of compound B were not used because of the likelihood of extracting compounded-in antioxidant during probing. Vulcanizates were probed with the following treatments: treatment P involved swelling samples in piperidine for 72 hours while treatment P+H involved probing samples with hexane-1-thiol (1M) in piperidine for 72 hours. These treatments are tabulated in table 6.6. This approach of modifying network structure was chosen in preference to the conventional technique of changing vulcanization system because it was felt that a change in vulcanization system may introduce modifications in vulcanization chemistry which would affect network oxidation.

Intermittent and continuous stress relaxation at 100°C of EA and PA vulcanizates which were treated in this way before ageing are shown in figures 6.28 and 6.29.

Compared to untreated EA and PA samples (figures 6.18 and 6.21), piperidine extracted samples exhibit more rapid scission and crosslink formation during oxidative ageing at 100°C. The difference in the rate of scission and crosslink formation between sample EA and PA is greatly minimised after extraction of vulcanizates with piperidine. The high stability of PA vulcanizate is therefore associated with piperidine extractable species, (such species may be antioxidant residues of section 4.1.3). This effect is similar to the deterioration in oxidative stability of N.R. vulcanizates after acetone extraction, which has been associated with extraction of antioxidant residue (Mazzeo, 1995).

Networks which were extracted with piperidine alone, (treatment P, table 6.6) exhibit less scission and initially less crosslink formation during ageing than samples which were treated with hexane-1-thiol (1M) in piperidine, (treatment P+H, table 6.6). Samples treated with P contain the original distribution of crosslink structures while samples treated with P+H contain crosslinks which are exclusively mono-sulphide although in addition to crosslinks they also contain pendant thiol groups which are introduced during the reaction of hexane-1-thiol with di-sulphide and poly-sulphide crosslinks, (section 2.2.3.2, reaction scheme VIII).

The continuous stress relaxation plots indicate that mono-sulphide crosslinks are readily oxidised and cleaved during ageing at 100°C. These results support the view that crosslinks which form during N.B.R. oxidation are not mono-sulphides since mono-sulphide crosslinks are readily oxidised and cleaved during heating at 100°C.

Designation	Treatments	Crosslink structure remaining
P	Piperidine treatment	$S_1 + S_2 + S_x$
P+H	Piperidine + hexane-1-thiol treatment	S_1
P+A	Piperidine treatment + 100°C exposure	S_1+ C-C
P+H+A	Piperidine + hexane-1-thiol treatment + 100°C exposure	S_1+ C-C
P+A>H	Piperidine treatment + 100°C exposure then hexane-1-thiol treatment	S_1+ C-C
P+A>MI	Piperidine treatment + 100°C exposure then methyl iodide treatment	C-C
P+H+A>MI	Piperidine + hexane-1-thiol treatment + 100°C exposure then methyl iodide treatment	C-C

TABLE 6.6. Chemical probe treatments and ageing conditions used in the study of the oxidation of chemically probed samples.

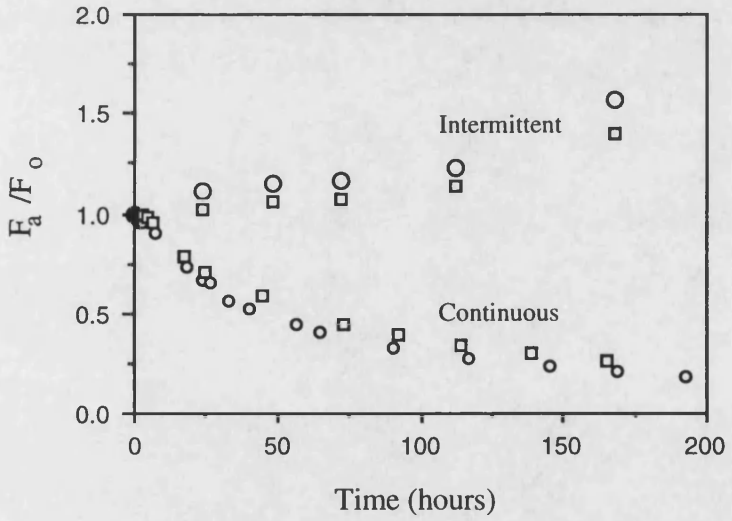

FIGURE 6.28. Air ageing at 100°C of N.B.R. vulcanizates EA

(a) □ treated with piperidine (P),

(b) ○ treated with hexanethiol in piperidine (P+H). Continuous and intermittent stress relaxation behaviour.

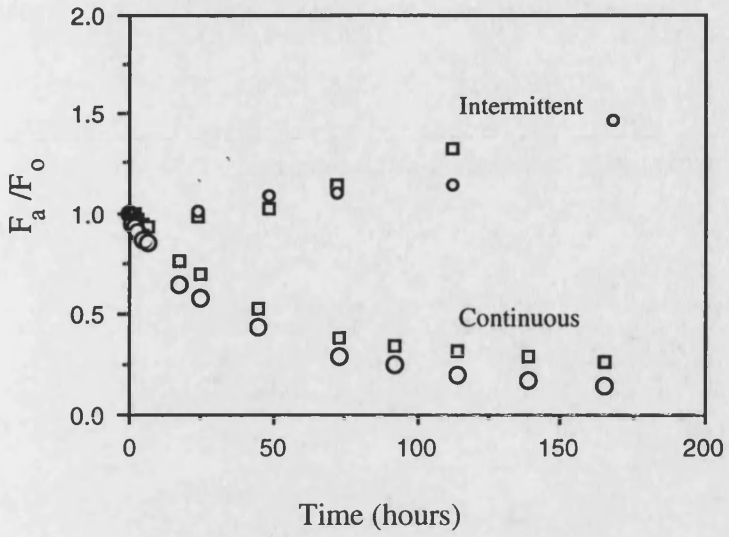

FIGURE 6.29. Air ageing at 100°C of N.B.R. vulcanizates PA
(a) □ treated with piperidine (P),
(b) O treated with hexanethiol in piperidine (P+H). Continuous and intermittent stress relaxation behaviour.

6.2.3.2. Weight Change During Ageing of Chemically Probed Samples

Weight change measurements of EA and PA vulcanizates which were treated with piperidine, (treatment P) and hexane-1-thiol (1M) in piperidine, (treatment P+H) during ageing at 100°C are shown in figures 6.30 and 6.31. Both treated samples show reduced induction times and increased oxygen absorption in comparison with untreated samples (figures 6.7 and 6.8). P+H treated samples, (containing mono-sulphide crosslinks and pendant thiols) show higher oxygen absorption than P treated samples, (containing original crosslink structure of table 4.26 and figure 4.17).

Differences in weight change between EA and PA samples after P and P+H treatment are negligible.

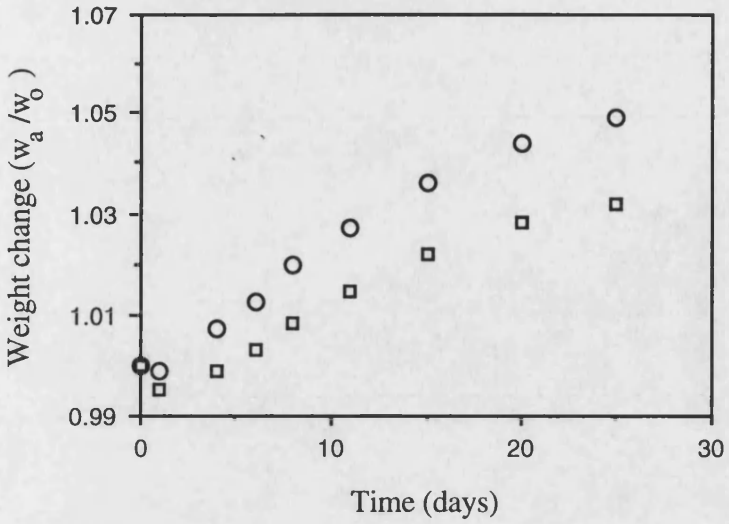

FIGURE 6.30. Air ageing at 100°C of N.B.R. vulcanizates EA

(a) □ treated with piperidine (P),

(b) O treated with hexanethiol in piperidine (P+H). Weight change.

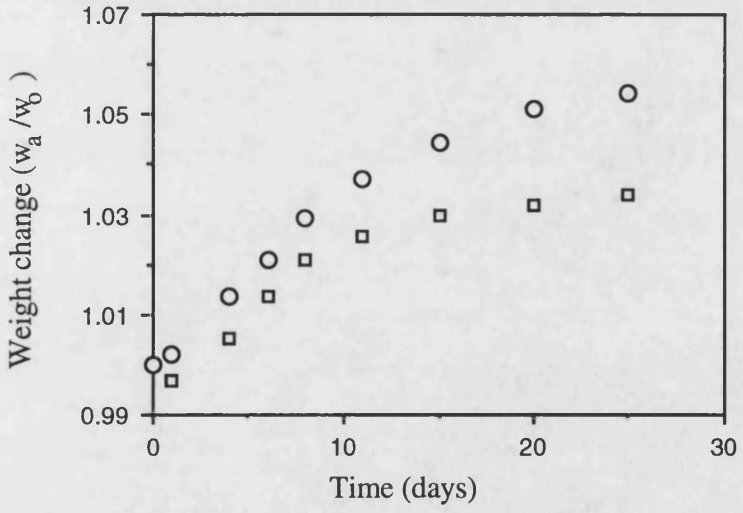

FIGURE 6.31. Air ageing at 100°C of N.B.R. vulcanizates PA

(a) □ treated with piperidine (P),

(b) O treated with hexanethiol in piperidine (P+H). Weight change.

6.2.3.3. Chemical Probe Treatment of Aged Chemically Probed Samples

6.2.3.3.1. Mooney-Rivlin Plots

Further elucidation of changes in crosslink structure was obtained from elastic deformation in tension measurements on treated EA and PA samples which were aged for 4 hours at 100°C. The treatment procedure used in the study of aged probed samples is shown in table 6.6. The ageing period of 4 hours was chosen from intermittent stress relaxation studies which showed that P+H treated samples exhibited significant crosslink formation after 4 hours heating at 100°C whilst samples which were treated with P exhibited no crosslink formation.

Mooney-Rivlin plots of EA samples before and subsequent to ageing and further chemical treatment are shown in figures 6.32 and 6.33. Treated PA samples are not shown because they exhibited identical behaviour to treated EA samples.

The Mooney-Rivlin plot of unaged EA, P treated sample, (figure 6.32) shows higher crosslink density than the P+H treated sample due to the presence of di-sulphide and poly-sulphide crosslinks. Poly-sulphide and di-sulphide crosslinks are removed from EA during treatment P+H.

The aged sample P+H (now designated P+H+A) shows an increase in crosslink density, although not to the level before probing, (the level of P). Thus not all crosslinks which were cleaved during hexane-1-thiol (1M) in piperidine treatment, (P+H) are reformed. In contrast unaged sample P, when aged, (P+A) shows no increase in crosslink density. This aged sample (P+A) is largely unreactive towards hexane-1-thiol (1M) in piperidine treatment following ageing (sample P+A>H), suggesting that crosslinks which were initially present as di-sulphides and poly-sulphides have largely been converted to mono-sulphides. The conversion of poly-sulphides to mono-sulphides has been greatly accelerated after piperidine extraction, (compare with figures 6.23 and 6.24). Therefore, amines, piperidine and diphenyl amine, both catalyse di-sulphide and poly-sulphide desulphurisation.

The structure of these newly formed crosslinks in P+A and P+H+A was further elucidated by probing with methyl iodide, which cleaves mono-sulphide crosslinks. The plots of these results are shown in figure 6.33. In figure 6.33 the Mooney-Rivlin plot for P+H+A is again shown for comparison. When this sample was probed with methyl iodide (P+H+A>MI), a reduction of crosslink density was observed, however some crosslinks remain. This implies that crosslinks which formed during ageing of

(P+H) sample are directly between carbon atoms (C-C). Sample P+A was also probed with methyl iodide (P+A>MI). The residual crosslink density (C-C) was similar to that of P+H+A>MI, although comparison with figure 6.32 shows that a larger concentration of sulphidic crosslinks had been cleaved by the methyl iodide in this sample. That these were reactive towards methyl iodide suggests that they were mainly mono-sulphidic. Di-sulphides and poly-sulphides are much less reactive towards methyl iodide.

Figures 6.32 and 6.33 confirm that C-C crosslink are not formed by poly-sulphide and di-sulphide oxidation decomposition products because the concentration of such crosslinks is similar in aged networks P+A and P+H+A.

These probed samples were further characterised by F.T.I.R. (A.T.R.) analysis. F.T.I.R. (A.T.R.) spectra of probed samples before and subsequent to ageing are shown in figure 6.34.

The spectrum of PA aged for 4 hr at 100°C shows absorption in the region of 1600 cm^{-1}, this is associated with zinc stearate, (figure 6.34a). Also shown are spectra of samples P+H+A and P+A referred to in table 6.6, (figures 6.34b and 6.34c). The 1600 cm^{-1} absorption is absent from the spectra of both P+A and P+H+A as the stearate had been extracted by the solvent.

The spectrum of P+A, (figure 6.34c) shows no remarkable features, but that of the P+H+A sample, (figure 6.34b) shows several absorption peaks which are not present in the other spectra. Absorption at 1000-1200 cm^{-1} is associated with S=O, C=S and RSO_2H structures while the bands at 880 cm^{-1} and 620 cm^{-1} are assumed to originate from -S-H and C-S-C, respectively. The appearance of these new bands is attributed to co-oxidation reactions of pendant thiols and polymers (see section 2.3.2.4, reaction schemes XVI and XVII).

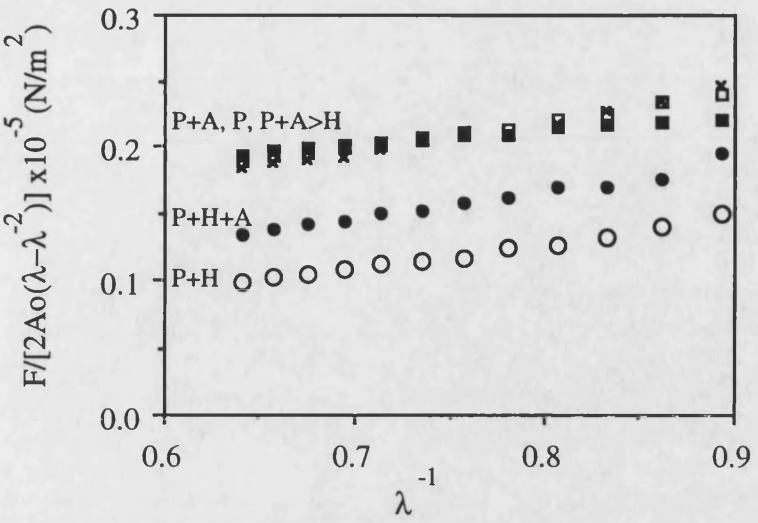

FIGURE 6.32. Mooney-Rivlin plots of probed N.B.R. EA vulcanizates

(a) Piperidine+hexanthiol treatment (P+H) ○
(b) Piperidine treatment (P) ■
(c) Piperidine+hexanthiol treatment+100°C exposure for 4 hours (P+H+A) ●
(d) Piperidine treatment+100°C exposure for 4 hours (P+A) □
(e) Treatment (P)+100°C exposure for 4 hrs then hexanthiol treatment (P+A+H) ×

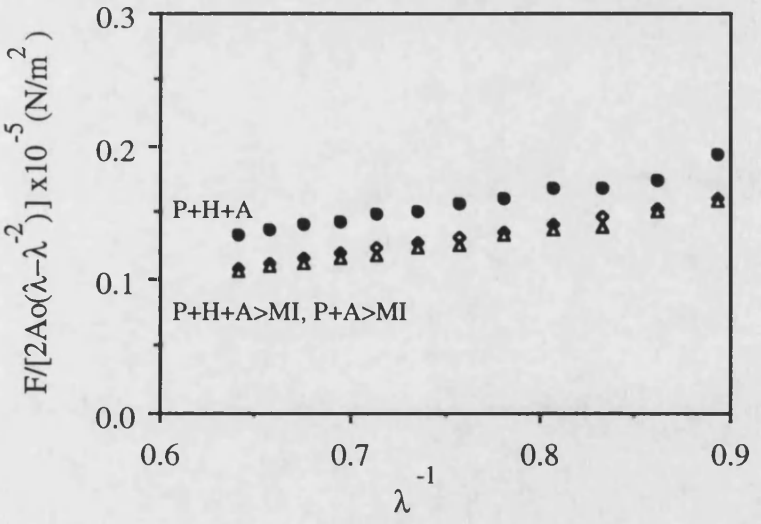

FIGURE 6.33. Mooney-Rivlin ploys of probed N.B.R. EA vulcanisates

(a) Piperidine+hexanthiol treatment+100°C exposure for 4 hours (P+H+A) ●
(b) Piperidine+hexanthiol treatment+100°C exposure for 4 hours then methyl iodide treatment (P+H+A>MI) △
(c) (P) treatment+100°C exposure for 4 hrs then methyl iodide treatment (P+A>MI) ◇

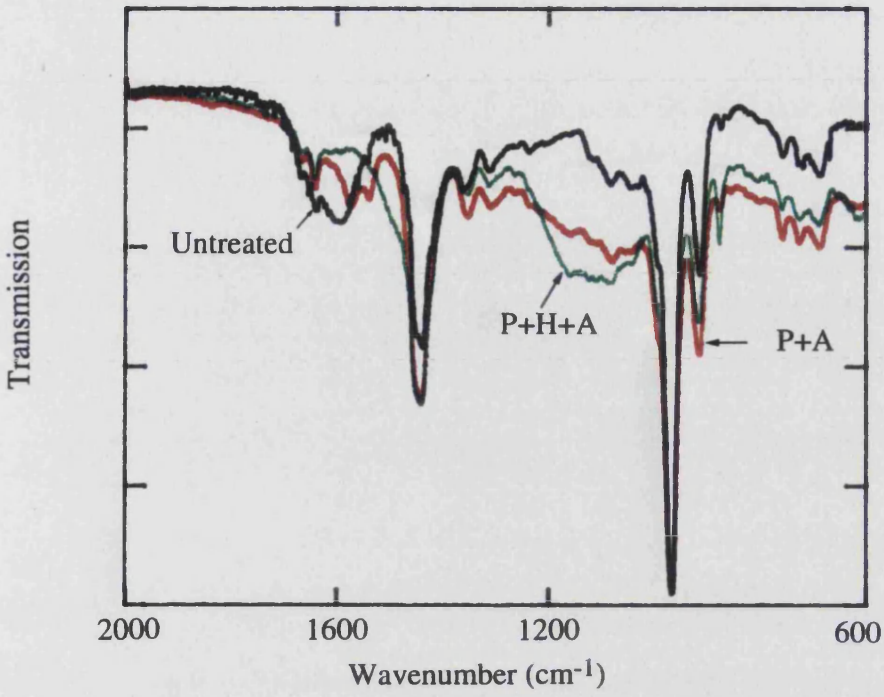

FIGURE. 6.34. F.T.I.R./A.T.R. Spectra of PA vulcanizates (aged at 100°C for 4 hours), (a) untreated, (b) treated with hexane-1-thiol then aged (P+H+A), (c) treated with piperidine then aged (P+A).

6.2.4. SUMMARY ON NETWORK OXIDATION

Oxidation of N.B.R. is accompanied by simultaneous crosslinking and scission reactions, crosslinking being the dominant process, (figures 6.18, 6.19, 6.21 and 6.22). Crosslinking and scission are influenced by base polymer and compound formulation.

In vulcanizates of compound A high rate of scission is accompanied by high rate of crosslink formation. For example compound EA shows highest rate of scission and highest rate of crosslink formation. In contrast compound PA shows lowest rate of scission and lowest rate of crosslink formation. These results are consistent with property change observed on oxidation, (section 6.1). Scission is thought to be caused by oxidative scission of mono-sulphide crosslinks. Di-sulphide crosslinks and poly-sulphide crosslinks are not reduced much in compound A during ageing while in compound B di-sulphides and poly-sulphides are rapidly converted to mono-sulphides. The mechanism of oxidative scission of mono-sulphide crosslinks is shown in section

2.3.2.4, (reaction scheme XVI). Crosslinks which form during N.B.R. oxidation are resistant to hexane-1-thiol and methyl iodide treatment and are thought to be C-C. The increase in C-C crosslinks occurs in the presence and absence of poly-sulphide and di-sulphide elimination. The C-C crosslinks may be formed by termination reactions in the free radical chain oxidation process, (section 2.3.1, reaction schemes IX and X).

In compound A the increase in total crosslink density is accompanied by little change in the concentration of poly-sulphide and di-sulphide crosslinks, (figures 6.23 and 6.24). The increase in C-C crosslinks is less in compound PA than EA, (figure 6.27).

Addition of diphenyl amine antioxidant, (compound B) causes a reduction in crosslink formation in all compounds but no reduction in the rate of scission in compounds other than those based on polymer E. Ageing is accompanied by an increase in total crosslink density after an induction time during which there is little change in crosslink density, (figures 6.25-6.27). In compound B early stages of ageing are accompanied by rapid conversion of poly-sulphide and di-sulphide crosslinks to mono-sulphide. These mono-sulphide crosslinks are cleaved and are replaced by C-C crosslinks. This rapid loss of sulphide crosslinks appears to be accompanied by a small reduction in total crosslink density. Rapid desulphurisation of poly-sulphide and di-sulphide crosslinks with formation of C-C crosslinks is also observed in piperidine treated samples, (figures 6.32 and 6.33). The rapid crosslink modification in vulcanizates of compound B may be the cause of faster initial stress relaxation and property change in compound B. In a different context an increase in the proportion of mono-sulphide crosslinks was observed during vulcanization of E and P compounds by addition of diphenyl amine antioxidant, (section 4.4.3.4, table 4.26). This was thought to be caused by an increase in the zinc:sulphur ratio in the active sulphurating agent, (section 4.4.4.2, table 4.28) and a shift in the equilibrium of the exchange reaction between active sulphurating agent and sulphide crosslinks, (section 2.4.3, reaction scheme V). During further ageing there is additional formation of C-C crosslinks, this being more rapid in compound EA than PA and formation of di-sulphide crosslinks. Di-sulphide crosslinks may be introduced by bimolecular reaction of sulphide oxidation products, such as pendant thiols, sulphenic acid and thiosulphoxylic acid, (section 2.3.2.4, reaction scheme XVII). It is demonstrated in figure 6.32 that crosslinks form through oxidation of pendant thiols.

EA and PA vulcanizates which have been pre-extracted with piperidine show similar rates of scission and crosslink formation and similar weight change during ageing. Piperidine extracted samples exhibit higher rates of scission and crosslink

formation than unextracted samples due to the extraction of piperidine soluble antioxidant residues of section 4.1.3. The similar oxidative stability of EA and PA after extraction demonstrates that the difference in oxidative stability between PA and EA is caused by piperidine extractable antioxidant residues. EA and PA vulcanizates which had been treated with hexane-1-thiol (1M) piperidine before ageing to remove di-sulphide and poly-sulphide crosslinks show more rapid crosslink scission and oxygen absorption than piperidine extracted samples. This implies that mono-sulphide crosslinks are more rapidly oxidised and cleaved than di-sulphide and poly-sulphide crosslinks.

6.3. SPECTROSCOPIC CHARACTERISATION OF AGED VULCANIZATES

This section provides additional information on the mechanism of polymer and network oxidation using spectroscopic and analytical techniques. Results of section 6.3 clarify some points discussed in earlier sections of this chapter.

6.3.1. CHARACTERISATION OF AGED VULCANIZATES BY F.T.I.R.

Vulcanizates which were aged at 100°C were studied by F.T.I.R. (A.T.R.) to obtain further information on the mechanism of ageing. The results of these studies for compounds EA, EB, PA and PB are shown in figures 6.35-6.37 and discussed below. In compound B spectra of vulcanizates based on polymer B, G and N were similar to spectra of vulcanizates based on polymers E and P, while in compound A the build up of oxidation structures was intermediate.

Figure 6.35 shows the change in ketone absorption of wavelength 1735 cm^{-1} relative to the methylene group at 1445 cm^{-1}. Figure 6.36 shows the absorbance at 1090 cm^{-1} caused by C-O stretching of peroxide and other oxidation products relative to the methylene absorption. The change in the broad OH absorbance band, at approximately 3450 cm^{-1} relative to the methylene absorbance is shown in figure 6.37. In this treatment it is assumed that the 3450 cm^{-1} absorption band is associated primarily with hydroperoxide, however due to the low specificity of the OH absorbance peak it cannot be excluded that the measured absorbance will include contributions from other oxidation products such as water and alcohol. The methylene group is used as an internal reference in these plots because it is reported that its concentration in N.B.R. does not change on oxidative ageing (Bhattacharjee *et al.*, 1992).

All vulcanizates show an increase in the concentration of ketone and peroxide structures during oxidative ageing at 100°C. The build up of such structures is particularly rapid with EA. The increase in peroxide and ketone of compound PA, up to an ageing period of 42 days is not much higher than for compound B. In the first day of ageing at 100°C vulcanizates of compound B show a more rapid increase in ketone and peroxide structures. Significantly ketone and peroxide formation in compound B preceeds hydroperoxide formation. This early formation of ketone and peroxide structures in compound B is consistent with persulphenyl radical initiated oxidation, persulphenyl radicals being formed during poly-sulphide decomposition, (this is shown in figures 6.25 and 6.26). The initial increase in ketone and peroxide structures in compound B is consistent with rapid change in elongation at break and stress relaxation of this compound, (reported in sections 6.1 and 6.2).

The increase in ketone and peroxide absorbance during oxidative ageing shows good similarity to the increase in total crosslink density and C-C crosslink concentration. Ketone formation in the oxidation of sulphur cured networks through chain scission is illustrated in section 2.3.1, (reaction scheme XI) and through crosslink scission in section 2.3.2.4, (reaction scheme XVI).

Figure 6.37 indicates differences in the build up of OH between vulcanizates of compound A and B. Vulcanizates of compound A show much higher I.R. absorption in the OH region than vulcanizates of compound B before ageing. This suggests that with compound A hydroperoxides are introduced during the mixing process. Absorption at 3450 cm^{-1} in unaged EA vulcanizates is much higher than in PA vulcanizates. This implies greater degradation in EA during mixing. Hydroperoxide formation in compound EB and PB is delayed and maximum hydroperoxide concentration occurs after approximately 7 days ageing at 100°C.

In all compounds the ratios of absorbance at 2150 cm^{-1} (attributable to -CN) and 910 cm^{-1} (attributable to vinyl-1,2 unsaturation) relative to the absorbance of methylene was not affected by ageing at 100°C, which implies that both structures are unreactive.

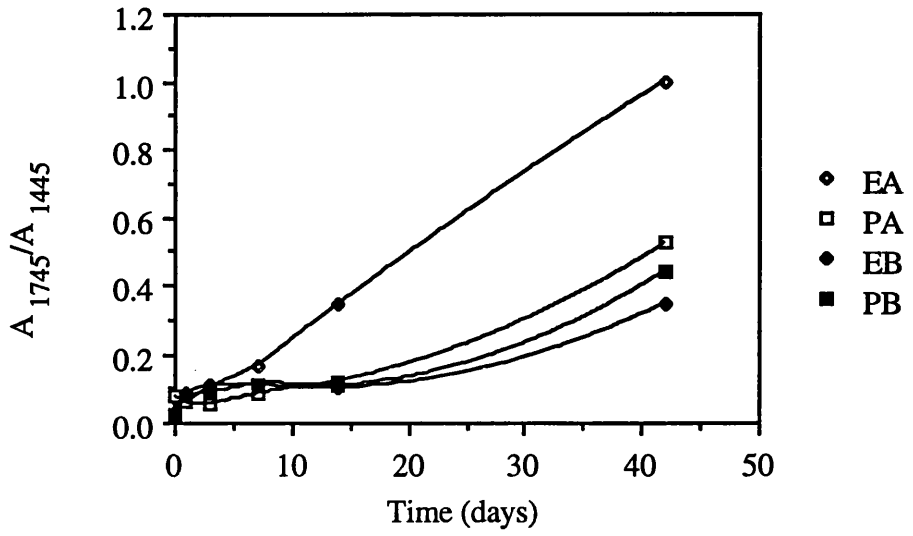

FIGURE 6.35. Change in I.R. absorption ratio, (ketone/methylene) with ageing time, at 100°C.

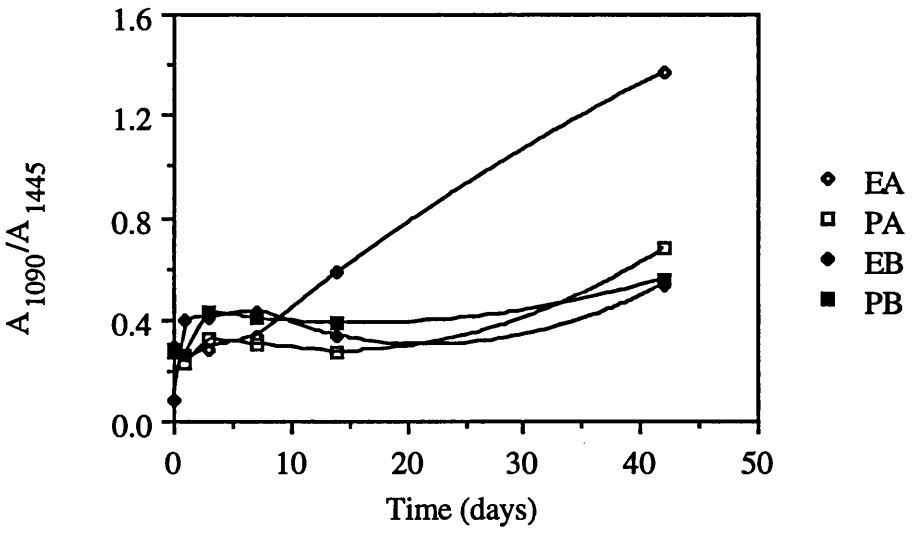

FIGURE 6.36. Change in I.R. absorption ratio, (peroxide/methylene) with ageing time, at 100°C.

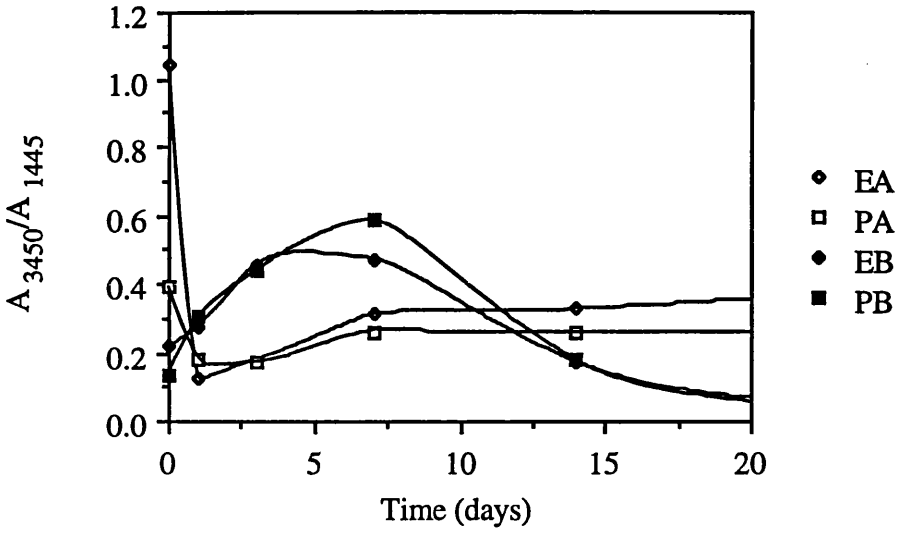

FIGURE 6.37. Change of I.R. absorption ratio, (OH/methylene) with ageing time, at 100°C.

6.3.2. CHARACTERISATION OF AGED SURFACES BY X.P.S.

The study of aged vulcanizates was supplemented by X.P.S. analysis. X.P.S. was regarded as a complimentary technique in the study of oxidation and as a means of obtaining additional information on crosslink oxidation, this being possible because binding energy of elements is influenced by bonding, (see section 2.3.5.2). In these studies work was restricted to compounds EA, EB, PA and PB because these compounds exhibit the largest difference in oxidative stability.

The concentration of sulphur and zinc on surfaces of vulcanizates which have been aged at 100°C for 14 days is shown in table 6.7. Results of table 6.7 should be compared to the concentration of sulphur and zinc on the equivalent unoxidised surfaces of table 4.28. The binding energies of zinc, sulphur and nitrogen species on the surfaces of aged vulcanizates are shown in table 6.9. The binding energies of these elements should be compared to their binding energies on unoxidised surfaces, (table 4.29). The concentrations of C_{1s}, N_{1s} and O_{1s} on oxidised surfaces relative to the concentration on unoxidised surfaces is shown in table 6.8 and figure 6.38. N_{1s} and O_{1s} values were not converted into C_{1s} ratios because the concentration of C_{1s} was similar for all compounds and was unaffected by ageing. Because C_{1s} values were

similar for all samples before and after ageing N_{1s} and O_{1s} concentrations may be compared directly.

The results of table 6.7 show an increase in the concentration of zinc and sulphur (with a binding energy in the region of 164 eV) on all surfaces after oxidation. The binding energy of zinc on the surfaces of oxidised vulcanizates, shown in table 6.9, indicates that such residues are not in the form of ZnS and ZnO, (compare with model compound binding energies of table 4.29). This is contrary to published results on the oxidation of sulphur cured E.P.D.M. systems where an increase in zinc sulphide, thought to be caused by desulphurisation of poly-sulphide crosslinks was observed (Deuri and Bhowmick, 1987). The binding energies of model compounds (table 4.29) suggest that zinc and sulphur species on the surfaces of N.B.R. are more likely to be in the form of zinc stearate and zinc-accelerator-sulphur complexes.

Oxidised vulcanizates of polymer P show an increase in the concentration of S_{169eV}, (oxygen bonded sulphur), (compare table 6.7 with 4.28). This increase in the concentration of S_{169eV} is likely to be associated with migration of sulphate/sulphonate emulsifier species to the surface. Migration of sulphate/sulphonate emulsifier species to N.B.R. surfaces and interfaces has been reported by Reeves and Packham (1992). S_{169eV} is unlikely to be associated with sulphide oxidation since no S_{169eV} could be detected on the oxidised EA surface.

In table 6.8 and figure 6.38 it is shown that surfaces oxidised at 100°C for 14 days contain more oxygen than unoxidised surfaces. It is thought that this oxygen is caused by oxidation, rather than migration of oxygen containing species. This is thought to be the case because oxygen concentration on aged EA compound is high. It has already been established that EA is most extensively oxidised. The increase in oxygen on the surface of compound EB is low. The difference in oxygen concentration between aged EA and EB vulcanizates support the view that the additional oxygen on the surface of vulcanizates is attributable to oxidation, rather than differences in migration species since the main difference between EA and EB is the extent of oxidation. The increase in oxygen is associated with a reduction in nitrogen while the ratio of the C_{1s} signal on aged to unaged vulcanizates is little affected. Nitrogen reduction is not associated with loss of cyanide since the level of hydrogen cyanide given off from aged vulcanizates under high vacuum, during X.P.S. analysis was insignificant, (see section 6.3.2.1) and the concentration of nitrile groups on aged surfaces, measured by F.T.I.R. was not changed, (section 6.3.1).

The preferential reduction in nitrogen with an increase in oxygen concentration on aged vulcanizate surfaces suggests inhomogeneous distribution of oxygen on aged N.B.R. vulcanizates, with more oxygen being in the vicinity of the nitrile group. Association can occur through strong dipole-dipole interaction between the nitrile group and sulphoxides, as reported in section 2.3.2.1. This interaction can be easily visualised since in N.B.R. most crosslinks are thought to be attached to a methylene of a butadiene unit adjacent to a nitrile group (Kirkham, 1978). Further association of the nitrile group may be through hydrogen bonding of the nitrogen with oxidation structures such as sulphenic acid, thiosulphoxylic acid, hydroperoxides and secondary alcohols. In a different context inhomogeneous oxygen distribution on the surface of S.B.R. vulcanizates measured by X.P.S. has been reported by Lin (1986).

In all vulcanizates the referenced binding energy of the N_{1s} signal is seen to shift to higher binding energy after oxidation, (compare tables 6.9 and 4.29). This shift in binding energy supports the postulate that the nitrile group is associated with oxidation structures since it is well known that binding energy is sensitive to environment (see section 2.3.5.2). It should be noted that Bhattacharjee *et al.* (1991) reported a shift in the binding energy of N_{1s} from 400.8 eV to 406.0 eV in H.N.B.R. during oxidation at 150°C for 48 hours. This shift in N_{1s} binding energy was attributed to conversion of -CN groups to -CNH (see section 2.3.1, reaction scheme XII). No comment was made on the possibility of hydrogen bonding and dipole-dipole interactions between the nitrile group nitrogen and oxidation structural groups. The observed increase in oxygen during ageing of N.B.R. and the preferential reduction in nitrogen is not explained by reaction XII and is more consistent with association between the nitrile group and oxidation structures.

Atomic ratio	PA	PB	EA	EB
$*S_{164eV}:C_{1s}$	$20.5x10^{-3}$	$20.3x10^{-3}$	$14.3x10^{-3}$	$14.2x10^{-3}$
$\wedge S_{169eV}:C_{1s}$	$25.1x10^{-3}$	$27.5x10^{-3}$	~	~
$Zn_{2p}:C_{1s}$	$13.6x10^{-3}$	$13.5x10^{-3}$	$14.1x10^{-3}$	$20.4x10^{-3}$

~None detected. *Bonded to S, C or H, ^bonded to O.

TABLE. 6.7. Mole ratios of N:C, O:C, S:C, Zn:C and S:Zn found on the surfaces of N.B.R. by X.P.S. after ageing for 14 days at 100°C.

Atomic ratio	PA	PB	EA	EB
$C_{1s(a)}:C_{1s(o)}$	0.96	0.94	1.08	1.02
$N_{1s(a)}:N_{1s(o)}$	0.83	0.70	0.56	0.60
$O_{1s(a)}:O_{1s(o)}$	1.43	1.60	2.39	1.80

(a) - aged, (o) - unaged.

TABLE 6.8. Mole ratios of C, N and O on surfaces of vulcanizates aged at 100°C for 14 days and on surfaces of unaged vulcanizates.

	Binding energy, eV		
Compound	Zn_{2p3}	S_{2p}	N_{1s}
EA	1022.50	163.65	400.4
EB	1022.70	163.90	400.2
PA	1022.75	163.75	399.9
PB	1022.75	163.20	400.3

TABLE 6.9. X.P.S. Binding energies of sulphur, zinc and nitrogen in N.B.R. vulcanizates aged at 100°C for 14 days, referenced to the binding energy of C_{1s} at 285 eV.

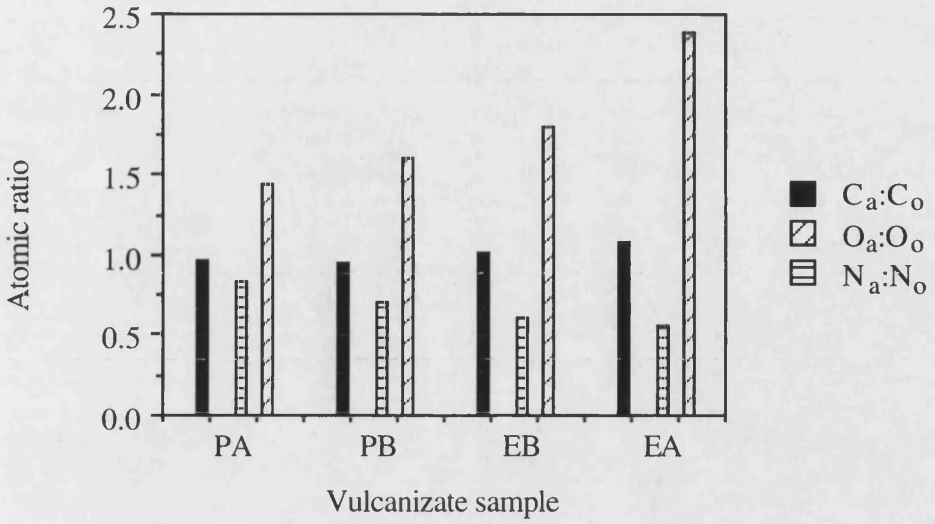

FIGURE 6.38. Atomic ratios of, carbon, oxygen and nitrogen on surfaces of vulcanizates aged for 14 days at 100°C, (a) relative to unoxidised surfaces, (o).

6.3.2.1. Mass Spectroscopy

During X.P.S. analysis vulcanizates gave off volatile material. The volatile material given off was analysed by mass spectroscopy. Concentrations of the four most abundant chemicals which were given off by vulcanizate surfaces during X.P.S. analysis are shown in figures 6.39-6.41.

The most abundant species evolved from vulcanizates, aged at 100°C for 14 days is water. The highest concentration of water is evolved from the aged EA sample (figure 6.39). It has been shown that this sample is most heavily oxidised, (section 6.1). Water is therefore likely to be introduced during oxidation. In sample PA the concentration of evolved water is similar for the aged and the unaged sample (figure 6.40). This is because sample PA is not appreciably oxidised after 14 days heating at 100°C. Samples of compound B which were aged at 100°C for 14 days, (figure 6.41) evolve less water than equivalently aged samples of compound A.

The concentration of water evolved from unaged samples based on polymer P is much higher than the concentration of water evolved from unaged samples based on

polymer E, due presumably to dehydration of coagulant hydrate residues of table 4.3. Polymer P contains 75 $x10^{-6}$ $mol.g^{-1}$ calcium whereas polymer E contains 28 $x10^{-6}$ $mol.g^{-1}$ magnesium. Dehydration is caused by heating up of sample surfaces during X-ray bombardment.

Other species such as nitrogen, carbon dioxide, hydrogen cyanide, methane and ethane were detected at much lower concentrations.

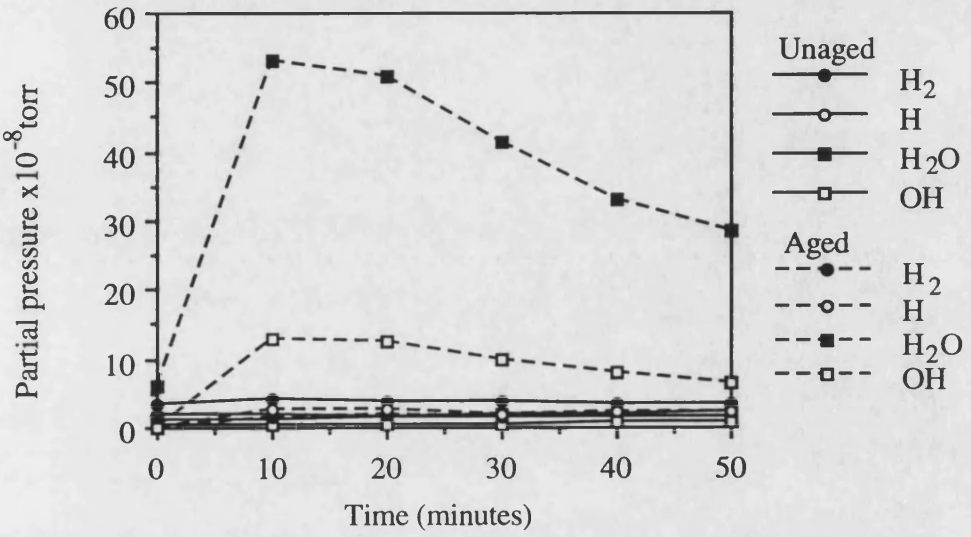

FIGURE 6.39. The four most abundant species evolved from, EA, unaged and aged at 100°C for 14 days, during X.P.S. analysis.

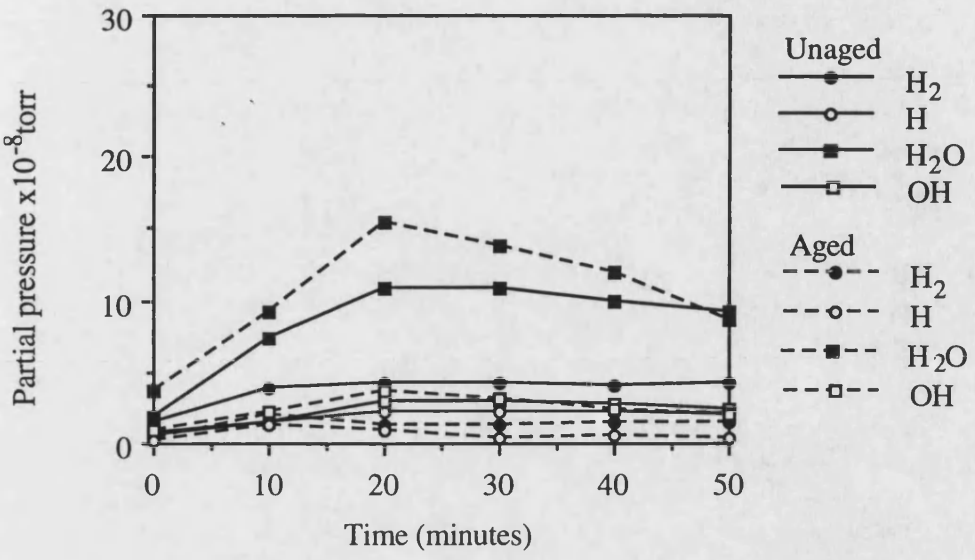

FIGURE 6.40. The four most abundant species evolved from, PA, unaged and aged at 100°C for 14 days, during X.P.S. analysis.

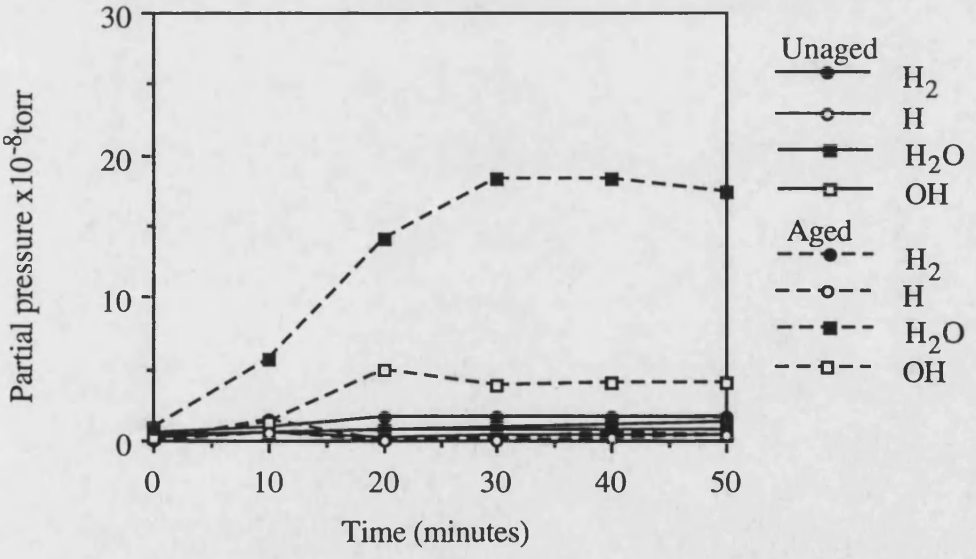

FIGURE 6.41. The four most abundant species evolved from, EB, unaged and aged at 100°C for 14 days, during X.P.S. analysis.

6.3.3. DIFFERENTIAL THERMAL ANALYSIS

6.3.3.1. Differential Scanning Calorimetry

Further study of the oxidation behaviour of polymers and vulcanizates was made by differential scanning calorimetry. Oxidation experiments involved heating samples at controlled heating rates in static air.

Figure 6.42 shows a D.S.C. oxidation curve of vulcanizate PA which was obtained by heating an 8.4 mg sample. This plot is similar to previously published D.S.C. oxidation scans of N.B.R. systems (Budrugeac and Segal, 1991; Budrugeac, Segal and Ciutacu, 1991).

In figure 6.42 the initial peak is attributed to oxidation, this being confirmed by its elimination when running experiments in nitrogen. The second peak was found to occur at 350±1°C in all samples and was unaffected in magnitude or position by running experiments in nitrogen. This peak is associated with thermal decomposition. At high temperatures, in excess of 400°C the heat flow signal becomes erratic due to sample volatilisation.

In order to obtain more detailed information on D.S.C. oxidation additional experiments were made by reducing sample size. This was a means of enhancing the oxidation peak and reducing oxygen diffusion effects, (see figures 6.43 and 6.44). Under these conditions the oxidation peak is enhanced and the thermal decomposition peak is greatly reduced. This effect of sample size has been reported by Goh (1987). D.S.C. oxidation peak parameters of polymers and vulcanizates obtained by running 0.2 mg samples are tabulated in tables 6.10 and 6.11. D.S.C. oxidation scans of EA and PA vulcanizates of section 6.2.3, (probed with, piperidine alone and hexane-1-thiol (1M) in piperidine) are shown in figures 6.45 and 6.46.

D.S.C. oxidation scans of figures 6.43 and 6.44 show that the oxidation peak of the raw polymers is a composite peak. Slusarski (1984) has reported similar results in the study of acetone extracted cis-1,4-butadiene and has attributed the initial peak to hydroperoxide formation and the latter peak to crosslinking, degradation and decomposition. D.S.C. oxidation scans of polymer E and P show differences in the position and character of the hydroperoxide formation peak. The higher onset temperature of oxidation of polymer P implies delayed hydroperoxide formation. Hydroperoxide formation may be delayed by antioxidant species of section 4.1.3. The

onset temperature of D.S.C. oxidation, (hydroperoxide formation) of table 6.10 is inversely related to oxidative stability of polymers compounded with formulation A.

Vulcanizates oxidise at higher temperatures than raw polymers and exhibit higher oxidation exotherms. The higher oxidation exotherms of vulcanizates may be associated with crosslink oxidation and crosslink maturation, (section 4.3.3, figures 4.10 and 4.11). These results show that sulphur compounds which are introduced into N.B.R. during compounding and vulcanization act as antioxidants. The antioxidative properties of sulphur compounds are well known and were reviewed in section 2.3.3.2. Compounding in of diphenyl amine antioxidant induces a shift in the D.S.C. oxidation peak to higher temperatures and a reduction in the oxidation peak exotherm for all compounds other than those based on polymer N. This is consistent with published results on the effect of antioxidants on the D.S.C. oxidation peak exotherm (Sircar, 1982).

EA and PA vulcanizates which were treated with piperidine start to oxidise at lower temperatures than untreated samples, (figures 6.45 and 6.46). This effect is likely to be associated with antioxidant extraction during piperidine treatment. EA and PA samples which were treated with hexane-1-thiol in piperidine treatment, (these samples contain only mono-sulphide crosslinks and pendant thiols) exhibit similar oxidative stability to samples which were treated in piperidine alone.

F.T.I.R., (A.T.R.) analysis of samples which were subjected to controlled heating rate treatments up to temperatures in the region of the D.S.C. oxidation peak did not show any build up in oxidation structures. This may be because under such conditions the depth of I.R. penetration is greater than the depth of oxidation. A visible colour change in such samples confirmed that surface oxidation had taken place.

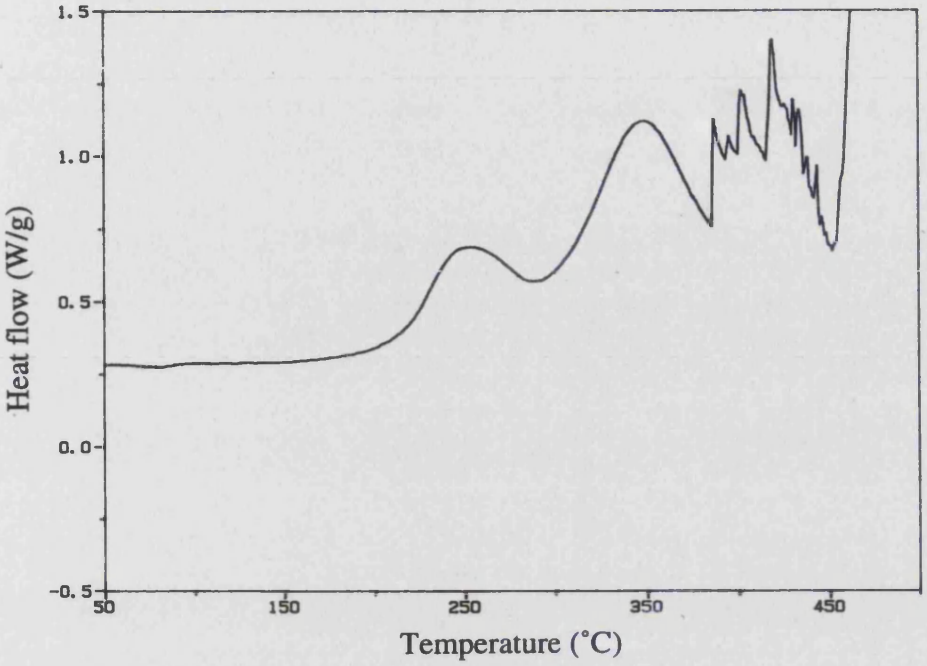

FIGURE 6.42. D.S.C. Oxidation scans of PA, obtained by heating samples of 8.4 mg in static air at 5°C/minute.

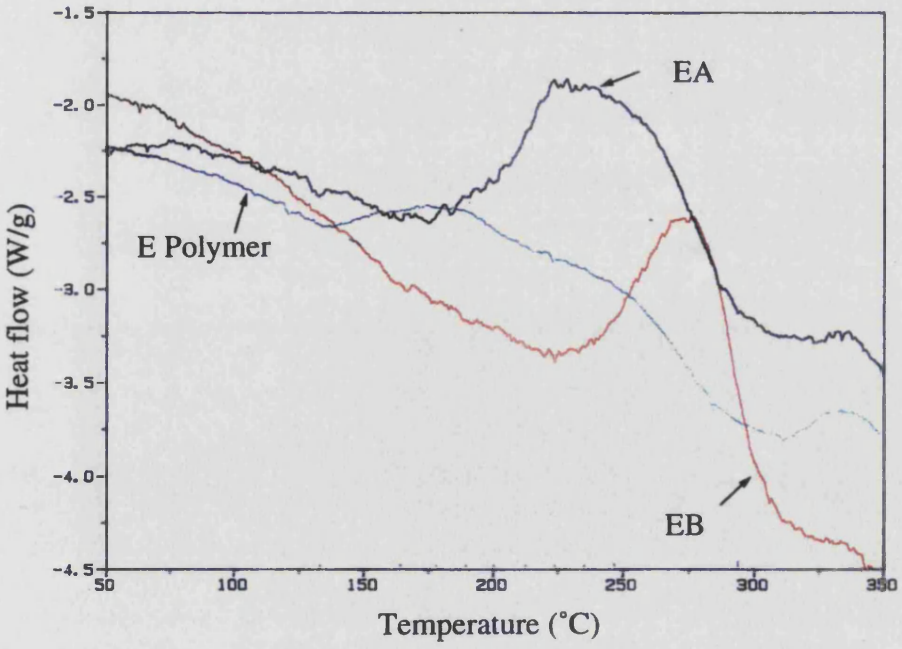

FIGURE 6.43. D.S.C. Oxidation scans of E polymer and vulcanizates, obtained by heating samples of 0.2 mg in static air at 5°C/minute.

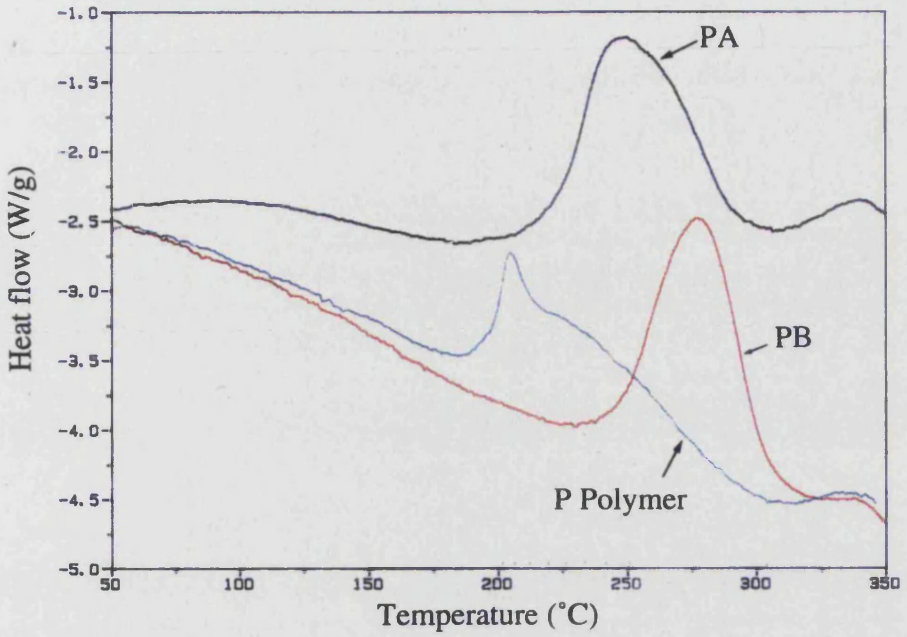

FIGURE 6.44. D.S.C. Oxidation scans of P polymer and vulcanizates, obtained by heating samples of 0.2 mg in static air at 5°C/minute.

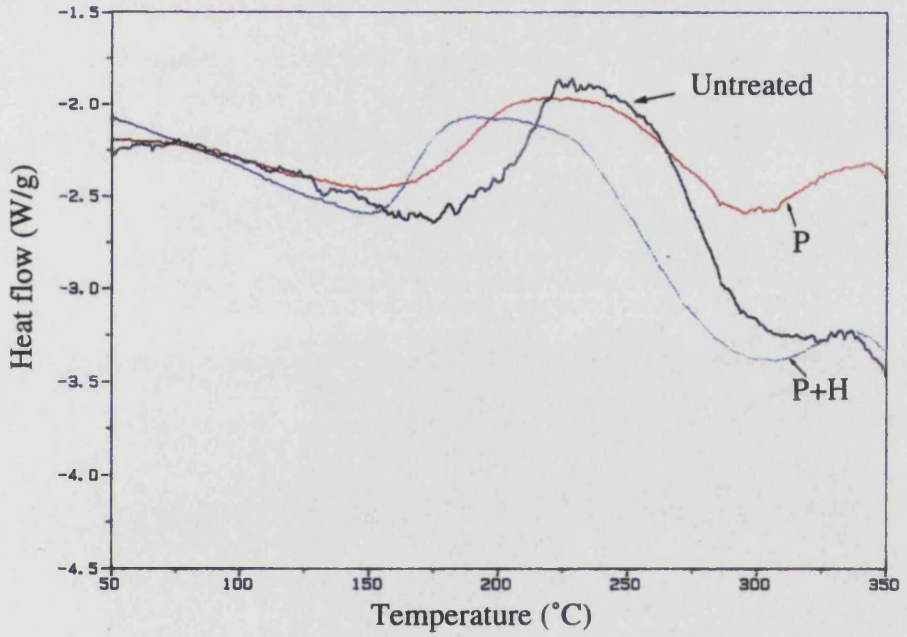

FIGURE 6.45. D.S.C. Oxidation scans of EA vulcanizates obtained by heating samples of 0.2 mg in static air at 5°C/minute, (untreated; treated with piperidine, P; treated with hexane-1-thiol (1M) in piperidine, P+H).

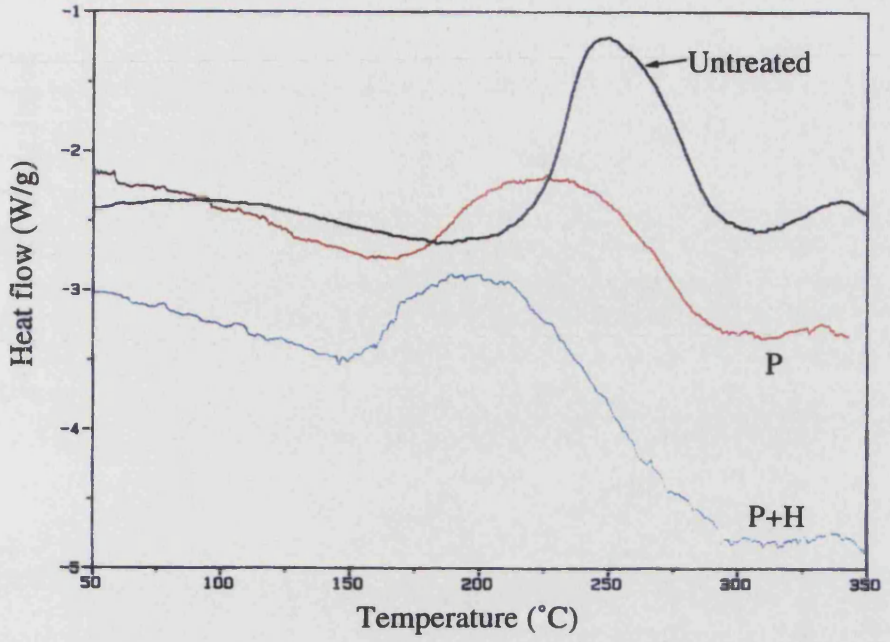

FIGURE 6.46. D.S.C. Oxidation scans of PA vulcanizates obtained by heating samples of 0.2 mg in static air at 5°C/minute, (untreated; treated with piperidine, P; treated with hexane-1-thiol (1M) in piperidine, P+H).

Polymer	Onset temp. of D.S.C. oxidation peak (°C)	Temp. at D.S.C. oxidation peak maximum (°C)*	Oxidation exotherm (J/g)
B	160	184	547
E	136	190	569
G	156	173	624
N	156	183	530
P	194	205	540

*These temperatures are of the first oxidation peak.

Table 6.10. D.S.C. oxidation peak parameters of raw N.B.R. polymers of sample weight in the region of 0.2 mg, heated at 5°C per minute.

Vulcanizate	Onset temp. of D.S.C. oxidation peak (°C)	Temp. at D.S.C. oxidation peak maximum (°C)	Oxidation exotherm (J/g)
BA	216	233	876
BB	238	274	684
EA	200	232	907
EB	235	277	651
GA	209	262	903
GB	245	263	670
NA	197	257	706
NB	246	279	831
PA	223	250	805
PB	246	278	787

Table 6.11. D.S.C. oxidation peak parameters of N.B.R. vulcanizates of sample weight in the region of 0.2 mg, heated at 5°C per minute.

6.3.3.2. Differential Thermogravimetric Analysis

Simultaneous differential thermal analysis and differential thermo-gravimetric analysis was carried out on vulcanizate samples to gain further information on the oxidation exotherm.

The scan of compound EA obtained by heating a sample of 0.8 mg is shown in figure 6.47. The scans of other compounds are similar to figure 6.47.

These scans show that the oxidation exotherm is accompanied by weight increase due to reaction with oxygen.

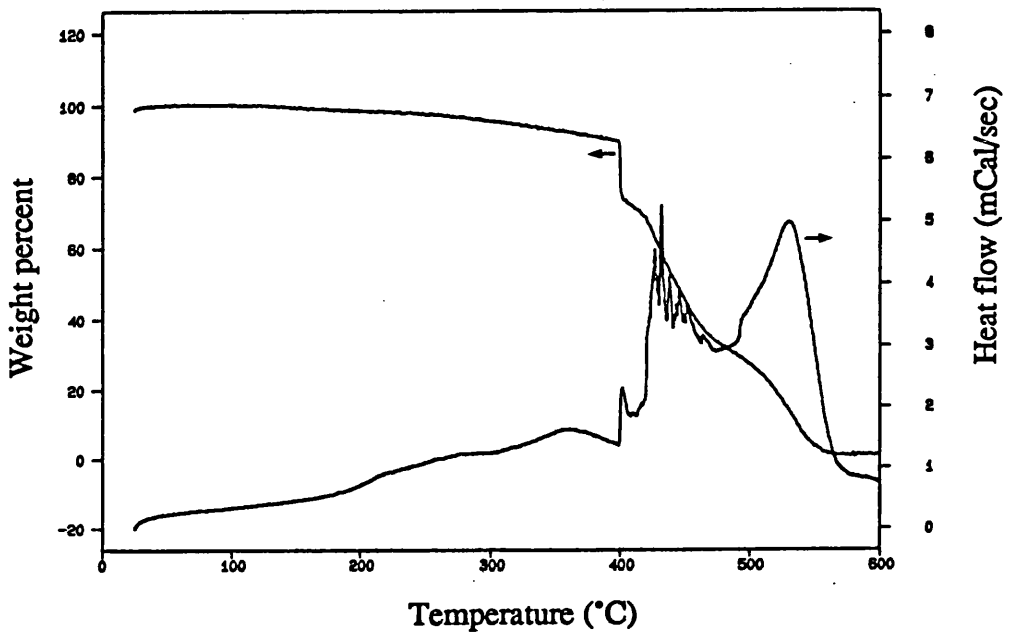

FIGURE 6.47. D.S.C./D.T.G. Scan of compound EA, (0.8 mg sample), heated in static air at a heating rate of 10°C/minute.

6.3.4. OXYGEN DIFFUSION COEFFICIENT

Oxygen diffusion coefficients in EA and PA were measured in order to see whether these could explain observed differences in oxidative stability of EA and PA.

Diffusion coefficients of these compounds are shown in figure 6.48. These values may not be absolute because in their determination an integral technique was used. In the integral measurement of diffusion one side of the membrane is at maximum concentration while the opposite side is at zero concentration only at the beginning of the experiments, (see section 5.4). The time lag calculation used for measurement of diffusion, (equation 5.1) is derived for steady state diffusion where one side of the membrane is maintained at zero concentration.

Results of figure 6.48 show that measured diffusion is similar for compounds EA and PA. The observed differences in oxidative stability between these two compounds are therefore caused by chemical factors.

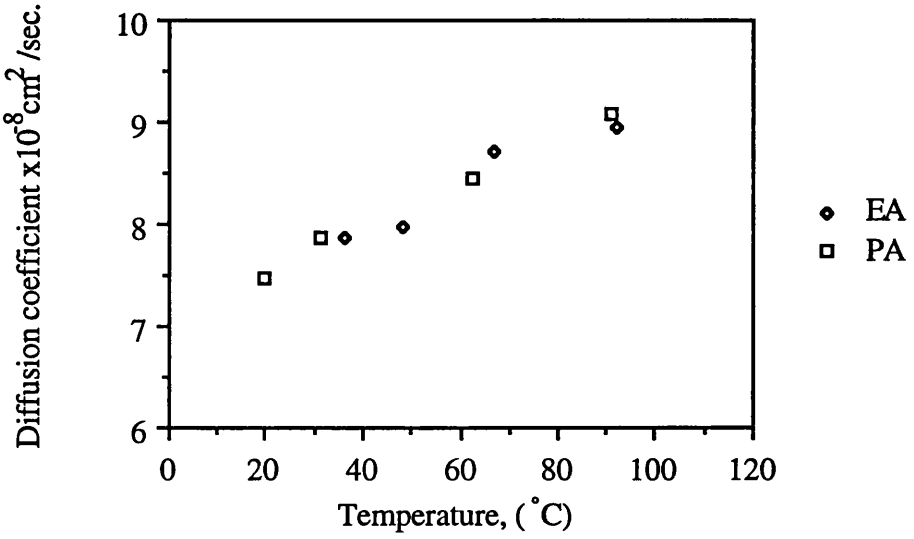

FIGURE 6.48. Oxygen diffusion coefficients of N.B.R. measured under isobaric conditions.

6.3.5. SUMMARY ON SPECTROSCOPIC CHARACTERISATION OF AGED VULCANIZATES

Ageing of all samples is accompanied by an increase in oxygen concentration, the increase being much higher on surfaces of EA than PA, EB and PB vulcanizates, (table 6.8). This oxygen is covalently bonded with polymer in the form hydroperoxide, peroxide, ketone and other oxidation structures, (figures 6.35-6.37). Water is a major product of oxidation, (figures 6.39-6.41).

Hydroperoxide formation is rapid in vulcanizates with no compounded in antioxidant, (compound A). In these vulcanizates hydroperoxide concentration appears to be at its maximum in unaged samples. Hydroperoxide concentration on the unaged EA surface is much higher than on the unaged PA surface. This suggests that in vulcanizates of compound A hydroperoxide formation occurs during mixing and is a

useful early indicator of relative stability. In vulcanizates with compounded-in diphenyl amine antioxidant (compound B) hydroperoxide formation is delayed.

Peroxide and ketone build up is rapid in EA and less rapid in PA and vulcanizates of compound B. In compound B peroxide and ketone build up is more rapid than in compound A within the first day of ageing at 100°C. This is consistent with the observed rapid change in elongation at break, stress relaxation and desulphurisation in vulcanizates of compound B during this ageing time. The more rapid initial peroxide and ketone build up in compound B may be associated with persulphenyl radical initiated oxidation.

On all surfaces there is an increase in the concentration of sulphur, (binding energy 164 eV) and zinc species after ageing at 100°C for 14 days, (table 6.7). The increase in these species during ageing at 100°C may be associated with migration of such species to surface regions. The binding energy of the zinc on oxidised surfaces, (table 6.9) is consistent with it being in the form of zinc stearate and zinc-accelerator species rather than zinc sulphide and zinc oxide, (see section 4.4.4.2, table 4.29). Zinc stearate has been determined on surfaces of vulcanizates by F.T.I.R., (figure 6.34a). The high concentration of oxygen bonded sulphur on the surfaces of vulcanizates of polymer P is associated with migration of sulphate/sulphonate species to surface regions rather than oxidation since no increase is observed in vulcanizates of polymer E.

The increase in oxygen concentration of aged vulcanizates is accompanied by little change in carbon concentration and a rapid reduction in nitrogen concentration. The inverse relation between oxygen and nitrogen concentration, (figure 6.38) suggests oxygen-nitrogen association, possibly through dipole-dipole interaction of sulphoxides with the nitrile group and hydrogen bonding of oxidation structures with the nitrogen of the nitrile group. Nitrogen reduction is accompanied by a shift in its binding energy, (referenced to the binding energy of C_{1s} at 285.0eV), (compare table 6.9 with table 4.29).

D.S.C. oxidation scans show that hydroperoxide formation is exothermic. The onset temperature of hydroperoxide formation in polymers, (136°C in polymer E and 194°C in polymer P) gives a good early indication of oxidative stability in vulcanizates of compound A. Vulcanizates of compound A show an increase in the temperature of D.S.C. oxidation, (200°C for EA and 223°C for PA) a reduction in the hydroperoxide formation peak and an increase in the magnitude of the oxidation exotherm in comparison with polymers. The higher oxidative stability of vulcanizates may be

associated with the hydroperoxide decomposing antioxidative properties of sulphur compounds reviewed in section 2.3.3.2. The higher magnitude of the D.S.C. oxidation exotherm of vulcanizates in comparison with polymers is caused by crosslink modification reactions which are shown to occur in this temperature region, (section 4.3.3, figures 4.10 and 4.11). Addition of diphenyl amine causes a shift in the D.S.C. oxidation peak to higher temperatures, (235°C for EB and 246°C for PB) and the oxidation peak exotherm is generally reduced.

Diffusion coefficients values for samples EA and PA are in the range 7.5-9.5 $x10^{-8}$ cm^2/sec between 20°C and 100°C and are not significantly different for these two base polymers. Differences in oxidative stability between E and P are therefore not associated with differences in diffusion coefficient.

6.4. POLYMERISATION RESIDUES INTERACTIONS

It is shown throughout this work that compounds of different polymers exhibit differences in the rate of tensile property change and viscoelastic property change during oxidative ageing, greatest difference being shown by compounds of polymers E and P. In compound A polymer P exhibits significantly superior oxidative stability to polymer E, (contrast a change in elongation at break of -323 % in EA and -101 % in PA, after 14 days ageing at 100°C). In compound B polymer P exhibits similar oxidative stability to polymer E, (after 42 days at 100°C PB shows a decrease in elongation at break of -213 % while EB shows a decrease in elongation at break of -274 %).

Differences were also shown in vulcanization behaviour. In compounds of polymer E, optimum vulcanization time, (Tc 95 %) was 35 minutes for EA and 23 minutes for EB, while in compounds of polymer P Tc 95 % was 30 minutes for PA and 24 minutes for PB.

The major differences between polymers P and E are emulsion residues, notably the high calcium, chlorine and oxygen bonded sulphur species of polymer P, (table 4.3). In order to study the effect of these residues on vulcanization and oxidation of N.B.R. additional compounds were prepared by compounding in such residues.

6.4.1. VULCANIZATION BEHAVIOUR

Additional compounds of EA and EB were prepared by compounding-in calcium chloride hydrate, sodium dodecyl sulphate and sodium dodecane sulphonic acid, at concentrations similar to those found in polymer P. Sodium dodecyl sulphate and sodium dodecane sulphonic acid were added at equimolar addition levels. The effect of compounded-in calcium chloride hydrate, sodium dodecyl sulphate and sodium dodecane sulphonic acid on vulcanization time (Tc 95 % at 150°C) of EA and EB compounds is illustrated in figure 6.49.

Calcium chloride hydrate retards vulcanization and reduces torque modulus in EA and EB vulcanizates. Sodium dodecane sulphonic acid has essentially no effect in EA and EB compounds. Sodium dodecyl sulphate has little effect on the vulcanization of compound EA but retards vulcanization in compound EB. It was previously shown that acceleration of the vulcanization process by diphenyl amine antioxidant in compounds E is greater than in compounds P. Coincidentally polymer E contains little sulphate/sulphonate emulsifier residue while polymer P contains oxygen bonded sulphur residue, thought to originate from sulphate/sulphonate emulsifiers at 1585 ppm. This implies that oxygen bonded sulphur emulsifier residue of polymer P affects vulcanization similarly to compounded-in sodium dodecyl sulphate.

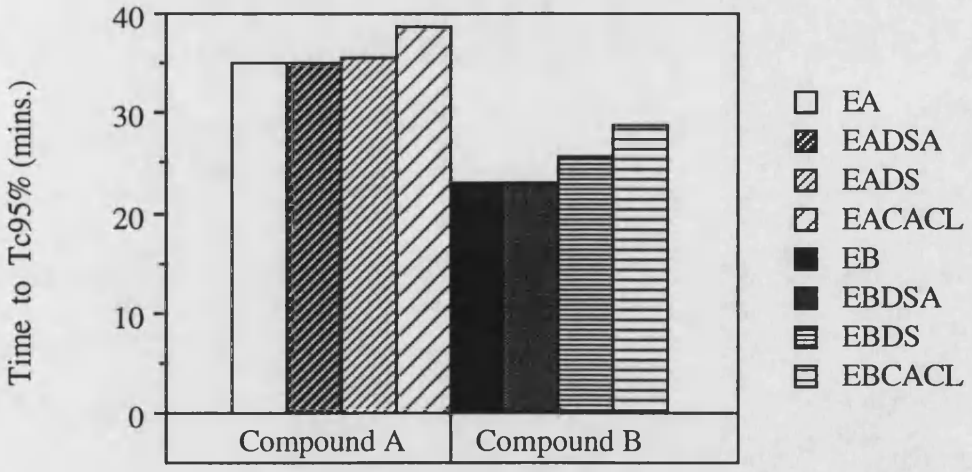

FIGURE 6.49. Effect of calcium chloride, (CACL), sodium dodecyl sulphate, (DS) and sodium dodecane sulphonic acid, (DSA) addition on vulcanization times of EA and EB compounds.

6.4.2. CHANGE IN TENSILE PROPERTIES ON AGEING

The effect of compounded-in calcium chloride hydrate, sodium dodecyl sulphate and sodium dodecane sulphonic acid on retention of elongation at break of EA and EB compounds is shown in figures 6.50 and 6.51, respectively.

In compound EA these additions have little effect on oxidative stability. Calcium chloride hydrate exhibits a mild antioxidative effect. In compound EB the antioxidative effect of calcium chloride hydrate is enhanced which implies synergism with diphenyl amine. The mechanism of calcium chloride action is further discussed in section 6.4.4. Sodium dodecane sulphonic acid has no significant effect on oxidative stability of EA and EB compounds while sodium dodecyl sulphate, which is added at the same molar concentration has a pro-oxidative effect in EB but no effect in EA. This implies antagonism between sodium dodecyl sulphate and diphenyl amine.

The interaction between compounded-in sodium dodecyl sulphate and diphenyl amine appears to be similar to the interaction between polymer P and diphenyl amine. Polymer P contains high levels of oxygen bonded sulphur which is presumed to be emulsifier residue. Further consideration to the mechanism of sodium dodecyl sulphate-diphenyl amine interaction is given in section 6.4.5.

6.1.3. STRESS RELAXATION

The effect of calcium chloride hydrate, sodium dodecyl sulphate and sodium dodecane sulphonic acid on stress relaxation of EA and EB vulcanizates is illustrated in figures 6.52-6.55. Addition of calcium chloride hydrate is seen to reduce crosslink formation in EA and EB, and reduce the rate of scission in EB. Sodium dodecane sulphonic acid has little effect on stress relaxation in EA and EB while sodium dodecyl sulphate is seen to increase the rate of crosslink formation and scission in EB but has little effect in EA.

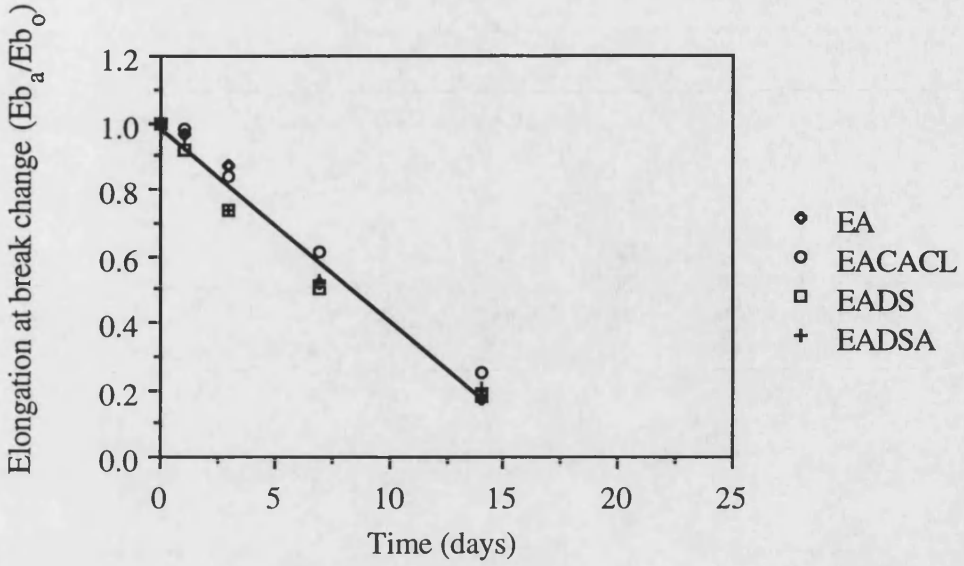

FIGURE 6.50. Change in elongation at break, (Eb) in vulcanizates of compounds EA during oxidative ageing at 100°C.

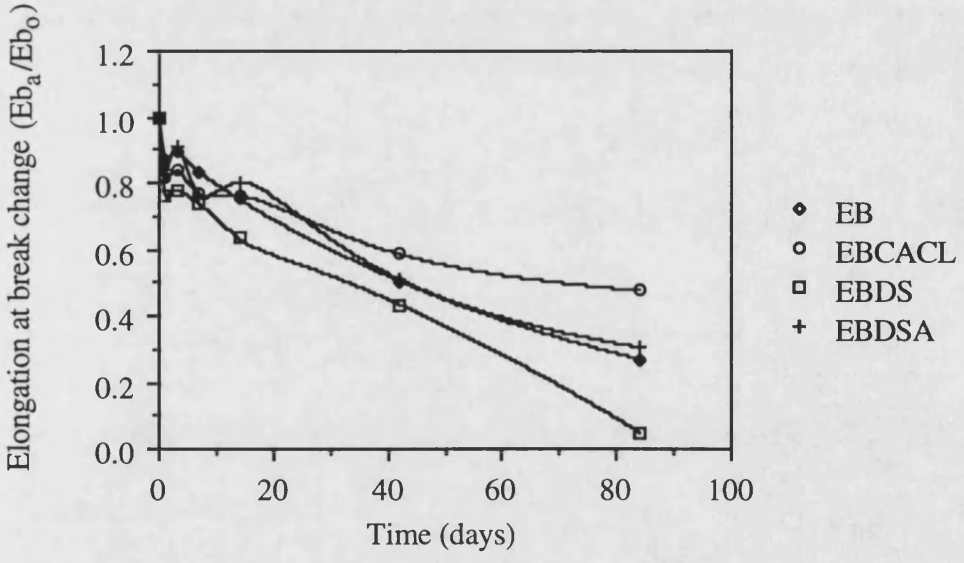

FIGURE 6.51. Change in elongation at break, (Eb) in vulcanizates of compounds EB during oxidative ageing at 100°C.

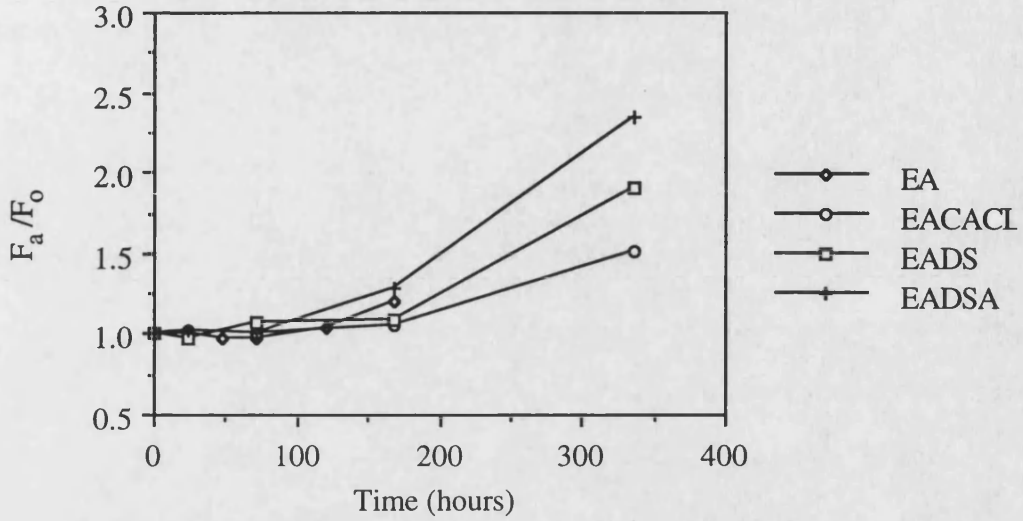

FIGURE 6.52. Intermittent stress relaxation in vulcanizates of compounds EA during heating in air at 100°C.

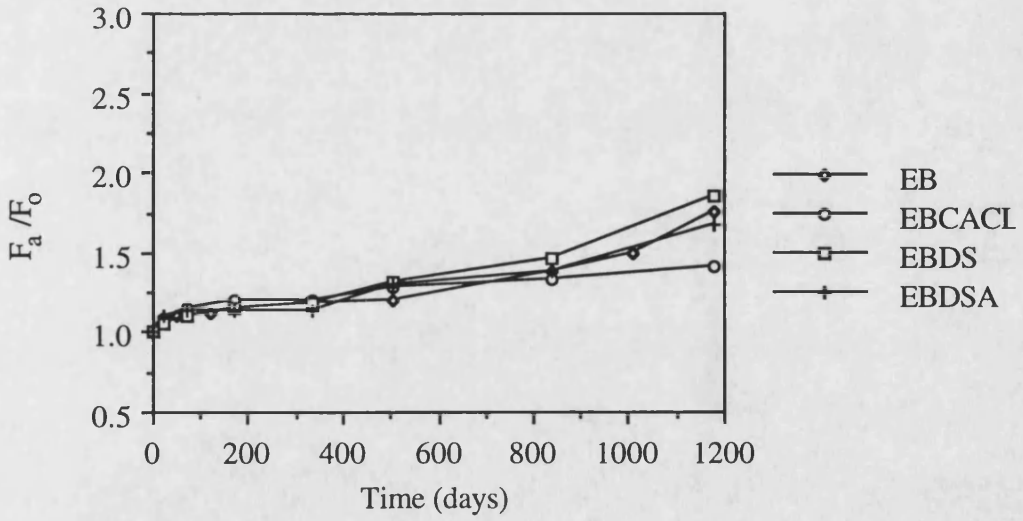

FIGURE 6.53. Intermittent stress relaxation in vulcanizates of compounds EB during heating in air at 100°C.

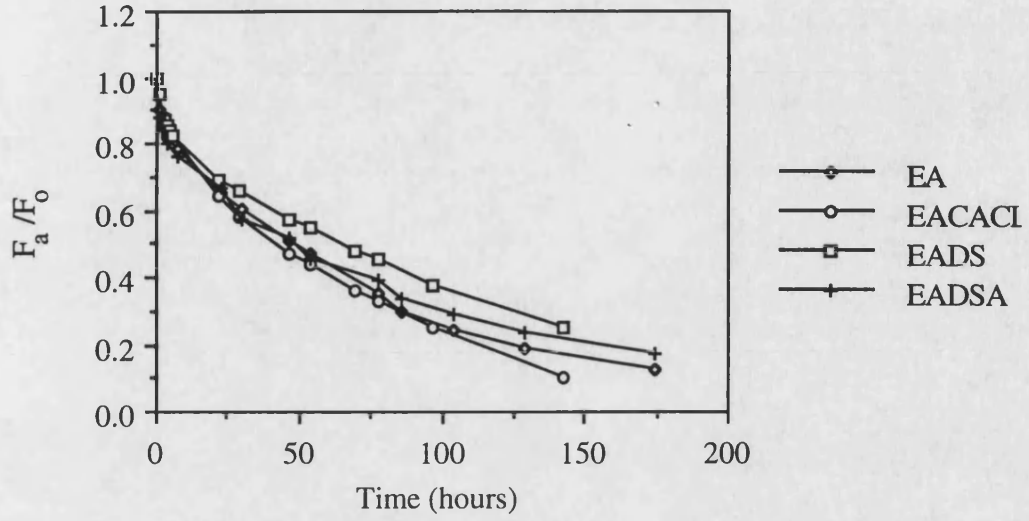

FIGURE 6.54. Continuous stress relaxation in vulcanizates of compounds EA during heating in air at 100°C.

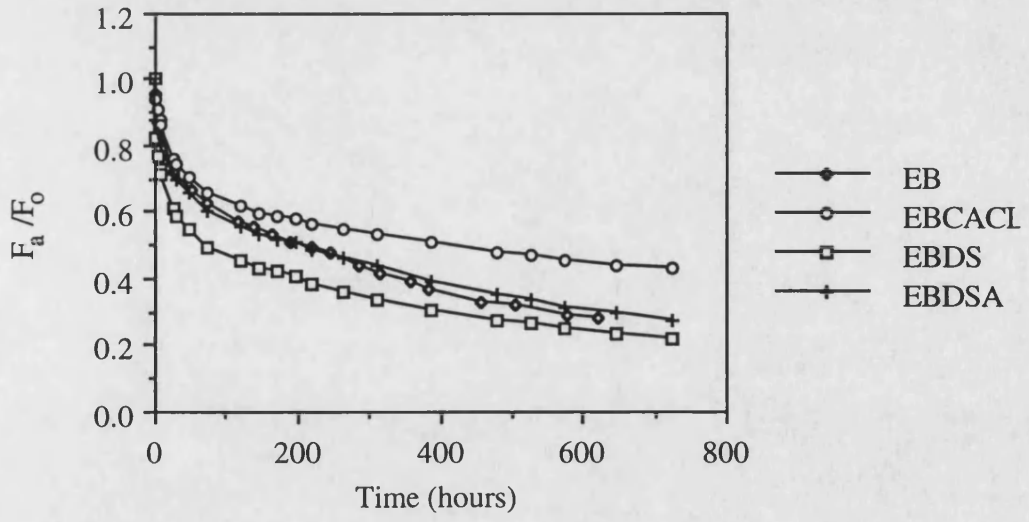

FIGURE 6.55. Continuous stress relaxation in vulcanizates of compounds EB during heating in air at 100°C.

6.4.4. MECHANISM OF CALCIUM CHLORIDE ANTIOXIDANT ACTION

In earlier sections 6.4.2-6.4.4 it was shown that calcium chloride hydrate has mild antioxidative properties when compounded into EA and strong antioxidative properties in compound EB. This suggests synergism between the antioxidative mechanisms of calcium chloride and diphenyl amine. Such synergism is usually displayed by antioxidants which act by a complementary mechanism. This would imply that calcium chloride hydrate acts by hydroperoxide stabilisation or decomposition.

In order to assess the mechanism of calcium chloride reaction additional experiments were made. A free radical mechanism was discounted following observations that calcium chloride hydrate has no effect on free radical peroxide vulcanization of N.B.R.. This is shown in figure 6.56.

Interaction between calcium chloride hydrate and hydroperoxides was measured by adding calcium chloride into compound EA which was compounded with pre-oxidised base polymer. The base polymer was oxidised in sheet form in an ageing oven at 100°C, for 24 hours to the point of extensive hydroperoxide formation. Addition of calcium chloride hydrate in increasing amounts to compounds based on pre-oxidised polymer resulted in an increase in torque modulus during vulcanization, (figure 6.57). Such increase was not observed in compounds based on unoxidised polymer. The increase in torque modulus in in pre-oxidised polymer in the presence of calcium chloride hydrate suggests interaction of calcium chloride with in excess of one hydroperoxide, leading to crosslink formation.

Evidence for interaction between calcium chloride hydrate and hydroperoxide is shown in F.T.I.R./A.T.R. spectra of figures 6.58 and 6.59. These spectra show that addition of calcium chloride hydrate causes an increase in hydrogen bonded OH functional groups in vulcanizates which are based on pre-oxidised polymer and no increase in vulcanizates which are based on unaged polymer. This is further confirmation of the view that calcium chloride hydrate acts as an antioxidant through interaction with hydroperoxide.

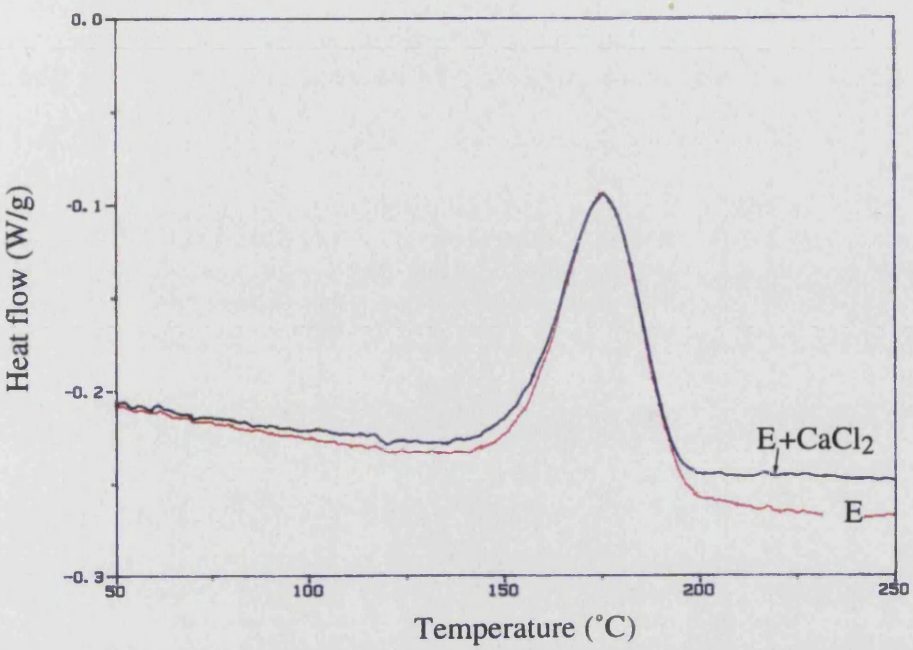

FIGURE 6.56. Effect of calcium chloride hydrate addition on free radical dicumyl peroxide vulcanization of N.B.R..

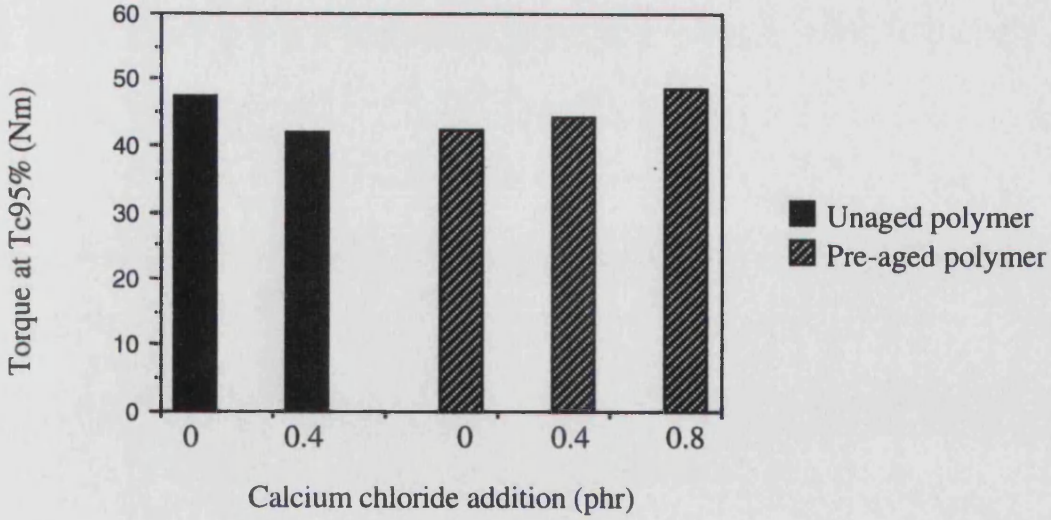

FIGURE 6.57. Effect of calcium chloride hydrate addition on torque maximum in EA compounds, based on unaged and pre-oxidised base polymer.

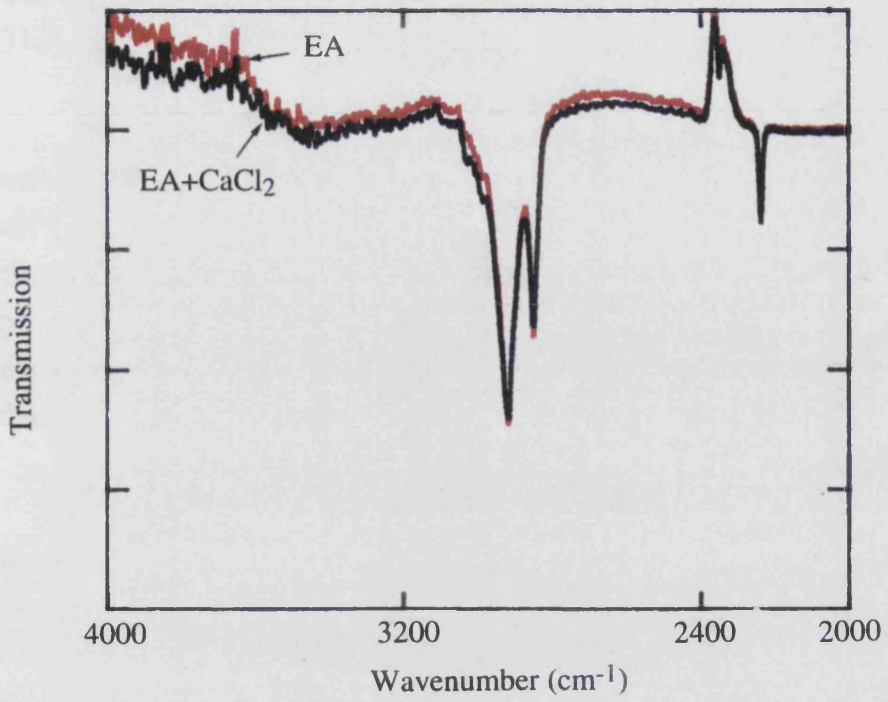

FIGURE 6.58. Effect of the addition of calcium chloride hydrate, (at 0.4 phr) on I.R. absorbance of EA vulcanizate compounded with unaged base polymer.

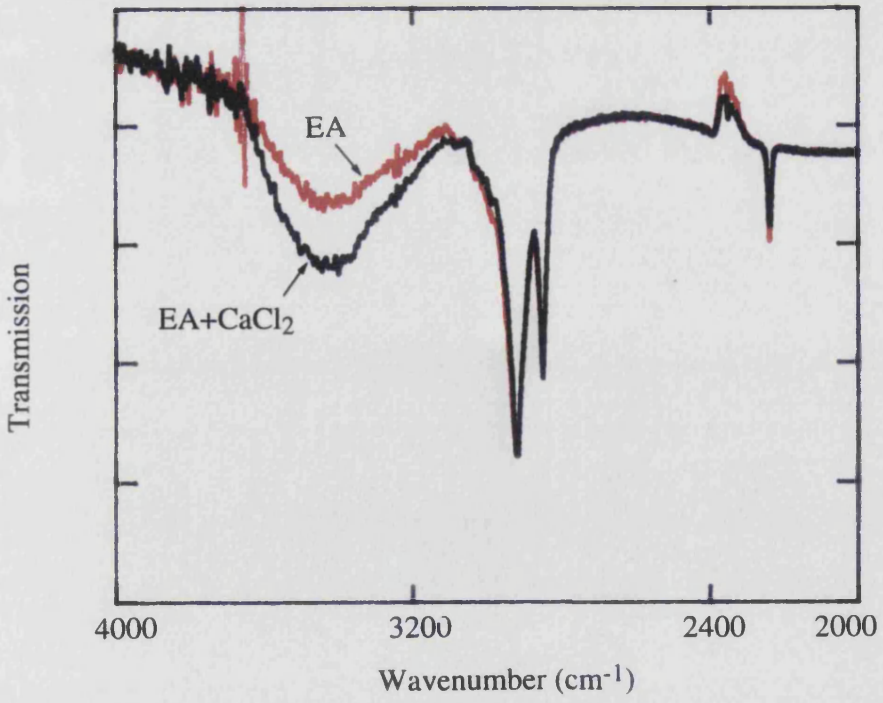

FIGURE 6.59. Effect of the addition of calcium chloride hydrate, (at 0.4 phr) on I.R. absorbance of EA vulcanizate compounded with pre-oxidised base polymer.

6.4.5. MECHANISM OF SODIUM DODECYL SULPHATE-DIPHENYL AMINE INTERACTION

The interaction between sodium dodecyl sulphate and diphenyl amine was examined in great detail by Meridith (1995) as part of a final year project. This work could find no evidence of direct reaction of sodium dodecyl sulphate and sodium dodecane sulphonic acid with diphenyl amine by controlled heating rate D.S.C. experiments, however in the presence of diphenyl amine the melting point of sodium dodecyl sulphate was shifted to higher temperatures. This implied association between sodium dodecyl sulphate and diphenyl amine.

Further information on the mechanism of interaction was obtained by heating individual components and mixtures to temperatures in the region of dehydration of hydrated water and measuring weight loss. This was followed by allowing dehydrated chemicals to stand in a humid atmosphere and measuring weight gain. The results from this study, which are tabulated in tables 6.12 and 6.13 show that in equal weight mixtures of sodium dodecyl sulphate and diphenyl amine weight loss is higher upon heating and weight gain is lower upon standing, than would be expected from individual components. This is not the case for mixtures of sodium dodecane sulphonic acid. This implies that there is association between sodium dodecyl sulphate and diphenyl amine. Interaction between the sodium cation and the lone electron pair of the nitrogen or hydrogen bonding between the tertiary hydrogen of the amine and the sulphate would explain the reduced ability of diphenyl amine to accelerate vulcanization and protect from oxidation. The complexed amine would not associate with the zinc ion of the active suphurating agent and would also presumably be unable to initiate heterolytic splitting of S_8 and poly-sulphides. Deactivation of the antioxidative properties of diphenyl amine could arise through a reduction in the lability of the tertiary hydrogen of the amine through steric hindrance.

Compound	Weight loss, % at 200°C	Weight gain, % at room temperature
NaDS	2.20	0.78
Diphenyl amine	6.90	1.35
1:1 weight mixture of diphenyl amine and NaDS	6.18 (expected 4.55)	0.59 (expected 1.06)

TABLE 6.12. Weight loss of compounds during heating under nitrogen for 30 minutes and weight gain during standing for 2 hours at room temperature, 80 % relative humidity.

Compound	Weight loss, % at 235°C	Weight gain, % at room temperature
NaDSA	2.08	0.22
Diphenyl amine	20.66	1.77
1:1 weight mixture of diphenyl amine and NaDSA	9.04 (expected 11.37)	1.30 (expected 1.00)

TABLE 6.13. Weight loss of compounds during heating under nitrogen for 30 minutes and weight gain during standing for 2 hours at room temperature, 80 % relative humidity.

6.4.6. SUMMARY ON THE EFFECTS OF COAGULANT AND EMULSIFIER CHEMICALS ON OXIDATION

It is demonstrated that calcium chloride hydrate acts as an antioxidant in EA and EB compounds. It is likely that other divalent metal coagulants will act in a similar way. Recent work of Gan and Ting (1993) reported that magnesium chloride forms an ionic association with aldehyde and carboxylate groups during storage hardening of N.R.. Calcium chloride and magnesium chloride are present in polymers as coagulant residues, (table 4.3). It is argued that stabilisation occurs through hydroperoxide interaction. This proposed mechanism is consistent with the increase in torque modulus and hydrogen bonded absorption of pre-oxidised compounds after addition of calcium chloride hydrate.

Sodium dodecyl sulphate and sodium dodecane sulphonic acid emulsifiers, (present in polymers at significant concentrations) have no significant effect on vulcanization behaviour and oxidation of EA compound. In compound EB sodium dodecyl sulphate retards vulcanization and reduces oxidative stability. Both effects are thought to be caused by sodium dodecyl sulphate-diphenyl amine interaction. This postulate is consistent with the observed increase in melting point of sodium dodecyl sulphate in the presence of diphenyl amine and the reduced uptake of water of dehydrated sodium dodecyl sulphate in the presence of diphenyl amine.

The interaction between sodium dodecane sulphonic acid and diphenyl amine is less because the sulphur in the sulphonic group is bonded to carbon, whereas the sulphate group is bonded to oxygen. Because of differences in charge distribution the sulphonate group is more stable with the sodium being more tightly bound and therefore less reactive.

6.5. CONCLUDING REMARKS ON THERMO-OXIDATIVE AGEING

The ageing process of N.B.R. is of great practical importance because of its effect on mechanical properties. Results of chapter six showing large differences in thermo-oxidative stability between polymers have important implications for service performance and ageing life of N.B.R..

The most significant differences in thermo-oxidative stability between polymers, obtained from different manufacturers occur in the absence of compounded-in antioxidant, (compound A). Of practical significance are studies showing that early indication of ageing performance in such systems can be obtained by measuring the onset temperature of hydroperoxide formation in raw polymers and vulcanizates and hydroperoxide concentration in vulcanizates. The gel content of raw polymers is an indication of storage ageing and has some bearing on thermo-oxidative stability of vulcanizates. Differences in thermo-oxidative stability between polymers are associated mainly with the type of residue antioxidant, its concentration and the extent of storage ageing of the raw polymer. Coagulant residues such as calcium chloride hydrate exhibit mild antioxidative properties. Vulcanizates exhibit improved thermo-oxidative stability to polymers due to the antioxidative properties of sulphur species.

Addition of diphenyl amine antioxidant, (compound B) to N.B.R. improves thermo-oxidative stability, however diphenyl amine is appreciably deactivated by polymerisation residues of sodium dodecyl sulphate. Such residues are present in some

polymers. The antioxidative properties of calcium chloride hydrate are enhanced in compound B due to synergism with diphenyl amine.

The mechanism of vulcanizate oxidation at 100°C is simultaneous crosslink scission and crosslink formation, with water being given off as an oxidation product. During oxidation crosslink formation is the dominant process. Cleaved crosslinks are predominantly mono-sulphide. In networks containing diphenyl amine and those treated with piperidine the concentration of poly-sulphide and di-sulphide crosslinks is reduced rapidly during heating at 100°C. In compounds without diphenyl amine antioxidant poly-sulphide and di-sulphide crosslinks remain during oxidative ageing at 100°C. Crosslinks which form during ageing are C-C, although at extended ageing times di-sulphide crosslinks reform due to interaction of oxidation structures such as pendant thiols. Oxidation structures, such as peroxide, ketone, hydroperoxide, alcohol, sulphoxide, sulphenic acid and thiosulphoxylic acid may be associated with the nitrogen of the nitrile group through dipole-dipole interactions and hydrogen bonding.

CHAPTER VII

7.0. GENERAL DISCUSSION

N.B.R. polymer is shown to contain residues of the emulsion polymerisation process. These polymerisation residues were found to differ between commercial N.B.R. grades of equivalent specification, obtained from different manufacturers. Differences in elemental residue composition were seen to affect the glass transition, rheological behaviour, vulcanization and oxidation. Differences in molecular weight and molecular weight distribution could be associated with differences in rheological behaviour, overall crosslink density and mechanical properties.

The following chapter is a general discussion of these points, however for more detailed discussion of individual subjects the reader is referred to specific discussions of results in chapters four and six.

7.1. THE NATURE OF N.B.R. BASE POLYMER

Five polymers were selected being representative of commercial N.B.R. of 28 weight % combined ACN content and Mooney viscosity c. 45 Mooney units, (table 3.1). They shared many features in common, being random co-polymers of ACN and butadiene with a high degree of monomer alternation, in most instances, (table 4.11). The butadiene monomer is enchained in trans-1,4-addition, cis-1,4-addition and vinyl-1,2-addition in the approximate ratio 75:15:10, (table 4.11). Despite the identical specification of the polymer samples used, (table 3.1) a number of differences in molecular structure were found, such as differences in molecular weight, molecular weight distribution and gel content, (tables 4.7-4.9). Average molecular weight is in the range 2.55-6.18 $x10^5$ $g.mole^{-1}$, molecular weight distribution, ($\bar{M}_W/\bar{M}_n$) is in the range 3.72-8.89 and gel content is in the range 0-8.8 %. In polymer E it was found that low molecular weight polymer contains a higher concentration of nitrogen than the bulk, considered to be caused by preferential polymerisation of ACN during early stages of polymerisation, (tables 4.1 and 4.4). This low molecular weight high ACN content polymer is distributed on polymer and vulcanizate surfaces, due to migration.

All samples contain trace elemental residues at significant concentrations, (table 4.3). Elemental residues are sodium, calcium, magnesium, chlorine, sulphur and iron. Sodium, calcium, magnesium and chlorine are coagulant residues such as sodium

chloride, calcium chloride and magnesium chloride. A fraction of the sulphur residues in some polymers is bonded to carbon, hydrogen or sulphur. These residues are thought to be alkyl mercaptan transfer agents and elemental sulphur in polymer N. Oxygen bonded sulphur residue which is present in all polymers is associated with sulphate/sulphonate emulsifiers. All polymers also contain a range of carboxylic acid emulsifier residues of several different molecular weights, (tables 4.5 and 4.6). In the polymer a proportion of these residues may be in the form of carboxylic acid salts. Iron which is present at concentration below 30 ppm may be associated with initiator residue and contamination from polymerisation equipment. All polymers are stabilised during latter stages of polymerisation by addition of non staining antioxidants, (section 4.1.3). Such antioxidants are mostly substituted phenols such as, 2,6-di-tertiary butyl-p-cresol, 2,2-methylene bis-(4-methyl-6-tertiary butyl phenol) and octadecyl-3-(3',5'-di-tertiary butyl-4'-hydroxyphenyl) propionate. Polymer E also contained di-naphthyl sulphone while polymer N contained the dioctyl ester of hexanedioic acid and rosin soap.

7.2. EFFECT OF BASE POLYMER ON PROPERTIES

7.2.1. THE GLASS TRANSITION

The D.S.C. glass transition temperature of N.B.R. polymers measured by heating at 5°C/minute is in the range -32°C to -35°C and does not appear to be affected by identified differences in molecular weight, molecular weight distribution, gel content and elemental residue composition, (table 4.12). The average width of glass transition is 7.6°C for polymer E, 18-19.5°C for polymers B, N and P and 36.0°C for polymer G, (table 4.13). The wide transition of polymer G may be associated with the high concentration of methanol extractable residue, (5.4 %) of polymer G while the narrow transition of polymer E may have its origin in the low average molecular weight and low molecular weight distribution. Polymer G also exhibits a lower apparent activation of energy of structural activation, obtained from Arrhenius plots of the glass transition dependence on heating rate, (table 4.14). In vulcanizates, D.S.C. glass transition temperature is in the region -27.7 to -30.3°C, (table 4.32). The width of transition is 7.0°C for vulcanizates of polymer E, 10°C to 16.8°C for vulcanizates of polymers B, N and P and 18°C to 19.5°C for vulcanizates of polymer G. The increase in glass transition and reduction in width of transition after vulcanization is associated with the restriction in molecular mobility caused by crosslinking. Reduction in the width of transition of polymer G may be higher because this polymer contains significant concentration of unsaturated carboxylic

acid, (oleic acid) which becomes combined into the network during vulcanization, (section 4.3). Glass transition temperature in vulcanizates, obtained from viscoelastic peak maxima is in the range of -13.4°C to -17.7°C, (table 4.33). Of practical interest are results showing that the width of the viscoelastic loss peak at its base and the width of D.S.C. glass transition in polymers are related.

7.2.2. POLYMER VISCOSITY

Polymer Mooney viscosity, ML 1+4 at 100°C is c. 45 Mooney units for polymers E, G, N and P, and 50 Mooney units for polymer B, (table 4.15). The higher Mooney viscosity of polymer B is associated with the higher molecular weight of polymer B. Viscosity at 120°C is also high for polymer B, at shear rates below 3.0 s^{-1}. At higher shear rates, where viscosity is affected less by molecular weight, polymer P exhibits higher viscosity, (figure 4.8). These difference are associated with differences in emulsifier residue composition between polymer B and P. Polymer G exhibits low viscosity at 120°C, within the range 1-3000 s^{-1}. It is argued that this is caused by the plasticising action of methanol extractable carboxylic acid emulsifier residues of polymer G.

7.2.3. VULCANIZATION AND NETWORK STRUCTURE OF COMPOUND A

Vulcanization is an exothermic process, (sections 4.3.2 and 4.3.3). The magnitude of the vulcanization exotherm during heating at 150°C is in the range 9.8-10.7 J/g for compounds BA, EA, NA and PA, and 7.9 for compound GA, (table 4.17). During scanning conditions, where samples were heated at 10°C/minute the cure exotherm is 18.7-20.6J/g for BA, EA, NA and PA, and 14.8 J/g for GA, (table 4.18). The higher cure exotherm under scanning conditions is caused by contribution to the measured exotherm by crosslink maturation and degradation reactions. This low cure exotherm of compound GA is reflected in a low torque modulus, (35 Nm) compared to a torque modulus of approximately 50 Nm for other polymers. The low torque modulus of GA is consistent with its low network chain density, (1.48×10^{-4} mol.cm^{-3}). Low torque modulus of GA is associated with its unsaturated carboxylic acid, (oleic acid) residue, a similar reduction in torque modulus being obtained in compound NA by compounding-in 1 phr of oleic acid.

Crosslink density is strongly influenced by molecular weight, due to its effect on the ratio of elastically active network chains to chain ends. High molecular weight

of polymer B, (6.18×10^5 g.mol^{-1}) is associated with high network chain density, (in BA, $N_v = 2.10 \times 10^{-4}$ mol.cm^{-3}). The low molecular weight of polymer E, (2.55×10^5 g.mol^{-1}) is associated with low network chain density, (in EA, $N_v = 1.61 \times 10^{-4}$ mol.cm^{-3}).

Crosslinked networks contain a distribution of crosslink structures, (table 4.26, figure 4.17). The poly-sulphide crosslink concentration is 44-54 %, the mono-sulphide crosslink content 14.6-21 % and the remainder di-sulphide. Direct crosslinks between carbon atoms are not introduced during vulcanization. During chemical probing of swollen networks it was found that significant weight loss occurred, (29.5 % with GA in table 4.20). This extracted material was N.B.R. polymer of average molecular weight below M_c. The result that polymer chains are extracted from networks during swelling has important practical implications for measurement of network chain density by techniques involving swelling. In determination of crosslink density material which is lost during swelling is usually not included in the calculation since it is assumed that such material is extra-network material. Calculation of network chain density of hexane-1-thiol (1M) in piperidine treated GA sample when omitting the volume element which is lost during swelling gives a value of 0.44×10^{-4} mol.cm^{-3} while correcting for the lost volume element gives a value of 0.31×10^{-4} mol.cm^{-3}. Values of M_c obtained from weight loss and molecular weight distribution curves give somewhat lower values than those which are obtained from compression deflection measurement, (tables 4.27 and 4.24, respectively). For GA the value of network chain density obtained from weight loss is 0.14×10^{-4} mol.cm^{-3}. A lower value of network chain density is obtained from weight loss data because unlike compression deflection measurements weight loss data do not include physical contributions.

7.2.4. VULCANIZATION AND NETWORK STRUCTURE OF COMPOUND B

Compounded-in diphenyl amine antioxidant, (compound B) accelerates vulcanization for all samples, (tables 4.16-4.18). The extent of acceleration is high in E, (34 % reduction in Tc 95 vulcanization time) and low in P, (20 % reduction in Tc 95 vulcanization time). Deactivation of diphenyl amine in polymer P is caused by sulphate emulsifier residues. The effect was reproduced by compounding in similar levels of sodium dodecyl sulphate in polymer E. The exothermic heat change of vulcanization of compound B is similar to compound A and affected by base polymer as in compound A. Addition of diphenyl amine causes an increase in the proportion of mono-sulphide crosslinks but overall network density is little affected, (tables 4.26

and 4.19, respectively).

Experimental evidence suggests that the effects of diphenyl amine are caused by catalysis of S_8 splitting and an increase in the zinc:sulphur ratio in the zinc-accelerator-thiolate complex, (figures 4.13 and 4.14, table 4.28). Elemental surface analysis also shows interesting differences in the concentration of sulphur and zinc species between vulcanizates of polymer E and P. The concentration of sulphur, (expressed as a ratio to carbon) whose binding energy is consistent with it being in the form of a zinc-accelerator complex, (table 4.29) is 6.8 $x10^{-3}$ and 40.7 $x10^{-3}$ on the surfaces of PA and EA vulcanizates, respectively and 2.9 $x10^{-3}$ and 16.3 $x10^{-3}$ on the surfaces of PB and EB vulcanizates, respectively. This implies differences in mobility of the zinc-accelerator-thiolate complex between polymers. These elemental surface analysis results were supported by ^{13}C N.M.R. studies were it was found that vulcanizates of polymer P contain an additional ^{13}C N.M.R. active sulphurated methylene structure, at 46 ppm thought to be associated with pendant sulphur-accelerator fragment, (figures 4.20 and 4.21).

7.2.5. MECHANICAL PROPERTIES

Tensile strength and tear strength of BA, EA, NA and PA are in the range 2.14-2.42 MPa and 1.52-1.79 kN/m, respectively while tensile strength and tear strength of GA is 2.92 MPa and 2.42 kN/m, (table 4.30). The higher tensile strength and tear strength of GA may be associated with the reduction in tensile strength and tear strength of vulcanizates beyond an optimum value of crosslink density. BA compound shows higher modulus and lower elongation at break than other compounds due the high crosslink density of polymer B. The viscoelastic loss angle peak tan δ is strongly affected by base polymer, (table 4.33). For compound EA, tan δ = 1.84 while for compound GA tan δ =1.38. The differences in viscoelastic properties at the glass transition are reflected in differences in D.S.C. glass transition behaviour of raw polymers. In polymer E, D.S.C. glass transition occurs over a narrow temperature range, (width of transition 7.6°C, change in specific heat capacity 0.66 J/g), while in polymer G transition occurs over a wide temperature range, (width of transition 36.0°C, change in specific heat capacity 0.98 J/g).

Tensile strength and tear strength properties of vulcanizates of compound B, are higher than for vulcanizates of compound A, (compare table 4.31 with 4.30). The higher strength properties of vulcanizates of compound B are likely to be associated with reported differences in crosslink distribution. Viscoelastic loss properties of

vulcanizates of compound A and compound B are not significantly different.

7.2.6. OXIDATION OF COMPOUND A

Oxidation of N.B.R. is accompanied by an increase in modulus, tensile strength, density and weight, and a reduction in elongation at break, (section 6.1). In terms of dynamic properties, ageing is accompanied by an increase in storage modulus and a reduction in loss modulus. The viscoelastic loss angle peak tan δ is reduced and its position is shifted to higher temperatures. The rate of property change is strongly affected by polymer. Lowest rate of property change is exhibited by polymer P while greatest rate of property change is exhibited by polymer E. Ageing is accompanied by simultaneous scission and crosslink formation, scission and crosslink formation being highest in EA and lowest in PA, (figures 6.18 and 6.21). The differences in oxidative stability between E and P are not associated with physical effects, since the diffusion coefficients of EA and PA are not significantly different, (figure 6.48). Diffusion coefficient increases from 7.5 to 9.0 $x10^{-8}$ $cm^2/sec.$ from 20°C to 100°C. Hydroperoxide formation measured by D.S.C. gives a good indication of relative rate of property change in compound A during ageing, (table 6.10). The temperature of hydroperoxide formation in polymers E and P is 136°C and 194°C, respectively. In compounds EA and PA the onset of the D.S.C. oxidation exotherm is shifted to 200°C and 223°C, respectively, (table 6.11). The improved stability of vulcanizates is associated with the antioxidative properties of sulphur compounds. Hydroperoxide concentration in unaged vulcanizates of compound A is high, due to hydroperoxide formation during mixing, (figure 6.37). Differences in stability between polymers E and P are associated with differences in antioxidant residues of section 4.1.3. Polymer P contains mostly 2,2-methylene bis-(4-methyl-6-tertiary butyl phenol). Polymer E contains the less efficient and more volatile 2,6-di-tertiary butyl-p-cresol as the main antioxidant type. Differences in gel content between polymers E and P, (8.8 % and 0 %, respectively) suggest differences in storage ageing of the base polymers. Extraction of EA and PA with piperidine reduces their oxidative stability and both samples exhibit similar stability. A contribution to the good oxidative stability exhibited by polymer P is its high concentration of calcium chloride hydrate coagulant residue. Calcium chloride hydrate was demonstrated to have mild antioxidative properties when compounded into compounds at 0.4 phr, (section 6.4).

Apparent activation energies of ageing measured from fitting tensile property change data and viscoelastic property change data to the Arrhenius model are not affected by polymer, (tables 6.4-6.6). Values are in the range 80-100 kJ/mole, with

the exception of a few values which are thought not to be significant because of high scatter in individual tensile property measurements. Arrhenius plots of ageing data however show high correlation coefficients. Differences in oxidative stability between EA and PA are caused by piperidine extractable antioxidant residues, (section 6.2.3).

7.2.7. OXIDATION OF COMPOUND B

In vulcanizates of compound B mechanical properties are affected in the same manner by ageing as in vulcanizates of compound A, (section 6.1). The rate of property change of vulcanizates of compound B during thermo-oxidative ageing is however less than in vulcanizates of compound A, beyond the first few days of heating. In the first few days of heating property change, (scission and crosslink formation) is greater in vulcanizates of compound B, (figures 6.19 and 6.22). The onset temperature of the D.S.C. oxidation exotherm is higher in vulcanizates of compound B than vulcanizates of compound A and the magnitude of the oxidation exotherm is lower, (table 6.11). In vulcanizates of compound B differences in the rate of property change between polymers are low. Best oxidative stability is displayed by GB and worst oxidative stability by EB. The relatively poor oxidative stability of PB is thought to be associated with deactivation of diphenyl amine antioxidant by sulphate emulsifier residues of polymer P, (section 6.4). Deactivation of diphenyl amine by compounding-in of sodium dodecyl sulphate at concentrations similar to those present in polymer P was demonstrated.

7.3. OXIDATION MECHANISM

Oxidation of N.B.R. networks at 100°C is accompanied by simultaneous scission and crosslink formation with the latter process being dominant, (section 6.2.1). Hydroperoxide formation in vulcanizates of compound A is rapid and is at its maximum following vulcanization, (figure 6.37). This implies hydroperoxide formation during mixing. In compound B hydroperoxide formation is delayed due to the antioxidative action of diphenyl amine. The rate of property change in properties such as modulus, tensile strength and weight change is characterised by an induction time. Induction time is longer for vulcanizates of compound B than vulcanizates of compound A. Crosslink formation is less rapid in compound B, while crosslink scission, (with the exception of polymer E) is similar to compound A. Within the first few days of ageing at 100°C there are some unexpected differences in ageing between compounds A and B. Ketone and peroxide formation is more rapid in compound B

than compound A, (figures 6.35 and 6.36). This more rapid ketone and peroxide formation is reflected in greater weight loss, more rapid rate of continuous stress relaxation, more rapid reduction in elongation at break and more rapid increase in modulus. Ketone and peroxide formation in compound B precedes the hydroperoxide peak. Formation of ketone and peroxide in compound B before appreciable hydroperoxide formation, is consistent with persulphenyl radical initiated oxidation. Persulphenyl radicals can form during decomposition of poly-sulphide crosslinks. Network density measurements on aged samples show that diphenyl amine catalyses crosslink desulphurisation and decomposition, (figures 6.25 and 6.26).

Crosslinks which form during oxidation at 100°C are directly between carbon atoms, (figure 6.27). At 100°C such crosslink formation is very rapid such that after a few days heating the highest proportion of crosslinks in vulcanizates are C-C. At extended ageing times di-sulphide crosslinks reform due to further oxidation of sulphide oxidation structures.

Scission occurs through scission of sulphide crosslinks, (predominantly mono-sulphide). In compound A di-sulphide crosslinks and poly-sulphide crosslinks remain during ageing at 100°C, (figures 6.23 and 6.24) while in compound B di-sulphide and poly-sulphide crosslinks are rapidly converted to mono-sulphide. A similar effect was reported within four hours ageing of piperidine treated vulcanizates. Both amines catalyse desulphurisation, (figures 6.32 and 6.33).

Calcium chloride hydrate was demonstrated to have antioxidative properties in compound EA, (section 6.4). Calcium chloride hydrate acts as an antioxidant by interaction with hydroperoxides and their stabilisation. The antioxidative properties of calcium chloride hydrate in the presence of diphenyl amine are strong due to synergism.

CHAPTER VIII

8.0. CONCLUSIONS

Five different N.B.R. polymers of c. 28 weight % combined ACN content and Mooney viscosity c. 45 Mooney units were studied and found to differ in polymerisation residues and in molecular constitution. Some of these differences exerted a significant effect on particular properties.

Glass transition temperature of the five polymers was within a narrow range of -32.0 to -34.0°C, while the width of glass transition , (7.6°C for polymer E, 36.0°C for polymer G and 18.0 to 19.5°C for polymers B, N and P) was significantly different. The temperature at viscoelastic loss peak maximum of vulcanizates was found to be in the range -13.4 to -17.7°C. The viscoelastic loss peak maximum was 1.84 and 1.94 for vulcanizates of polymer E, 1.38 for vulcanizates of polymer G and 1.48-1.78 for vulcanizates of polymers B, N and P.

The narrow width of transition of polymer E may partly be associated with the low molecular weight, low molecular weight distribution and high gel content of polymer E. Crosslinks introduced during vulcanization reduce the width of glass transition. The greater width of glass transition of polymer G may be associated with its higher concentration of methanol extractable residue, (5.4 weight %), a high proportion of which is carboxylic acid.

When vulcanized under similar conditions, differences in overall crosslink density were found. Vulcanizates of polymers N and B showed the highest crosslink density. This was a result of the elemental sulphur residue present in polymer N and the high molecular weight of polymer B. In contrast the crosslink density of vulcanizates of polymer G was lowest. This was associated with the presence of the unsaturated emulsifier oleic acid as a residue. Oleic acid reduces physical crosslink density by reacting preferentially with the active sulphurating agent. Vulcanizates of polymer E also showed low crosslink density. This was associated with the low molecular weight of polymer E.

Vulcanizates of compound A contain a distribution of crosslink structures. Inclusion of diphenyl amine antioxidant (compound B) results in acceleration of the vulcanization process and an increase in the proportion of mono-sulphide crosslinks. This could be understood in terms of amine catalysis of sulphur exchange in crosslinks and the active sulphurating agent. The extent of these effects varied with base polymer.

Thus in compounds of polymer E addition of diphenyl amine antioxidant caused a reduction in vulcanization time of 34 % while in compounds of polymer P addition of diphenyl amine caused a reduction in vulcanization time of 20 %. Retardation of the accelerating effect of diphenyl amine could be achieved by compounding-in sodium dodecyl sulphate at concentrations similar to those found as residue in polymer P.

During treatment of networks involving swelling uncombined polymer of average molecular weight in the vicinity of average molecular weight between crosslinks is extracted. In measurement of crosslink density by compression-deflection measurement this extracted volume element should therefore be included in sample volume. Measurement of the weight of extracted polymer and integrating of molecular weight distribution curves was found to be a suitable method for determination of chemical crosslink density.

The principal features of N.B.R. oxidation are loss of elongation at break, increase in modulus, increase in tensile strength, increase in density, reduction in viscoelastic loss peak maximum and a shift in glass transition to higher temperatures. At ageing temperatures of 70°C-130°C, loss of elongation at break and increase in modulus is rapid in the first day of heating and is followed by an induction period. These changes are accompanied by increase in ketone and peroxy oxidation structures. Diphenyl amine antioxidant reduced the rate of property change beyond the first few days of heating.

In vulcanizates of compound A oxidative ageing at 100°C causes an increase in total crosslink density. The concentration of poly-sulphide crosslinks remains unchanged, the concentration of di-sulphide crosslinks is reduced and mono-sulphide crosslinks are eliminated. Newly formed crosslinks are thought to be directly between carbon atoms. Such crosslinks may form through free radical and persulphenyl radical initiated degradation.

Addition of diphenyl amine catalyses crosslink desulphurisation and decomposition during early stages of ageing at 100°C. Crosslinks which form during ageing are mainly C-C, however at extended ageing times di-sulphides form through oxidation of sulphide oxidation structures.

Many differences in oxidation behaviour between polymers were observed. In raw polymers onset temperature of hydroperoxide formation, (measured by D.S.C. during controlled heating rate experiments) was 136°C for polymer E, 194°C for polymer P and 156-160°C for polymers B, G and N. This temperature of

hydroperoxide formation gives an indication of the relative stability of A compounds. For example, after 14 days ageing at 100°C, the change in elongation at break and stress at 100 % elongation of PA was -101 % and +0.18 MPa, respectively while the change in elongation at break and stress at 100 % elongation of EA was -323 % and +0.84 MPa, respectively.

This difference in oxidative stability between EA and PA was principally associated with differences in antioxidant residues. Evaluation of the oxidative stability of EA and PA after extraction with piperidine, and also treatment with hexane-1-thiol (1M) in piperidine showed reductions in oxidative stability and equivalent oxidative stability.

Some of the individual differences in stability were results of differences in coagulant and emulsifier residues. Compound PA which showed good stability had high calcium and chloride residues, presumed to originate in calcium chloride coagulant and high oxygen bonded sulphur species, presumed to originate in sulphate/sulphonate emulsifier residues.

An antioxidant effect of calcium chloride was demonstrated, by compounding-in such species. Stabilisation by calcium chloride appears to be through hydroperoxide association and stabilisation.

Sulphoxy emulsifier residues produce interesting effects. Compound EB containing compounded-in sodium dodecyl sulphate showed less oxidative stability than EB without such species compounded-in. Sodium dodecane sulphonic acid addition to EB at the same molar ratio had no effect. In compound EA (no added antioxidant) both additions had no effect. This interaction between diphenyl amine and sodium dodecyl sulphate may be through the lone electron pair of the amine and the sodium cation or through hydrogen bonding with the nitrogen of the amine. Such interaction is consistent with experimental results showing that the effectiveness of compounded-in diphenyl amine is less in polymer P which has a high concentration of oxygen bonded sulphur residue.

9.0. SUGGESTIONS FOR FURTHER WORK

In this work it was shown that traces of unsaturated carboxylic acid become bound to N.B.R. by preferential reaction with the crosslinking agent. The practical implications of this type of reaction were not fully considered because there was insufficient time, however it was shown that traces of oleic acid have a disproportionately large effect on the reduction in crosslink density resulting in significant changes in mechanical properties. Detailed study into the effect of attaching carboxy terminated short chain branches into N.B.R. by this means would be of considerable theoretical and practical interest in modification of network structure and static-dynamic tensile properties.

Network density determination from measurement of polymer loss during swelling is potentially a valuable method for determination of chemical crosslink density, particularly in low crosslink density networks. This method needs to be further tested by calibrating results with results obtained by an independent method of chemical crosslink density determination. This may be done by extracting networks of known chemical crosslink density. Networks of known chemical crosslink density may be prepared by crosslinking with a crosslinking agent of known functionality, (such as dicumyl peroxide) (Lorenz and Parks, 1961).

In this study the mechanism of network oxidation, was mainly studied at 100°C. Further study of network oxidation over a range of temperatures, perhaps down to room temperature would shed additional information on the mechanism of network oxidation. It would be of further interest to study the oxidation behaviour of vulcanizates cured to different degree in order to further evaluate the relative stability of specific crosslink structures. Study into the effect on oxidisability of low molecular weight polymer with different monomer composition would also be of interest since low molecular weight polymer migrates to surfaces where its effect may be disproportionately large.

It was demonstrated that calcium chloride coagulant exhibits antioxidative properties. Other coagulants, such as magnesium chloride and sodium chloride are also present in N.B.R. as polymerisation residues and their effect on oxidation should be studied.

Bibliography

Abu-Zeid M. E., Yousseff Y. A. and Abdul Razoul F. A. (1986). Thermal Degradation of Butadiene-Styrene Based Rubber. *Journal of Applied Polymer Science*, **31**, 1575.

Al-Malaika S. (1991). Mechanism of Antioxidant Action and Stabilisation Technology-The Aston Experience. *Polymer Degradation and Stability*, **34**, 11.

Aminabhavi T. M., Harrogoppad S. B., Khinnavar R. S. and Balundgi R. H. (1991). Rubber Solvent Interactions. *JMS-REV. Macromolecular Chemistry and Physics*, **C31**, 433.

Avramov I., Grantscharova E. and Gutzow I. (1988). Structural Relaxation. II. Metaphosphate Glasses. *Journal of Non-Crystalline Solids*, **104**, 148.

Banerjee B. (1989). Sulphenamide Accelerated Sulphur Vulcanization of Natural Rubber in the Presence of N-Cyclohexylthiophthalimide- Applications of E.S.R. Technique to Elucidate the Mechanism of Vulcanization. *Kautschuk + Gummi Kunststoffe*, **42**, 217.

Barker L. R. and Tinker A. J. (1989). Accelerated Testing and its Relevance to Service Performance. A.C.S. Rubber Division Meeting, October 17-20, Detroit (1989), paper 31.

Barlow F. W. (1988). "Rubber Compounding", New York: Mercel Dekker Inc., chpt. 5.

Barnard D. and Lewis P. M. (1988). in "Natural Rubber Science and Technology", Roberts A. D., ed., Oxford Science Publishers, chpt. 13.

Bateman C., Moore C. G., Porter M. and Saville B. (1963). in "The Chemistry and Physics of Rubber Like Substances ", Bateman L., ed., London: Maclaren press, chpt. 15.

Bertram H. H. (1981). 50 Years of Perbunan N. *Technical Notes for the Rubber Industry*, **53**, 3.

Bhattacharjee S., Bhowmick A. K. and Avasthi B. N. (1991). Degradation of Hydrogenated Nitrile Rubber. *Polymer Degradation and Stability*, **31**, 71.

Bhattacharjee S., Bhowmick A. K. and Avasthi B. N. (1993). in "Elastomer Technology Handbook", Cheremisinoff N. P., ed., Boca Raton, Florida: C.R.C. Press Inc., chpt. 13.

Bhowmick A. K. and Sadham K. De. (1980). Effect of Curing Temperature and Curing System on Network Structure and Technical Properties of Styrene Butadiene Rubber. *Journal of Applied Polymer Science*, **26**, 529.

Bille H. and Fendell H. (1993). How to Do Hot Air Ageing Tests Properly; A Survey of Influencing Parameters and Practical Guidance on Dealing with Them. A.C.S. Rubber Division Meeting, May 18-21, Denver (1993), paper 67.

Björk F., Dickman O. and Stenberg B. (1989). Long Term Studies of Rubber Materials by Dynamic Mechanical Stress Relaxation. *Rubber Chemistry and Technology*, **62**, 387.

Björk F. and Stenberg B. (1985). Influence of the Formation of an Oxidised Layer on the Dynamic Mechanical Properties of Natural Rubber. *Polymer*, **5**, 245.

Björk F. and Stenberg B. (1990). Stress Relaxation of a Nitrile Rubber Surrounded by an Oil that Increase the Network Density. *Polymer*, **31**, 1649.

Boruta J. and Petrujova A. (1987). Method of Predicting Service Life of Strain-Free Carbon Black Filled Rubber Vulcanizates Subjected to Natural Ageing. *International Polymer Science and Technology*, **14**, T59.

Brajko V., Duchacek V., Tauc J. and Tumova E. (1980). Determination of Poly-sulphide Crosslink Content in Rubber. *Plasty a Kaucuk*, **17**, 166.

Brazier D. W., Nickel G. H. and Szentgyorgyi Z. (1980). Enthalpic Analysis of Vulcanization by Calorimetry. Thiuram Monosulphide/Sulphur Vulcanization of N.R., B.R. and S.B.R.. *Rubber Chemistry and Technology*, **53**, 160.

Brown R. P., Morrell S. H. and Norman R. H. (1973). Tensile Stress Relaxation. *Journal of the I.R.I.*, **August**, 158.

Brown P. S., Porter M. and Thomas A. G. (1985). Influence of Crosslink Structure on Properties of Crystallizing and Non-Crystallizing Polyisoprenes. International Rubber Conference, Kuala Lumpur (1985), 1100.

Brydson J. A. (1988). "Rubbery Materials and their Compounds", New York: Elsevier, chpt. 9.

Budrugeac P. (1992). Thermo-oxidative Degradation of Some Nitrile-Butadiene Rubbers. *Polymer Degradation and Stability*, **38**, 165.

Budrugeac P. and Segal E. (1991). Thermo-oxidation and Non-isothermal Kinetic Study of Thermally Aged Nitrile Butadiene Rubber. *Thermochimica Acta*, **184**, 25.

Budrugeac P., Segal E. and Ciutacu S. (1991). Thermo-oxidative Degradation of Nitrile-Butadiene Rubber. *Journal of Thermal Analysis*, **37**, 1179.

Butler J. and Freakley P. K. (1992). Effect of Humidity and Water Content on the Cure Behaviour of a Natural Rubber Accelerated Sulphur Compound. *Rubber Chemistry and Technology*, **65**, 374.

Campbell D. S., Chapman A. V., Goodchild I. R. and Fulton W. S. (1992). Experimental Determination of the Mooney-Rivlin Constant for Natural Rubber Vulcanizates. *Journal of Natural Rubber Research*, **7**, 168.

Campbell D. S. and Saville B. (1967). Current Principles and Practices in Elucidating Structure in Sulphur Vulcanized Elastomers. Proceedings of the First International Rubber Conference, Brighton, (1967) p. 1-14.

Chang D. M. (1981). Investigation of the Structure-Property Relationship of Improved Low Compression Set Nitrile Rubbers. *Rubber Chemistry and Technology*, **54**, 170.

Chapman A. V. and Porter M. (1988). in "Natural Rubber Science and Technology", Roberts A. D., ed., Oxford Science Publishers, chpt. 12.

Colclough T., Cunneen J. I. and Higgins G. M. C. (1968). Oxidative Ageing of N.R. Vulcanizates. Part III Crosslink Scission in Mono-sulphide Networks. *Journal of Applied Polymer Science*, **12**, 295.

Coulthard D. C. and Gunter W. D. (1977). New Compounding Approaches to Heat Resistant N.B.R.. *Journal of Elastomers and Plastics*, **9**, 131.

Crowther B., Lewis P. M. and Metherell C. (1988). in "Natural Rubber Science and Technology", Roberts A. D., ed., Oxford Science Publishers, chpt. 6.

Cunneen J. I. and Lee D. F. (1964). Effect of Sulphur Compounds on the Autoxidation and Stress Relaxation of Peroxide Vulcanizates of Natural Rubber. *Journal of Applied Polymer Science*, **8**, 699.

Cunneen J. I. and Russell R. M. (1969). Occurrence and Prevention of Changes in Chemical Structure of Natural Rubber Tyre Tread Vulcanizates During Service. *Journal of the Rubber Research Institute Malaya*, **22**, 300.

Denisov E. T. (1980). in "Developments in Polymer Stabilisation-3", Scott G., ed., London: Applied Science Publishers, chpt. 1.

Deuri A. S. and Bhowmick K. A. (1987). Ageing of E.P.D.M. Rubber. *Journal of Applied Polymer Science*, **34**, 2205.

Devlin E. F. (1986). The Effect of Cure Variables on Cis/Trans Isomerisation in Carbon-Black Reinforced Cis-1,4-Polybutadiene. *Rubber Chemistry and Technology*, **59**, 666.

Dilks A. (1983). in "Degradation and Stabilisation of Polymers", Jellinek H. H. G., ed., N. Y.: Elsevier, chpt. 12.

Dinzburg B. N., Keller R. W. and Bond R. (1988). Heat Resistance Evaluation for Rubber Compounds. *Rubber World*, **February**, 28.

Dollimore D. (1992). in "Thermal Analysis-Techniques and Applications", Charsley E. L. and Worrington S. B., eds., Cambridge: Royal Society of Chemistry, p. 31.

Doyle G. M., Humphreys R. E. and Russell R. M. (1971). The Influence of Chemical Structure on the Dynamic Properties of Sulphur-Vulcanized Carbon Black Reinforced Natural Rubber. *Journal of Applied Polymer Science*, **15**, 1855.

Dunn J. R. (1984). Compounding N.B.R. for High Temperature Applications. *Rubber World*, **June**, 16.

Dunn J. R. (1981). in "Developments in Polymer Stabilisation-4", Scott G., ed., London: Applied Science Publishers, chpt. 7.

Eliseeva V. I., Ivanchev S. S., Kuchanov S. I. and Lebedev A. V. (1981). "Emulsion Polymerisation and its Application in Industry", New York: Plenum Publishing Corporation, p.18.

Engels H. W. (1994). p-Phenylenediamines: Correlation of Molecular Structure and Effectiveness. *Kautschuk + Gummi Kunststoffe* , **47**, 12.

Field L. (1977). in "Organic Chemistry of Sulphur", Oae S., ed., New York: Plenum Press, chpt 7.

Flory P. J. (1953). "Principles of Polymer Chemistry", New York: Cornell University Press.

Franta I. (1989). "Elastomers and Rubber Compounding Ingredients", New York: Elsevier.

Frenkel R., Duchacek V. and Maksutov G. (1992). Hydrolysis of Acrylonitrile Butadiene Rubber. *Plastics Rubber and Composites Processing and Applications*, **17**, 19.

Gan S.-N. and Ting K.-F. (1993). Effect of Treating Latex With Some Metal Ions on Storage Hardening of Natural Rubber. *Polymer*, **24**, 2142.

George A. P. (1980). Temperature Dependence of Wall-Slip in Milk Liner Compound. Avon Industrial Polymers Internal Assignment 3561.

Gillen K. T. and Clough R. L. (1989). Time-Temperature-Dose Rate Superposition: A Methodology for Extrapolating Accelerated Radiation Ageing Data to Low Dose Rate Conditions. *Polymer Degradation and Stability*, **24**, 137.

Gillen K. T. and Clough R. L. (1992). Rigourous Experimental Confirmation of a Theoretical Model for Diffusion-Limited Oxidation. *Polymer*, **33**, 4358.

Gillen K. T., Clough R. L. and Dhooge N. J. (1986). Density Profiling of Polymers. *Polymer Testing*, **27**, 225.

Goh S. H. (1987). Thermoanalytical Studies of Rubber Oxidation: Characterisation of Nitrile Rubbers. *Thermochimica Acta*, **113**, 387.

Gronski W. and Hoffman U. (1992). Structure and Density of Crosslinks in Natural Rubber Vulcanizates. A Combined Analysis by N.M.R. Spectroscopy, Mechanical Measurements and Rubber Elasticity Theory. *Rubber Chemistry and Technology*, **65**, 63.

Haslam J, Willis H. A. and Squirrel D. C. M. (1972). "Identification and Analysis of Plastics", London: Butterworth Publishers.

Hamed G. R. (1994). Fundamental Characteristics and Properties of Crosslinked Elastomers. *Rubber World*, **October**, 25.

Hanthal H. G. (1975). in "The Preparation and Manufacture of Dimethyl Sulphoxide", Martin D. and Hanthal H. G., eds., New York: Wiley Press, chpt. 1.

Harris B., Braddell O. G., Almond D.P., Lefebvre C. and Verbist J. (1993). Study of Carbon Fibre Surface Treatments by Mechanical Analysis. *Journal of Materials Science*, **28**, 3353.

Hertz D. L. (1984). Theory and Practice of Vulcanization. *Elastomerics*, **November**, 17.

Hertz D. L., Bussem H. and Ray T. W. (1994). Nitrile Rubber- Past, Present and Future. A.C.S. Rubber Division Meeting, October 11-14, Pittsburg (1994), paper 58.

Hoffman U., Gronski W., Simon G. and Wutzler A. (1992). Determination of Crosslink Densities of Carbon Black Filled Natural Rubber Sulphur Vulcanizates by ^{13}C N.M.R. Spectroscopy and ^{1}H N.M.R. Transversal Relaxation. *Die Agnewandte Makromolekulare Chemie*, **202/203**, 282.

Hoffman W. (1968). in "Polymer Chemistry of Synthetic Elastomers", Kennedy J. P. and Tornqwist E. G. M., eds., New York: Interscience Publishers, chpt. 4.

Hoffman W. (1984). Influence of Crosslinking on Permanent Set Especially Compression Set of Nitrile Rubbers at Elevated Temperatures. *Plastics and Rubber Processing and Applications*, **4**, 191.

Hoffman W. (1985). Review of Improvements in Sulphur Cured Nitrile Rubber Compounds. *Plastics and Rubber Processing and Applications*, **5**, 209.

Horvath J. W., Purdon J. R. and Meyer G. E. (1974). Polymerisation Stabilised N.B.R.: A Significant Advance in Age Resistance Via Non-Extractable Antioxidants. *Applied Polymer Symposium*, **25**, 187.

Husbands M. J. and Scott G. (1979). Mechanism of Antioxidant Action: The Behaviour of Sulphur Dioxide in Auto-Oxidising Systems. *European Polymer Journal*, **15**, 249.

Hummel D. O. and Scholl F. (1981). "Atlas of Polymer and Plastics Analysis", Volume 3, Second edition, Weinheim: Verlag Chemie.

Ishida H. (1987). Quantitative Surface F.T.I.R. Spectroscopic Analysis of Polymers. *Rubber Chemistry and Technology*, **60**, 497.

Kirkham M. C. (1978). Current Status of Elastomer Vulcanization. *Progress of Rubber Technology*, **41**, 61.

Kiroski D., Burke D. and Packham D. E. (1994). Effect of Substrate on Adhesion in Rubber Moulding. *Vide-Couches Minces*, **272**, 454.

Koenig J. L. and Patterson D. J. (1986). Application of Solid State ^{13}C N.M.R. Spectroscopy to Sulphur Vulcanized N.R.. *Elastomerics*, **November**, 21.

Kotani T. and Teramoto T. (1980). Compound Formulation for Heat Resistant Nitrile Rubber. *International Polymer Science and Technology*, **7**, T/18.

Krejsa M. R. and Koenig J. L. (1993a). A Review of Sulphur Fundamentals for Accelerated and Unaccelerated Vulcanization. *Rubber Chemistry and Technology*, **66**, 376.

Krejsa M. R. and Koenig J. L. (1993b). Solid State Carbon-13 N.M.R. Studies of Elastomers. XI. N-t-Butyl Benzothiazole Sulfenamide Accelerated Sulphur Vulcanization of Cis-Polyisoprene at 75 MHz. *Rubber Chemistry and Technology*, **66**, 73.

Kruger F. W. and Mc.Gill W. J. (1991a). A D.S.C. Study of Curative Interactions.III. The Interaction of T.M.T.D. with ZnO, Sulphur and HSt", *Journal of Applied Polymer Science*, **42**, 2661.

Kruger F. W. and Mc.Gill W. J. (1991b). A D.S.C. Study of Curative Interactions.IV. The Interaction of T.M.T.D. with ZnO, Sulphur and HSt. *Journal of Applied Polymer Science*, **42**, 2669.

Kruger F. W. and Mc.Gill W. J. (1992a). Study of Curative Interactions in Cis-1,4-Polyisoprene.VI. Interactions of Some Combinations of Sulphur, T.M.T.D. and ZnO. *Journal of Applied Polymer Science*, **44**, 581.

Kruger F. W. H. and Mc.Gill W. J. (1992b). Study of Curative Interactions in Cis-1,4-Polyisoprene. XI. Network Maturing Reactions in the Cis-1,4-Polyisoprene-Sulphur-Zinc Dimethyldithiocarbamate-ZnO Systems. *Journal of Applied Polymer Science*, **45**, 1491.

Lautenschlaeger F. K. (1977). The Structure of Accelerated Sulphur Vulcanizates based on Model Compound Vulcanization. Rubbercon '77 Conference, Brighton (1977), paper 16.

Lee L.-H., Stacy C. L. and Engel R.G. (1966a). Mechanism of Oxidative Degradation .I. Oxidation of Synthetic Rubbers Catalysed by Metallic Ions. *Journal of Applied Polymer Science*, **10**, 1699.

Lee L.-H., Stacy C. L. and Engel R.G. (1966b). Effect of Metallic Salts and Metal Deactivators on the Oxidation of Polybutadiene. *Journal of Applied Polymer Science*, **10**, 1717.

Lee T. C. P. and Morrell S. H. (1973). Network Changes in Nitrile Rubber at Elevated Temperature. *Journal of the I.R.I.*, **February**, 27.

Layer R. W. (1991). Recuring Vulcanizates, a Novel Way to Study the Mechanism of Vulcanization. *Rubber Chemistry and Technology*, **65**, 211.

Lin D.G. (1986). High Temperature Contact Oxidation and Adhesion to Metals of Butadiene Styrene Acrylonitrile Rubber. *Kautchuk iRezina*, **1**, 13.

Lorenz O. and Parks C. R. (1961). The Crosslinking Efficiency of some Vulcanizing Agents in Natural Rubber. *Journal of Polymer Science*, **50**, 299.

Lotfipour M. (1990). Unpublished Work.

Lotfipour M, Packam D. E. and Turner D. (1991). Interfacial Layers and Adhesion in the Moulding of Rubber. *Surface and Interface Analysis*, **17**, 516.

Lotfipour M., Reeves L., Kiroski D. and Packham D. E. (1994). The Interphase in Rubber-Metal Moulding: the Influence on Adhesion of Sulphur-Containing Emulsifier Residues in Nitrile Rubber. *Journal of Adhesion*, **47**, 33.

Luston J. (1980). in "Developments in Polymer Stabilisation-2", Scott G., ed., London: Applied Science Publishers, chpt. 5.

Malek K. A. B. and Stevenson A. (1992). A 100-Year Old Study of the Life Prediction of Natural Rubber for an Engineering Application. *Journal of Natural Rubber Research*, **7**, 126.

Mark J. E. (1982). Experimental Determinations of Crosslink Densities. *Rubber Chemistry and Technology*, **55**, 762.

Mark J. E. (1992). Molecular Aspects of Rubberlike Elasticity. *Die Angewandte Makromolekulare Chemie*, **202/203**, 1.

Martin D. (1975). in "The Preparation and Manufacture of Dimethyl Sulphoxide", Martin D. and Hanthal H. G., eds., New York: Wiley press, chpt. 4.

Mayer R. (1977). in "Organic Chemistry of Sulphur" Oae S., ed., New York: Plenum Press, chpt. 2.

Mazzeo R. A. (1995). Preventing Polymer Degradation During Mixing. Rubber World, **February**, 22.

Meissner B. (1987). Ageing of Sulphur Vulcanizates and Possibilities of its Retardation. *International Polymer Science and Technology*, **14**, T62.

Melley R. E. and Stuckey J. E. (1970). A Determination of Crosslink Density from Compression Modulus Data. *Journal of Applied Polymer Science*, **4**, 2327.

Meridith P. (1995). "Final Year Project", School of Materials Science, University of Bath.

Meyer K. H. and Hohenemser W. (1936). Contribution to the Study of the Vulcanization Reaction. *Rubber Chemistry and Technology*, **9**, 201.

Mifune N., Nagai Y., Nishimoto K and Ishimaru S. (1991). Study on Change of Material Properties and Dynamic Properties of Styrene-Butadiene Rubber. *Kobunshi Ronbunshi*, **48**, 437.

Milner P. W. (1987). in "Developments in Rubber Technology 4", Whelan A. and Lee K. S., eds., London: Elsevier Applied Science Publishers, chpt. 2.

Moakes R. C. (1975). Long Term Natural Ageing. *R.A.P.R.A. Members Journal*, **July/August**, 57.

Morrison N. J. and Porter M. (1984). Temperature Effects on the Stability of Intermediates and Crossinks in Sulphur Vulcanization. *Rubber Chemistry and Technology*, **57**, 63.

Morrison R. T. and Boyd R. N. (1987). "Organic Chemistry", 5th Edition, Boston: Allyn and Bacon Inc, p.76, 251.

Moynihan C. T., Eastal J. A., DeBolt M. A. and Tucker J. (1976). Dependence of the Fictive Temperature of Glass on the Cooling Rate. *Journal of American Chemical Society*, **59**, 12.

Musci R. (1995). Europrene N Green: A New Line of Top Performance Nitrile Elastomers. Rubbercon '95 Conference, Göteborg, paper 65.

Narayaswamy O. S. (1986). A Model of Structural Relaxation in Glass. *Journal of American Chemical Society*, **54**, 491.

Parks C. R., Parker D. K. and Chapman D. A. (1972). Pendant Accelerator Groups in the Ageing of Rubber. *Rubber Chemistry and Technology*, **45**, 467.

Poehlein G. W. (1986). in "Encyclopedia of Polymer Science and Engineering", Mark H. F., Bikales N. M., Overberger G. G. and Menges G., eds., New York: John Wiley & Sons, p.1.

Porter M. (1968). in "The Chemistry of Sulfides", Tobolsky V. A., ed., New York: Interscience Publishers, p.165.

Rana M. A. and Koenig J. L. (1993). Solid State C-13 N.M.R. Studies of Vulcanized Elastomers.XII. Accelerated Sulphur Vulcanized High Vinyl Polybutadiene. *Rubber Chemistry and Technology*, **66**, 242.

Reading M. (1992). in "Thermal Analysis-Techniques and Applications", Charsley E. L. and Worrington S. B., eds., Cambridge: Royal Society of Chemistry, p.108.

Reeves L. and Packham D. E. (1992). Effect of Compounding on the Adhesion of Rubber to Medium Carbon Steel. *Journal of Physics: D: Applied Physics*, **25**, A14.

Reeves L., Kiroski D., and Packham D. E. (1993). Weak Boundary Layers: Adhesion in Rubber Moulding. Adhesion '93 Conference, York.

Ridland J. J. and Pfisterer H. A. (1983). Compounding N.B.R. to Specification. *Rubber World*, **March**, 20.

Rosin J. (1967). "Reagent Chemicals and Standards", 5th Edition, Princetown N.J.: D. Van Nostrand Company Inc..

Saville B. and Watson A. A. (1967). Structural Characterisation of Sulphur Vulcanized Rubber Networks. *Rubber Chemistry and Technology*, **40**, 100.

Scherer G. W. (1986). "Relaxation in Glasses and Composites", London: Wiley Publishers.

Schneider B., Doskocilova D., Stokr J. and Suoboda M. (1993). Study of Thermal Degradation of Polybutadiene in Inert Atmosphere: Evidence of Temperature and Time of Heating in I.R. and N.M.R. Spectra. *Polymer*, **34**, 432.

Seah M. P. and Briggs D. (1990). in, "Practical Surface Analysis", Briggs D. and Seah M. P., eds., 2nd Edition, New York: John Wiley & Sons Ltd., chpt. 1.

Selker M. A. and Kemp A. R. (1994). Sulphur Linkage in Vulcanized Rubbers. Reaction of Methyl Iodide with Sulphur Compounds. *Industrial and Engineering Chemistry*, **36**, 16.

Shelton J. R. (1981). in "Developments in Polymer Stabilisation-4", Scott G., ed., London: Applied Science Publishers, chpt. 4.

Shelton J. R. (1983). Oxidation and Stabilisation of Rubbers. *Rubber Chemistry and Technology*, **56**, G71.

Sircar A. K. (1982). Characterisation of Elastomers by Thermal Analysis. *Journal of Scientific and Industrial Research*, **41**, 536.

Sims J. (1988). Studies on the Crosslink Structure and Mechanical Properties of Natural Rubber and Nitrile Rubber Vulcanizates. MPhil Thesis, University of Bath.

Skinner T. D. (1972). The C.B.S.-Accelerated Sulfuration of Natural Rubber and cis-1,4-Polybutadiene. *Rubber Chemistry and Technology*, **45**, 182.

Slusarski L. (1984). Thermal Stability of Elastomers. *Journal of Thermal Analysis*, **29**, 905.

Starmer P. H. (1993a). Swelling of Nitrile Rubber Vulcanizates by Polar and Non Polar Liquids-Part 1: Review of Parameters. *Journal of Elastomers and Plastics*, **25**, 59.

Starmer P. H. (1993b). Swelling of Nitrile Rubber Vulcanizates by Polar and Non Polar Liquids-Part 2: Swelling Curves. *Journal of Elastomers and Plastics*, **25**, 121.

Starmer P. H. (1993c). Swelling of Nitrile Rubber Vulcanizates by Polar and Non Polar Liquids-Part 3: Factors Affecting Maximum Swelling. *Journal of Elastomers and Plastics*, **25**, 188.

Stolfuss B. and Warrach W. (1981). High Performance Nitrile Rubber for Low Temperature Applications. *Elastomerics*, **October**, 51.

Studebaker M. C. (1972). The Oxidative Hardening of S.B.R.. *Rubber Chemistry and Technology*, **45**, 450.

Tobolsky A. V., Prettyman I. B. and Dilton J. H. (1944). Stress Relaxation of Natural and Synthetic Rubber Stocks. *Journal of Applied Physics*, **15**, 380.

Treloar L. R. G. (1975). "The Physics of Rubberlike Elasticity", 3rd. Edition, Oxford: Clarendon Press.

Varughese S and Tripathy D. K. (1992). Dynamic Mechanical Properties of Epoxidised Natural Rubber Vulcanizates: Effect of Curing System and Ageing. *Polymer Degradation and Stability*, **38**, 7.

Wagner C. D. (1990). in "Practical Surface Analysis", Briggs D. and Seah M. P., eds., 2nd Edition, N. Y.: John Wiley & Sons, Appendix 5.

Wanyn G. (1990). The Changes in Low Temperature Properties of N.B.R.-26 Vulcanizates During Thermo-oxidation. *China Synthetic Rubber Industry*, **13**, 266.

Wunderlich B. (1992). New Directions in Thermal Analysis. *Thermochimica Acta*, **212**, 131.

Wells G. M. (1991). "Handbook of Petrochemicals and Processes", Aldershot: Gower Publishing Company.

Yasuda H. and Rosengren K. J. (1970). Isobaric Measurement of Gas Permeability of Polymers. *Journal of Applied Polymer Science*, **14**, 2839.

Yehia A. A. and Stoll B. (1982). Kinetics of Vulcanization of Nitrile Butadiene Rubber. *Kautschuk + Gummi Kunststoffe*, **40**, 950.

Yongjin L. (1989). Calculation Methods for Predicting the Ageing Property or Life Time Period of Rubber. *China Synthetic Rubber Industry*, **12**, 205.

Zachoval Z. and Brajko V. (1989). in "Elastomers and Rubber Compounding Ingredients", Franta I., ed., New York: Elsevier, chpt. 3.